Stony Brook University

Investigation of Bio-Inspired Hybrid Materials through

Polymer Infiltration of Thermal Spray Formed Ceramic Templates

A Dissertation Presented

by

Katherine Claire Flynn

to

The Graduate School

in Partial Fulfillment of the

Requirements

for the Degree of

Doctor of Philosophy

in

Materials Science and Engineering

Stony Brook University

August 2014

Stony Brook University

The Graduate School

Katherine Claire Flynn

We, the dissertation committee for the above candidate for the

Doctor of Philosophy degree, hereby recommend

acceptance of this dissertation.

Dr. Sanjay Sampath – Dissertation Advisor
Professor, Department of Materials Science and Engineering

Dr. Jason Trelewicz - Chairperson of Defense
Assistant Professor, Department of Materials Science and Engineering

Dr. Dilip Gersappe
Associate Professor, Department of Materials Science and Engineering

Dr. Andrew Gouldstone
Assistant Professor, Department of Mechanical and Industrial Engineering
Northeastern University

This dissertation is accepted by the Graduate School

Charles Taber
Dean of the Graduate School

Abstract of the Dissertation

Investigation of Bio-Inspired Hybrid Materials Through

Polymer Infiltration of Thermal Spray Formed Ceramic Templates

by

Katherine Claire Flynn

Doctor of Philosophy

in

Materials Science and Engineering

Stony Brook University

2014

High strength and toughness are often mutually exclusive in engineered materials. This is especially true of ceramics and polymers. Ceramics exhibit high strength and stiffness, but are brittle while polymers are flaw tolerant but prone to deformation at low stresses. Nature overcomes this restriction in materials by strategically combining brittle components with tough organics, leading to materials with both a high strength and toughness. One of the most impressive natural composites is nacre consisting of mainly a brittle mineral phase, 95vol% calcium carbonate (aragonite), and 5vol% biopolymer (a combination of proteins and polysaccahrides). Nature combines constituents with poor macroscale properties and achieves levels that surpass those expected despite being formed of mostly mineral $CaCO_3$ tablets. Interestingly, nacreous assemblies can display a toughness 3,000 times higher than their major constituent, aragonite.

Similarities have been observed between nacre and sprayed ceramics in terms of their microstructures and mechanical behavior. Both assemblies follow a design hierarchy and layered organization over several length scales. The mineral phase in nacre has evolved on the microscale and nanometer interlayers of biopolymer bond neighboring tablets. In addition, these tablets have a certain degree of waviness, nanoscale roughness, and mineral bridges thereby further enhancing linkages to one another. These inherent microstructural features significantly improve the mechanical properties of nacreous assemblies. On the other hand, sprayed ceramics are formed from micron sized splats, larger than aragonite nacreous tablets, with comparable

(nanoscale) roughness, resulting from grain termination sites. Together these features of sprayed ceramics respond similarly to nacre, showing a great extent of mechanical nonlinearity and hysteresis, which is mostly absent in structural ceramics.

Due to the splat-by-splat deposition process, sprayed ceramics contain a certain degree of porosity (up to approximately 20%). Often, porosity is interconnected and is controlled by varying processing parameters. Through the introduction of an appropriate polymer at the porosity interface, it may be possible to achieve synergistic benefits in terms of both strength and toughness of the sprayed material. This dissertation will focus on the fabrication and evaluation of property enhancements of bio-inspired materials based on ceramic thermally sprayed scaffolds through post deposition polymer impregnation.

Table of Contents

List of Figures

List of Tables

List of Abbreviations

AIBN:	Azobisisobutyronitrile
Al_2O_3:	Alumina
APS:	Atmospheric plasma spray
ATBN:	Amine-terminated butadiene acrylonitrile
CTBN:	Carboxyl-terminated butadiene acrylonitrile
DSC:	Differential Scanning Calorimetry
E:	Modulus
E_{oc}:	Open circuit potential
E_{corr}:	Corrosion potential
FS:	Flame spray
HT:	Heat treated
HVOF:	High-velocity oxy fuel
I_{corr}:	Corrosion current
K_{IC}:	Fracture toughness
m_i:	Weight
M_i:	Molecular weight
MMA:	Methyl methacrylate
n_i:	number of molecules with i repeat units
OCP:	Open circuit potential
PDMS:	Polydimethylsiloxane
PMMA:	Poly(methyl methacrylate)
PVA:	Polyvinyl alcohol

SCE:	Saturated calomel electrode
STA:	Simultaneous Thermal Analysis
SI:	Simple immersion
TGA:	Thermogravimetric Analysis
TS:	Thermal spray
VI:	Vacuum infiltration
YSZ:	Yttria stabilized zirconia
σ_{flex}:	Flexural strength

1. Introduction

Millions of years of evolution have allowed nature to produce materials some would call ideal. High performance natural materials possess unique combinations of mechanical properties rarely seen in engineered materials. Natural materials often occur as laminated or layered structures and exhibit a high degree of strength, toughness, and stiffness making them noteworthy. These materials differ from the usual inverse relationship observed between strength and toughness or stiffness and toughness. It is often necessary for natural materials to possess this unique combination of properties because of their functions, including protection from predators and skeletal support. In this chapter, natural composites including bone and nacre will be discussed.

1.1. Biogenic Materials

Approximately 60 biogenic materials have presently been identified [1]. Organic materials produced by living organisms or a biological process are referred to as biogenic materials. Perhaps the most common of these materials include silica in radiolarians and diatoms (marine organisms), hydroxyapatite in bones and teeth, and calcium carbonate in seashells [2, 3]. Biologically produced materials come in a variety of sizes and shapes depending on the application. For example, the basic components of bone are hydroxyapatite crystals embedded in collagen fibrils. These hydroxyapatite crystals are on the order of nanometers [4]. However, a sea urchin spine is formed from a single crystal of calcium carbonate and its length can vary in size from 10 to 50mm [2]. This provides evidence that nature has been able to evolve materials that are designed for a specific purpose and application which display a unique set of properties.

The effective combination of brittle ceramics and tough biopolymers into a biological composite can be seen in the property map showing toughness and modulus, Figure 1.1 [5]. The top left portion is dedicated to natural elastomers. This category contains biological materials like skin that are compliant and soft. These materials are tough and rather than cracking, they will tear. In the lower right portion of the property map, are materials that are prone to cracking. They are ceramics and although harder and stiffer than the elastomers, they are also more fragile. The upper right domain is where nature has combined the ideal properties of elastomers (toughness) and minerals (stiffness) into one biological composite. In fact, the combination of

elastomers and minerals can result in properties that are far superior to the individual ingredients. Through alterations of the mineral and biopolymer content in the composites, the degree of stiffness can vary. For instance, tooth enamel which is 99% mineral in composition is 1000 times stiffer than collagen, while antler bone which is only 30% mineral is nearly 100 times stiffer than collagen [2].

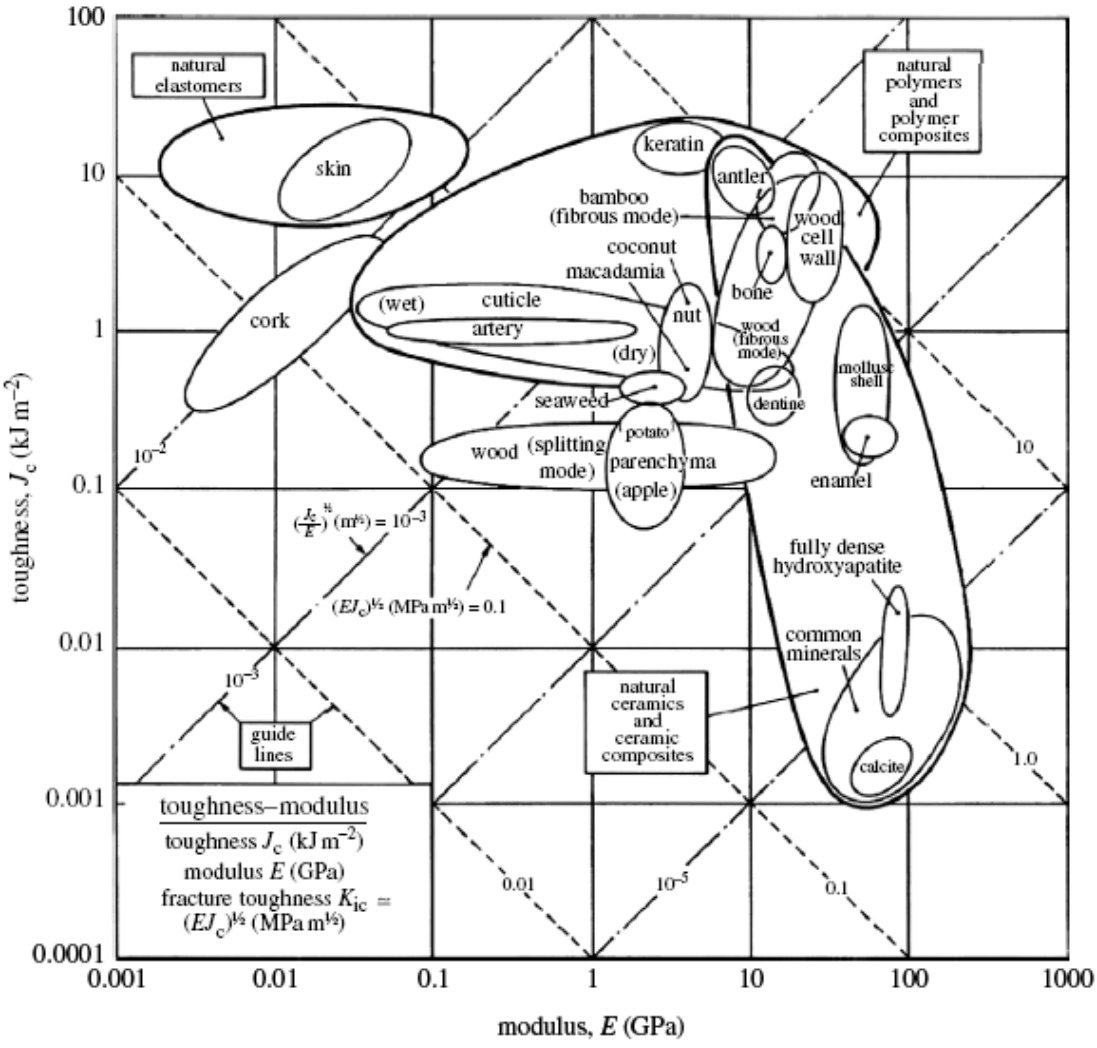

Figure 1.1. Material properties chart for natural material composites as well as their individual constituents. The modulus, or stiffness of the material is provided on the horizontal axis while toughness, or the material's resistance to crack propagation is provided on the vertical axis [5].

The combination of natural elastomers and minerals results in materials with a high degree of stiffness and therefore, it could be expected that these composites would also be brittle. However, this is not the case and in fact as observed in the property map, natural composites like bone and nacre when compared to their major mineral constituents are orders of magnitude tougher. This is a result of the distinctive way in which brittle minerals and soft proteins are arranged.

1.2. Nature's Design of High-Performance Materials

Nature has had years to evolve and has achieved exceptional natural laminated materials including bone and nacre. Mineralization is one technique that allows for natural materials to exhibit both a high hardness and stiffness [6]. It is widely known in the materials science community that materials with a high mineral content are rather brittle and therefore would not necessarily exhibit outstanding combinations of stiffness, strength, and toughness. However, in materials like bone and nacre, this remarkable combination exists because of the way nature designs and merges the specific constituents.

Certain features in bone and nacre can be found over several distinct scales ranging from the macroscale to the nanoscale. For example, the mineral phase is designed on the nanoscale or microscale and in the form of layers, rods, grains, or platelets. Then brittle materials are bonded to one another by a ductile organic material that is a combination of proteins and polysaccharides. By using ductile and soft proteins and tissues to form a network with the incorporation of much stiffer minerals, nature is able to create a material that has both stiffness and toughness. Although these mechanical properties are measured at the macroscale, they are a result of the design features at work over several distinct length scales. The hierarchical arrangement is involved in energy dissipation, the transfer of stresses and loads as well as distribution of damage which can aid in resistance to cracking. In fact, some argue that the hierarchical arrangement is necessary for hard biological materials [7].

1.3. Examples of Biological Composites

There are several natural laminated composites that display exceptional mechanical properties. Of them bone and nacre will be discussed in further detail below.

1.3.1. Bone

Another natural material with exceptional properties is bone. Bone is the combination of hydroxyapatite, a mineral, and collagen, a softer material. The hydroxyapatite is a stiff inorganic mineral phase and the collagen is a softer organic phase that is mostly collagen but contains a small amount of proteoglycans and noncollageneous proteins [4, 8]. The structure of bone is organized over six to seven hierarchical levels, Figure 1.2 [2, 4, 9]. The combination of these two materials results in a high stiffness material that is also extremely tough. Collagen fibrils are embedded with nanoscopic mineral crystals. The displacement of the nanoscopic mineral crystals is the basic deformation mechanism of the collagen fibrils [10, 11]. The three-dimensional arrangement of the collagen fibrils governs the properties of the bone. The arrangements can include:

- Woven
- Plywood
- Aligned

Collagen fibrils that are aligned form collagen fibre, which serve as the basis for forming other structures like lamellae and osteons. The interactions of cracks with these features is not completely understood. However, it is thought that the mechanisms at the larger scale are just as important as the mechanisms at the nanoscale. At the microscale there are a number of mechanisms that come into play. They include viscoplastic flow, crack deflection, crack bridging, and microcracking [2, 12, 13]. Nalla *et al.* found that crack bridging seems to be the main toughening mechanism. Crack bridging is a way of impeding the advancement of a crack, by ligaments of intact bone material forming bridges along the crack faces. This serves as a means of pulling crack faces together and through this, crack advancement is hindered or blocked [13].

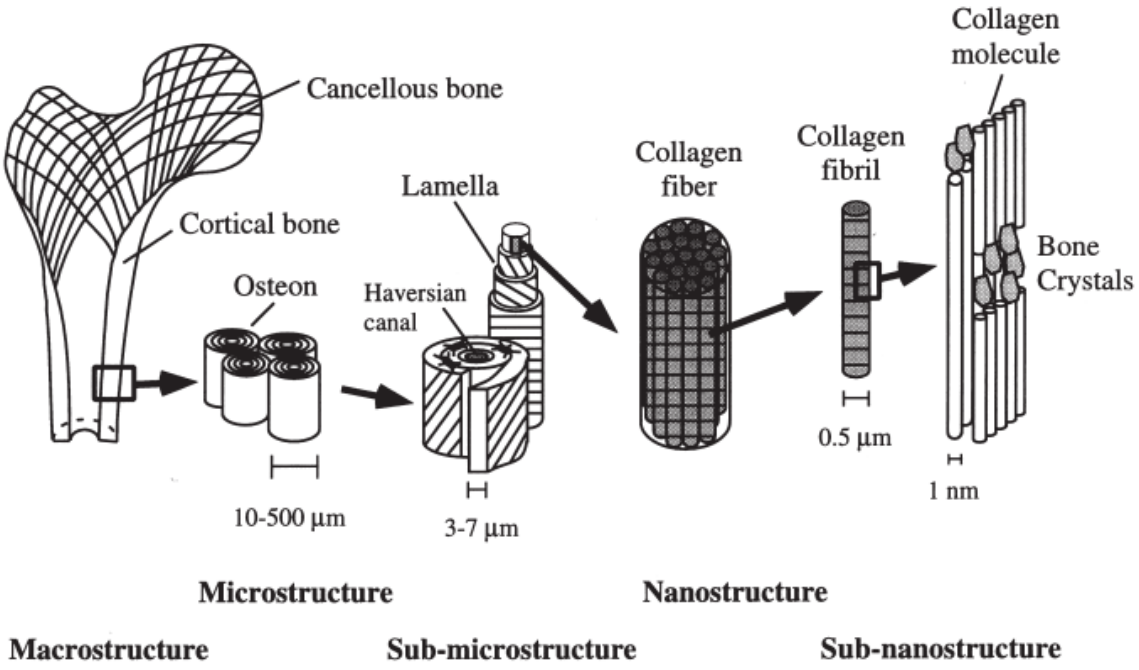

Figure 1.2. The hierarchical structure of bone. The structure ranges from the macroscale, down to subnanoscale [9].

1.3.2. Nacreous Assemblies

Perhaps the most impressive of all natural materials is nacre and will therefore be discussed in great detail. Nacre, the combination of calcium carbonate platelets and an organic biopolymer, results in a material with properties that widely outperform its major constituents. To date, there are no man-made composites that result in such a synergistic combination of properties. For this reason, nacre is one of the most widely studied natural material systems.

It was approximately 545 million years ago when mollusks first appeared. However, it was 440-500 million years ago when the mollusk family diversified quite a bit leading to the separation of various classes. Previously, mollusks were all rather small; only 2 to 5mm in size. Today, there are approximately 60,000 different species and their shells are still similar in structure to the earlier forms. The Gastropoda class is composed of the most species (~35,000) followed by the Bivalvia with nearly 10,000 species. The Gastropoda class contains Conch shell, top shell and abalone while the Bivalvia class includes oysters and clams. [14]. Of all nacre, columnar nacre from the red abalone is the most widely studied [15].

Most mollusks grow a hard shell which serves as armor for the soft mollusk. The inside of the shell has a soft tissue covering called the mantle which is responsible for growing the shell.

The shell offers a tremendous level of protection to the soft mollusk and for this reason it is essential it be both stiff and strong. A mollusk shell can be thought of as a two layered system; the first is the hard calcite shell and the softer inner layer called nacre, Figure 1.3. Nacre is the most widely studied aspect of a mollusk shell.

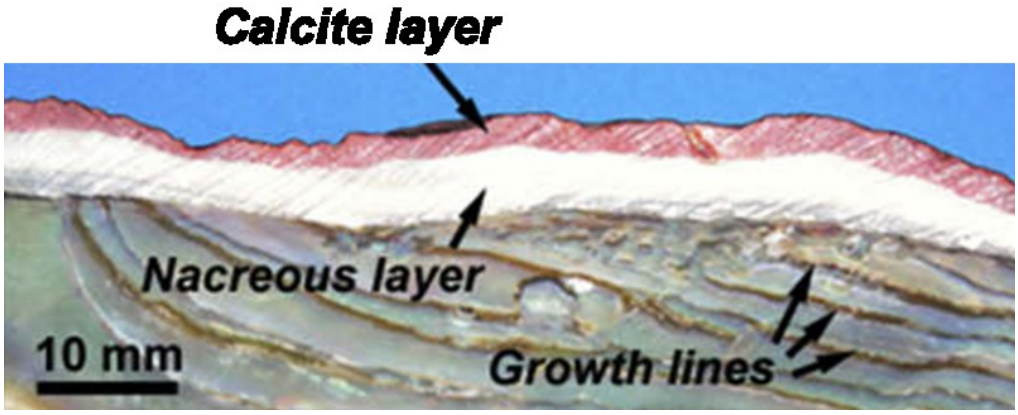

Figure 1.3. A macroscopic view of a mollusk shell. Here it is apparent that it the shell is two layer armored structure. The top layer is the hard and brittle calcite layer and the nacreous layer is the inner lustrous layer [16].

The hard outer calcite layer of a mollusk shell is extremely difficult for a foreign object to penetrate but once penetrated will experience brittle fracture. In coupling with nacre, this mollusk shell is an ideal armor system and this is because the inner nacreous layer can provide structural integrity when the outer shell has cracked. The body of a mollusk is rather soft so nacre provides protection from predation or from rocks or debris that may be moved by the current that could cause harm. Furthermore, nacre contains growth lines which are a few sub-layers of weaker material that may even serve as crack deflectors. [14]

Nacre is grown from the epithelial cells in the mantle of a mollusk [17]. There are two types of nacre, columnar and sheet. From their mantle, gastropods and cephalopods form columnar nacre [18-20] and bivalves form sheet nacre from their mantle [21, 22]. Irregular shaped polygonal tablets grow in between the previously deposited organic layers in both sheet and columnar nacre but during their formation there are differences in the growth of sheet and columnar nacre, Figure 1.4. Only two or three consecutive crystalline layers grow at once in sheet nacre while columnar nacre grows in multiple stacks or columns at once. Each growing column contains about 20 to 30 different tablet layers. The largest tablet is at the bottom and each consecutive tablet decreases in size, resulting in columns forming conical stacks. Although the formation mechanism differs across species, they have a similar appearance visually. [17].

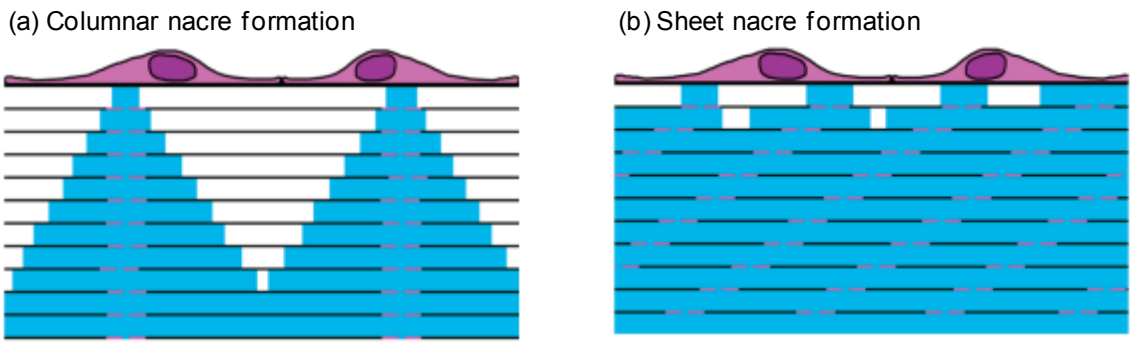

Figure 1.4. Schematic illustrating the difference in the way sheet and columnar nacre form from the growing surface. (a) Columnar nacre forms in multiple conical columns at once in stacks of about 20 to 30 layers. Each tablet layer increases in size as the distance from the growth surface increases. (b) Formation of sheet nacre occurs in two or three consecutive crystalline layers at once. In this schematic the first two layers after the growth line are still forming and will eventually fill in and new layers will form. [17].

Nacre is composed of alternating layers of platelets and organic polymer layers. The hard mineral calcium carbonate platelets occur most often as aragonite. The organic layers are comprised of proteins and polysaccharides. Overall, the structure of nacre is 95vol% calcium carbonate and 5vol% polymer and the microscale architecture is described as having a brick and mortar structure, Figure 1.5 [23-25]. The brittle platelets are densely packed microscopic aragonite polygonal tablets, approximately 5-8μm in diameter and nearly 0.5μm in thickness. There are approximately 20-30nm thick interlayers of organic materials that anchor the platelets together. Depending on the type of mollusk the nacre can be arranged in coulumns, and thus referred to as columnar nacre (abalone shell and other gastropods) or more randomly, as sheet nacre (bivalves like oyster and mussels). [14].

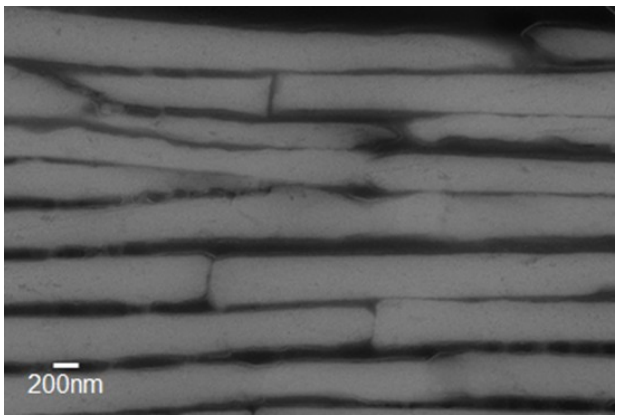

Figure 1.5. Microstructure of a nacreous assembly illustrating it's similarity in appearance to a brick and mortar architecture.

A number of features are present in nacre, from the macroscale all the way down to the nanoscale. The overall macroscopic mechanical performance of nacre is due to the combination of mechanisms working over several length scales, Figure 1.6. Each aragonite tablet tends to have a certain degree of waviness that conforms to the adjacent tablets, so that they fit together. The organic interlayers between the aragonite tablets is actually a number of layers of various proteins and chitin, containing pores with spacing of 20-100nm. This leaves gaps for mineral bridges and asperities, two different aragonite structures. Mineral bridges are aragonite connections that form between adjacent tablets and help hold tablets in position. During the application of a load, and in order for deformation to occur, work must be done to fracture the mineral bridge interconnections. Following fracture of the mineral bridges, the fragments can act as asperities. Asperities are bumps or rough portions on the surface of aragonite tablets that make contact with asperities on adjacent tablets when deformation occurs, causing sliding of tablets. Energy dissipation occurs as a result of the frictional sliding of asperities on one another. [14].

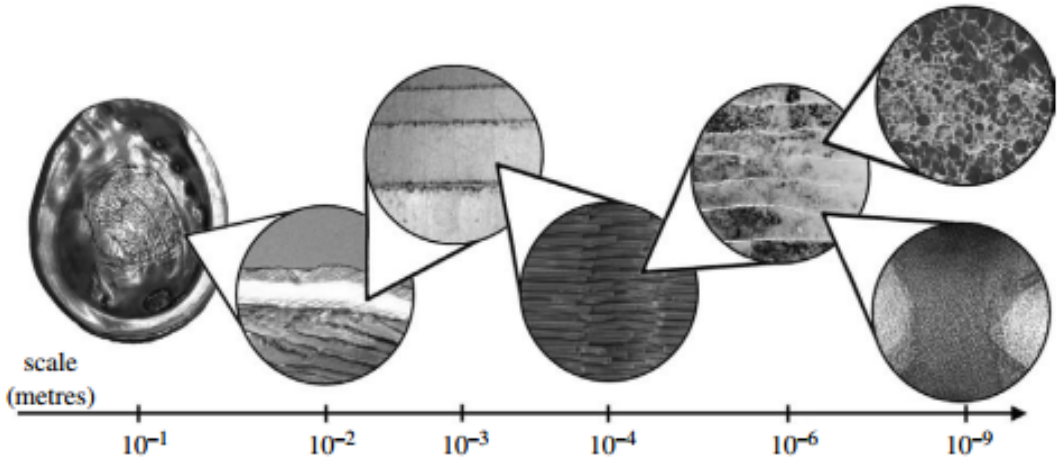

Figure 1.6. Depiction of the features present in nacre over several length scales, from the macroscale to the microscale, down to the nanoscale [2].

The role of the organic matrix is substantial in the determination of the properties of nacre. The stiffness of nacre is on the same order as that of its major constituent aragonite, however, the strength is two to three times greater than that of aragonite. The 5vol% organic polymer in nacre contributes to the increased fracture toughness of the composite. In fact, the major contributor to an increased fracture toughness displayed by nacre is the polysaccharide and protein layers [26]. The polysaccharide matrix provides the framework for the soluble proteins [26].

The organic matrix in nacre has been the focus of much attention because it is one of the main reasons nacre exhibits its high level of mechanical properties. The role of the organic

matrix goes much further than simply nucleating and organizing the calcium carbonate crystallites. This is apparent because some shell materials contain more organic matrix than is required to nucleate the crystallites. Through its intrinsic properties and its ability to control mechanically significant features like size, shape, and the distribution of the calcium carbonate crystallites, the organic matrix plays a major role in the determination of the mechanical properties of the composite system. [24].

Compared to most engineered composites, nacre has an exceptionally high ceramic content. Nacre is 95vol% calcium carbonate, while the remaining 5vol% is an organic matrix of polysaccharides and protein. Due to this high volume percent of ceramic, nacre should behave in a brittle manner, but in fact it does not. The synergistic combination of aragonite and the protein and polysaccharide organic matrix results in a material that has 3,000 times the toughness as aragonite alone. [24, 25, 27]. The structure is composed of polygonal platelets of aragonite. Each platelet interlocks with its neighboring platelets. This forms a sheet of platelets and there are numerous sheets stacked on top of each other. [24, 28]. Layers of calcium carbonate platelets alternate with layers of the nanometer organic polymer matrix [29]. Nacre has a "brick and mortar" structure with the aragonite acting as the bricks and the protein and polysaccharide matrix serving as the mortar [25]. The combination of plate like ceramics in combination with the organic polymer matrix yields a natural composite material with the ability to withstand a high degree of applied stress and show a tolerance to flaws that makes it a superior material. [24, 28].

High strength and tolerance for flaws are essential characteristics for structural materials to exhibit [28]. Ceramics are usually strong, but it is not practical to use them as structural materials because of their brittleness [30]. Polymers are extremely flaw-tolerant but do not have the ability to withstand a high level of stress. In fact, polymers significantly deform at low levels of applied stresses. [28]. Nature has engineered a near perfect material in nacre, found as the inner lustrous layer of some mollusk shells such as the red abalone. It meets the challenges of being both strong and flaw tolerant. Due to the highly ordered calcium carbonate bricks (95vol%), with a nearly continuous jacket of organic material (5vol%) surrounding them, nacre exhibits a toughness that is much higher than would be expected. [31]. Each ceramic platelet in the red abalone shell has a thickness of approximately 400nm and an edge length of approximately 5μm. These platelets are separated by a biopolymer layer that varies from about 5 to 20μm in thickness. [26]. Although there is an extremely low polymer content, the precise and ordered arrangement also helps contribute to the substantial mechanical properties.

1.4. Mechanical Response of Natural Materials

Not only do biological materials possess impressive mechanical properties due to their layered structure, but the design architecture guides the mechanical response to stress and strain. Natural composites like nacre and bone exhibit an anelastic response to cyclic loading which is also characteristic of other materials like rock. Anelasticity is a mechanical response that is characterized by both nonlinearity and hysteresis when a material is exposed to cyclic loading conditions. Nonlinearity and hysteresis occur as a result of the way the layered materials and their defects respond to cyclic loading conditions. Nonlinearity provides for an increased strain tolerance by allowing for the accommodation of a greater degree of deformation. Hysteresis is an energy dissipative mechanism caused by friction when layered interfaces experience sliding on each other.

1.4.1. Anelasticity in Rock

Under mechanical loading, the majority of rocks exhibit anelastic behavior, which are due to cracks, Figure [32, 33]. During uniaxial compression, the cracks present in rocks will close. At low stresses, the cracks remain open and as the stress increases, the cracks close resulting in stiffening of the rock. Mostly all of the cracks are closed at low stresses because the majority are flat. A certain stress level is reached, above which there is no additional change in stiffness because all cracks are already closed. This results in a linear portion of the stress-stain curve. Also apparent from Figure 1.7 [32], is the hysteretic loop. Hysteresis is a result of the friction between the crack surfaces during sliding. Even though cracks can be closed due to compressive stresses, the crack faces may slide against each other. The sliding is hindered by friction and thus the presence of hysteresis. The behavior of rocks under uniaxial compression is similar to that observed during hydrostatic pressure, except that hysteresis is not observed during hydrostatic compression because there is no frictional sliding.

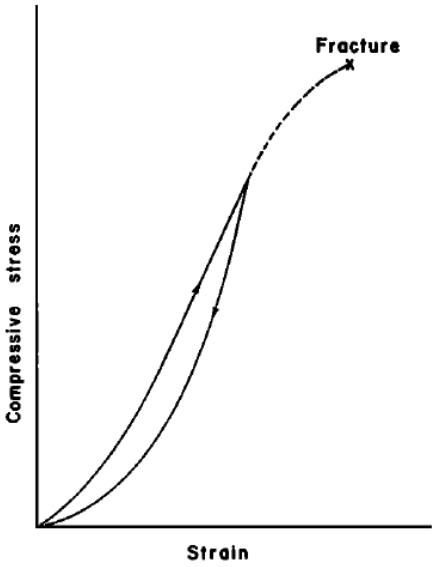

Figure 1.7. Stress-strain curve for rocks in compression [32].

1.4.2. Anelasticity in Bone

Figure 1.8 shows the stress-strain behavior typical of trabecular bone. This behavior is observed due to cracks, plasticity, and viscous creep. The presence of cracks introduce discontinuities which are responsible for degradation in material properties like strength and stiffness. What is particularly noteworthy of the mechanical behavior of bone, is the complexity of the resulting strain behavior. The strain behavior observed is a combination of the effects of elastic strain, inelastic strain (from damage accumulation), plastic strain, and anelastic strain [34]. Through multiple loading cycles, the strain behavior can be distinguished. Trabecular bone displays behavior similar to what is observed in composites [35], in that when loaded and unloaded, bone recovers about three-quarters of the total inelastic strain [34], and thus hysteresis is present. At low strain levels, and during the initial application of a reload, very small changes are observed in the stiffness or elastic modulus of bone. As the load increases and the strain rate becomes higher, nonlinearity is observed [36]. This is due to the propagation of cracks and the relieving of residual stresses. Through cyclic loading and unloading in bone, the strength and stiffness will show a reduction because of resulting bone fatigue [37-41].

There is an elastic (or linear) response to load for deformations that are below 1%, Figure 1.8. When the strain begins to increase at a greater rate than stress, the behavior becomes nonlinear. This is referred to as the yield point. After which, there is permanent deformation of bone that occurs. Nonlinearity is a result of the porous trabecular bone structure. As the pores are compressed, they collapse and trabeculae collide and compress reducing the bone-volume fraction because of the porosity reduction leading to stiffening. [42]. The layered and porous

architecture of bone governs its anelastic behavior and is also responsible for the impressive strength, toughness, and stiffness displayed by bone.

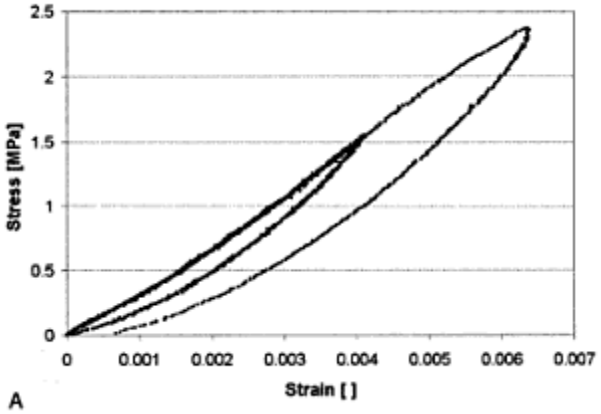

Figure 1.8. An experimental stress-strain curve displaying the stress-strain behavior during cyclic loading for trabecular bone [42].

1.5. Natural Composites as a Driving Force for Man-Made Materials

The attractive combination of properties achieved when nature combines mineral and biopolymer into a composite to form materials like bone and nacre is currently unsurpassed by manufactured materials. For this reason, especially in the past several years there has been an upswing in investigations that seek to mimic these mechanical responses in man-made materials. Applying natural design principles to human engineered materials is referred to as biomimetics. Nacre is one of the most widely studied materials that pose as a model for a biomimetic material. Nature has had millions of years to evolve and perfect material combinations and designs. Researchers and scientists are becoming increasingly aware that there is a tremendous amount that can be gained from examining natural materials and their design principles.

Although there has been some work in engineering composites similar to nacre, the work thus far has been with templates that are difficult and time consuming to produce. Composite materials are those formed from the combination of two or more different materials. These materials have properties that complement each other and when united lead to the arrangement of attractive properties that would not be achievable in the monolithic material [43]. For this reason, composites are engineered and found in naturally occurring materials. One of the most amazing

natural creations is nacre formed from brittle calcium carbonate platelets and layers of an organic material of proteins and polysaccharides. Although synthetic materials formed from interlocking ceramic tablets and a few weight percent polymer in the form of adhesive may show an improvement in being able to resist fracture, the improvements cannot compare to the fracture toughness of nacre [44]. Attempts at engineering a composite with the degree of strength, toughness, and stiffness that nature has evolved in nacre have not been successful to date. Setbacks are also encountered when it comes to scaling up as well as producing composites with the degree of order and sophistication in their hierarchy that naturally occurring materials exhibit. These are some of the reasons that using thermally sprayed templates for nacre-like composites is so desirable. Producing a coating via TS is a quick process that easily offers large scalability and with the appropriate secondary phase introduced these hybrid materials may be engineered to exhibit both a high strength and flaw tolerance.

One attempt at mimicking nacre involves creating a hybrid composite utilizing alumina (Al_2O_3) and the polymer poly methylmethacrylate (PMMA) formed through freeze casting. Ceramic based suspensions in water were frozen, forming porous scaffolds with ice crystal template architectures. The templates were then infiltrated with PMMA. Along with structures like the one just described. Additional ones were prepared in which the infiltrated scaffolds were compressed perpendicularly to the lamellae, thus forming a 'brick and mortar' structure. In order to promote densification of the structure, as well as to form ceramic bridges between the bricks, a sintering step was carried out. [45, 46]. Compared to a process like thermal spray that could be used to manufacture templates that can be used for a biomimetic structure, this one is rather complex and extensive.

The flexural strength and fracture toughness of the engineered composites were measured. It was found that the flexural strength of the ice-templated structures were on the same order as that of bulk alumina in the direction perpendicular to the lamellae. The flexural strength values were approximately 120 to 210 MPa. When the fracture toughness was examined, the values were almost double what could be expected from the simple "rule of mixtures" between Al_2O_3 and PMMA. [45, 46].

Thus far, attempts at mimicking nacre a natural hybrid material have centered around forming nacre like materials through synthetic mineralization [47], self-assembly of nacre-like thin films [48, 49], clay nanocomposites [50] and freeze casting [45, 46, 51]. These methods face challenges when it comes to scalability. The processes to form the bio-inspired nacre-like assemblies are time consuming and not tailored to making large quantities of samples.

The following chapter will focus on the application of thermally sprayed materials, a man-made arrangement, as templates for nacre-like biomimetic coatings. Before a biomimetic nacre-like material can be designed around a thermally sprayed scaffold, it is important to understand

what exactly is required in order to successfully engineer a biomimetic material. Barthelat *et al.* has outlined this process in three key steps:

- A natural model to mimic needs to be identified. In nature, there are a large number of materials that could pose as the model for a biomimetic design. The function of the manmade design needs to be selected and the natural model identified. Often, manmade biomimetics that are the most successful have functions similar to the natural material they are modeled after. [52]

- It is essential to next select the key mechanisms, structures, and design principles that make the natural material noteworthy and apply a number of them to the engineered material. [52]

- Finally, the manmade biomimetic material needs to be designed and fabricated. Often this last step is complicated due to the complexity of natural materials and the fact that natural materials are arranged in a hierarchical structure over several length scales. [52]

The unique anelastic response of the coatings resulting from their layered structure and inherent defects due to the nature of the deposition process will be discussed. An advantage associated with the use of thermal spray is it is an industrial process that can quickly generate a large volume of sprayed material that is of a rather uniform nature. To date, no process has the ease of manufacturing as that of composite materials utilizing thermally sprayed scaffolds. Ease of specimen generation is important, especially in the testing phase. Through the infiltration of these porous templates, it is likely that certain property enhancements will be made. In addition, the similarity of thermally sprayed materials and nacre in terms of their microstructures and behavior under mechanical loading and unloading cycles will be addressed.

2. Unique Attributes of Thermally Sprayed Coatings and Nacreous Assemblies

As discussed in Chapter 1, nonlinearity and hysteresis, or anelasticity is displayed by natural materials such as nacre as a result of their microstructural attributes. Not only is anelasticity displayed in natural materials but also in thermally sprayed coatings as a response to either mechanical or thermal cycling. In this chapter, similarities between nacre and thermal spray formed deposits will be addressed. This includes their microstructure and fracture behavior. Based on the commonalities in mechanical behavior and microstructure of nacreous assemblies and thermally sprayed materials, attempts to fabricate a biomimetic nacre-like material using thermally sprayed scaffolds will be investigated in this dissertation.

2.1. Thermal Spray Deposition Processes

The presence of thermally sprayed coatings is apparent in a number of industries. TS coatings have industrial applications in aerospace, biomedical, electronic and transportation fields. The purpose of a coating is to provide a cost effective means of protection to a base material or substrate that would otherwise not be achievable. Thus their presence, is significant because it allows for a material to be used in a situation where it otherwise would not have been possible.

Thermal spray is a versatile technology used for coating deposition that is becoming more widespread due to advances in materials and processing. The thermal spray processes generate layered materials that are formed through the successive impact of molten droplets on a substrate. In this process, molten or semi-molten particles are accelerated at high velocities and continuously directed toward a substrate. Once impingement on a substrate, the particles rapidly solidify forming thin splats which undergo high quenching stresses. Depending on the material, ceramics or metals, these splats yield to cracking or high dislocation density respectively. Further, a coating is formed through continuous impingement and interbonding of the splats. The properties of a thermally sprayed coating depend significantly on the process parameters. [53].

Background

Thermal spray is a generic term used to describe a class of coating deposition processes to form metallic and nonmetallic coatings. Thermal spray processes include:

- Flame spray (ceramic rod or powder)
- Plasma spraying
- High velocity oxy-fuel (HVOF) spray
- Wire arc spray
- Cold spray
- Warm spray
- Detonation spray

Thermal spray can be further divided into three categories (flame spray, electric arc spray, and plasma arc spray). These categories are organized according to the energy source (chemical or electrical) used to heat the feedstock material, in wire, rod, or powder form. The particles in a molten or semimolten state are directed toward a prepared substrate using atomization jets or process gases to accelerate them toward the surface. When the particles impact the prepared substrate, they form a bond with the surface, and spread out forming a splat. Upon reaching the substrate, the splats undergo rapid cooling which can be in excess of 10^6 K/s. Subsequent particles keep impinging on the surface, causing a thickness buildup and the formation of a lamellar microstructure. [53, 54].

A typical thermal spray system will include:

Spray torch	Melts and accelerates the particles toward a surface
Robot	Controls the spray torch
Power supply	Required for the spray torch
Feeder	To supply feedstock to the spray torch in powder, wire, or rod form
Media supply	Required gases or liquids to generate the plasma plume or flame to carry the feedstock

Console for the controller	Either integrated or stand alone for the equipment

2.2. Characteristics of a Thermally Sprayed Deposit

During the spray process, particles travel through process jets or spray plumes before reaching a substrate, thus experiencing huge temperature and velocity gradients. Powders are the most commonly used feedstock in thermal spray. Within a particular powder, it is normal for there to be a distribution of particle sizes. The size of each particle results in a different path through the plume depending on the inertia of each particle. This means that the preferred path of some particles may result in a particle having a short dwell time and thus remaining completely unmelted or only semi melted. The particle dwell period is controlled by a number of factors like distribution of powder size, flame characteristics, spray distance, and the carrier gas flow rate. Depending on the particle size and particle dwell period, particles can vaporize before reaching a substrate, be unmolten when reaching the substrate, or somewhere in between. Through continual particle deposition, a lamellar coating can build up rather quickly. Due to the wide range of process parameters and feedstock, coating morphology can vary significantly, especially between TS processes. There are several interactions that come into play prior to and during the deposition of thermally sprayed coatings, which contribute to the microstructural evolution.

Thermal spray processes result in the generation of coatings that tend to be uniform in their nature but contain a number of defects. A deposited coating may be composed of particles in various forms. For instance, particles may be fully unmelted, partially melted, or completely melted. During coating deposition, defects such as porosity or voids can result when unmelts or semi molten particles and gases are entrapped in a coating. There may also be variability in particle size when a wire or rod is used as feedstock because there may be non uniformity in the heating of the wire or rod.

Post deposition, particles undergo rapid solidification and spreading to form a splat on the substrate, Figure 2.1. It is important the substrate be of appropriate roughness and temperature to ensure bonding (mechanical locking) between the substrate and particle. As a particle is undergoing rapid solidification on the substrate, a number of things are happening that affect the microstructure of the coating. For instance, there can be splat spreading, splashing, splat locking with the substrate, grain growth, splat shrinking, or intrasplat cracking. Upon a ceramic particle impinging on a substrate, rapid quenching of the splat leads to the evolution of vertical cracks, or mud cracks which lead to an uneven or rough splat top surface. As more splats are deposited and there is successive buildup of the splats to form layers and particles are interacting with each other. Interactions among particles are dependent on particle flux which refers to the number of

particles impinging on the substrate per unit time, as well as whether or not the particles are molten.

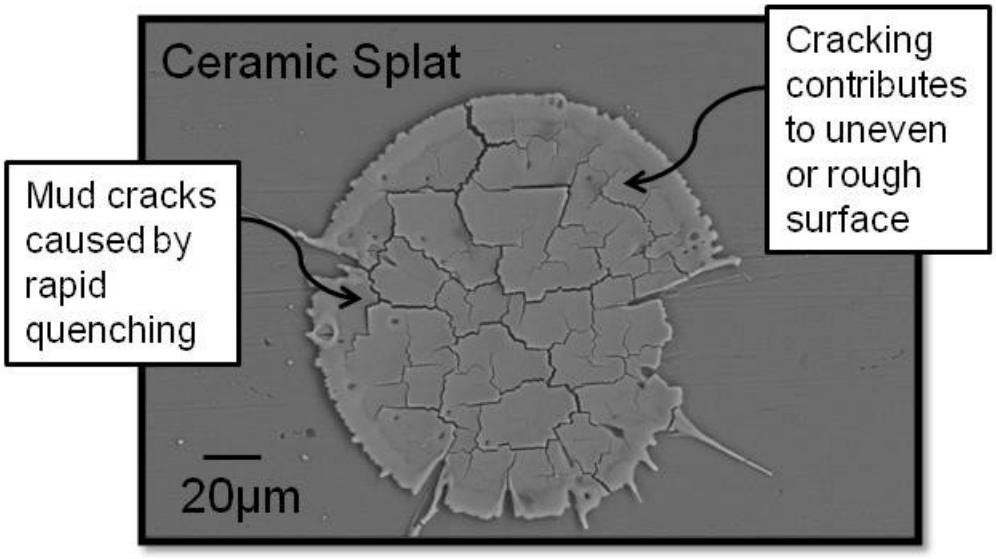

Figure 2.1. SEM micrograph of a ceramic splat. During thermal spray processes molten or semi-molten particles are accelerated at high velocities and directed toward a substrate. Once impingement on a substrate, a particle rapidly solidifies forming a splat.

Characteristic of coatings is some degree of porosity. Entrapped air within a coating can also lead to oxidation depending on the sprayed material. Depending on the spray process, plasma, twin wire arc, combustion spray, or high velocity oxy-fuel, there is variable oxide content in a coating. Oxide content may not always be detrimental. For example, it can provide lubrication, increase coating hardness and wear resistance.

2.3. Defect Formation During the Thermal Spray Process

It is well known that thermally sprayed coatings have a number of defects. During coating deposition, there are often unmolten or semi-molten particles which result in the presence of porosity and voids. Interlamellar cracks and pores can originate from gas becoming entrapped during coating deposition. Rapid solidification of particles and splat spreading can result in intersplat boundaries, which is especially common in ceramic materials. All of these defects can lead to interconnected porosity and defects.

Depending on the feedstock material being sprayed, i.e. ceramics or metals, the deposited coating will vary tremendously in its microstructure and defect distribution. Metallic coatings, Figure 2.2, undergo a lesser degree of cracking as the molten splats plastically deform prior to cracking, which leads to a more ordered structure. The layered nature of the coating is also clearly defined. Metallic coatings are more prone to oxidation when sprayed in air due to interactions between the metallic particles and oxygen during the spray process. Ceramic coatings, Figure 2.2 , tend to have a more chaotic structure. Identifying specific layers of ceramic coatings is more difficult than for metallic coatings. The rapid solidification of ceramic particles upon impingement on a substrate leads to a high population of cracks which are more prevalent in ceramic coatings. Ceramic splats cannot undergo the same level of plastic deformation as metallic splats. The above mentioned characteristics of a ceramic or metallic coating are variable depending on spray conditions. Altering spray parameters can affect the structure of a coating, although the microstructures of metallic and ceramic coatings usually tend to be identifiable based on the specified characteristics.

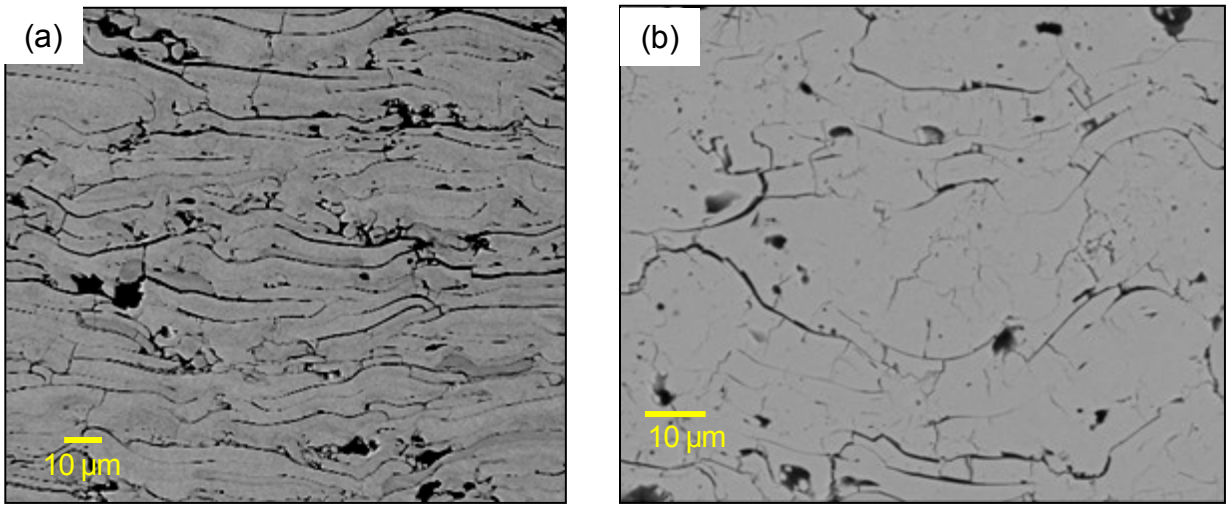

Figure 2.2. a) A typical metallic microstructure and b) a typical ceramic microstructure. Notice the differences in terms of defects and the layered build up between metallic and ceramic thermally sprayed coatings.

Focusing on thermally sprayed ceramic coatings such as zirconia or alumina, which are commonly used to provide high temperature protection or wear resistance respectively, to an underlying substrate; the evolution of the microstructure is more complex. The defect density for ceramic coatings is higher and there is a wide distribution of various types of defects. Figure 2.3 presents a typical fracture surface for a sprayed ceramic coating [55]. The defects include, porosity and voids, intrasplat cracks, intersplat boundaries, and interlamellar pores. Most of these defects arise during the spray process. Defects can be created from unmolten or partially molten

particles, inadequate flow or the molten particles becoming fragmented upon impact on the substrate, shadowing effects during spraying caused by an improper spray angle, or entrapped gas. Vertical and horizontal cracks originate due to a high cooling rate of specific splats or weak interlamellar bonding.

Although a number of defects are introduced during the spray process, a significant number of microcracks are generated during the cooling process. During the initial cool down period, a number of cracks can form due to the generation of thermal stresses caused by the thermal expansion mismatch of the coating with the underlying substrate. Deposition processes and the processing conditions play a major role in defect architecture which is strongly correlated to the mechanical properties of a coating. Basically, process parameters control the nature of the deposit formation dynamics which aid in defining the microstructure and thus highly influence coating properties. [56].

It is believed that various defects contribute differently to a particular coatings properties because of the nature of the defects as well as the mobility of splats. For this reason, porosity alone is not enough to understand the property and performance relationship of a thermally sprayed coating. A more in depth understanding of the types of defects present is necessary, especially whether these defects can be exploited to provide further benefits to a thermally sprayed material.

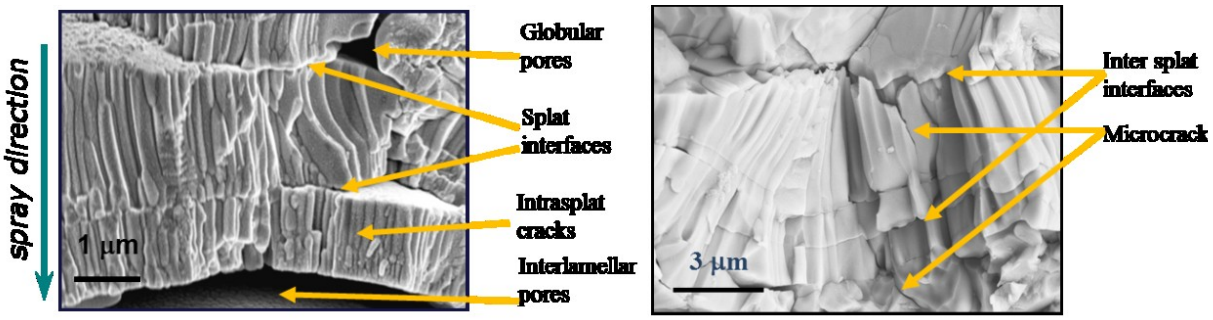

Figure 2.3. A number of present defects in a thermally sprayed coating are indicated. These defects contribute to a thermally sprayed coating's properties [55].

2.4. The Layered Nature of Thermal Spray Formed Deposits and Natural Nacre

Another similarity between thermally sprayed coatings and natural materials like nacre is their microstructure. Impingement of splats on a substrate lead to the formation of a thermally sprayed coating which is described as having a 'brick-wall' structure while nacreous assemblies display a 'brick and mortar' structure, Figure 2.4. The semi-continuous thermal spray process in which particles are directed toward a substrate, flatten and rapidly solidify results in a brick-wall formation of deposited splats. In between splats, there are different types of porosity or voids filled with air. This structure is rather similar to some naturally layered materials like nacre that contain biopolymer interlayers instead of the air filled interfaces and gaps present in sprayed deposits. As in nacreous assemblies, the layered nature of coatings contributes to the unique mechanical response that is observed when thermally sprayed materials are exposed to cyclic loading. This response will be discussed in the next section.

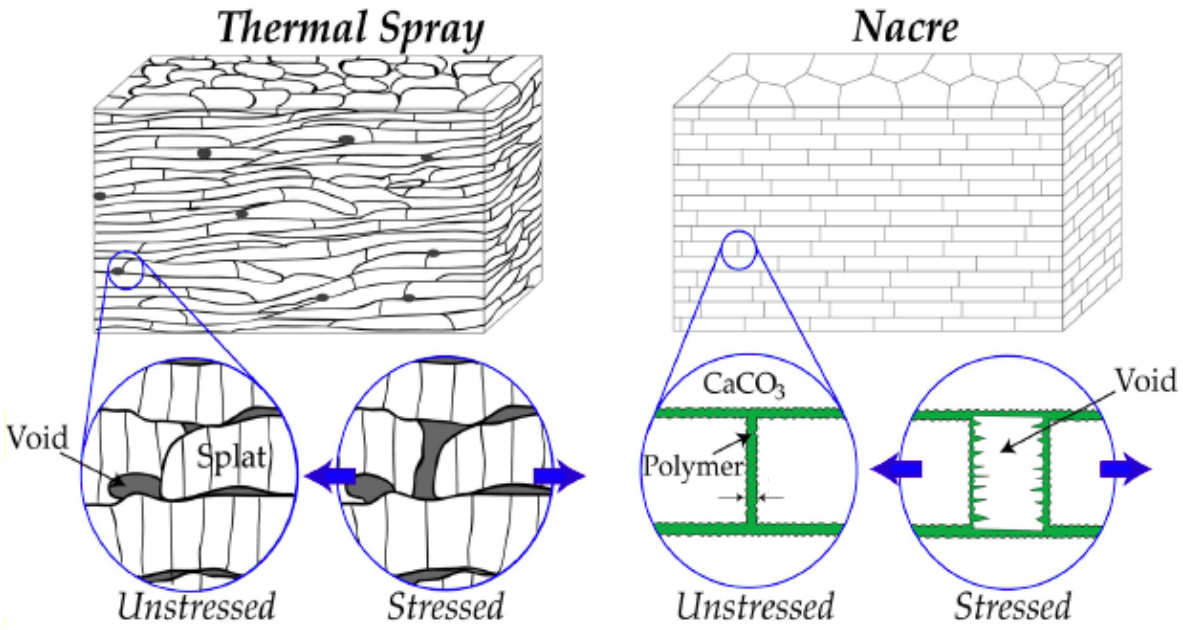

Figure 2.4. Schematic showing the microstructure of a thermally sprayed material and a nacreous material. Both exhibit a layered microstructure.

2.5. The Presence of Anelasticity in Thermally Sprayed Materials

Ceramic coatings deposited via thermal spray display some unique properties, namely nonlinear behavior in terms of their stress-strain relationship and a hysteretic response during thermal and/or mechanical loading and unloading cycles. Together nonlinear and hysteretic behavior is referred to as anelasticity [57]. Recently, it has even been shown that certain metallic coatings such as molybdenum or nickel display anelastic behavior under thermo-mechanical cycling. Interestingly, naturally layered materials like nacre also exhibit anelasticity.

Anelastic behavior in coatings has been attributed to the distinctive microstructural features that are inherent in sprayed deposits. Figure 2.5 shows such a response of a yttria stabilized zirconia coating measured using the bi-layer curvature method. This method includes the heating and cooling of a coated beam in a controlled environment. The thermal mismatch between the coating and underlying substrate introduce interfacial strain which causes the system to undergo a change in curvature. Bi-layer temperature-curvature measurements have shown that ceramic coated beams and even metallic coated beams experience an anelastic response during thermal cycling.

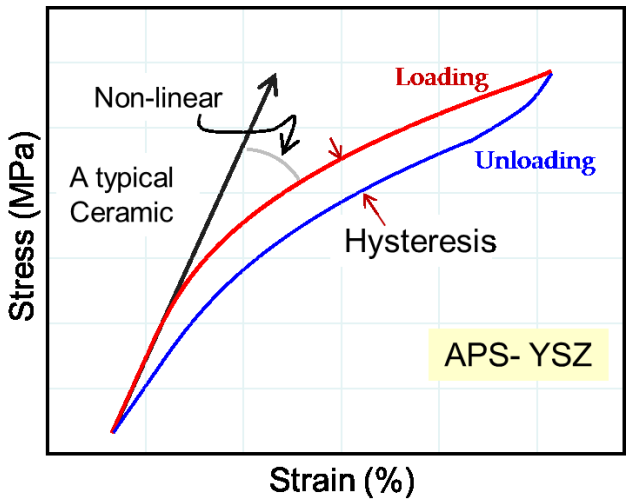

Figure 2.5. The stress/strain relationship for a plasma sprayed YSZ coating deposited on an aluminum 6061 substrate that has been derived from the temperature-curvature response measured during thermal cycling.

Under thermo-mechanical loading, anelasticity arises from splats and porosity responding in a way that results in the unique nonlinear and hysteretic response. During cycling, the coating

will undergo both tension and compression. In tension, cracks, porosity and other voids are opening while in compression these defects are closing leading to nonlinearity. Nonlinearity contributes to enhanced material performance because it serves as a way of redistributing stresses allowing for greater levels of deformation, resulting in a ductility-like response in solids that otherwise tend to be brittle. Hysteresis results from the frictional sliding of loosely or unbonded splats or crack surfaces. Both nonlinearity and hysteresis operate together during loading and unloading cycles.

Anelastic behavior is generally observed because of two main factors, phase transformations and geometrical attributes [58]. Based on the fact that this work examined partially stabilized zirconia and alumina at temperature ranges below those at which any phase transformation occurs, phase transformations were concluded to not contribute to the anelastic behavior. This means the observed anelasticity is due to geometrical attributes of thermally sprayed coatings.

A thermal spray deposit is produced when thousands of micrometer sized droplets are directed at a high velocity toward a prepared substrate. Before impingement on the substrate, the feedstock material is melted in either a plasma or combustion flame. Upon impacting on the substrate, molten or semi-molten particles flatten and then rapidly solidify resulting in the formation of disk-shaped splats. The diameter of a splat is typically 50 to 200μm and the thickness is approximately 0.5 to 5μm. Coatings are formed from splats in a chaotic assembly which results in coatings with interlamellar porosity due to gaps from poor contact between splats and globular pores or voids which are a result of incomplete filling of impinging splats [59]. Other present defects in a coating are referred to as mud cracks and these arise when ceramic splats undergo rapid quenching on a substrate [60, 61].

Splat interfaces and intrasplat cracks are likely contributors to the anelasticity observed in thermally sprayed ceramics. While splat interfaces and intrasplat cracks affect anelasticity, other defects like larger pores and cracks probably do not have as great an impact on anelasticity. However, they most likely influence other properties such as the modulus. Mechanistically, in thermally sprayed ceramic coatings, hysteresis is caused by frictional sliding of crack faces [32, 62-64] and the opening and closing of microcracks and smaller pores and voids [32, 65-67]. Hysteresis, which is the difference in paths between the loading and unloading of some stresses, is significant because it is a means of energy dissipation.

Prior to the work being carried out that will be discussed in this dissertation, Liu and Dwivedi extensively studied the anelastic behavior of thermally sprayed coatings and factors affecting this unique behavior. Liu explored anelasticity through modeling. By using both single and multiple crack and interface systems a Coulomb friction model was examined to mimic the sliding that occurs in a ceramic coating across splat interfaces during crack closure. The nonlinear and anelastic response was accurately captured using the model and Liu provided two key findings. The first being that friction is necessary for hysteresis to occur and when the

coefficient of friction, μ, is 0.5 the hysteresis produced is at a maximum. When μ is much larger than 0.5, sliding of splat interfaces is prevented and no hysteresis is observed. The second finding dealt with the effects of initial crack opening. The dimensionality of the gap between splat interfaces governs the hysteretic response, with smaller splat interface gaps tending toward larger hysteresis effects. This work provided evidence that anelastic behavior can be controlled by altering the friction coefficient and initial crack opening. Therefore, through varying process parameters, the anelastic response of a thermally sprayed coating can be influenced.

It is significant that thermally sprayed coatings show an anelastic response to cyclic thermal and mechanical loading because natural materials exhibit the same kind of response. The fact that both nacreous assemblies and thermally sprayed coatings exhibit anelasticity, Figure 2.6, help to make thermally sprayed templates an ideal candidate for templates for biomimetic nacre-like materials.

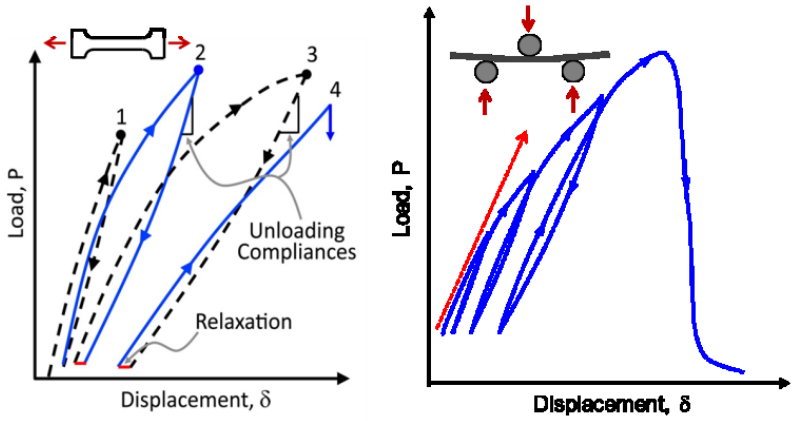

Figure 2.6. The left shows modeled behavior for nacre as presented by Currey *et al.* **[23]**. On the right, behavior for a plasma sprayed YSZ coating is presented. Both show anelastic mechanical behavior; that is they both are nonlinear and hysteretic.

Nacre is a material that exhibits exemplary properties such as strength and toughness. The past few decades have shown a growing interest in developing manmade materials that can mimic or come close to the properties of nacre. For this reason, the microstructure and mechanisms behind the properties have been studied extensively. Nacre is perhaps such an exemplary material because it is nearly completely composed of a brittle material but yet so tough, due to the addition of a few volume percent biopolymer. Just as in bone, nacreous assemblies have hierarchical structures that are highly organized over several length scales, all the way down to the nanoscale. [14].

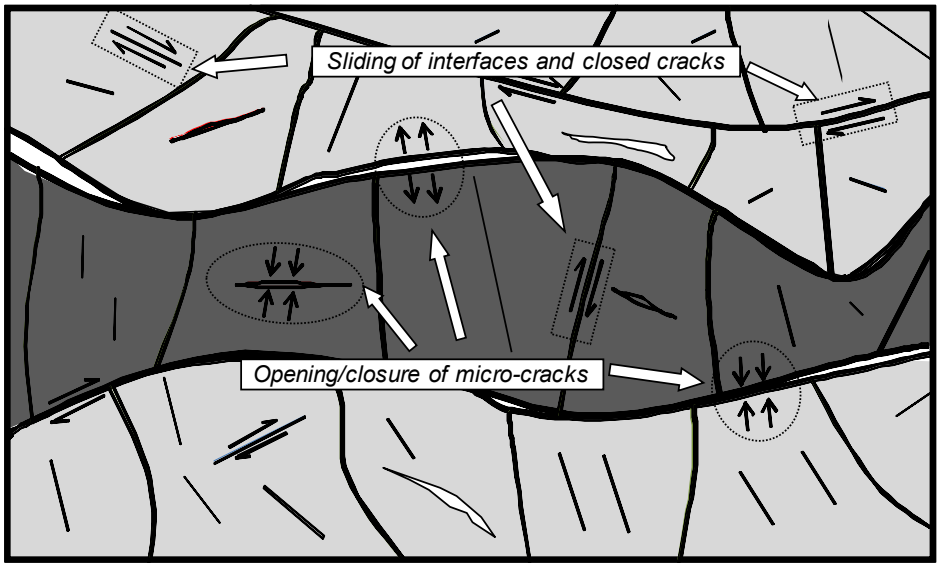

Figure 2.7. Schematic of the mechanisms that contribute to anelasticity in thermally sprayed coatings. The two mechanisms are the opening and closing of defects combined with the sliding of interfacial surfaces [68].

2.6. Deformation Behavior of TS Coatings and Nacreous Assemblies

2.6.1. Deformation Behavior of Nacre

Both nacre and thermal spray deposits contain a myriad array of defects and flaws. For instance, porosity and defective growth sites in the case of nacre, while TS contain porosity and voids, intrasplat cracks, intersplat gaps, and interlamellar pores. In both nacreous assemblies and thermally sprayed materials, these imperfections serve as potential sites of origin for cracks which can lead to catastrophic failure under applied tensile loads [69]. Just as in TS deposits, flaws in nacre cannot be eliminated, so it is essential that the material be robust enough even with defects incorporated in their design to resist crack propagation and growth originating from defective sites. [14].

Despite the fact that nacreous assemblies are comprised of 95vol% hard mineral, they have ductile-like behavior and pretty large strains to failure due to several microscopic mechanisms that have been outlined by Barthelat *et al.* Interfaces begin to yield in shear at tensile stresses of 60MPa. This causes tablet sliding which results in localized deformation of the structure. Eventually, deformation can spread so that a large volume of the nacre is affected causing

significant straining at the macroscale. After all of the sliding sites have been affected, failure will occur by pullout of the aragonite tablets, after local sliding distances of 100-200nm. This behavior is due to the way nacre has evolved, and is as follows:

- The interface is weaker than the aragonite tablets. It is also important to note that due to the small size of the aragonite tablets they are afforded a higher tensile strength than that of bulk aragonite. This is because materials become more tolerant of flaws at the nanoscale [70, 71]. If the organic interface was not weaker than the tablets, the tablets would not experience sliding and instead fail under the tensile stress [14]. This would be more characteristic of brittle fracture and not the ductile like behavior that actually exists in nacre.

- The aspect ratio of the aragonite tablets is optimized. There are a couple of restrictions that are faced by the aragonite tablets. If the tablets, are too thin then nacre faces the risk of premature fracture and thus failure, showing brittle behavior. Yet it is important that the aspect ratio be high enough so that the surfaces of the sliding tablets and the cohesion of the organic layer and tablet surface is maximized [72].

- A hardening mechanism occurs at the local scale. This is necessary to ensure that sliding is spread throughout the entirety of the nacreous assembly. Once the aragonite tablets begin to slide, in order for them to slide further, higher stresses are required. This is why it is beneficial for new sliding sites to be initiated and the area experiencing deformation to spread over a large volume. During this process, the tablets will for the most part remain elastic. This means that the hardening mechanism must occur at the tablet and organic phase interface. Barthelat *et al.* examined how the interface behaved by performing a shear test along the layers and observed that in order to slide along one another, the tablets need to climb some obstacles. This led to the conclusion by Barthelat *et al.* that strain hardening is required for deformation over large volumes and critical for the mechanical performance of nacre in both tension and shear. [14, 73].

Based on the above conclusions by Barthelat *et al.*, it was concluded the behavior of nacre is driven by specific mechanisms that occur at the interfaces between the aragonite tablets and a number of these nanoscale mechanisms are provided below.

- The adhesion between the organic biopolymer layer and the tablets is quite strong and under applied tensile loads some of the molecules in the organic layer can unfold. This enables the organic material to stretch while still adhering to the tablets. It isn't until the elongation of the organic material reaches about 100nm that all of the modules contained in the molecule will unfold, and up until this point little hardening

is expected under tensile stresses because this is on the same order as the sliding distance of the tablets in nacreous assemblies. However under shear stress, shear strains at the interface are higher and therefore hardening occurs at the macroscale which is believed to be due to the polymer. [14, 44, 71, 74].

- Another mechanism that is believed to cause strength and hardening in nacre is when nanoasperities on surfaces of adjacent tablets make contact as nacre experiences shear stress, Figure 2.8. Nanoasperities on opposing surfaces of platelets lead to resistance in sliding which cause strain hardening. In order for platelets to slide, they must climb over each other which require a certain stress. [14].

- Mineral aragonite bridges provide some reinforcement for interfaces and serve as a means of locking tablets in place, Figure 2.8. It hasn't been verified, but Barthelat *et al.* believe if sliding occurs and bridges become fractured, further sliding could cause them to make contact again and serve as a means of almost relocking aragonite tablets. [14].

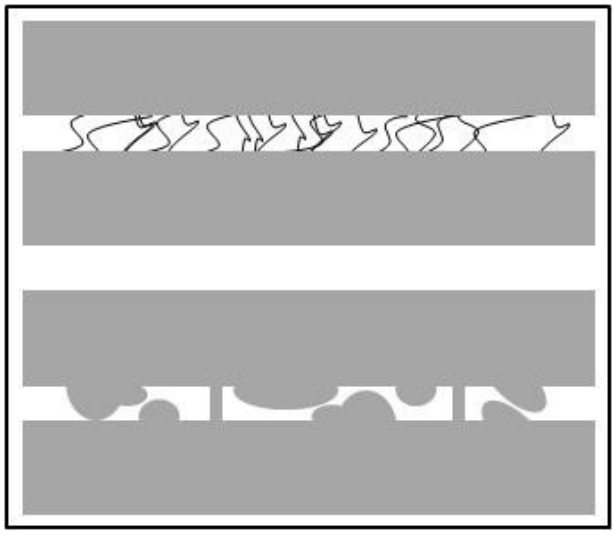

Figure 2.8. The top is a schematic of the organic layer in a nacreous assembly and the bottom is a schematic of the mineral bridges and nanoscale asperities on the surfaces of opposing tablets.

- The last proposed nanoscale mechanism is due to the waviness of individual aragonite tablets which is thought to be the reason hardening occurs. This is because as each layer slides over one another, they need to slide past each tablets waviness, Figure 2.9. By climbing over these obstacles, tablets become locked and resistance to sliding is increased. [14]

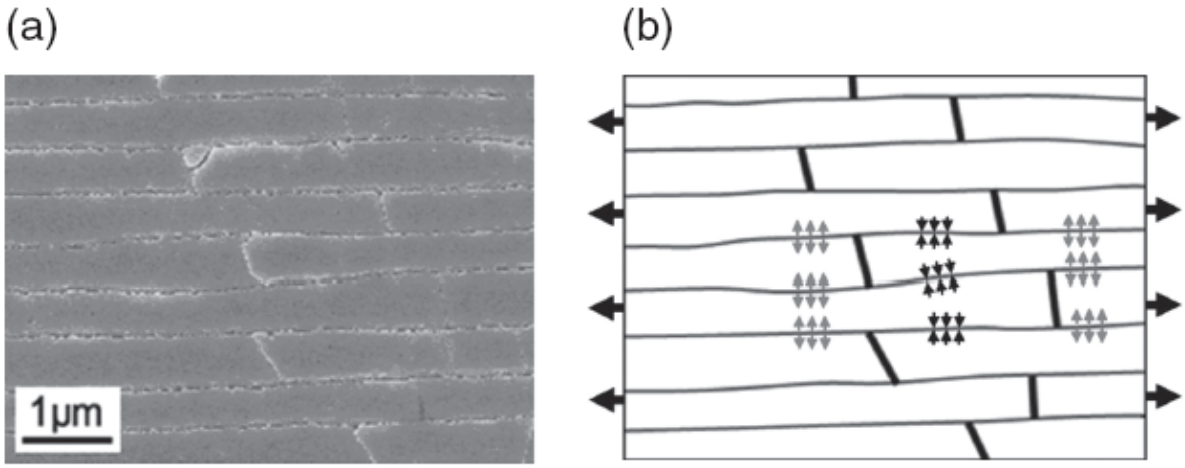

Figure 2.9. a) An SEM micrograph of nacre tablets and b) schematic of the waviness present in the tablet structure [75]. Illustrated in the schematic are the stresses nacre is subjected to as it experiences shear stress. It is also worth noting that nacre also experiences some compressive stresses in shear.

2.6.2. Similarities in Deformation Behavior of Thermally Sprayed Ceramics and Nacreous Assemblies

Deformation mechanisms of spray formed ceramics and nacreous assemblies are also somewhat similar. For instance, thermally sprayed coatings and nacre can both sustain some integrity even while sacrificing some layers. Unlike bulk ceramics, thermally sprayed ceramics are non-linear solids and exhibit some degree of ductility, as they have the ability to withstand levels of strain that bulk ceramics cannot. The nonlinearity of the coatings has already been discussed earlier, however the ductility part of the mechanical behavior can readily be seen under bending conditions. Figure 2.10 illustrates the schematics of the deformation mechanisms for sprayed ceramics and nacre. Due to the nature of loading, both systems will experience compression on the top surface where the load is being applied. Free standing thermally sprayed coatings will fracture from the bottom surface due to tensile stresses when experiencing applied loads at their top surface. In actuality, the fracture mechanisms will be different with nacreous materials, which are covered by an outer hard and brittle calcite layer. Nacreous layers under three-point loading still attached to the hard calcite layer will fracture from the top surface. The outer calcite layer acts as a bulk ceramic with low strain tolerance. Most of the load is resisted by the calcite layer within its elastic region, however the nacreous structure becomes important

when the calcite layer gives way. At this time the nacreous layer under the hard calcite layer dissipates a large amount of applied energy by performing nonlinearly. It has been reported if the hard calcite layer is removed from the nacreous layer, and load is applied at the top surface, nacre will deform at the surface in tension [76], in a similar way to thermally sprayed ceramics.

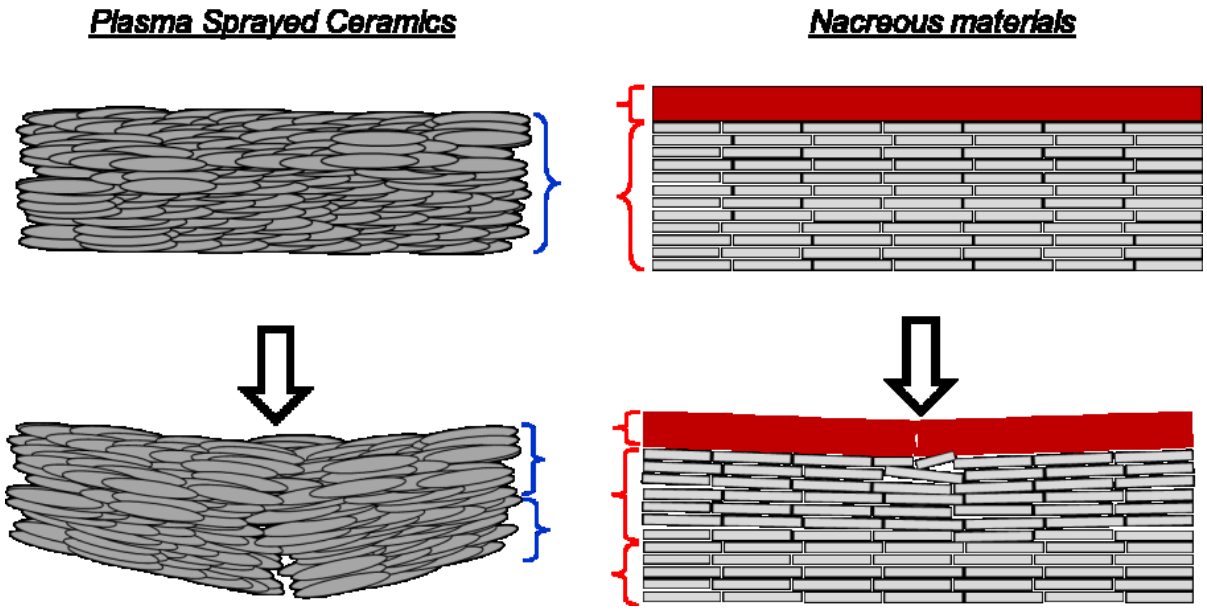

Figure 2.10. Observed deformation mechanisms of thermally sprayed coatings and nacreous assemblies in cases where load is applied to the top surface. It is important to note that there is a harder calcite layer on the top surface of the nacreous assembly in the schematic which is the reason it fractures from the top surface.

This dissertation examines the potential of thermally sprayed coatings to serve as templates for a biomimetic nacre-like composite. Through infiltration of a polymer into the porosity and voids of a coating, the microstructure of a thermally sprayed coating can be made to be more like that of a natural composite material. The enhancement of properties of polymer infiltrated thermally sprayed composites will be examined. Developing a composite containing a hard brittle ceramic and softer polymer has been studied for quite some time, yet there has not been any engineered composite able to compete with nacre in terms of its mechanical properties like both fracture toughness and strength.

2.7. Thermally Sprayed Materials as Scaffolds for Nacre-like Materials

Thermally sprayed coatings and nacre have been shown to have a number of similarities in terms of both their microstructures and anelastic response to loading. Through post deposition infiltration to alter the surfaces of splat interfaces these similarities can be increased. One such aspect that makes TS coatings promising templates for nacre-like assemblies is their inherent defects, which have been discussed earlier in more detail. In addition, the properties of thermally sprayed materials can be tailored through changes in the spray process. The three point bend data presented in Figure 2.11, is for high and low porosity coatings. By simply altering the number of defects, the mechanical behavior of a coating will change. A more porous microstructure leads to more defects and interface surfaces, contributing to a higher degree of anelasticity. It is important to note that if defects are too large and splats are too loosely bonded there will be no friction due to splat sliding and therefore no anelasticity. This is an important finding in synthesizing a composite that behaves like nacre.

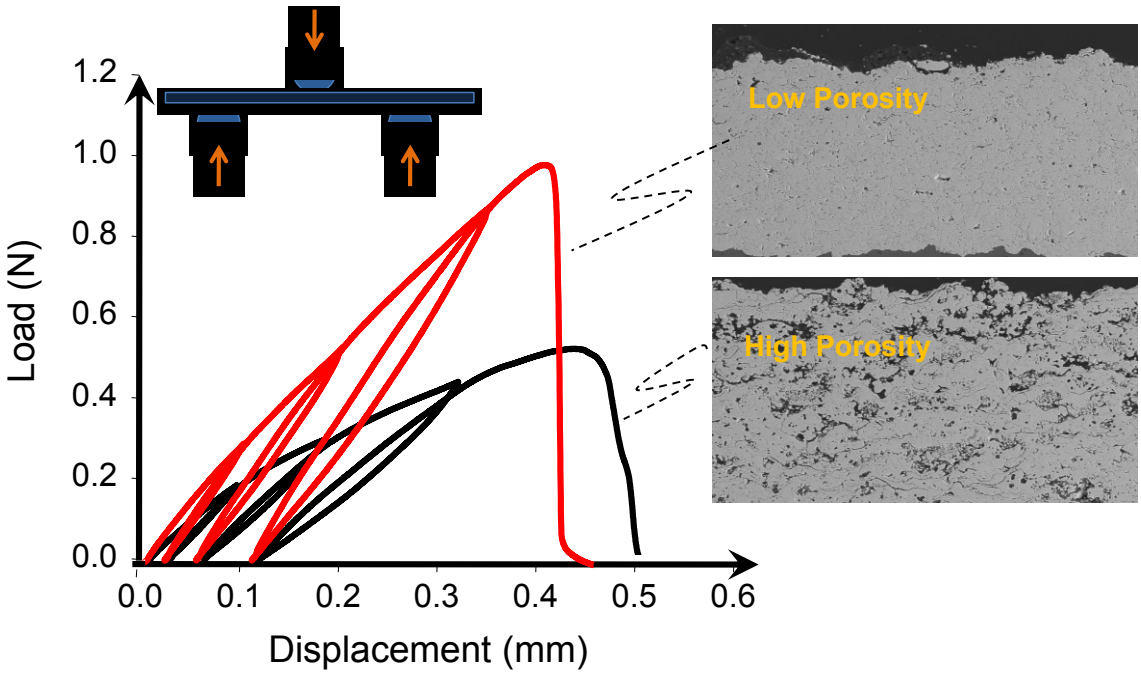

Figure 2.11. By tailoring the porosity of a thermally sprayed structure, the mechanical behavior of a thermally sprayed coating can be affected due to the changes in defects present. Both low and high porosity TS coatings show anelastic behavior. That is they are nonlinear and hysteretic.

Of particular interest regarding these structures are the interfaces that exist between splats which are on the order of nanometers. During solidification interlamellar grain growth of splats

locks splats together, similar to nacre tablets being joined together. Some of the calcium carbonate platelets are anchored together by the growth of mineral bridges from one tablet to another, Figure 2.12.

Figure 2.12. In the image on the left, the organic biopolymer layer is shown which serves as an adhesive that binds the two layers together. The schematic in the center shows how the mineral bridges, asperities and biopolymer work to keep the platelets anchored together. The right most figure is a thermally sprayed YSZ coating that has been infiltrated post deposition. As in the image of nacre, there is clear bonding and anchoring of the two splats with the polymer phase that has been introduced post deposition.

Spray parameters can be adjusted so particles reaching the substrate will be fully molten allowing for continued grain growth of one layer of splats into another. Like in nacre, where mineral bridges provide some stiffness to the structure, continued grain growth in TS coatings may serve the same function as mineral bridges. It is also well known that nacre has asperities on the top surfaces of the $CaCO_3$ bricks. Exposure to stresses can lead to some sliding or shifting of the bricks. However, the asperities provide some friction and prevent bricks from sliding past each other, serving as a way to add increased toughness to the nacreous assembly. At grain growth termination sites of TS materials, there is some roughness which may serve the same function as the asperities of nacre. For these reasons, as well as the tunability of thermal spray microstructures through alterations in the spray process TS materials have the potential to serve as templates for nacre like structures.

The microstructure of thermally sprayed coatings is often referred to as having a “brick wall” microstructure, with each splat analogous to a brick. Nacre is said to have a “brick and mortar” microstructure, Figure 2.4. The inorganic calcium carbonate platelets serve as the bricks and the organic biopolymer acts as mortar. Thermally sprayed coatings have gaps filled with air at their interfaces which varies from the organic polymer layer between the calcium carbonate platelets in nacre. Therefore, nonlinearity that TS coatings display is due to geometric effects. Another difference is that nacreous assemblies are highly ordered materials whereas thermally sprayed materials lack this degree of order. Even with these differences in their corresponding

microstructures, TS materials and nacreous hybrid assemblies show similar responses when introduced to mechanical loads.

Due to the impressive properties of nacre, there have been many attempts to engineer a hybrid material that can display properties comparable to the natural material. Thus far, a number of challenges have been presented. The scale of nacre ranges from bricks which are approximately 0.5 microns thick with polymer interlayers approximately 20 to 30 nm in thickness. Architectures of this dimension have been difficult to replicate, with scale up challenges being a major hurdle. Using thermal spray materials as templates for these hybrid materials is one possible solution. Thermal spray is an industrial process and is therefore relatively easy to replicate and control. Not to mention that large volumes of materials can be sprayed rather quickly, making the process rather fast compared to other techniques such as freeze-casting [45, 46, 51] or synthesis of nacre like films through self-assembly [48, 49].

3. Statement of the Problem

It is not often that a material exhibits both a high degree of stiffness or strength paired with a high toughness. Usually these properties are mutually exclusive. However, there are some materials that exhibit both which is why natural materials like bone, tooth enamel, and nacre are so impressive. What is particularly noteworthy is that nacre displays such extraordinary properties despite being composed mainly of brittle components. In fact, nacre's structure is composed of 95vol% mineral calcium carbonate and 5vol% organic biopolymer. The reason its strength and toughness relationship deviates from the usual inverse one displayed by most materials is not only the result of the biopolymer interlayers, but its highly organized design structure.

The pairing of exceptional strength and toughness by nacre has led to a tremendous effort in replicating these properties in synthetic materials. Thus far, attempts have only produced materials on a small scale due to certain challenges and costs associated with manufacturing techniques. Thermal spray is a technique that can produce materials on a large scale, rather quickly and at low cost making it an ideal choice for manufacturing nacre-like biomimetic materials. Another, perhaps more important advantage associated with the application of thermally sprayed coatings in creating nacre-like materials is that the microstructure is somewhat similar to that of nacre. Nacre is said to have a "brick-and-mortar" structure; calcium carbonate platelets, or bricks, while the organic interlayers serve as mortar. TS coatings have what is referred to as a "brick wall" microstructure with each splat analogous to an aragonite brick in nacre. Coatings deposited via thermal spray processes have gaps instead of mortar, or organic biopolymer at their interfaces. The porosity and voids, interlamellar pores, intrasplat cracks, and splat interfaces are considered defects and contribute to the lower overall strength and toughness when compared to bulk materials. However, exploiting these defects may lead to a manmade composite through the introduction of a second organic phase that exhibits synergistic effects in terms of strength and toughness as displayed in natural nacre.

Not only do TS materials have a similar microstructure to naturally layered materials like nacre, but they also show similarities in their nonlinear stress-strain behavior and hysteretic response under mechanical loading. The mechanical response of coatings can also be altered through manipulations of the microstructure. Microstructures can be tailored through processing which results in modifications to their properties and behavior. The types of defects and porosity can be altered through not only changes in processing conditions, spray process, starting material etc. but following deposition. Post deposition the porosity is introduced to an external polymeric media, which significantly modifies the overall coating properties.

Of significant importance to this dissertation is understanding the relationship between the structure of thermally sprayed hybrid materials and their mechanical properties. Previous work has shown that interfacial features, opening dimension and metrology, can be influenced through spray process conditions. Thermal spray materials will be explored to determine how best to deposit scaffolds and yield an ideal template for bio-inspired materials. This will be completed by changing coating deposition processes, parameters, and materials to further enhance the staggered/organized arrangement inherent of thermally sprayed materials that is so important to the exceptional properties displayed by nacreous assemblies. In terms of their microstructures, both nacre and TS materials display similarities resulting in parallels in terms of their mechanical behavior under applied loads, and ways to further these similarities will be studied.

Of particular interest is how to optimize the mechanical response of thermally sprayed coatings. In order to accomplish this feat, infiltration with an organic material into the interlamellar gaps and voids helps provide strength and toughen the system, resulting in strength and toughness levels that cannot be achieved in each individual phase separately.

Further tailoring the structure of coatings post-deposition was investigated to achieve properties more similar to nacre, i.e. synergistic effects of the microstructure in providing simultaneous improvements in strength and toughness. Nacreous materials have organic biopolymer layers that surround the calcium carbonate bricks, while TS materials are comprised of gaps surrounding the deposited splats. The introduction of organic media into the interfaces of a TS template thus effectively modifying the interfacial layers, results in enhanced properties such as strength and fracture toughness. The biopolymer layers in nacreous assemblies are understood to be one of the main factors for the superior properties exhibited by the natural assemblies. The importance and type of polymer (thermoplastic, thermoset etc.) is scrutinized and methods leading to the maximum property enhancements are examined.

Polymer content in a solution or heat treatment of the polymers effect on the properties of an infiltrated coating is surveyed. Different weight percentages of a polymer dissolved in a solvent affect properties differently due to a higher concentration of polymeric material. Higher weight percent solutions have a greater viscosity, so examining whether polymer solution can effectively penetrate defects and interconnected porosity, to expose interfaces to polymer needs to be addressed.

Another meaningful aspect of this research will be exploring appropriate template materials that can be infiltrated with polymers or sealants. Thus far, alumina and zirconia have been studied the most extensively, but will altering the interfaces of other ceramics and metallic TS coatings provide increased strength, toughness, or damage tolerance? It will be useful to understand the benefits that various polymers or sealants provide in property improvements to thermal spray scaffolds. It is likely not all structures will be improved to the same degree, if at all by each of the materials chosen for infiltration. Exploring a variety of materials for TS templates

in this study seeking to mimic nacre a hybrid natural material can provide insight into what materials could be improved through modifications of their interfaces.

Investigations will scrutinize methods to successfully infiltrate thermally sprayed materials with polymer or sealants in a manner such that there are enhancements of strength, toughness, and other mechanical properties. For instance, various methods such as brushing, simple infiltration and vacuum infiltration can introduce polymer into defect sites and interconnected porosity of TS structures, but not all methods may lead to the same improvements in terms of properties. Polymer infiltration methods may also be dependent on the polymer.

Finally, a connection needs to be made to industry and potential applications of this study need to be presented. Polymer infiltrated coatings may provide solutions when it comes to more damage tolerant coatings or coatings in which porosity is detrimental to the properties. Due to the presence of polymer as a secondary phase, applications for these materials would need to be for lower temperatures. The majority of the investigations in this dissertation will focus on freestanding coatings. However the effect on wear properties and corrosion resistance of coatings on substrates is addressed. In addition, to infiltration with several polymers, coatings will also be impregnated with several industrial sealers. Thermal spray sealers are often applied to coatings to enhance wear properties and corrosion resistance. Therefore, the effectiveness of sealers is studied and whether or not their application results in unintended improvements in mechanical properties such as strength and fracture toughness.

4. Experimental Procedures

In this chapter, different experimental techniques used for the fabrication and property evaluation of biomimetic nacre-like materials will be discussed in detail. This includes the various spray processes used for the generation of TS scaffolds, infiltration processes for interfacial modifications of the scaffolds, as well as characterization techniques to evaluate properties of such composites.

4.1. The Thermal Spray Process

Coatings produced via thermal spray are used in a wide variety of industrial fields for a number of industrial applications including in aerospace, biomedical devices, electronics and transportation fields. Coatings are deposited to provide benefits including wear resistance, traction, sealing, corrosion resistance, and oxidation resistance.

Thermal spray encompasses a number of processes that are extremely versatile; virtually any material can be sprayed onto a wide range of substrates. As long as a material can undergo melting without experiencing decomposition, it is a likely candidate for thermal spray. Additionally, feedstock material can be sprayed in a wide range of forms, powder, rod, or wire. Another major advantage associated with thermal spray processes is that coatings are deposited on substrates without a huge thermal load on the substrate. This is significant because it allows for deposition of a coating from a material with a high melting point onto a substrate without altering the properties of the substrate or causing major distortion of the part which can occur as a result of a high thermal load. Thermal spray processes also allow for a coated part to be recoated if the coating becomes worn or damaged. Through removal of the original coating from a substrate or part, a coating can be resprayed without altering the dimensions or properties of the part. Due to these advantages associated with thermal spray processes, they are often used as a method for depositing a coating. Coatings produced through thermal spray are used extensively due to their ease of application and cost effectiveness.

Although there are a number of advantages associated with this family of spray processes, there are some disadvantages as well. For instance, a coating can only be deposited on a surface in the line of sight of a torch. This means only areas directly visible to the torch can be

effectively coated. In addition, areas where a torch cannot reach, like a deep cavity smaller in size than a torch cannot be coated.

As mentioned, there are a number of thermal spray processes. However, only flame spray and plasma spray will be discussed in detail because those were the deposition processes relevant for scaffolds examined in this dissertation.

4.1.1. The Flame Spray Process

The flame spray process makes use of combustible gas as the heat source for melting the feedstock material, either in powder, wire or rod form. Often a combination of gases is selected so that the operating costs and coating properties are balanced. Possible gases for the flame spray process include, oxygen with either acetylene, propane, hydrogen, and methyl-acetylene-propadiene (MAPP) fuel gas. Usually flame spray torches can be adapted for different gases by variations in the nozzle and/or air cap. Modifications of the nozzle and/or air cap can also outfit the gun for various alloys or wire sizes. Depending on the oxygen-to-fuel gas ratio and pressure, characteristics and temperature of the combustion flame will vary. [54].

The flame spray process when compared to other thermal spray processes tends to require low capital investment and requires less equipment maintenance. It is also characterized by its somewhat high deposition rates and efficiencies, as well as being somewhat easier to operate. Characteristic of flame spray deposited coatings, are lower bond strengths and higher porosity levels. [54].

Flame spray coatings are utilized in a number of areas. For instance, alloys that are nickel based can be flame sprayed for the reclamation of worn out parts. Bronze based alloys can be sprayed to seal areas or for bearings, and tungsten carbide and nickel based alloy blends can be sprayed to increase the wear resistance of a base material. Zinc flame spray coatings can also be deposited as a means of corrosion resistance. [54].

Powder Flame Spray

As the name suggests, powder is the feedstock form for the generation of coatings in powder flame spray. During this process, powder is fed through the center of a nozzle where it

encounters elevated temperatures and melts, Figure 4.1. Molten particles are accelerated and propelled toward the substrate by combustion gases. The amount of powder that can be carried in the gas stream is dependent upon powder characteristics, the velocity and volume of the gases used.

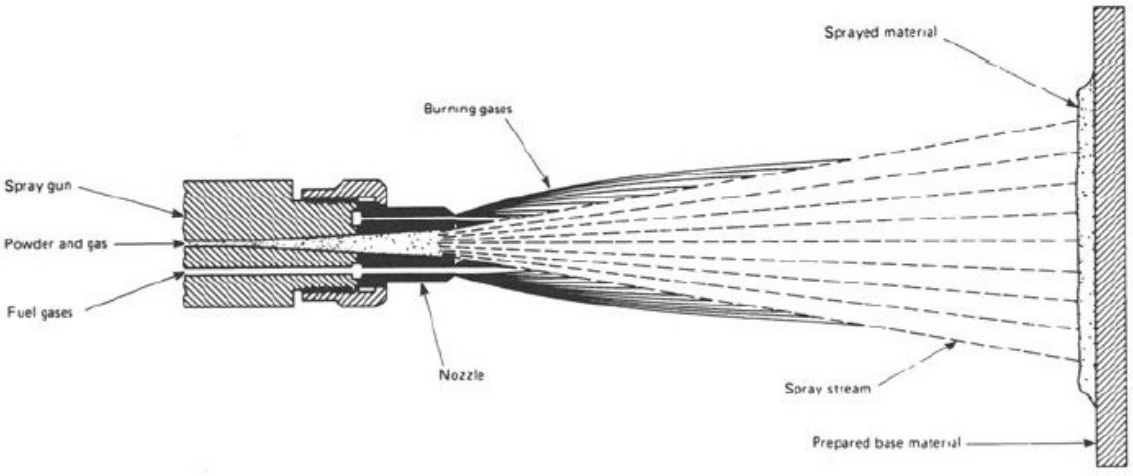

Figure 4.1. Cross section of a typical powder flame spray torch [54].

Ceramic Rod Flame Spray

Saint-Gobain manufactures the Rokide® spray system which is a flame spray process with ceramic rod feedstock, Figure 4.2. The Rokide® spray torch has "V" slotted fiber rolls that grip the ceramic oxide rods and feed them forward where they are melted. An advantage associated with the Rokide® spray system ensures particles do not leave the spray system until fully molten. Due to their high kinetic energy and thermal mass, the particles remain molten until reaching the substrate. This is significant because it results in coatings with a high particle-to-particle cohesive bonding. Coatings deposited via this system also have a lower degree of globular pores and voids, which are defects that can be caused by the deposition of semimolten or unmolten particles.

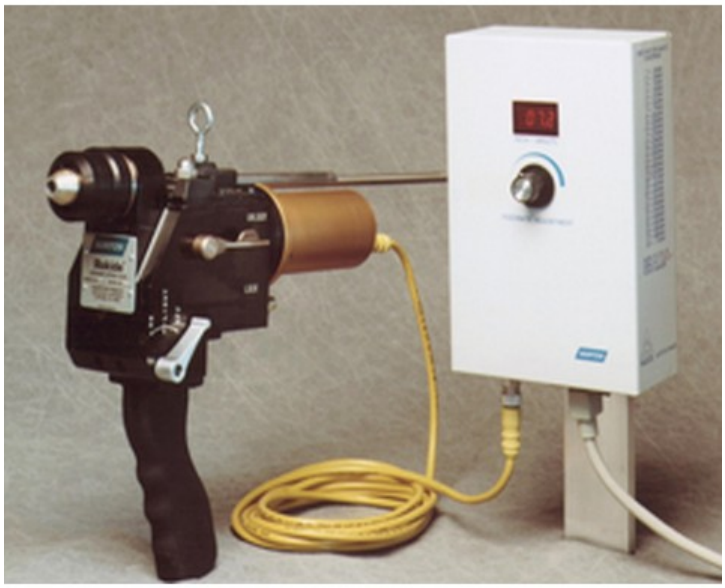

Figure 4.2. The Rokide® spray system [77].

4.1.2. The Plasma Spray Process

The plasma spray process most often involves argon gas, but may include other gases, such as nitrogen, hydrogen, or helium. Gas flows between a water-cooled copper anode and tungsten cathode, Figure 4.3. Argon tends to be the gas of choice because it is chemically inert. By adding additional gases, the enthalpy of the gas can be increased.

A high frequency discharge is used to ignite an electric arc between the cathode and anode. A dc power source then ensures maintenance of the arc. A plasma plume is an ionized gaseous cloud comprised of positive ions, free electrons, neutral atoms, and molecules. Plasma, sometimes referred to as a fourth state of matter, is created when a gas is heated above 5,000˚C and chemical bonds are broken. Atoms begin to experience random movements resulting in violent collisions which lead to the detachment of some electrons from their nuclei. When heavier nuclei lose an electron they become positively charged. [78]. Ionization of the gas occurs creating plasma. The temperature of the plasma can surpass 30,000˚C and as it exits the spray nozzle the volume, pressure and velocity also increase. [54].

Virtually any metallic, ceramic, or cermet coating can be deposited via the plasma spray process. The feedstock powder can be injected directly into the gas stream outside the torch or in the exit region of the anodic nozzle. The high temperature and velocity stream is what heats and accelerates the particles, propelling them to the substrate for deposition. Powder temperature and velocity are affected by the operating parameters and design of the spray torch. Operating

parameters include power levels, gas flows, powder feed rate, carrier gas flow, angle of deposition, and standoff distance. Standoff or spray distance is extremely significant in coating deposition because the distance feedstock travels to the substrate should be long enough to undergo sufficient melting and acceleration. However, too long of a distance can result in cooling and slowing of the traveling particles. Particle melting and acceleration play a major role in overall coating quality and the deposition efficiency. Particle size and morphology of powder is also of great importance because of its affect on the rate of heating and acceleration. Particles can also react with the process gases or gases in the surrounding environment, affecting coating quality. This is especially true of metallic feedstock which can undergo oxidation. A high degree of oxidation can drastically reduce coating density, cohesive strength, and bond strength. [54].

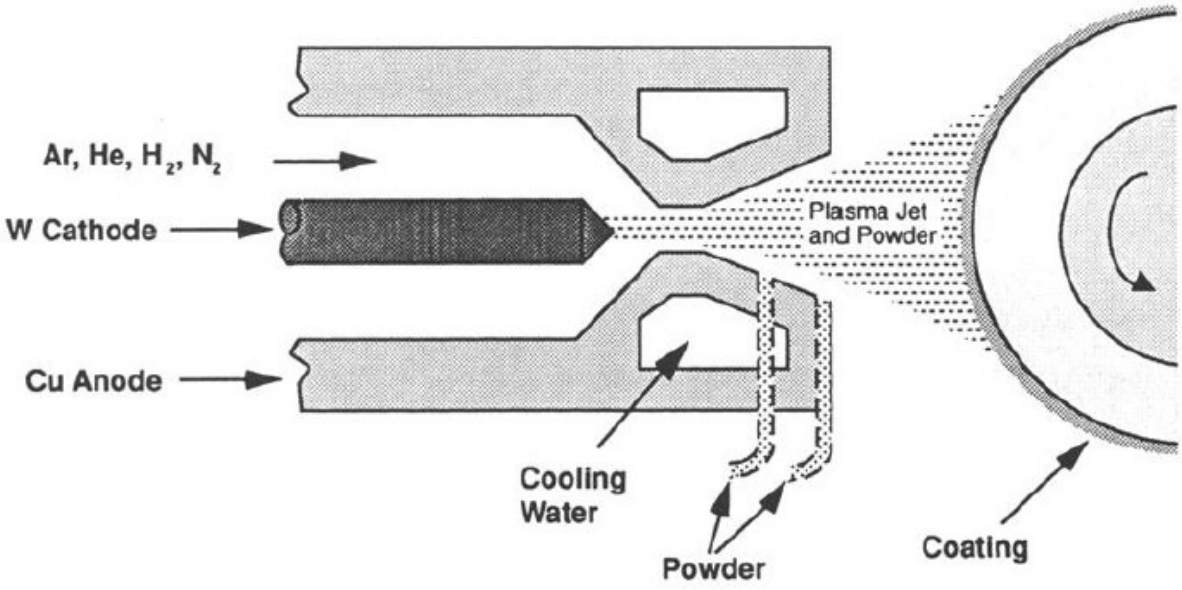

Figure 4.3. Schematic of the plasma spray process [54].

4.2. Processing of Thermally Sprayed Coatings

Flame spray and plasma spray processes were selected for template deposition based on microstructural attributes of coatings deposited with these processes, including the nature and level of porosity. A benefit of using TS templates for the fabrication of nacre-like materials is the wide range of materials that can be thermally sprayed. For this study, the most widely studied coating materials were alumina and YSZ, both brittle ceramics just as the calcium carbonate tablets in nacre.

Many of the attempts discussed thus far in the literature regarding fabrication of nacre-like materials have dealt with alumina templates. Therefore, this provided a good starting point for investigation into nacre-like composites based on thermally sprayed scaffolds. As discussed by Barthelat *et al.* when selecting a natural material that will inspire the design of a biomimetic material, key characteristics of the natural material need to be identified so they can be applied to the manmade material. It is well known and has been discussed extensively in Chapter 1 that calcium carbonate platelets in nacreous assemblies have nanoscale asperities or surface roughness. This surface roughness plays a role in the impressive properties that nacre displays. In order for deformation to reach a certain level, asperity jump or climb must occur in which the asperities slide over each other. This requires a great deal of energy and hence leads to toughening. In addition to alumina, yttria stabilized zirconia was selected in part for the roughness caused by grain termination sites of splats which could also hinder splat mobility. Another major reason for YSZ selection is due to its frequent use in applications requiring thermally sprayed coatings. It is one of the most commonly sprayed and understood materials deposited in coating form via thermal spray processes.

Powder flame spray coatings were deposited using the Terodyne torch and Micro Abrasives aluminum oxide powder while alumina ceramic rod flame spray coatings were formed using Saint-Gobain's Rokide® spray system. The plasma spray process was used to deposit both Al_2O_3 and YSZ scaffolds. Coatings were sprayed on both stationary fixtures and a rotating carousel, Figure 4.4 at various spray distances. The use of the carousel was important in helping to deposit a coating with a sufficient degree of porosity. As the carousel rotates in a counterclockwise direction, the torch raster pattern is vertical. Particles are continually being aimed at the rotating carousel. As it rotates deposited particles cool significantly before another layer is deposited on the sprayed surface. Air cooling jets were also used during the spray process to increase cooling and therefore, allow for deposition of a coating with a greater porosity. Spray distance is also important because it can influence the coating microstructure. A fairly long spray distance of approximately 5in or 6in will further enhance the porosity level of a given coating. By increasing the standoff distance, particles have a longer dwell time in the spray plume and their velocity decreases as they reach the substrate. A lower velocity as particles impinge on the substrate limits interfacial interactions. Therefore, a decrease in particle velocity and temperature caused by the cooling jets and carousel, combined with an increase in spray distance creates a porous coating.

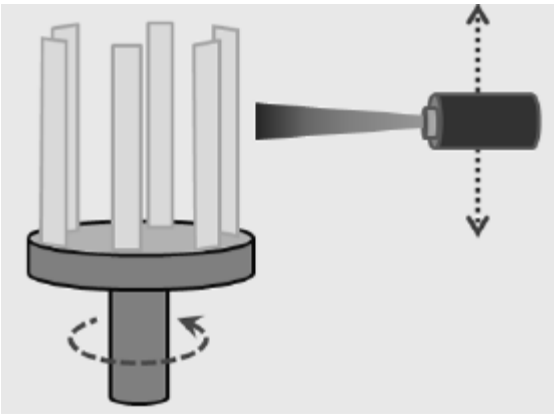

Figure 4.4. A schematic of a carousel that was used in the processing of thermally sprayed coatings for this study. The torch is depicted in this diagram and it's movements labeled with arrows showing a vertical raster pattern. While the torch is programmed to move vertically, the carousel rotates in a counterclockwise direction. Using a carousel helps to increase the porosity of the coating and allows for splats to cool considerably before a new layer of material is sprayed on the substrate and coating deposit.

4.3. Free Standing Coating Preparation

Method of Substrate Removal to Yield a Freestanding Coating

The majority of experiments performed in this study required coatings to be freestanding, meaning they would need to be removed from the substrate. Following coating deposition, coatings were made freestanding through substrate dissolution using an aqua regia mixture. In order for this to be accomplished, coatings on a substrate were cut to a size of approximately 25.4 x 40mm using a Buehler a division of Illinois Tool Works Inc. Isomet 1000 precision saw with an abrasive diamond blade. An aqua regia solution was then prepared from 75vol% hydrochloric acid and 25vol% concentrated nitric acid. Aqua regia is an extremely corrosive mixture, and many metals are not able to withstand its corrosivity. In this case, Al6061 was the substrate material and coatings on the Al6061 substrates were placed in the aqua regia solution immediately after preparation and left for approximately 3 to 4h. In some cases, the substrate did not completely dissolve so an additional aqua regia mixture was prepared and the above procedures were repeated.

Plasma spray YSZ and Al_2O_3 and powder flame spray Al_2O_3 coatings on Al6061 substrates were the only coating and substrate systems introduced to this acid dissolution method. Rokide® Al_2O_3 coatings were made freestanding mechanically with no chemical exposure. It was found

that acid exposure negatively impacted the measured coating enhancements of the Rokide® samples following the introduction of a second organic phase.

Rokide® Al_2O_3 coatings were separated from their substrates by grinding the sample edges on a belt sander to remove overspray that provided further anchoring of the coating on the substrate. In addition, the Al6061 substrates were only lightly grit blasted at a pressure of 40psi to provide minimal surface roughening and thus a lower mechanical bond strength of the coating to the substrate. During spraying, the substrates were affixed to the carousel with binder clips, such that approximately 15mm on both ends of the longer direction were left uncoated. This allowed for an area to grip when the substrate was bent backwards for removal. This mechanical removal process did not work for all spray processes and materials due to the higher bond strength of some coatings.

Processing of Freestanding Coatings for Testing the Effect of a Secondary Phase on Coating Enhancements

Following substrate removal, freestanding coatings were cut to size for infiltration followed by characterization. For the majority of three-point bend tests, coatings were sliced to an approximate size of 25.4 (length) by 6mm (width). Following flexural strength or fracture toughness measurements, fractured test pieces were used for other tests such as indentation and thermogravimetric analysis. There are some cases when the width of the samples was varied and those cases are discussed in further detail in the following chapters.

Freestanding coatings were cut to the appropriate dimensions using a Buehler a division of Illinois Tool Works Inc. Isomet 1000 precision saw with an abrasive diamond blade. Eventually a more reliable method for sectioning specimens was developed. This method is the same as for notching fracture toughness samples, and made use of a diamond coated abrasive blade with a thickness of 0.007in, Figure 4.5.

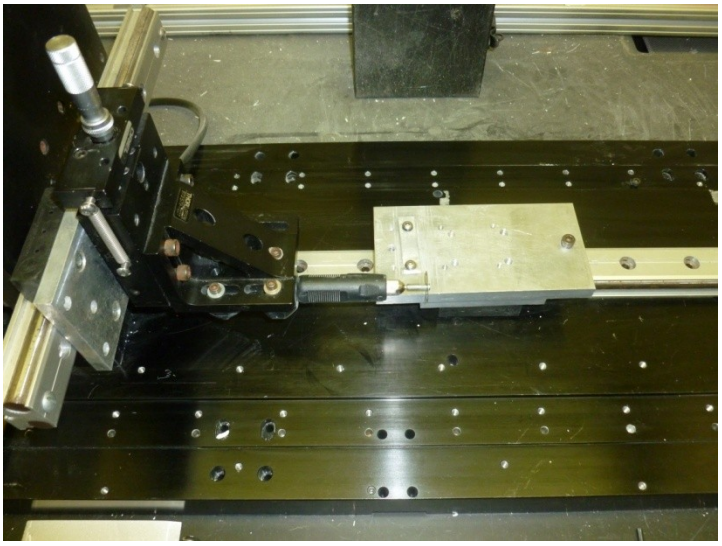

Figure 4.5. A top view of the notch machine that was used to cut freestanding coating three-point bend and fracture toughness specimens to their appropriate widths for testing. In addition, it was also used to notch fracture toughness specimens.

4.4. Chemical Treatments of Thermally Sprayed Materials

In selecting a secondary organic phase for impregnation post deposition, there were a number of considerations taken into account to ensure selection was appropriate. The idea was to select a material that would provide some cushioning against stress and also increase the toughness of the material by preventing cracks. Finding a secondary phase that allows for sliding of the ceramic splats helping to dissipate strain energy with the application of a load is a key purpose of the organic phase. Just as in nacre, the majority of the composite would be the hard and stiff ceramic material while there would be a few percent polymer dispersed throughout the structure. By combining these two materials, the idea would be to amplify properties.

4.4.1. Classification of Polymers

A polymer is a chemical substance composed of molecules containing one or more sequences of atoms with primary bonds, usually covalent linking them together. The small units, or mers are repeated a number of times to form larger molecules. Polymers are synthesized through polymerization processes which link a number of monomers together.

Normally commercial polymers are formed from at least 100 monomers but the number can vary. This is referred to as the degree of polymerization, *n*, and has the most important effect on the properties of a given polymer.

Polymers can be classified as thermosets, thermoplastics, or elastomers, Figure 4.6.

- Thermoplastics

As a polymer cools, it begins to solidify and long molecules are prevented from freely moving. If a thermoplastic is reheated, it will melt and be able to freely flow again. The ability to be reheated after solidifying is characteristic of a thermoplastic. Thermoplastics can be further divided into amorphous or crystalline polymers. Amorphous polymers are those that have a disordered molecular structure, even as they cool or solidify. Those thermoplastics that are semi-crystalline display a certain level of order as they are cooled and experience solidification. Although some regions of semi-crystalline polymers may be ordered, other areas remain amorphous and thus are randomly oriented. [79].

- Thermosets

In order for a thermoset to solidify, it must be cured or cross-linked. Cross-linking is a chemical reaction and during the process, macromolecules will form linkages with each other. As a result, an immobile network of molecules is formed. Because this formation of a network is a chemical reaction, the molecules are not able to flow even after reheating, hence this reaction is not reversible. Due to the high degree of cross-linking associated with thermosets, they tend to be the most brittle and stiff of all polymers. [79].

- Elastomers

Elastomers are polymers that are only lightly cross-linked. The glass transition temperature is significantly lower than room temperature so elastomers are soft and compliant at room temperature. In addition, elastomers can recover from large deformations. [79].

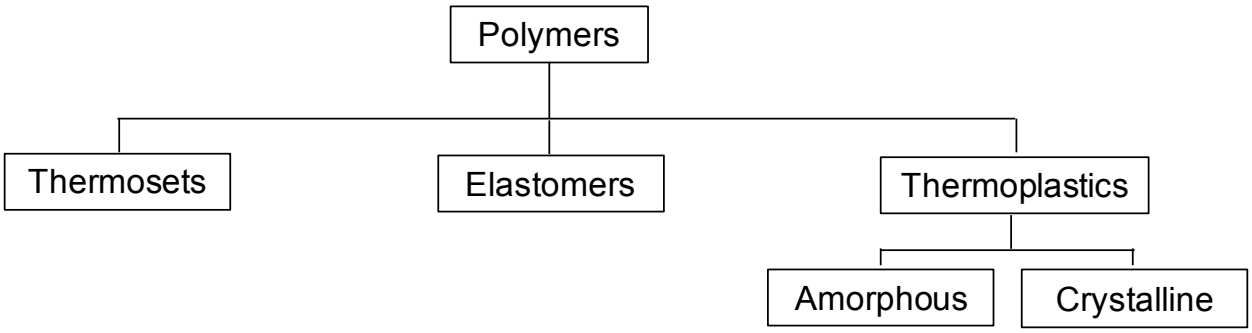

Figure 4.6. Classification system of polymers.

Classification of the Molecular Structure of a Polymer

The skeletal structure of a polymer can either be linear, branched, or network, Figure 4.7. A linear polymer is one in which there is a single carbon backbone and is simply a chain with two ends. A branched polymer has a main carbon backbone with side chain bonds at what are called junction points or branch points. The number and branch size can help to characterize these polymers. Network polymers have a three dimensional structure with several connected chains and are said to be cross-linked. Network polymers can either be highly cross-linked, in the case of thermosets or lightly cross-linked, as in elastomers. [79, 80].

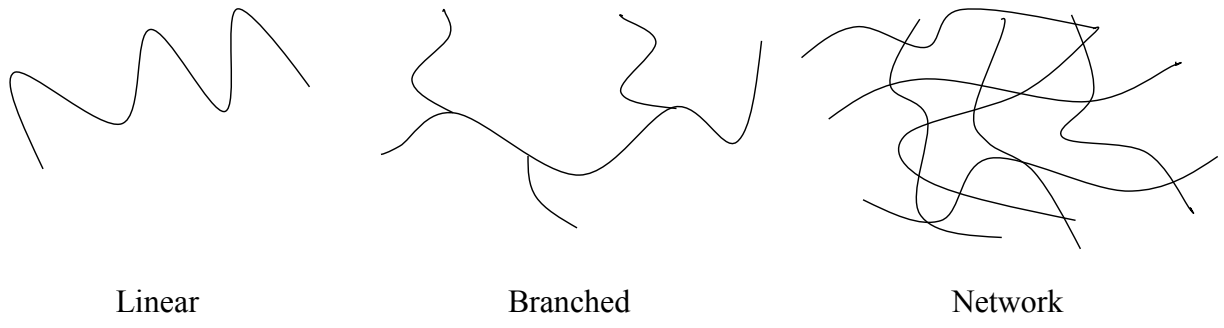

Figure 4.7. Skeletal structures of polymers.

Molecular Weight of Polymers

A number of polymer properties are dependent on molecular weight of the polymer. These properties include transition temperatures, strength, stiffness, toughness and viscosity. For

example, when polystyrene has a degree of polymerization of 1,000 it is stiff and brittle at room temperature. If the degree of polymerization is approximately 10 then at room temperature it will be sticky and soft. Polymers with molecular weights that are too low have transition temperatures and mechanical properties that are also too low and therefore, have limited commercial applications. [79, 80].

It is important to note that the molecular weight of a polymer does not refer to one specific value. Instead, molecular weight of a polymer refers to a molecular weight distribution or the average molecular weights, and so is determined by:

$$\bar{M} = \frac{W}{N}$$

where N is the number of moles in the sample and W is the sample weight. In order to achieve a certain set of properties in a polymer, the molecular weight distribution can be manipulated. Polymers that are composed of long chains have higher molecular weights and those with shorter chains have a lower molecular weight distribution. There is a distribution of molecular weights because during the polymerization process, polymer chains do not all grow to the same length and so an average molecular weight is often reported. [79, 80].

Often properties will saturate upon reaching a large molecular weight, above which there is no additional benefit to a further increase in molecular weight, Figure 4.8. In addition, as the molecular weight increases the viscosity also increases. This is because larger polymer molecules make a solution more viscous than smaller ones. Although as the molecular weight increases, the degradation temperature of the polymer decreases. [79, 80].

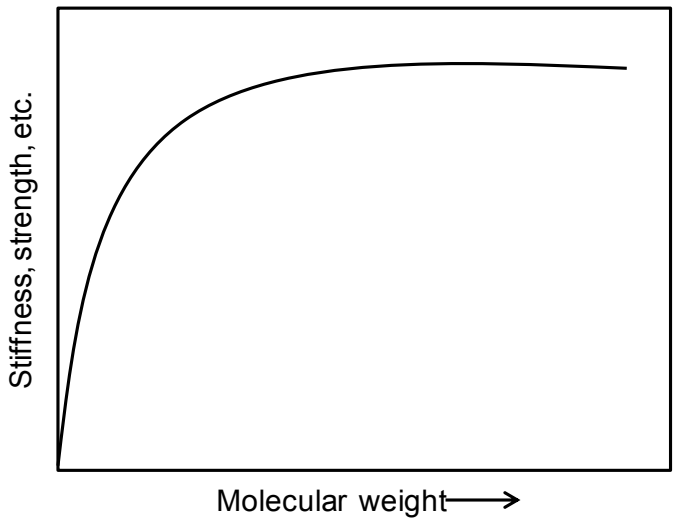

Figure 4.8. The relationship between mechanical properties and the molecular weight of polymers. As the molecular weight increases, there is an increase in mechanical properties such as strength and stiffness until the values become saturated and above which no further improvements are observed.

The majority of polymers (not including natural polymers) have a molecular weight distribution that follows the one in Figure 4.9. There are several ways of determining the average molecular weight. They include:

- Number average molecular weight

$$\bar{M}_n = \frac{\sum m_i}{\sum n_i} = \frac{\sum n_i \sum M_i}{\sum n_i}$$

- Weight average molecular weight

$$\bar{M}_w = \frac{\sum m_i M_i}{\sum m_i} = \frac{\sum n_i M_i^2}{\sum n_i M_i}$$

- Viscosity average molecular weight

$$\bar{M}_V = \left(\frac{\sum m_i M_i^{1/\alpha}}{\sum m_i} \right)^{1/\alpha}$$

where m_i represents the weight, M_i represents the molecular weight and n_i refers to the number of molecules with i repeat units. [79, 80].

For polymers that are formed from a single molecular weight species, referred to as monodispersed, the following relation exists:

$$\bar{M}_w = \bar{M}_n = \bar{M}_v$$

Usually polymers are not monodispersed but instead polydispersed meaning they are composed of a range of molecular weights. For polydispersed systems, the following relation exists:

$$\bar{M}_w > \bar{M}_v > \bar{M}_n$$

A polydispersity index can be calculated for a polymer system. It is given by:

$$PI = \frac{\bar{M}_w}{\bar{M}_n}$$

In general, polymers with a low polydisperity index tend to have higher strengths and flowability, which is related to the ease of processing than those materials with a higher polydisperity index.

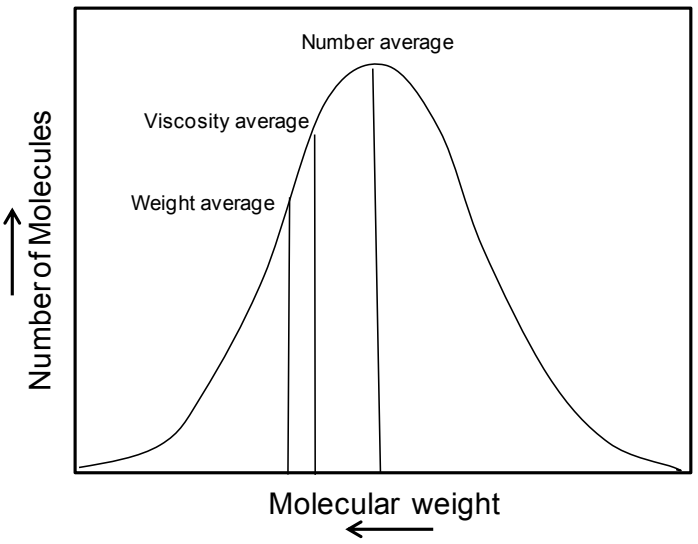

Figure 4.9. The molecular weight distribution for a typical thermoplastic. The number average, weight average, and viscosity average are labeled.

4.4.2. Selected Polymers for Infiltration into Thermal Spray Scaffolds

Polymers that were the most essential in this dissertation included PMMA, PVA, epoxy, and PDMS. The characteristics of each and their properties will be discussed.

PMMA

As already discussed, there has been previous work focused on the synthesis of biomimetic nacre-like materials. A great deal of this work has centered on alumina scaffolds and PMMA organic interlayers. Therefore, previous work as well as the properties of PMMA made it a polymer of choice for this study.

PMMA is the polymer formed from methyl methacrylate (MMA), with the following chemical formula, $(C_5H_8O_2)_n$. It is a linear amorphous thermoplastic polymer. PMMA is known for having a high strength and Young's modulus. However, one of the drawbacks associated with PMMA is its low impact strength and rigidity.

PMMA polymerizes in the presence of free-radical initiators and its repeat unit, Figure 4.10, links together in large numbers. The presence of the pendant methyl group (CH_3) prevents the close packing of the polymer chains to form a crystalline structure. In addition, the present

pendant methyl group restricts the free rotation around the carbon-carbon bonds which result in PMMA being a rigid polymer. A pendant group is a group that is connected to the polymer backbone and occurs in the repeating monomer unit.

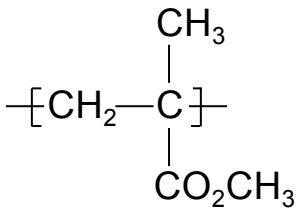

Figure 4.10. The methyl methacrylate repeat unit.

PVA

PVA is formed through the polymerization of the monomer vinyl acetate and then the full or partial hydrolysis of polyvinyl acetate (PVAc). It is unusual among the polymers for the reason that it is not synthesized from polymerization of monomers. Instead, PVAc is polymerized and PVA is formed through its dissolution in an alcohol and treatment with an alkaline catalyst. In the hydrolysis reaction, the acetate groups are removed from the PVAc chains. It has a chemical formula of $(C_2H_4O)_n$ with a repeat unit showed in Figure 4.11, and is a semi-crystalline thermoplastic. PVA was selected for infiltration due to its adhesive properties [81]. Introducing a secondary phase into a TS template with good adhesive properties could enhance the splat anchoring which would help resist deformation when a load is applied. PVA is also known to have a fairly high tensile strength and flexibility.

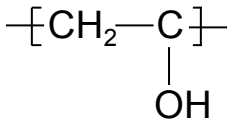

Figure 4.11. The vinyl alcohol repeat unit.

PDMS

PDMS has the empirical formula $(C_2H_6OSi)_n$ and depending on the number of monomer repeat units, Figure 4.12, it can range from almost a liquid when there is no cross-linking to a semi-solid after some cross-linking. Unlike an epoxy which exhibits a high degree of cross-linking, PDMS is a thermoset that only lightly cross-links. After cross-linking or curing it is a flexible elastomer. PDMS was selected for infiltration into TS scaffolds based on its ability to withstand high deformation rates at room temperature.

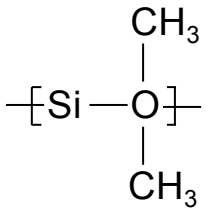

Figure 4.12. The repeat unit composing PDMS.

Epoxy

Epoxy is the cured product of an epoxy resin that has either been cross-linked or cured with themselves or with a co-reactant usually referred to as hardeners or curatives. The curing reaction is initiated when an epoxy resin is reacted with a hardener or catalyst. The curing process involves the chemical reaction of molecular chains at active sites. Cross-linking occurs when covalent bonds are formed between epoxide groups of the epoxy resin and amine groups of the hardener. The cross-linking is what governs properties of the epoxy such as strength and rigidity.

The most widely used epoxies occur as either one or two component mixtures. One component epoxy systems are pre-catalyzed and require temperatures between 250-300˚F to cure. Two component epoxy systems undergo cross-linking at room temperature. However, cross-linking can also be completed at higher temperatures. In fact, often room temperature epoxies may only be able to reach their maximum mechanical properties with the application of heat.

The properties of an epoxy system can be further altered through the introduction of second phase particles into the epoxy mixture. The use of a secondary phase in an epoxy mixture is to provide additional sites for the initiation of energy absorption in the polymer rather than only at the head of the crack tip. Through the addition of second phase particles, the epoxy system can

be toughened, making it less brittle. This is a significant improvement for epoxies, which are thermosetting polymers. Thermosets are among the strongest polymers but also prone to brittle fracture.

A commercial two component epoxy from Buehler a division of Illinois Tool Works Inc. was used for infiltration by mixing EpoThin hardener and EpoThin resin. Epoxy, a thermosetting polymer was selected for infiltration into TS scaffolds due to the fact that epoxies tend to be the strongest of all polymers. Due to their high degree of cross-linking to form a three-dimensional network, thermosets are strong. Unlike thermoplastics with weak attractive forces between chains, cross-linking is completed by chemical bonding so thermosets tend to be the strongest of polymers. However, thermosets are also more brittle. The fact that epoxies have good adhesive properties and are relatively easy to work with made them a good choice for impregnation into TS templates.

4.4.3. Other Considerations in Polymer Selection

In addition to the relevant mechanical properties of polymers including strength, there are also other characteristics of concern when selecting polymers, such as polymer viscosity and molecular weight. A polymer with a low viscosity and molecular weight is desired so that it can impregnate the coating template and achieve a high level of penetration. However, certain polymer properties such as strength are higher when viscosity is higher. The molecular weight of a polymer plays an important role in the overall behavior of a polymer and therefore its properties. In the case of PVA, as the molecular weight increases, there is an increase in viscosity, adhesive strength, and tensile strength. Therefore, it is important to maximize properties such as adhesive strength yet still have a polymer with a viscosity such that infiltration into the interfacial porosity of the thermal spray templates is possible.

Table 2 provides the typical viscosity and molecular weight of the polymers used in this study. Polymers such as epoxy with a lower molecular weight and viscosity had a better ease of infiltration while polymers such as PDMS are rather difficult to incorporate into the open porosity of a thermal spray coating. Both epoxy and PDMS are two component systems while PMMA and PVA polymers were dissolved in a solvent. In some cases, PMMA was polymerized in-situ in thermal spray scaffolds. These procedures will be further discussed in section 4.4.4.

Table 2. Typical viscosities and molecular weights of polymers selected for fabrication of ceramic/polymer composites [82-85].

Polymer	Viscosity (cP) at 25˚C	Average Molecular Weight Range
Epoxy	~200	~700
PDMS	~3500	~500,000- 3,000,000
PMMA	~700-1000	~120,000-131,000
PVA	~600-800	~31,000-124,000

Epoxy, a thermoset, is one of the strongest polymers making it a logical choice for selection to interfacially modify thermal spray scaffolds. In order to show improvements in strength and fracture toughness of thermal spray templates when impregnated with polymeric media, it is necessary that the polymer have good mechanical properties. Although it is known to be rather brittle, the high strength of the epoxy and relatively low viscosity when compared with other materials still warrants exploration of ceramic/epoxy composites.

Despite the somewhat higher viscosities of PMMA and PVA, these polymers were selected for investigation. One of the major benefits of PMMA, is that it has carbonyl groups which can form secondary hydrogen bonds with the OH groups of the alumina. A polymer that would be able to form bonds to serve as a means of anchoring splats together as in the case of natural nacre is highly desirable. As will be discussed in further detail in section 4.4.4, the etching and grafting steps of the in-situ polymerization of PMMA served as a means of enhancing the bonding between the inorganic ceramic and organic polymer. PVA is often used in adhesives making it a desirable polymer for modification of interfaces of ceramic TS templates. PVA and PMMA are both thermoplastic polymers, and thus are somewhat less brittle than epoxies which could possibly lead to polymer/composite TS materials having a higher fracture toughness.

Although PDMS has an extremely high viscosity, and thus molecular weight, it can recover from large strain levels at low stresses. Elastomers can elastically recover from large strains thus they can experience a high level of deformation before fracture. A polymer that can deform to a high degree prior to fracture is desirable in the fabrication of biomimetic nacre-like composites and therefore, PDMS was chosen for a secondary phase.

4.4.4. Infiltration of Polymer Solution or Thermal Spray Sealers into Thermally Sprayed Scaffolds

Depending on the polymer type (thermoset, thermoplastic, or elastomer) or sealer, infiltration was completed in a different manner to maximize the content that could be introduced into a given TS template. The following section will discuss the methods used for infiltration which were optimized for this study.

Infiltration of PMMA and PVA Solution

PMMA and PVA solutions were prepared at two different concentrations each by dissolution of the polymer in an appropriate solvent. Water was used as the solvent for both the 6wt% PVA and 22wt% PVA. Based on preliminary studies, it was originally thought that the highest weight percent PVA that could be dissolved in water was 6wt%. However, with the application of heat, it was found that 22wt% could be prepared in solution. Following this, external heat was applied to make all PVA solutions due to the ease of dissolution. Preparation of the PVA polymer solutions included using a beaker with water on a hot plate. In order to make the dissolution process faster, a magnetic stirrer was added to prevent the polymer from settling on the bottom. The hot plate was turned to approximately 60°C and the appropriate wt% of both polymer and solvent were added to the vial. The polymer was left to dissolve in the solvent until clear. This took no longer than 3h for each solution.

In order to prepare PMMA solutions, 8wt% PMMA was dissolved in toluene or 22wt% PMMA was dissolved in chlorobenzene. Preliminary dissolution experiments only allowed for 8wt% PMMA in solution. However, with the application of heat and other solvents, 22wt% PMMA could be dissolved. Again, these beakers were placed on a hot plate at approximately 60°C with a magnetic stirrer and left until clear. This took no longer than 3h for both 8wt% and 22wt% solutions of PMMA.

Solutions of PVA and PMMA were left to cool to room temperature. Once at room temperature coatings were immersed in the solutions and placed at room temperature under 0.1mm Hg vacuum for 4min. Through investigation of infiltration times, 4min was found to be sufficient to allow for polymer infiltration. Samples were removed from solution and excess PMMA and PVA on sample surfaces was wiped clean. Infiltrated coatings were then left overnight. The remaining polymer solution could be stored for future use.

Epoxy Infiltration

A commercial epoxy from Buehler a division of Illinois Tool Works Inc. was used for infiltration by mixing EpoThin hardener and EpoThin resin. Recommended by Buehler for curing is a ratio of 5g resin to 2g hardener. In some cases, 6g of resin to 1g of hardener was chosen in order to provide an epoxy that did not fully harden when cured. The desired masses of resin and hardener were mixed 60s until a homogenous mixture. Coatings were then immersed in the mixture gradually allowing for entrapped air to escape thus making way for the epoxy mixture. Infiltration occurred under 0.1mm Hg vacuum for 4min. Samples were removed from the epoxy mixture and excess epoxy was removed from the sample surfaces. Samples were left overnight to allow the epoxy adequate time to cure.

In addition, to the above epoxy procedures a number of epoxy infiltrated samples were processed further by performing an additional heat treatment step. Epoxy infiltrated coatings (5:2 or 6:1) were placed in a furnace at 200˚C for 2hr to promote further cross linking of the epoxy by performing a staged cure. This is discussed in more detail in Chapter 5.

Application of Thermal Spray Sealers

Three common sealers were applied to TS scaffolds by brushing the top and bottom surfaces of freestanding coatings for a total of 30min, 15min on each side. Sealers selected for these experiments were Diamant Dichtol, Metcoseal URS, and Metcoseal AP. They were chosen for based on their recommended application and service temperature limits which are presented in Table 3. Samples were then left overnight to allow the sealants enough time to cure.

Table 3. Thermal spray sealers used for coating impregnation, their recommended applications and the maximum service temperatures for which the sealers are designed.

Sealer	Recommended Application	Maximum Service Temperature
Diamant Dichtol	Provides corrosion resistance	500˚C (932˚C)
Metcoseal URS	Increased corrosion, impact, and abrasion resistance for ceramic and metallic coatings Resists a number of solvents, acidic, basic, and atmospheric environments	205˚C (400˚F)
Metcoseal AP	When it is necessary for coatings to be impermeable for use in high pressure applications Resists a number of solvents, acidic, basic, and atmospheric environments	205˚C (400˚F) continuous service 260˚C (500˚F) intermittent service

Impregnation of PDMS

Sylgard® 184 silicone elastomer kit was purchased from Dow Corning for interfacial modifications of ceramic templates. This set included PDMS base and a curing agent. In order to prepare the PDMS mixture, the base and curing agent were combined in a 10:1 ratio by weight and mixed manually for approximately 10min. The samples are then placed in the mixture and left under 0.1mm Hg vacuum for 4min to help force the PDMS into the open coating porosity. Freestanding coatings are removed from the PDMS and placed in a furnace at 80˚C for 2hr to promote cross-linking of the polymer chains. The coatings are then left overnight.

In-situ Polymerization of PMMA from MMA Monomer into Thermally Sprayed Templates

A final method of introducing a second organic phase into TS scaffolds consisted of a series of steps to polymerize PMMA in-situ. This procedure was similar to what Munch *et al.* followed to fabricate nacre-like coatings [45] and was adapted from procedures followed at VTT Technical Research Centre of Finland. In-situ polymerization was accomplished by first completing an etching step followed by a grafting step, and then two polymerization steps.

A Piranha etching solution was made by mixing 25vol% hydrogen peroxide solution and 75vol% concentrated sulfuric acid in a small beaker with a magnetic stir bar. The beaker was placed in a larger beaker to function as a water bath. Sulfuric acid was added to a hydrogen peroxide solution a single drop at a time while being constantly stirred. No external heat should be applied, as the process is exothermic. The dry sample was inserted into the beaker using Teflon tweezers. Teflon tweezers are used because Piranha solution is acidic and an oxidizer, so it will corrode metals. Ensure that the stir bar will not make contact with the samples. The samples should be left in the etchant for 20min. Following 20min, the samples should be removed using the same Teflon tweezers and rinsed repeatedly with deionized water, so pH is neutral. Samples should be left overnight to dry.

Following the etchant step whose purpose is to leave hydroxyl groups on the surface of the alumina coatings, the sample surfaces were exposed to a grafting agent. The surface grafting agent (3-(Trimethooxysilyl)propyl methacrylate was diluted in acetone, such that the ratio of acetone to surface grafting agent was 1:10. This dilute mixture was prepared so there were 2.5mL for every 1g of sample. This means if the total sample weight was 10g, then 25mL of acetone and surface grafting agent should be made. In order to assist in the diffusion of the reagents, the flask containing the sample and reagents was placed in a sonicator and left for 30min. Upon the completion of 30min the sample were removed from the grafting solution and left to dry overnight prior to starting the first polymerization step.

A volume of liquid necessary for covering the sample in a flask was estimated. The sample and stirrer were inserted into the flask. Of this total volume, 25wt% methyl methacrylate (MMA) and 75wt% toluene was mixed. Then 1wt% (of the MMA mass) azobisisobutyronitrile initiator (AIBN) was added. A nitrogen atmosphere was inserted and the flask was placed in a sonicator for 30min to assist diffusion into the thermally sprayed scaffolds. Following this, the flask was wrapped in aluminum foil and placed in a 70˚C water bath for 1hr while being constantly stirred. Samples were then removed from solution and rinsed with toluene to remove excess monomer and AIBN. The TS coatings were allowed to dry overnight. The second polymerization step was similar to the first except this time 0.5wt% AIBN was added to the flask with MMA and toluene. The flask was also sonicated for 30min and upon completion was placed in a water bath for 8hrs at 50˚C while being constantly stirred. Samples were then removed and left overnight.

4.5. Surface Preparation of Samples Following Infiltration

Once samples have been cut to the appropriate size for three-point bend flexural strength and fracture toughness measurements and a second organic phase has been introduced, the specimen surfaces likely have a thin film of organic material, although much of the excess has already been removed following infiltration. Prior to testing, it is necessary to remove this layer of organic material and to reduce the roughness of the specimen surfaces. This was accomplished by polishing the surfaces to a finish of 9μm. As sprayed coatings, or those with no polymer present were also polished to a surface finish of 9μm.

Following surface polishing of samples, the thickness and width was measured five times at different locations and averaged. Taking five measurements of each helped to account for any variation within a sample. Fracture toughness specimens were notched using the notch machine, Figure 4.5. Samples were notched following the infiltration and polishing steps to minimize any type of machining following notching. The notch depth was measured by taking the average of three depth measurements using optical microscopy.

4.6. Characterization of Nacre-like Materials

Three-Point Bend for Flexural Strength and Fracture Toughness Measurements

Samples prepared for three-point bend tests were sliced to a size of approximately 25.4mm by 5mm, unless otherwise noted. The surfaces of these samples were polished to a finish of approximately 9μm. The three-point bend setup consists of two supports, or the load span. The sample is placed on these supports and a load is applied to the center of the sample from above, as can be seen in Figure 4.13. For all samples tested, the load span was kept at a constant 21.06mm. Three point bend tests were chosen as opposed to four point bend tests due to limitations of the instrument (TIRAtest 26005).

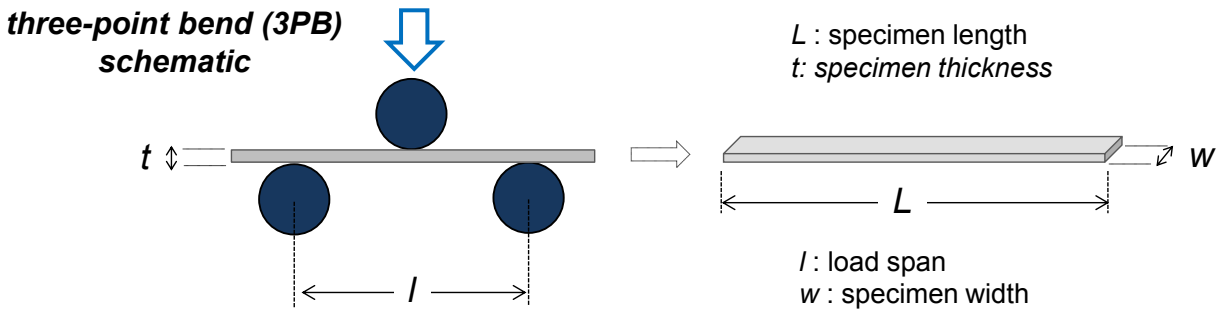

Figure 4.13. Schematic of a three-point bend test setup. The support span, or load span is identified in the figure and has a length of 21.06mm. The load is applied from the top of the setup in the center of the coating.

A load cell with a maximum load capacity of 0.5kN was used. The load cell was affixed to the crosshead of the screwdriven mechanical loading frame of the TIRAtest 26005. For the majority of tests, the crosshead speed was 0.2mm/min. Three-point bend tests were either conducted as single cycle tests or three cycles, meaning the sample would fracture after the first cycle or after the third cycle. Prior to beginning a test, a preload was applied to the sample of about 1.2N to ensure contact between the loading roller and sample surface.

Upon completion of three-point bend tests, the flexural strength of each coating was calculated according to equation 1.1;

$$\sigma = \frac{3LP}{2wt^2} \qquad \text{Equation (1.1) [86]}$$

where σ is the flexural strength, P is the maximum load, L is the load span, w is the width of the test specimen, and t is thickness. Due to the application of a preload force of approximately 1.2N prior to the start of the test, the preload was added to the maximum load measured. Three-point bend tests also allow for the calculation of maximum strain which is given by equation 1.2;

$$\varepsilon = \frac{6tv}{L^2} \qquad \text{Equation (1.2)}$$

where ε is strain, t is thickness, ν is deflection of the beam, and L is the load span. Based on the results of three point bend testing the effect of polymer infiltration on mechanical properties such as flexural strength can be calculated.

Fracture toughness of the as sprayed and infiltrated freestanding coatings was calculated according to ASTM E1820. Prior to notch fracture toughness measurements, a notch was made in the coating using the notch machine, Figure 4.5. Specimens were notched so as not to affect more than ½ of the coating thickness. Usually a fracture toughness specimen is then precracked, but this was not necessary for specimens based on TS scaffolds due to their highly defective nature. Coatings were sprayed to have a high level of porosity, so there are many defects inherent at the notch tip that serve as crack initiation sites. Fracture toughness provides a quantitative measure of the stress needed to cause a preexisting flaw to propagate. Filling the porosity of thermally sprayed templates with polymer and modifying interfaces, could provide enhanced protection against the propagation of cracks meaning infiltrated samples would have a higher fracture toughness.

Microindentation for Indentation Elastic Modulus and Hardness Testing

A Micromaterials LTD., micro/nano indenter was utilized to examine the local hardness properties of freestanding coatings, Figure 4.14. For indentation experiments, samples already fractured during three-point bend tests were indented. This allowed for the maximum number of experiments to be performed using each sprayed coating. In order to assess the effect of damage tolerance on polymer infiltrated coatings, static indentation experiments were conducted. A 1/16” tungsten carbide spherical indenter tip was used and the maximum load was set to 5N. For each as sprayed coating or polymer infiltrated coating, 30 indents were made on the top surface of each sample. Thermally sprayed coatings tend to have a number of pores, therefore the indentation results can be misleading because it is possible the indenter will impact on an area that is a pore or void. In order to avoid any misleading data, 30 indents are made and any hardness or modulus values that fall outside the standard deviation are discarded. Microindentation operates on the basis that an indenter tip with a known geometry makes contact with a sample surface while applying an increasing load. Upon reaching the specified maximum load value, the normal load reduces until either partial or complete relaxation. This is repeated for a preset number of indents. During each portion of the experiment, the indenter’s position relative to the sample surface is monitored. The applied load is plotted against the position of the indenter for each loading/unloading cycle. Based on results from static indentation experiments,

indentation and elastic modulus are determined. This allows for determination of the effect polymer as a second phase has on enhancements of TS scaffolds.

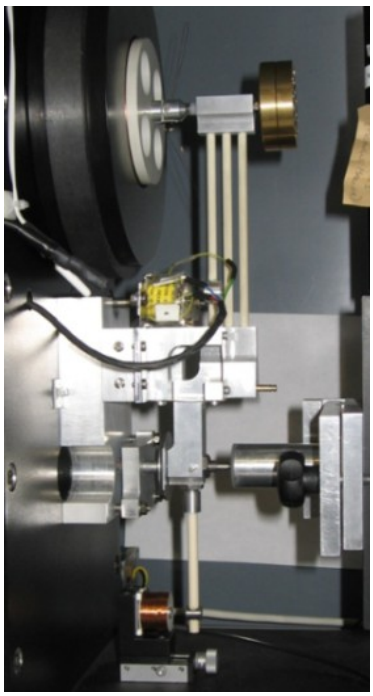

Figure 4.14. Image of the Micromaterials LTD. microindenter utilized in this study.

The microindenter is also equipped with the capability to perform dynamic indentation experiments. During a dynamic indentation test, the Berkovich indenter tip repeatedly strikes the localized sample area for 1h at a constant preset load. A Berkovich indenter tip is formed from a three sided pyramid. The profile of the Berkovich tip is rather flat with a face half angle of 65.27°. [87]. The indenter makes contact with the sample and holds for 3s. The indenter tip then retracts from the sample and holds its position for 5s before contacting the sample again and holding for 3s. This process is repeated for 1h, and can be seen in Figure 4.15.

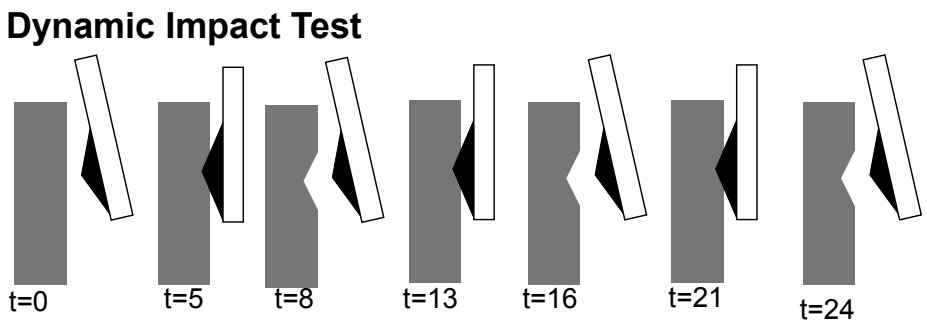

Figure 4.15. Schematic of dynamic indentation test. The indenter tip starts from a position not in contact with the sample. The tip then contacts the sample and holds for 3s, moves away from the sample for 5s, and contacts the samples again for 3s. This is repeated for a predetermined period (diagram courtesy Dr. Brian Choi).

Thermogravimetric Analysis for Mass Loss Determination

A Netzsch STA (simultaneous thermal analysis) 449C Jupiter was utilized for thermogravimetric analysis (TGA) measurements. Thermogravimetric analysis is a technique for monitoring the mass of a material as the temperature changes according to a controlled program in a controlled atmosphere. This instrument is advantageous because it is capable of simultaneous thermal analysis, meaning it can perform both differential scanning calorimetry (DSC) and TGA during the same sample run eliminating any inconsistencies. These include such parameters as the gas flow rate, sample size, heating rate, thermal contact of the sample crucible and sensor, etc. TGA is important because it allows for the mass of a sample to be measured continuously as a function of temperature and/or as a function of time at a set temperature. DSC is conducted by measuring the heat that is required to increase the temperature of a reference and sample as a function of temperature.

The instrument consists of a vertical, top-loading furnace with a sample crucible that is supported by a precision balance and located in the furnace, Figure 4.16. The sample crucible is supported by the sample carrier. During the experiment the mass of the sample is constantly measured.

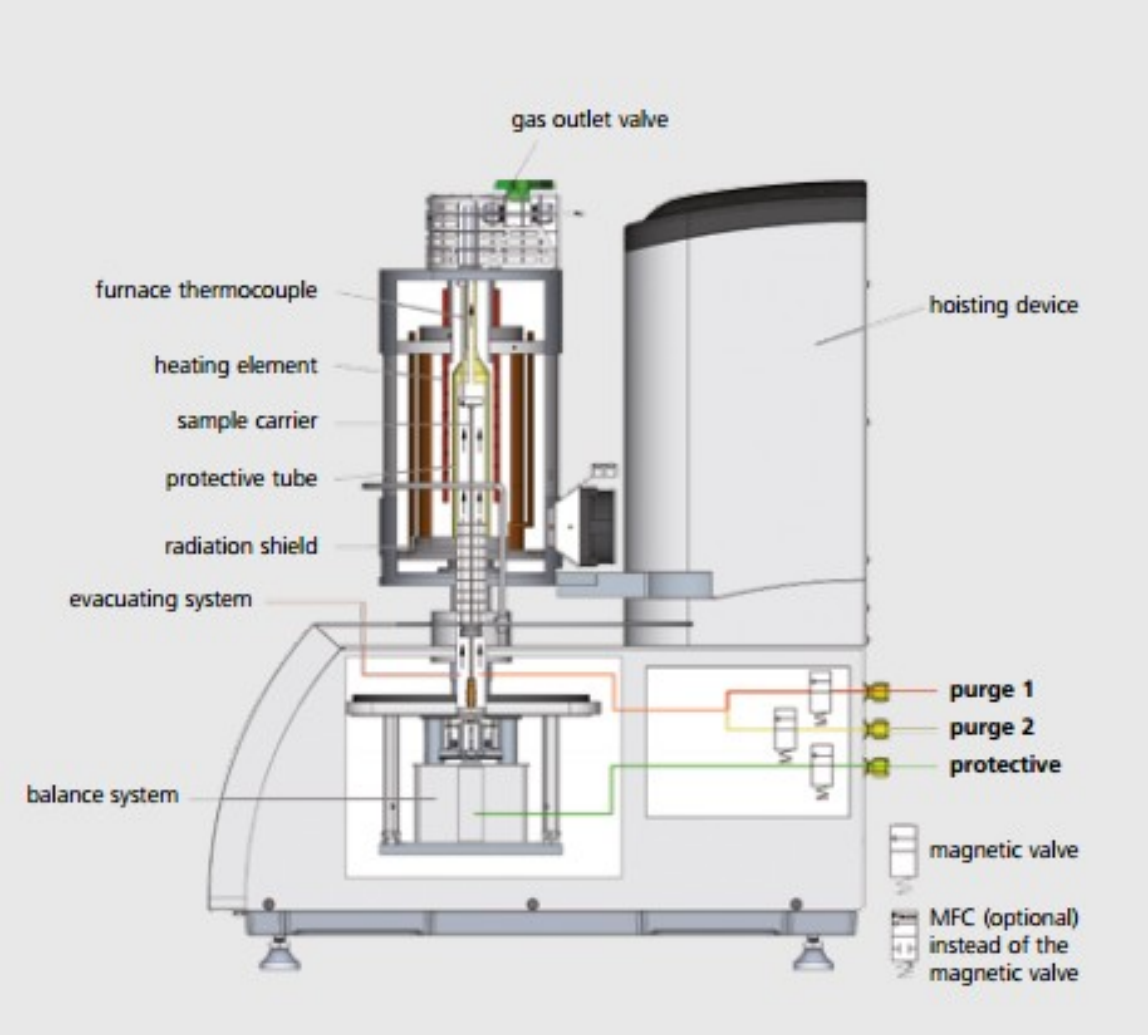

Figure 4.16. Cross section of the Netzsch STA 449C Jupiter used for thermogravimetric analysis [88].

Following fracture from three-point bend measurements, TGA of as sprayed and infiltrated coatings was completed providing an estimate of polymer content in a given scaffold. For analysis, the fractured coatings were further sectioned into pieces with a mass of less than 50mg. Prior to testing, a calibration run was performed using the same parameters as the test. Argon gas was used as a purge gas and was flowed at a rate of 5mL/min for the entire duration of the test. Samples were placed in platinum crucibles and heated at 10˚C/min until reaching 1000˚C, where there was an isothermal portion of the test and the maximum temperature was held for 15min. By heating the samples to 1000˚C, it was assumed all of the polymer would be burned off, and the mass loss calculated would give an indication of polymer content within a ceramic scaffold. Following completion of TGA, results were analyzed using Netzsch Proteus Analysis and mass loss in wt% was measured. All of the infiltrated coatings from the same sprayed coating were

compared against the as sprayed coating. Mass loss of the as sprayed coating was assumed to be due to moisture entrapped within a coating. The as sprayed mass loss was subtracted from infiltrated coatings of each particular scaffold to yield the mass loss due to the polymer.

Pin-on-Disk Wear Testing

One of the most widely used tribotesters is the pin-on-disk apparatus. The setup is comprised of a stationary pin that slides against a sample that is placed on a rotating stage or disk, Figure 4.17. ASTM G99-04 requires that a pin with a spherical tip be used. However, there a number of different tip geometries that can be selected. A motor driven carriage with a force/load sensor applies a load vertically downward. The sensor ensures that the load remains at the specified load for the duration of the test. Often the load is set to remain constant, but can be varied if the user desires.

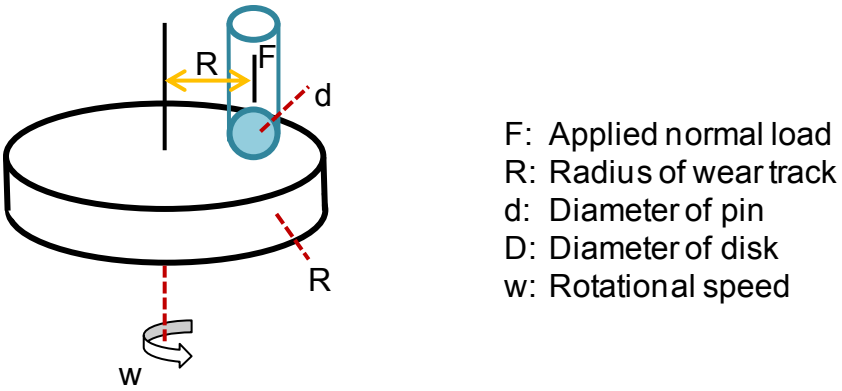

Figure 4.17. Schematic of a pin-on-disk wear test.

For wear testing, a coating and substrate system was sliced to a size of 1in by 1in using a Buehler a division of Illinois Tool Works Inc. Isomet 1000 precision saw with an abrasive diamond blade. After sectioning coupons to the appropriate size, one was left in the as sprayed condition and the others were infiltrated with selected polymers or thermal spray sealers. A CETR UMT-2 multi-specimen test system was used for the wear testing. For pin-on-disk testing, coatings were not made freestanding but left adhered to the substrate. Both as sprayed and

infiltrated coatings were polished to a surface finish of about 9μm. Coatings were not polished to a finer finish due to the fact that they were impregnated and should not be exposed to any diamond suspension that could possibly infiltrate any unfilled porosity, especially in the case of the as sprayed samples as this would have an impact on the tests. Each sample was affixed to the center of a sample holder using Loctite® 380™ Black Max® instant adhesive. When the glue sets, the mass of the sample and sample holder is measured. An alumina ball will be inserted as the pin tip for these tests so prior to beginning a sample run, the mass of the alumina ball is also measured. The plate and sample holder are tightly screwed into the rotating disk. The alumina ball is placed in its holder and the holder tightened, so it will not rotate during the experiment.

Before starting a run, the readout on the Extech hygro-thermometer clock should read 25%. If the readout is higher the heater should be placed in front of the tribometer for a few hours to dry the test chamber. Doors of the tribometer should be left ajar. For all pin-on-disk tests, the velocity of the rotating disk was set to 120rev/min for a test duration of 30min. The radius of the wear track was approximately 7mm. Depending on the template material, the force was varied. For all alumina and yttria stabilized zirconia templates, the force was set to -20N. Upon completion of the 30min, the sample and alumina ball were cleaned of all surface debris with compressed air and the masses measured. The sample coating and substrate system were removed from the sample holder by placing them on a hot plate for a few minutes.

Following the sliding wear test, the wear track is imaged and measurements are taken to give an idea of the width of the wear track. Based on the width of the wear track, conclusions can be made about the toughness of each material. The coefficient of friction is also calculated.

Corrosion Evaluation

Corrosion resistance of nacre-like composites was evaluated using an accelerated electrochemical test. Artificial seawater with a concentration of 3.5wt% NaCl and a pH of approximately 7 was prepared. Coating-substrate systems were used for the test with corrosion of the top surface of the coating being studied. Coatings were tested as sprayed and then following infiltration with thermal spray sealers. As sprayed coatings served as a benchmark so the corrosion resistance with sealers could be evaluated. Surfaces were polished to a surface finish of 9μm. Again, a finer surface finish is ideal but to avoid filling porosity with any diamond suspension the coatings were not polished to a finer surface finish. It was thought 9μm would be allowable because all coatings were polished to the same finish. Therefore, although the finish was not ideal, the presence of sealers would still give an indication as to the level of protection provided.

An electrochemical cell and a potentiostat (Gamry Reference 3000, Gamry Instruments) was used for the accelerated electrochemical testing, Figure 4.18. The glass electrochemical cell is capable of supporting three electrodes:

- Working electrode- the sample
- Counter electrode- platinum mesh (larger than the working electrode)
- Reference electrode- saturated calomel electrode (SCE)

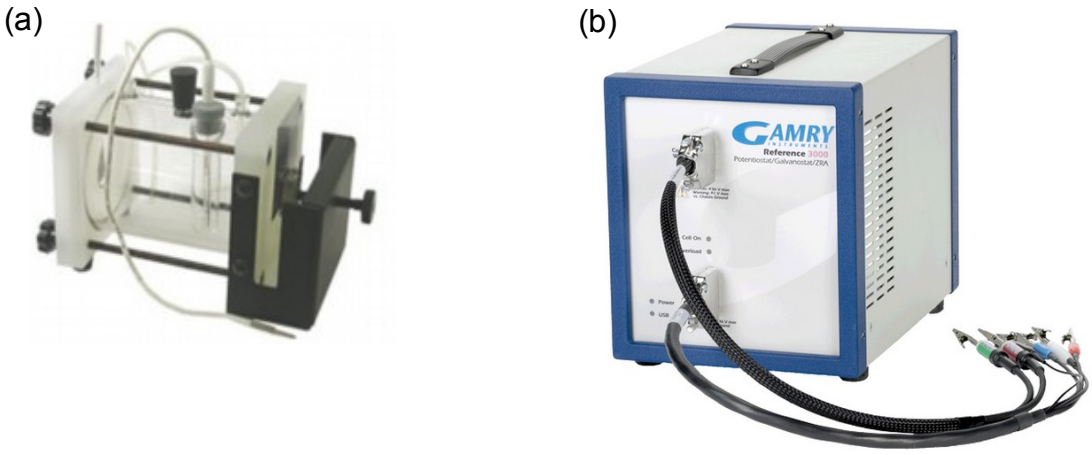

Figure 4.18. a) Gamry electrochemical cell serving as the galvanic cell and b) Gamry 3000 potentiostat used for potentiodynamic polarization [89].

Samples were placed in the galvanic cell with an area of $1cm^2$ exposed to the simulated seawater. Open circuit potential (OCP) measurements were conducted on the samples for approximately two hours to allow the system to stabilize prior to performing the potentiodynamic measurements. Potentiodynamic measurements were performed at the rate of 0.5mV/s between a voltage of -0.3 to 1.0V. The voltage is swept from negative to positive between the reference and working electrode while the response of the system is measured. The system response is measured at each voltage in the form of current density.

5. The Biomimetic Response of Interfacially Modified Thermal Spray Templates

In this chapter, interfacially driven property enhancements of deposited flame spray coatings using ceramic oxide rods will be discussed. Following the design requirements of natural nacre, ceramic rod flame spray was used to deposit alumina coatings with a brick wall microstructure. Through interfacial modifications via polymer infiltration, the biomimetic response of thermally sprayed materials can be tailored to more closely resemble that of nacre. Moreover, the thermal spray deposition process is quick and can be scaled up easily, and the ratio of polymer to ceramic closely resembles natural nacre making it an ideal template for this biomimetic material. In addition, of the approaches to fabricate nacre-like materials previously discussed, few of them actually have the volume ratio of brittle to ductile components observed in nacre. Some of these techniques can have more than 20% polymer. This chapter will focus on the interpretation of synergistic improvements in properties modified coatings display.

5.1. Application of Natural Design Requirements to Deposit a Template for a Nacre-like Material

As previously discussed, in order to engineer a biomimetic material three key steps should be met. The process includes, identifying a model natural material, identifying key mechanisms, structures, and design principles for application to man-made materials and finally the design and fabrication of a biomimetic material. Due to the fact, that natural materials such as nacre, are usually arranged in a hierarchical structure over several length scales, this process can be quite complex. However, the nature of thermal spray coatings provides an ideal template for the production of biomimetic nacre-like structures. Inherent in the thermal spray structure are several length scales. For instance, they contain micron thick bricks or splats with nanoscale interfaces. In addition, due to the spray process and processing parameters, microstructures with a varying degree of interfaces and arrangements can be deposited.

Saint-Gobain's Rokide® spray system was utilized to fabricate alumina coatings at a 4.5in standoff distance using alumina rods as feedstock. The Rokide® spray system is advantageous because particles are not able to leave the unit until fully molten. Therefore, all particles

deposited on the substrate are fully molten due to their high kinetic energy and thermal mass after leaving the unit. This eliminates any coating defects due to unmelts or semi-molten particles, leading to fewer globular pores and voids when compared to other spray processes. In fact, coating deposition via the Rokide® spray system leads to a relatively uniform and organized structure, Figure 5.1. Following deposition, Rokide® coatings were removed from substrates by mechanical means as opposed to dissolution of the substrate in aqua regia. Following substrate removal coatings were cut to appropriate dimensions for mechanical testing.

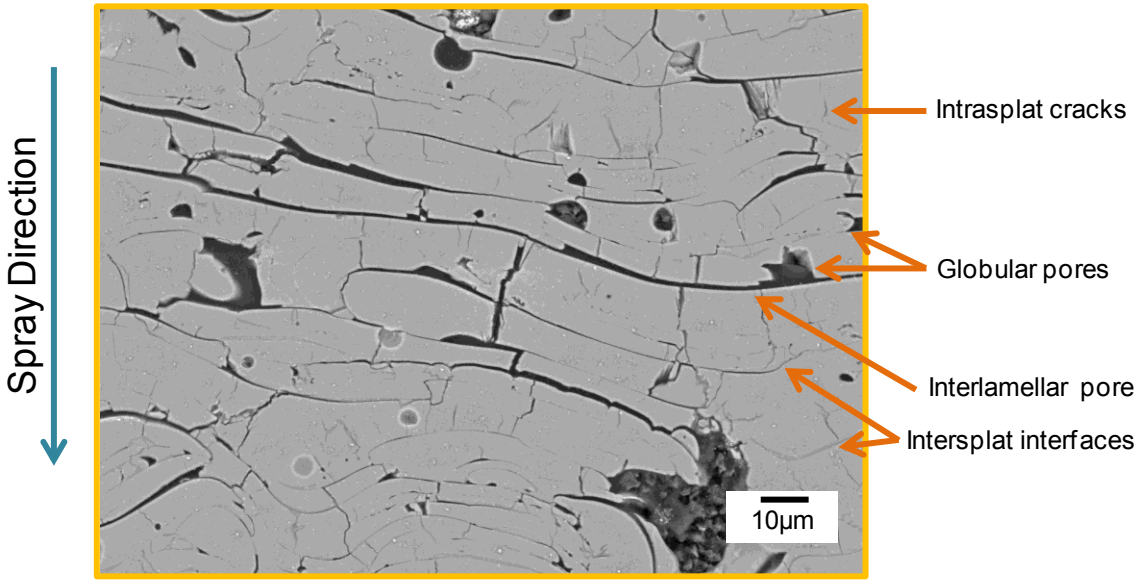

Figure 5.1. Typical cross section of an alumina coating deposited using the flame spray process and alumina rods as feedstock. Notice the highly layered and organized structure which is similar to natural nacre.

The staggered and lamellar microstructure observed from ceramic rod spray formed deposits is highly desirable for a biomimetic material. Natural materials like nacre also display an organized arrangement over several length scales as seen in Figure 5.1. This high order of organization helps to contribute to their outstanding properties. Furthermore, both nacre and thermal spray deposits have brittle and stiff tablets arranged in a staggered fashion.

Another benefit of the ceramic oxide rod deposition process is that individual tablets have some degree of waviness to them just as observed in natural nacre. Further examination of the splats indicates some degree of roughness to individual splats. This is analogous to nanoasperities on the surface of aragonite platelets in nacre. The presence of these design

features are contributing factors to the great potential TS materials possess as templates for biomimetic materials.

In addition to the microstructural resemblance of nacre and thermal spray materials is the similar mechanical response to applied loads. As discussed in detail in Chapter 2, both spray formed deposits and nacreous assemblies exhibit anelasticity, a combination of hysteresis and nonlinearity exposed to cyclic loading. Exhibition of nonlinearity is significant because its presence indicates high stresses are redistributed to allow for greater deformation. This is an indication of enhanced performance in a material, especially in ceramics where it introduces a quasi-ductile response in solids that should otherwise be brittle. Hysteresis is important because it is an energy dissipative process. The combined microstructural attributes and mechanical similarities between nacre and TS materials will be further enhanced when a second ductile phase is incorporated into a sprayed template post deposition leading to interfacial modifications.

5.2. The Effect of Interfacial Modifications on Ceramic Rod Thermal Spray

To build upon the nacre-like design of the laminated thermally sprayed templates they were treated post deposition with polymeric material. Incorporation of a softer and ductile phase into the interfacial gaps and coating defects results in a lamellar material that now displays a brick and mortar microstructure as observed in nacreous assemblies. Polymeric materials tend to be flaw tolerant, however, they experience deformation under the application of minimal stresses. Ceramic materials are extremely strong and also brittle. They have poor resistance to cracks or surface flaws. Therefore, the idea is to combine two materials, ceramic and polymer, with poor macroscale properties and achieve properties that surpass those that would be expected by the "rule of mixtures."

Samples were infiltrated with a number of different ductile phases as per the procedures in the experimental section. Testing under three-point bend loading conditions shows the presence of a softer organic phase at the interfacial spacing and defect sites leads to tremendous enhancements in the flexural strength of the oxide rod spray formed templates. As sprayed coatings were found to have a flexural strength of approximately 30MPa, Figure 5.2. Through post deposition chemical infiltration, the flexural strength was enhanced to over 200MPa, with the addition of less than 3.5wt% polymer in the case of the 5:2 epoxy heat treated sample, Figure 5.2.

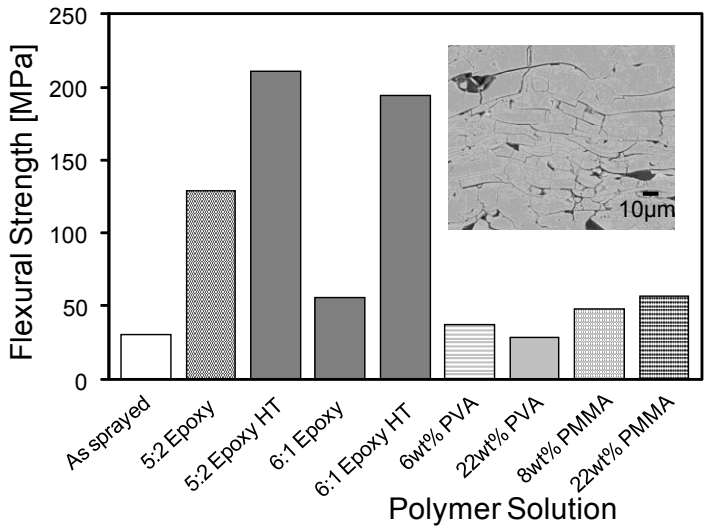

Sample	Polymer Content
5:2 epoxy	3.46%
5:2 epoxy HT	2.47%
6:1 epoxy	2.69%
6:1 epoxy HT	1.93%
6wt% PVA	0.15%
22wt% PVA	0.06%
8wt% PMMA	0.17%
22wt% PMMA	0.57%

Figure 5.2. Alumina Rokide® samples sprayed at a standoff distance of 4.5in on a carousel tested under three-point bend loading conditions in the as sprayed condition and after infiltration with various secondary phases.

Based on the results a 5:2 epoxy heat treated sample was notched and tested under three-point bend loading conditions for fracture toughness determinations because it showed the highest enhancement levels post deposition, Figure 5.2. It is likely that the presence of heat treated epoxy at defective sites of thermally sprayed coatings shows the highest property enhancements because this creates the strongest interfaces when compared with the other polymers tested. The heat treated epoxy serves as an adhesive which has the ability to allow splats to slide on one another but at the same time it can hinder and help limit the interfacial splat sliding in the same way the biopolymer does in nacreous assemblies. In the cases of PMMA and PVA, the overall properties of the composites are not as strong as for heat treated epoxy and this could be due to the weaker interfaces which do not serve as a means of locking splats to one another. Based on the results it is clear through post deposition treatment that properties of the nacre-like engineered composite can be tremendously enhanced.

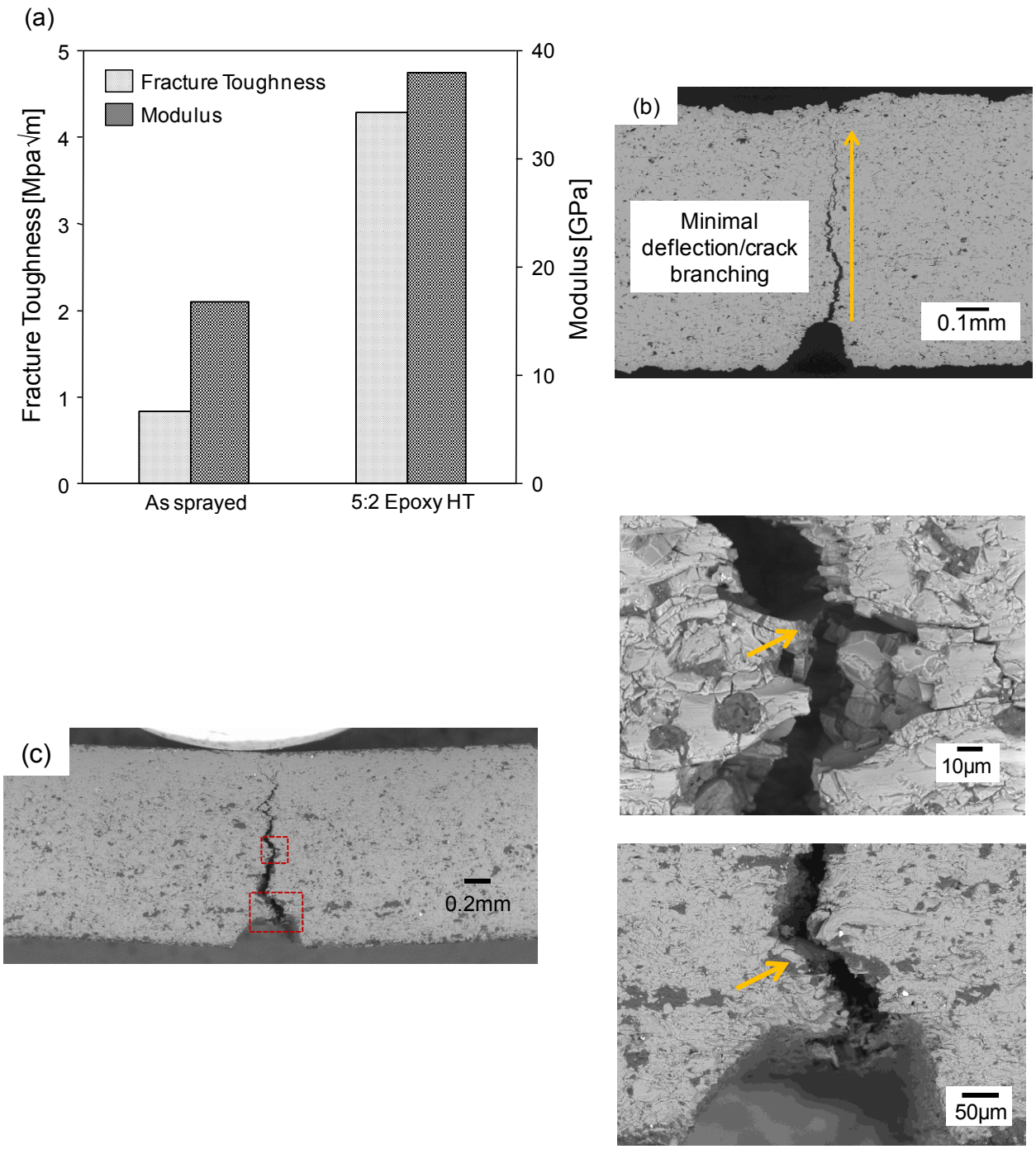

Figure 5.3. a) Fracture toughness versus modulus for alumina rod specimens tested under three-point bend loading conditions for fracture toughness and modulus measurements. b) SEM image of the crack path through an as sprayed coating. There appears to be little crack deflection through the through thickness of the specimen. c) SEM micrographs of the propagating crack through a staged cure epoxy sample. It appears that polymer ligaments or bridges are still intact.

Not only was flexural strength enhanced, but the fracture toughness, indentation modulus, and hardness as well Figure 5.3 and Figure 5.4. These results are important because of the

synergistic effects observed with the addition of a few wt% polymer which are comparable to what is observed in natural nacre. It is important to note that microindentation for modulus determination is an extremely localized test with only a few hundred microns of material being sampled, so results are likely to vary with each test. However, the main trend would still be the same; infiltration with a softer material leads to enhancements in modulus.

Addition of epoxy at the interfaces can enhance fracture toughness, Figure 5.3. The increase in toughness can be expected because polymer serves as a means of deflecting a travelling crack. SEM images indicate polymer stretching along the crack length, in the direction of the crack propagation, Figure 5.3. A crack tip can encounter polymer causing the sharp tip to become blunt, thus deflecting the traveling crack. The crack may even stop propagating until a critical stress is reached to result in the reinitiation of the traveling crack. The staggered arrangement of the ceramic splats can also serve as a means of increasing toughness because now the crack must travel in a zigzag pattern along the polymer interlayer between the splats. The deflection caused by the ductile interfaces is clearly observed in the crack path through the as sprayed and staggered epoxy infiltrated interface. There is little crack deflection in the as sprayed specimen as the travelling crack does not encounter the presence of any tough media at the interfaces. Therefore, it takes the shortest path. As a crack encounters polymer in the infiltrated specimen, it is deflected by the low stiffness interfaces. This is evidenced by the crack path in Figure 5.3 which encounters a number of changes in direction and crack branching.

Layer by layer materials can be deposited via thermal spray processes to produce manmade composites with properties such as strength and fracture toughness in the range of nacreous assemblies and in some cases properties that surpass those of natural nacre.

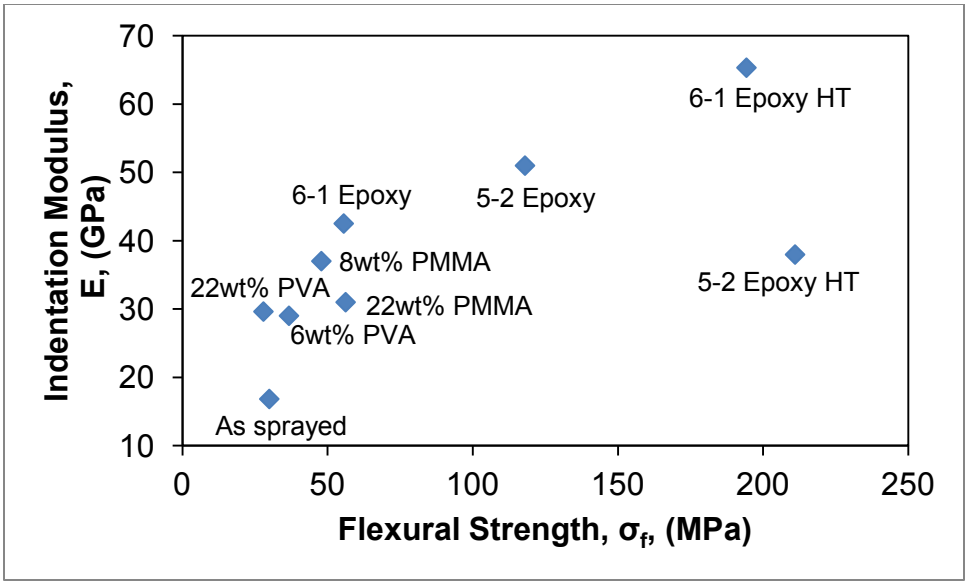

Figure 5.4. Indentation modulus vs. flexural strength of Rokide® coatings sprayed at a 4.5in spray distance on a rotating carousel. Results are important because there appears to be benefits associated with the presence of a softer and tougher material incorporated into a ceramic thermally sprayed template.

5.3. Effect of the Cross Linked Density of Epoxy on Thermal Spray Ceramics

In order to achieve optimal performance from an epoxy, the cure needs to be optimized, including the curing temperature and cure duration. Buehler EpoThin Resin and EpoThin Hardener are capable of curing or cross-linking at room temperature. When an epoxy is cured, it becomes cross-linked resulting in a complex three dimensional structure. Many epoxies can be cured at room temperature, resulting in a minimum cure, but can also be cured at an elevated temperature. A minimum cure is defined as one in which the epoxy is no longer wet to the touch. However, most epoxy mixtures will not achieve their full mechanical or physical property potentials if not cross linked at elevated temperatures.

Curing at room temperature allows for the cross-linked structure to form slowly and results in a more expanded structure. As the formation of the expanded network structure occurs, there is decreased mobility of any unreacted groups and they are blocked from reaching any open reactive sites preventing any further cross linking. By curing an epoxy at a higher temperature, the cross linking density is higher and a greater degree of cross linking occurs. Chemical reactions are initiated quickly and molecules can completely form an expansive three dimensional network if there is sufficient kinetic energy provided the system through curing at

an elevated temperature. Achieving a high degree of cross linking is what enables an epoxy to achieve its optimal mechanical and physical properties, including strength, hardness, and modulus. This is corroborated by the results shown in the previous section.

In order to overcome a major disadvantage associated with lower temperature cures in that the cross linked density is not as high, cures can be completed at higher temperatures. One way to accomplish this is by performing a staged cure which includes a high temperature post cure step following a room temperature cure. Infiltrated samples were left to cure for 8hr at room temperature so some-cross linking could initiate building a network structure. Following the room temperature curing, samples were placed in the furnace for a high temperature post cure allowing for a higher degree of cross linking and thus improved mechanical properties. Another way to accomplish this is by performing a fast cure in which the epoxy is simply cured at an elevated temperature for a couple of hours.

Experiments were performed to determine if an initial formation of a cross linked network at room temperature followed by a high temperature curing step was beneficial in achieving the highest flexural strength and fracture toughness levels. Results supported the fact that a staged cure led to higher property enhancements when compared to a fast cure. However, the benefits associated with a staged cure were slight when compared to the fast cure.

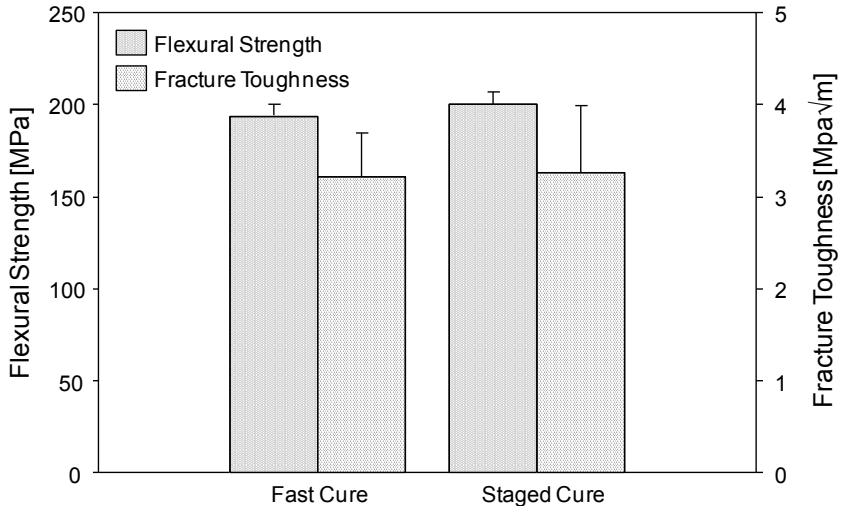

Figure 5.5. Flexural strength and fracture toughness measurements calculated from three-point bend loading of alumina rod flame spray freestanding coatings infiltrated with epoxy and cured through either a fast cure or staged cure. Results are almost equivalent, however, the staged cure has slightly higher mechanical properties.

5.4. Effect of Template Modifications on the Property Enhancements of Thermal Spray Composites

One of the major advantages in using thermal spray to deposit hard ceramic networks for nacre-like materials is the tunability of the spray processes and their effect on tailoring a unique microstructure for optimal templates. Using the Saint-Gobain Rokide® spray system, a number of coatings were deposited on a rotating carousel with identical spray parameters, but altering the spray distance or standoff distance. The idea is that by increasing spray distance, porosity level could also be altered allowing for a higher degree of interfacial modifications. Through increasing standoff distance, it was assumed it would be possible to increase interfacial gap size and therefore more polymer would be able to be incorporated into the brittle ceramic templates. ImageJ was utilized for image analysis on cross sections of the microstructures of coatings deposited at 4, 5, and 6in standoff distances and porosity level was analyzed. According to Table 4, this is exactly what happened. As the spray distance was increased from 4 to 6in, the percent of porosity increased from 12.9 to 17.6%.

Table 4. Porosity level and standoff or spray distance for three sets of Rokide® specimens.

Standoff Distance (in)	Porosity (%)
4	12.9
5	14.6
6	17.6

In the previous section it was shown that the greatest improvements in flexural strength occur when a thermally sprayed template is infiltrated with a 5:2 mixture of epoxy from Buehler a division of Illinois Tool Works Inc. and then heat treated for 2hr at 200˚C. Therefore, not all polymers were examined in determining the effect that standoff distance, and thus porosity level had on the level of property enhancements. Coatings were only tested as sprayed, infiltrated with a 5:2 epoxy, heat treated after infiltration with a 5:2 epoxy mixture, and 22wt% PMMA. Results of the three-point bend measurements proved to be very interesting. First, it was concluded that the standoff distances of 4in and 5in produced coatings with nearly identical flexural strengths and fracture toughnesses, Figure 5.6 and Figure 5.7. The flexural strength and fracture toughness of the sample sprayed at a 6in standoff were lower, although still relatively close. It is likely that the values were lower because there is a higher degree of porosity, and the splats are more loosely bonded. Due to the fact that there is probably a lower degree of cohesion between the splats and the structure is looser, when a load is applied, a lower level of deformation can be accommodated so specimens fracture sooner.

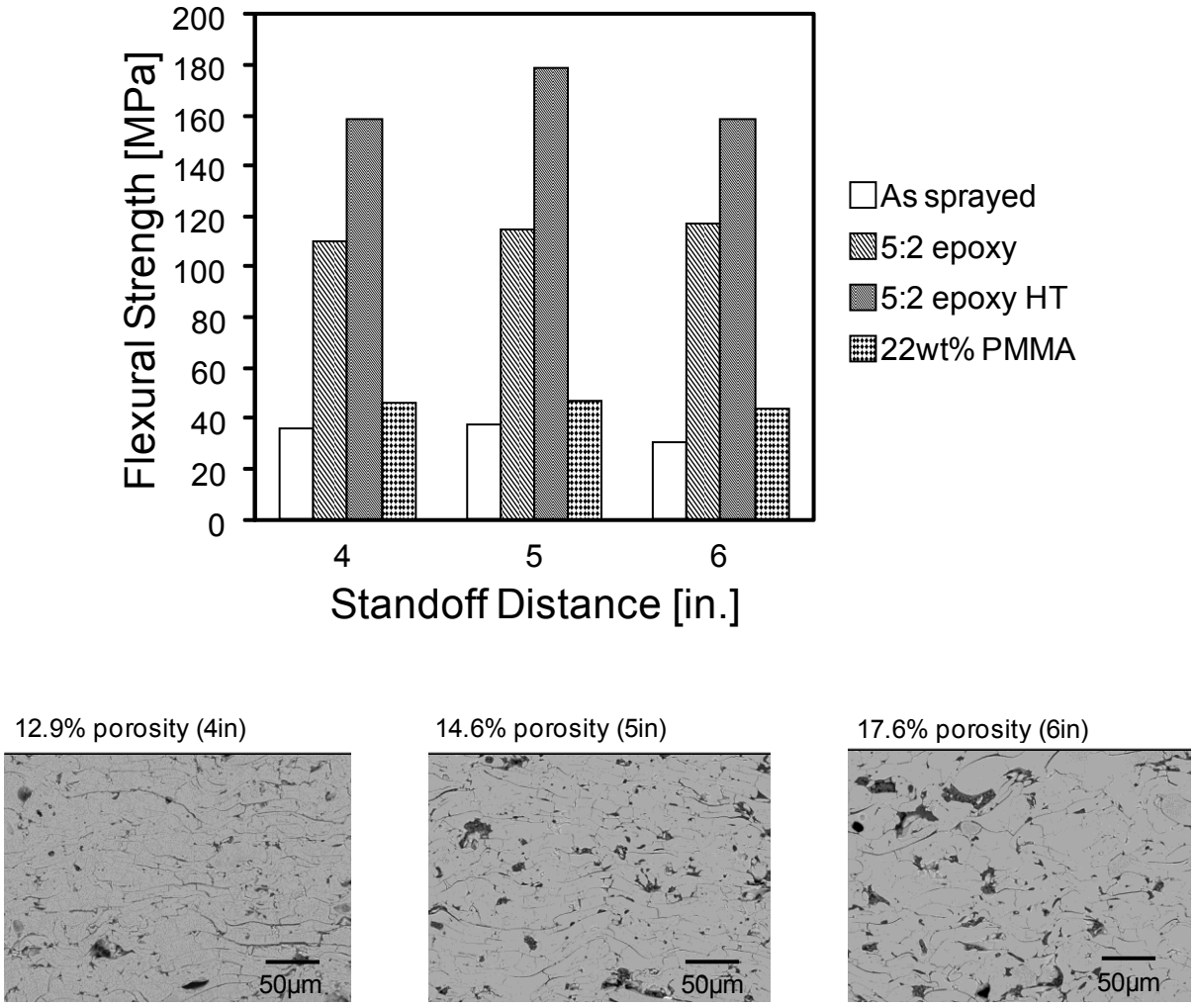

Figure 5.6. Flexural strengths of Rokide® samples sprayed at a spray distance of 4, 5, and 6 inches. In all cases, the maximum strengths are quite similar across all spray distances.

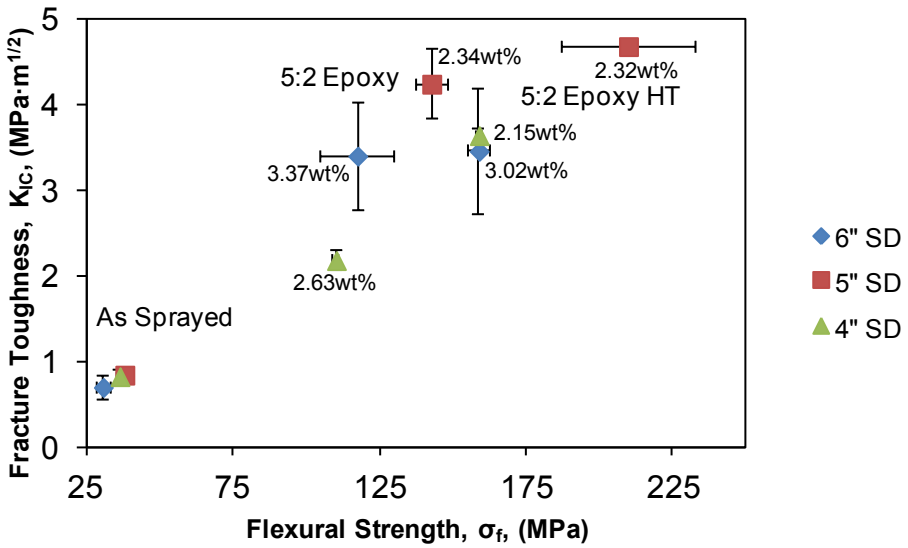

Figure 5.7. Specimens sprayed at a 5in SD have the highest fracture toughness and flexural strength for as sprayed and infiltrated conditions suggesting the porosity level of these specimens (14.6%) is optimum in replicating a nacre-like response. It is interesting to note the as sprayed fracture toughness and flexural strength for the 4in SD (12.9% porosity) specimen is nearly equivalent to that of the 5in SD specimen but a higher porosity level is more important when it comes to impregnation by a second phase. Polymer content (wt.%) of each infiltrated scaffold is provided on the graph.

What is particularly interesting about the results is that there appears to be a porosity level in which the increase in fracture toughness and flexural strength can be maximized. At a 5in SD (14.6% porosity) the alumina templates show the greatest enhancement in flexural strength and fracture toughness. When infiltrated with 5:2 epoxy and heat treated, the flexural strength increases from 37.7 ± 2.0MPa to 209.5 ± 22.7MPa. The fracture toughness is enhanced from from 0.85MPa·√m to 4.69MPa·√m. If interlamellar spacing is large, as in the case of the ceramic oxide rods sprayed at 6in, mechanical properties like flexural strength and fracture toughness will be lower than if the gap size is smaller. However, interlamellar spacing cannot be too small or the material would behave closer to a bulk ceramic. In order to achieve nacre-like mechanical properties, there needs to be tablet sliding. With gaps that are too large, the contact area between the splats is reduced which produces lower strength and fracture toughness. With a standoff distance of 5in., the contact area is optimized and this is observed in the highest as sprayed properties and the greatest property levels following post deposition infiltration.

Perhaps what is most impressive about the findings presented is thermally sprayed composite biomimetic materials have achieved properties in the range or that surpass those of natural nacre which nature has had millions of years to evolve and perfect. The flexural strength of nacre is approximately 135MPa [90] and some have found the fracture toughness to be 3.3-

9MPa·√m. The values obtained for thermally sprayed nacre-like composites have been as high as 225MPa and 4.69MPa·√m for flexural strength and fracture toughness, respectively.

5.5. Stress/Strain Behavior of Synthetic Biocomposites

Under three-point bend loading conditions, the fracture behavior of thermally sprayed biocomposites varies tremendously based on the characteristics of the secondary phase present, Figure 5.8. Due to the nature of the secondary phase, there is a different response to applied load. PMMA is a glassy thermoplastic polymer material. Thermoplastics are linear or branched polymers often having a high molecular weight and are considered simpler in terms of their structure than other polymers like thermosets. When heated thermoplastics melt, becoming pliable and upon cooling they return to their original state. At low temperatures PMMA undergoes brittle fracture which becomes more ductile as the temperature is raised toward the T_g, or the glass transition temperature. The glass transition temperature is different for each polymer and below this temperature a polymer will become hard and brittle. Other factors that can affect the glass transition temperature include the testing rate, sharpness of the notch tip, and specimen thickness. [91].

Although PMMA is a thermoplastic and exhibits brittle fracture, it is not as brittle as the fracture that is observed among thermosetting polymers which are some of the most brittle. Epoxy resins, are considered to be the strongest of the thermosetting polymers. Thermosets tend to be highly cross-linked. This cross-linking reaction is brought about by curing which causes irreversible setting of the polymer into a fused form with a complicated three-dimensional network.

(a) (b)

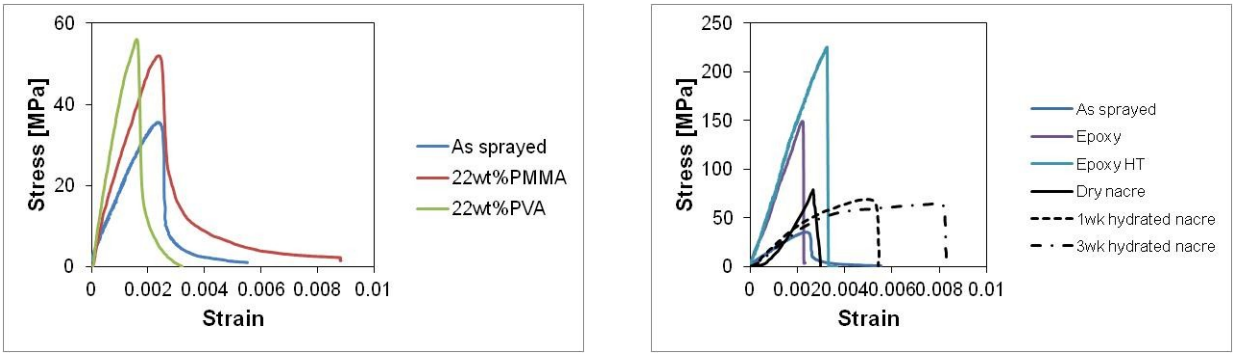

Figure 5.8. The differences in stress/strain behavior of coatings infiltrated with a) thermoplastic polymers, such as PMMA and PVA which experience more ductile fracture behavior as opposed to b) thermosetting polymers like epoxy that fail in a more catastrophic way. The stress/strain behavior of nacre from the literature is provided [92]in b) in both dry and hydrated conditions. Nacre that is hydrated shows a higher strain tolerance than the bio-inspired coatings, but the 5:2 epoxy HT sample shows a higher strain tolerance and strength than the dry nacre which is significant.

As observed in Figure 5.8, as the load being applied to the specimens is increased, the stress is increased and the energy being stored increases. The greater the amount of energy stored, the more brittle the fracture which is evidenced as a vertical line in the cases of the epoxy and epoxy heat treated samples. The energy absorption is also in extremely localized regions around the crack tip [91]. With the more ductile polymers such as PMMA and PVA, there is a more graceful failure of the specimen. The energy release rate is more gradual with the thermoplastic polymers.

The epoxy and epoxy heat treated specimens are quite impressive because they are able to tolerate a higher stress level than a dry nacre specimen and exhibit an almost equal strain tolerance. This is quite remarkable because it is possible with appropriate thermally sprayed templates and polymer choice hybrid composites can be tailored to achieve amplifications in properties comparable to nacreous assemblies. Nacre hydrated in water fails has a higher strain tolerance as the hydration period increases from 1wk to 3wk, but there is a drop in strength with the increased hydration time.

5.5.1. Examining Methods to Maximize and Improve the Toughness of Epoxies

Recently, there has been a tremendous amount of work dedicated to improving the properties of epoxy, namely the fact that it is highly susceptible to brittle failure. One method of improving the toughness of epoxy is to add second phase particles to the epoxy as either rubber particles or liquid rubbers. The idea behind the addition of a secondary phase in the polymer matrix is to provide more sites for initiation of energy absorption instead of the localized polymer region at the head of the crack tip.

Emerald Performance Materials provided four different additives to combine with the Buehler EpoThin resin and hardener. The four modifiers and their mixing directions are provided in Table 5. Following the instructions, the products were added to the epoxy mixture that was prepared as usual and heat treated for 2hr at 200˚C. Results of three-point bend experiments are provided in Figure 5.10. Based on the results the toughners provided benefits and allowed for further fracture toughness amplification. In fact, with Hypro 1300X16, the fracture toughness reached 5.7MPa√m and a flexural strength of 185MPa which is a significant improvement from the as sprayed value of 0.97MPa√m and 41MPa for flexural strength and fracture toughness, respectively.

Table 5. The name and type of the epoxy modifiers used in this study along with the recommended parts per hundred (phr) to be added to the specific side of the epoxy system as per directions from Emerald Performance Materials, Maple Shade, NJ.

Additive Name	Information	Parts per Hundred (phr)
HyPox RA840	Bis-A-Epoxy adduct of CTBN with 18% acrylonitrile in the polymer backbone. This is 40% CTBN and 60% epoxy resin	25 (added to the resin side of the system)
Hypro 1300X68	Glycidyl ester of a CTBN with 18% acrylonitrile in the polymer backbone	10 (added to the resin side of the system)
Hypro 1300X16	Amine-terminated CTBN with 18% acrylonitrile in the polymer backbone	10 (added to the curative side of the system)
Hypro 1300X21	Amine-terminated CTBN with 10% acrylonitrile in the polymer backbone	10 (added to the curative side of the system)

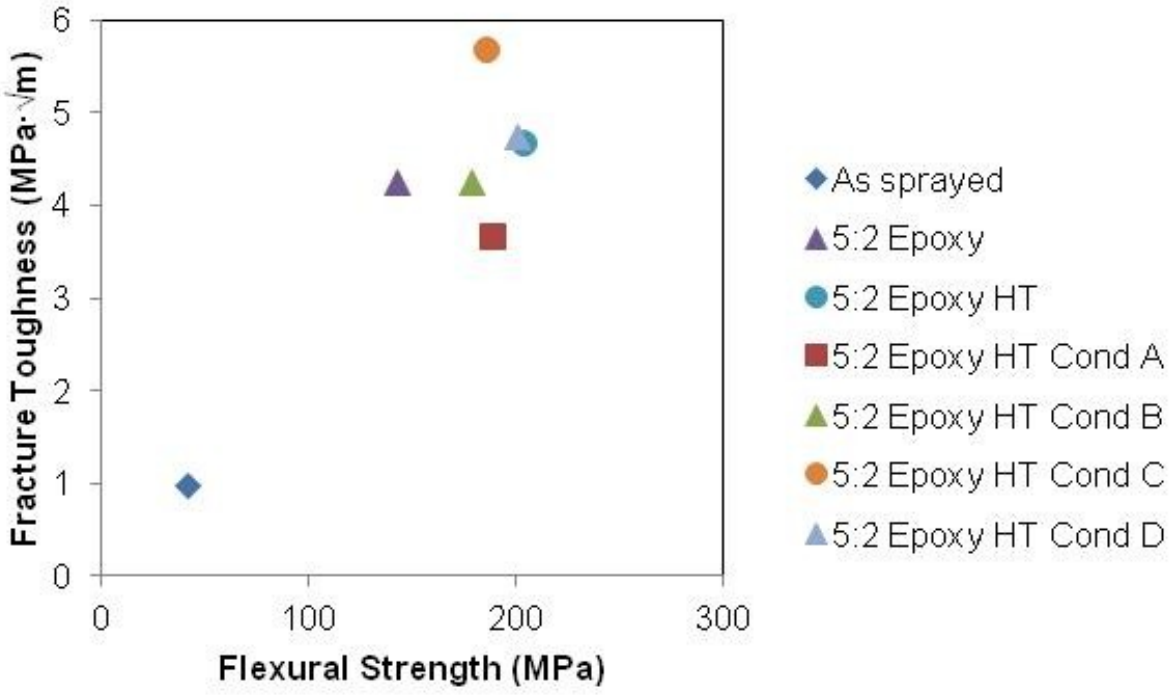

Figure 5.9. The flexural strengths and fracture toughnesses of freestanding ceramic rod flame spray samples infiltrated with epoxy. Based on the results, modifications to the epoxy can result in a higher fracture toughness but a somewhat lower strength (Condition C- HyproX16) than the highest strength observed in the sample infiltrated with epoxy and heat treated. Condition D (Hypro1300X21) modified epoxy samples has nearly the same strength and fracture toughness as the heat treated sample. In the case of Condition A (HyPox RA840) and Condition B (Hypro1300X68) the flexural strength and fracture toughness are both lower than the epoxy HT sample but both flexural strengths are higher than the epoxy sample. It appears that there is not as much of a benefit associated with HyPox RA840 and Hypro1300X68 modifiers.

5.5.1.1. Stress/Strain Behavior of Modified Epoxies

Thermoplastic and thermosetting polymers are both susceptible to brittle fracture caused by energy absorbing mechanisms such as crazing and shear yielding, only acting in regions localized to the crack tip. Thermosets are especially prone to brittle fracture, but they tend to be strong. Epoxies are among the strongest of the thermosetting polymers. With such energy absorption mechanisms being confined to highly localized regions around the crack tip, the volume of material involved in the energy absorption mechanisms compared to the overall specimen size is very low. Therefore, by increasing the volume of material involved in absorbing energy, it is possible to toughen the polymer. This is completed by initiating localized energy absorbing mechanisms from multiple sites so that a greater volume of polymer than just the

localized region around the crack tip is involved in energy absorption. Perhaps the most successful way of increasing the volume of polymer involved in absorbing energy is through incorporation of a second phase consisting of rubbery particles.

In the previous section, it was shown that the addition of a second phase in the polymer phase does lead to toughness enhancements. Examination of the stress/strain curve of these toughnened epoxies also indicates there is an increased toughness which is indicated by the slight improvement in strain tolerance and the higher degree of nonlinearity in the stress/strain curve prior to fracture, Figure 5.10.

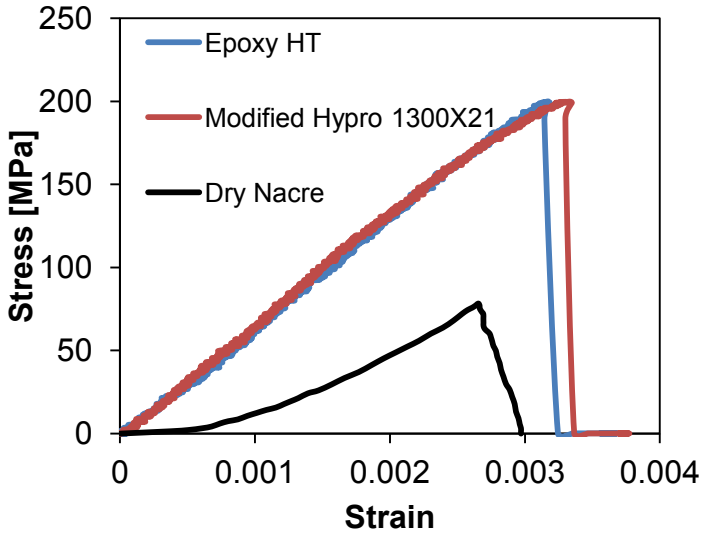

Figure 5.10. Stress/strain behavior of ceramic rod flame spray coatings infiltrated with epoxy and a modified epoxy mixture using 10phr (parts per hundred) of Hypro 1300X21 additive. Both samples were heat treated for 2hr at 200˚C. The stress/strain behavior from a sample of dry nacre is provided from the literature [92]. Modification of the epoxy mixture allows for a sample with nearly the same strength but with an enhanced strain tolerance. This suggests the modification had the desired impact of toughening the epoxy mixture.

5.6. Contributions of the Polymer Phase to the Biomimetic Nacre-like Response of Thermally Sprayed Coatings

Of all natural materials, nacre has gained the most notoriety and is of the most interest to scientists and researchers due to its superior mechanical properties despite having such a high mineral content. Nacre is the focus of numerous biomimetic studies which seek to apply features of biological materials to engineer synthetic materials. Thermally sprayed materials can be interfacially modified and shown to have properties that approach or surpass those of natural

nacre. The tremendous property enhancements that are measured in chemically treated TS coatings are due in part to the presence of polymer at the interfaces and also the inherent defects present in coatings.

Presence of a secondary more ductile phase incorporated into TS templates serve as a means of significantly enhancing mechanical properties of thermally sprayed coatings and thus the biomimetic response. Thermally sprayed coatings have a number of microstructural attributes that make them similar to nacreous assemblies, but the presence of polymer brings about striking similarities in the mechanical response of the hybrid composites. TS coatings which are formed from successive impingement of molten particles onto a substrate's surface result in the formation of splats which build up to form laminated materials. Each splat has some degree of surface roughness and is bonded to neighboring splats, however, some are more loosely bonded. When soft polymeric material is present at the interfacial gaps it serves as a means of providing cohesion between the splats over large sliding distances and possibly lubrication when loads are applied and the composite is in tension. This in combination with the surface roughness and waviness of individual splats helps provide initial resistance to splat sliding and generates hardness. In this chapter the biomimetic response of post deposition infiltration of thermally sprayed coating templates was discussed. The following chapter will examine what changes can be made to the coating templates and how these changes affect the nacre-like response.

6. Effect of Template Characteristics and its Role on Property Enhancements

The results in the previous chapter focused on alumina rod flame spray biomimetic nacre-like composites. It was concluded that an organized microstructural arrangement as that deposited during the Rokide® process can lead to significant property enhancements of the material when introduced to polymer media post deposition. However, thermal spray includes a number of different spray processes and allows for the deposition of coatings with various architectures, Figure 6.1. Therefore, powder flame spray and plasma spray processes were utilized to deposit a looser, disordered coating and a denser, semi-organized structure, respectively. The Rokide® structure discussed in detail in the previous chapter has the highest degree of organization of the coatings in this study. This chapter will focus on changes of the critical microstructure introduced through processing changes, and the role on the fabrication of nacre-like materials.

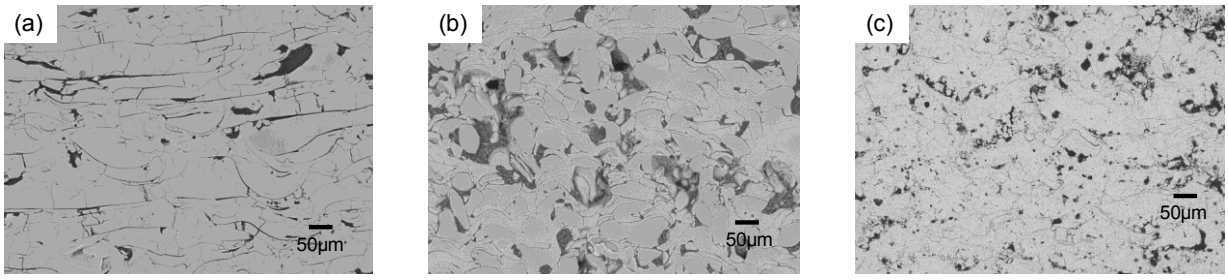

Figure 6.1. Three critical microstructures that are developed during the a) alumina rod flame spray, b) powder flame spray, and c) plasma spray process.

6.1. Loose and Disordered Powder Flame Spray Alumina

Post deposition alumina powder flame spray coatings were made freestanding and sectioned to the appropriate size as discussed in the experimental section. Substrate free specimens were then infiltrated and their surfaces polished for three-point bend testing to determine their flexural strengths. In each case, except for the in-situ polymerization samples, vacuum was used to assist in introducing the organic materials into the interfaces. Results showed that the flexural strength

of the alumina specimens were enhanced with the addition of each secondary polymer phase, Figure 6.2. The largest increase in flexural strength is for the FS alumina coating infiltrated with epoxy. PMMA dissolved in solvent and PMMA formed from in-situ polymerization both showed a similar improvement to the alumina scaffolds. PVA had a tremendous effect on improving the strength of the scaffolds, only second to the commercial epoxy. Epoxy and PDMS were both prepared in a similar manner. Specific ratios were suggested by each manufacturer of base material to hardener/curing agent, which is discussed in Chapter 4.

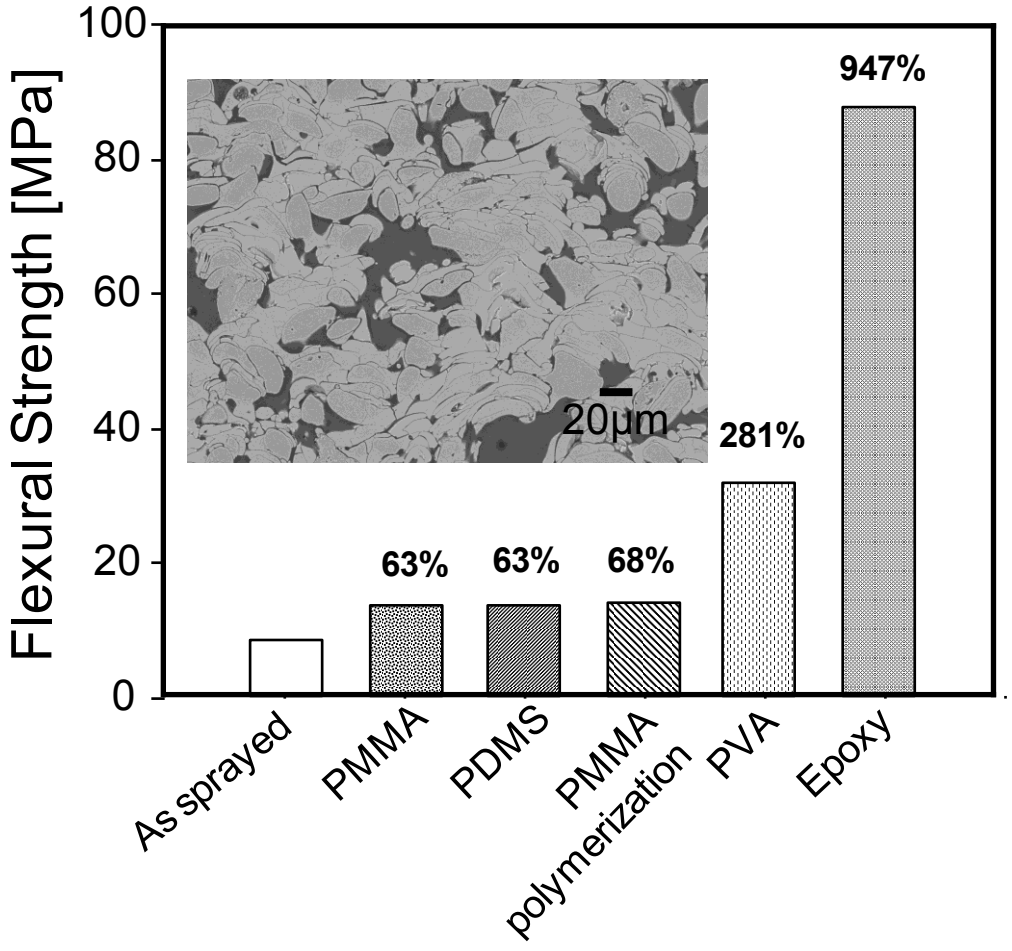

Figure 6.2. All of the polymers/sealants used to date in this study were introduced to flame spray alumina coatings. The percentage refers to the percent increase in flexural strength from the as sprayed alumina coating. Despite the introduction of a few weight percent polymer there are significant property enhancements. The epoxy infiltrated sample contains the greatest polymer percentage, 4.2wt%.

6.2. Hybrid, Dense and Semi-Ordered Plasma Sprayed YSZ Coatings

Results thus far have shown the addition of a few weight percent polymer in ceramic rod and powder flame spray alumina coatings result in synergistic improvements to biomimetic materials based on thermally sprayed scaffolds. That is, the resulting mechanical properties are far superior to what would be expected using simple composite models. This is the same observation that can be made with nacre. The addition of biopolymer interlayers that make up approximately 5vol% of the total structure result in properties far superior than what is expected based on the constituents. This is why nacre has been the focus of such intense studies. Based on observations with alumina, YSZ was plasma sprayed in order to study whether or not these same synergistic effects could be observed if the template material was changed. This could determine whether the role of property enhancements was template material dependent. As already determined, property enhancements are not polymer dependent.

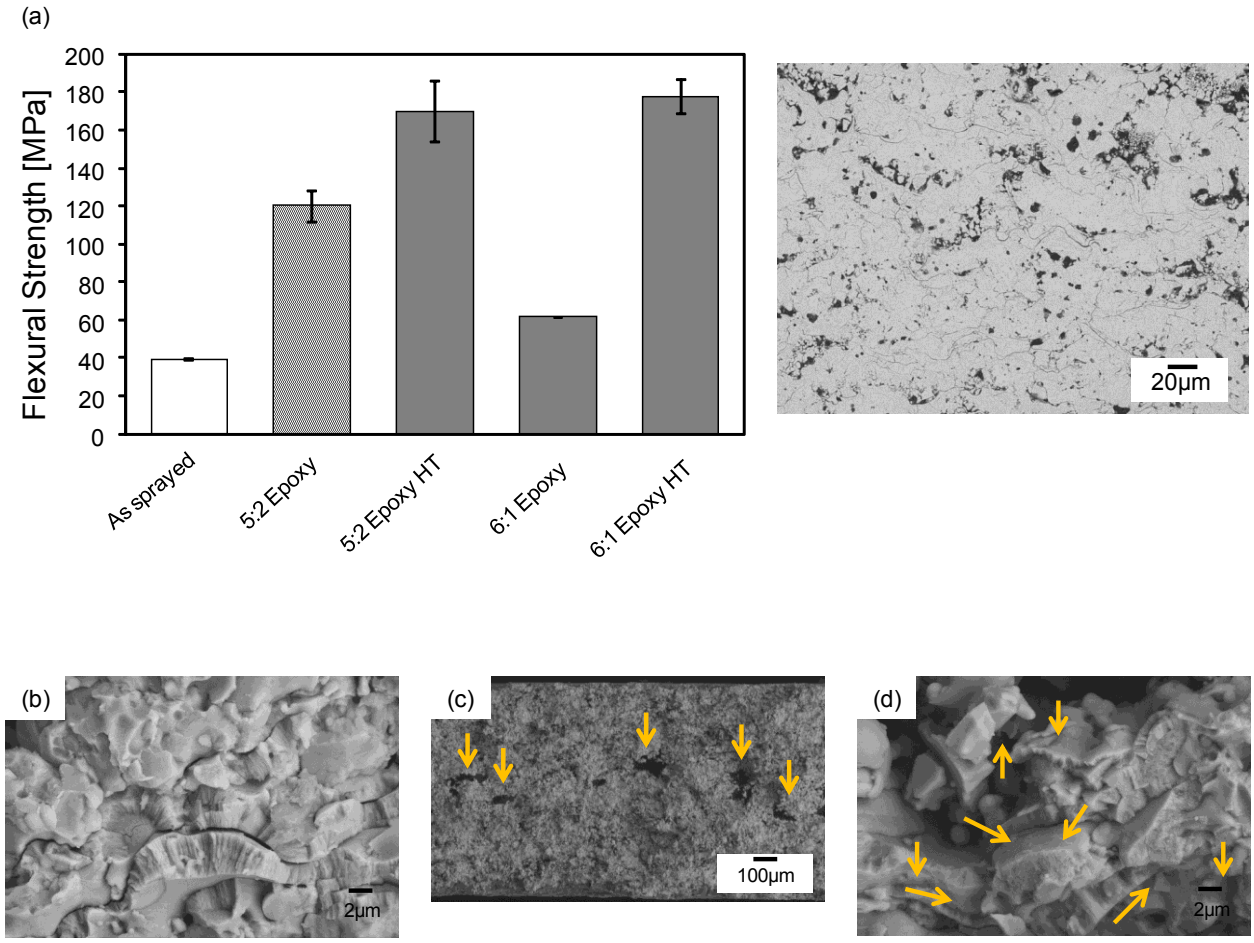

Figure 6.3. a) Microstructure of YSZ plasma sprayed on a stationary fixture and three-point bend flexural strength measurements of the as sprayed YSZ coating and following infiltration. b) As sprayed YSZ fracture surface. c) and d)YSZ infiltrated with epoxy in a 6:1 ratio of resin to hardener. Polymer is clearly throughout the entire cross section of the coating as indicated by the arrows.

Unlike ceramic rod flame spray coatings, these plasma spray coatings are more of a hybrid structure that is a cross between the layered Rokide® and disordered powder flame spray coatings. In the case of YSZ, a number of polymers were infiltrated into freestanding coatings. Again, the highest increase in flexural strength observed was with the YSZ and 5:2 epoxy heat treated. Therefore this composite system was tested under three-point bend loading conditions for fracture toughness determinations, Figure 6.4. Based on the fracture toughness experiments, the 5:2 epoxy HT and YSZ composite system displayed the greatest increase.

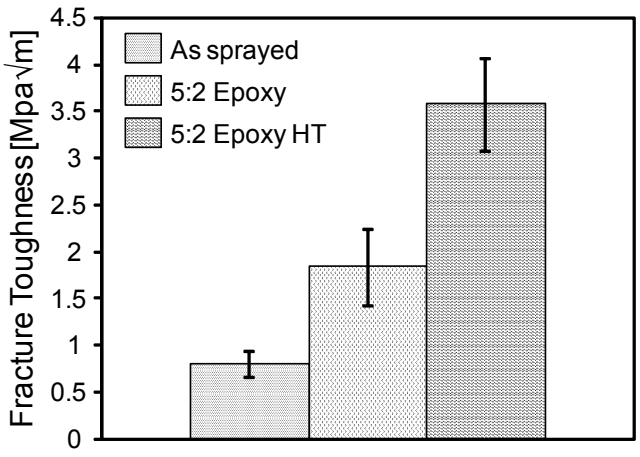

Figure 6.4. Fracture toughness measurements for as sprayed, 5:2 epoxy, and 5:2 epoxy HT YSZ specimens tested under three-point bend loading.

The presence of epoxy at coating interfaces plays a similar role as the combination of polysaccharides and proteins at the interfaces of the calcium carbonate platelets in nacre. Under a load and subjected to tension, YSZ splats slide on each other. Epoxy provides cohesion and possibly even lubrication during sliding. The grain termination sites provide roughness on the surface of the splats which also introduce some resistance to sliding, just as nanoasperities on the surface of the aragonite platelets resist sliding. The unique layered architecture of plasma sprayed coatings in combination with polymer lead to extraordinary mechanical performance.

6.2.1. The Effect of Surface Speed on Coating Property Enhancements

Two YSZ coatings were deposited on aluminum substrates using the same process parameters. However, one spray run was deposited using a stationary fixture and the second was deposited using a rotating carousel to determine how surface speed influences the microstructure of a coating and hence its properties. Altering surface speed during deposition ensured there was a porosity difference between the two yttria stabilized zirconia coatings allowing for the effect of porosity on the enhancement of coating properties to be determined. With an increase in surface speed, deposited particles experience a longer cooling period before a new layer is deposited. This leads to fewer surface interactions between the deposited layers and more porosity. A higher degree of porosity may lead to higher polymer content at the coating interfaces resulting in modification that can be related to enhancements in properties.

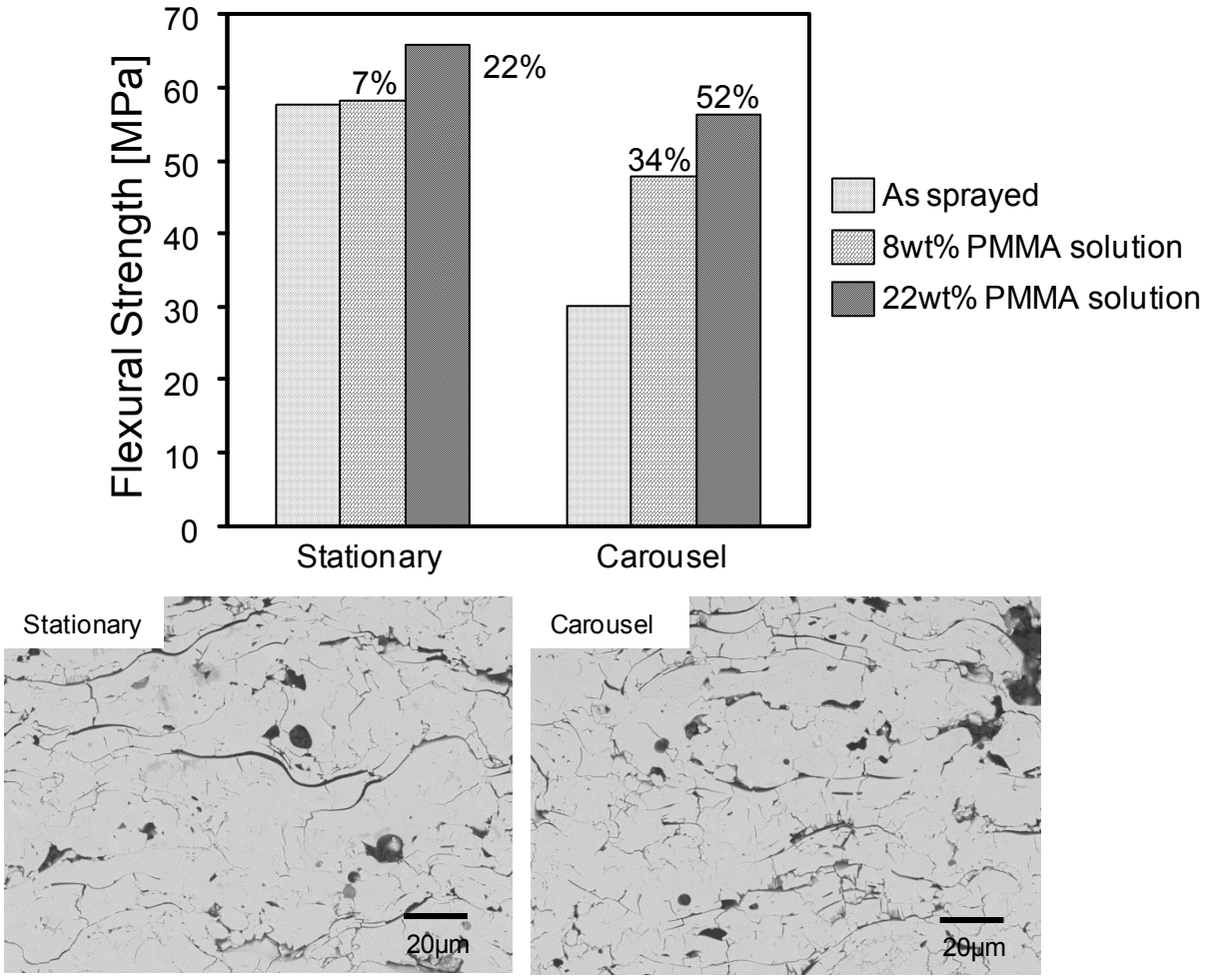

Figure 6.5. Yttria stabilized zirconia was sprayed using the same conditions on a stationary ICP beam and rotating carousel. Results from three point bend tests showed that the more porous samples (carousel) could be enhanced more as indicated by the percent increases provided on the graph, but the as sprayed denser coating had a higher flexural strength than either of the enhanced carousel samples.

Results from the three-point bend tests, Figure 6.5, confirmed that both specimens sprayed on the carousel and stationary fixtures can be enhanced in terms of their flexural strength. It makes sense the specimens sprayed on the rotating carousel can be enhanced further due to their higher inherent porosity and thus increased opportunity for polymer to be incorporated into the porous templates. However, infiltrated coatings deposited on a carousel do not reach the level of the as sprayed coatings deposited on a stationary fixture.

6.3. Low Porosity, Staggered Alumina Ceramic Rod Flame Spray Coatings

Ceramic rod flame spray coatings were discussed in detail in Chapter 5 in regard to property enhancements associated with infiltration by a secondary polymer phase and they will be briefly discussed in this chapter. Saint-Gobain's Rokide® Spray System was utilized to fabricate alumina coatings sprayed on a carousel at a 5in standoff distance. Using alumina rods, they are melted in a spray unit and projected at a surface being coated. This process is advantageous because all of the particles deposited on the substrate are fully molten due to their high kinetic energy and thermal mass after leaving the unit. Rokide® particles are not able to leave the unit until they are molten. This is different from other thermal spray processes that use powder feedstock. Powder enters a high-temperature gas stream, but do not have a sufficiently long enough dwell time allowing for all particles to melt completely. Deposition of only fully molten particles that undergo rapid quenching upon reaching the spray surfaces translates into a more organized and uniform structure that is free of defects associated with unmelts or semimolten particles.

Rokide® coatings were removed from substrates by mechanical means as opposed to dissolution of the substrate in aqua regia. Following substrate removal coatings were cut to appropriate dimensions for mechanical testing. As sprayed coatings were tested under three-point bend loading conditions and found to have a flexural strength of approximately 38MPa, Figure 6.6. Through post deposition chemical infiltration, flexural strength was enhanced to over 200MPa, with the addition of less than 3.5wt% polymer.

Not only was the flexural strength enhanced, but the fracture toughness, as well. These results are important because of synergistic effects observed with the addition of a few wt% polymer which are comparable to what is observed in natural nacre. Modification of the interfaces with epoxy leads to enhancements of coating properties, Figure 6.6. The increase in toughness can be expected because polymer serves as a means of deflecting and slowing a propagating crack. Analysis of SEM images show deflection of the crack, Figure 6.6. A crack tip can encounter polymer, blunting the sharp crack tip or deflecting the traveling crack. The crack may even stop propagating until a critical stress is reached, thus causing its reinitiation. Crack propagation can be through the polymer or around the polymer located at the interfaces. It is not likely the crack would take a path through the polymer so it would have to increase the length of its path by going around tough material at the interfaces.

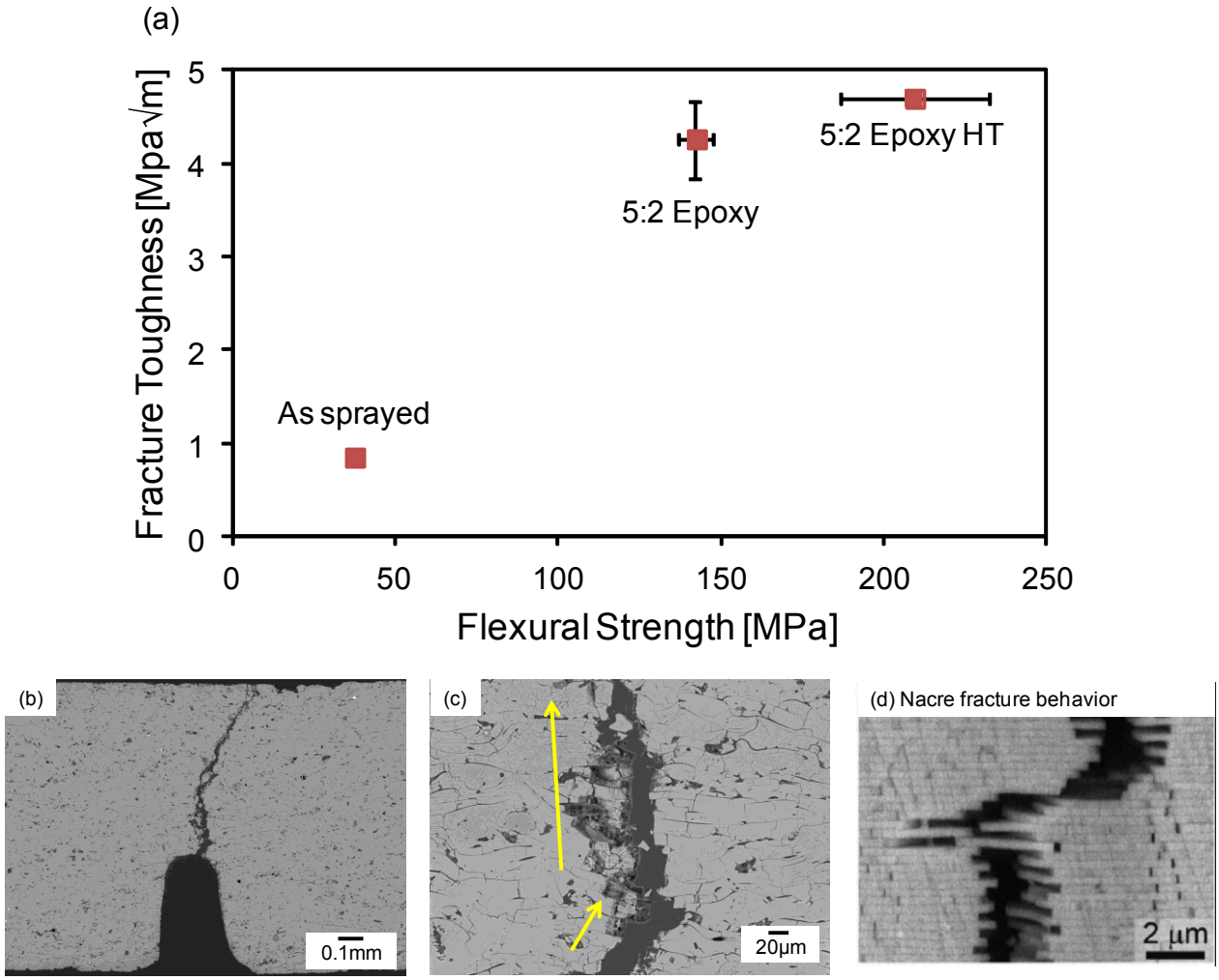

Figure 6.6. a) Alumina Rokide® samples sprayed at a standoff distance of 5in on a carousel tested under three-point bend loading conditions in the as sprayed condition and after infiltration with 5:2 epoxy as a second phase. b) and c) SEM image of the path the propagating crack followed through the through thickness of the alumina coating. The crack changes direction upon encountering polymer and shows some degree of splat pullout in its fracture surface which is similar to d) the tablet pull out observed in natural nacre [93].

6.4. Conclusions

Thermal spray encompasses a family of processes that are ideal for fabrication of nacre-like composites. Coating templates deposited via thermal spray processes are relatively inexpensive, can be deposited quickly and are easily scaled up. The key finding in Chapter 6 is that different starting templates allow for enhanced mechanical properties. However, of the three critical microstructures, greater percentage increases of coating properties and the accommodation of more polymer into the coating defects occurs when coatings are looser and more globular in their

microstructure. In Figure 6.7, the more organized alumina rod flame spray as sprayed flexural strength is in the range of 30 to 40MPa and fracture toughness is approximately 0.9MPa√m. The alumina powder flame spray with a more globular and irregular microstructure has a flexural strength of approximately 20MPa and a fracture toughness of 0.3MPa√m as sprayed. Using a commercially available epoxy from Buehler, the strength and fracture toughness can be significantly enhanced. But those more regular and organized structures show the greatest potential to reach properties exhibited by nacreous assemblies, even though, the lumpy and irregular templates can accommodate higher polymer content. For instance, the globular template containing epoxy has a polymer content of approximately 4.20% and the heat treated sample has a polymer content of 2.44% polymer. The more staggered and organized template can accommodate approximately 3.45% polymer, while the hybrid microstructure contains about 4.0wt% polymer. Globular microstructures can contain more epoxy because of the nature of the porosity, globular pores and voids. There are no regions in the staggered thermally sprayed templates containing the same level of globular pores and voids which mean epoxy is mostly be present at the interlamellar gaps. The powder flame spray coatings contain interlamellar gaps in addition to the globular pores and voids. Therefore, those templates with a higher porosity level can accommodate higher polymer content. Although more polymer is incorporated, the increases in mechanical properties associated with globular coatings thus far has not been able to reach the levels of the denser and more organized coatings because the as sprayed strength and fracture toughness is not there to begin with.

Ceramic rod flame spray coatings have a staggered microstructure, and are the most highly organized of all templates tested. Part of this reason is because the only particles deposited are in the molten state, so this eliminates defects caused by unmolten or partially molten particles. Therefore, the number of globular pores and voids are significantly reduced within a coating. The more organized ceramic rod templates were also the ones in which the highest property levels were observed, Figure 6.7. It appears that the remarkable improvements in coating properties are observed because of the organized arrangement in combination with the secondary ductile phase. This is similar to what Barthelat concludes [2, 6, 15, 52, 94] regarding the staggered arrangement of nacre from hard and stiff calcium carbonate platelets that are bonded and held together by softer materials. When a load is applied to the thermally sprayed templates, the splats can slide on one another. This is enhanced by the addition of the softer phases at the interfaces and in the defects. The thin organic layers help to control the sliding of the splats. According to the results presented thus far, with the softer secondary phase, the coating composite is able to withstand a greater degree of deformation while dissipating energy.

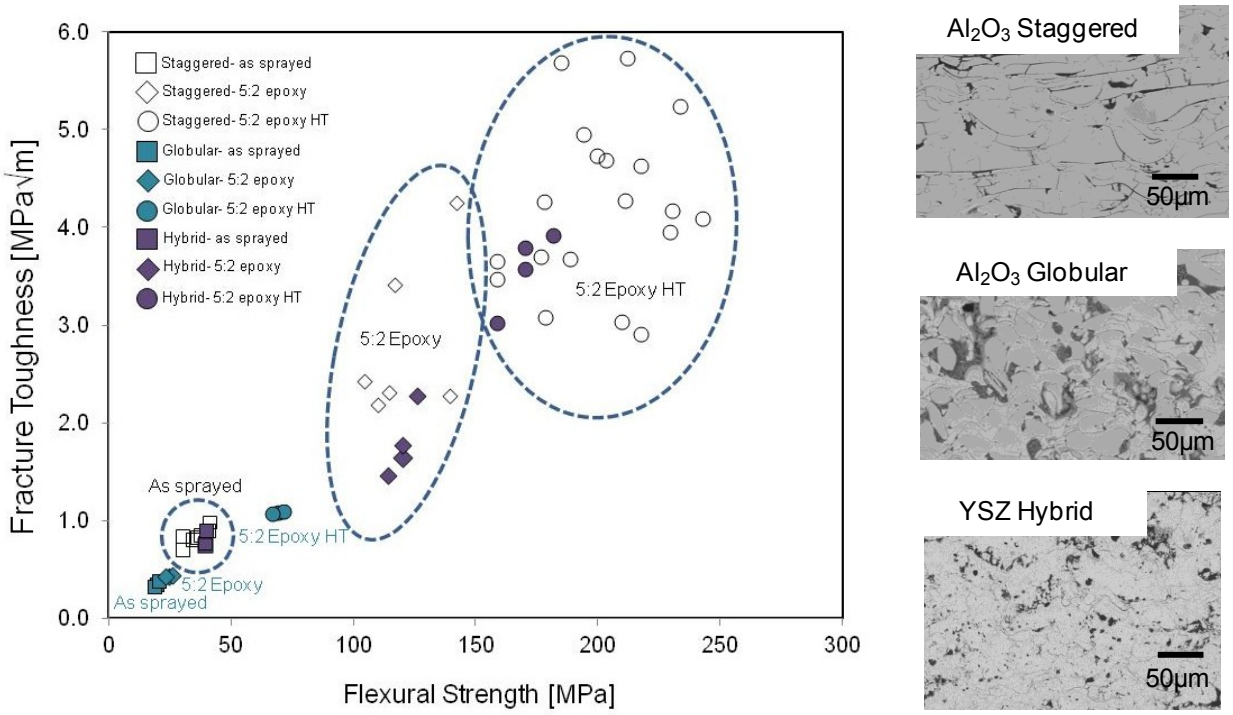

Figure 6.7. Fracture toughness and flexural strength of as sprayed and infiltrated scaffolds.

The focus of this chapter was on the three critical microstructures that can be deposited via plasma spray, powder flame spray, and ceramic rod flame spray and the improved properties that can be engineered. The following chapter will address alternate approaches to increasing the level of property enhancements through methods designed to increase the polymer content present in a given specimen.

7. Alternate Approaches to Property Enhancements of Thermally Sprayed Ceramic Templates

Image analysis of the infiltrated templates thus far have included porosity levels that range from 12% (plasma spray) to 22% (powder flame spray), while the ceramic rod flame spray coatings range from 12.9% to 17.6%. Despite these porosity levels, infiltration yielded about 2-4wt% polymer content determined by thermogravimetric analysis, depending on the sample architecture and polymer type. Therefore, four alternate approaches were devised in order to increase the polymer content for each specimen. These included, stacking a number of individual coatings, co-spraying a ceramic and metallic material so the metallic could be etched away, in-situ polymerization, and changing sample dimensions. This chapter will focus on the alternate approaches to increase the amount of polymer content in a thermally sprayed scaffold.

7.1. The Effect of Stacking Thermally Sprayed Templates on Flexural Strength

Stacked Ceramic Rod Flame Spray Templates

As previously mentioned, Rokide® coatings have porosity levels of 12.9-17.6%, but have been infiltrated with a maximum porosity level of about 4wt%. The idea was that if a higher polymer content could be incorporated into the Rokide® template then it would be possible to see a higher level of property enhancements. Through stacking several coatings, a polymer interlayer between two individual layers would be formed which is analogous to the biopolymer interlayers in natural nacre.

Several different stacked specimens were tested to examine the level of property enhancements. These systems included double and triple layer coatings that were left as sprayed and double and triple layer coatings that were separately infiltrated and then adhered together with additional epoxy. In addition, these coatings were also tested as single layer specimens both as sprayed and infiltrated with epoxy. Due to restrictions on the total number of samples the systems were infiltrated with epoxy and then heat treated. It has been shown previously that

infiltrating with a 5:2 ratio of epoxy followed by a heat treatment step of 2h at 200˚C results in the greatest coating property enhancements. Therefore, this was the only polymer tested.

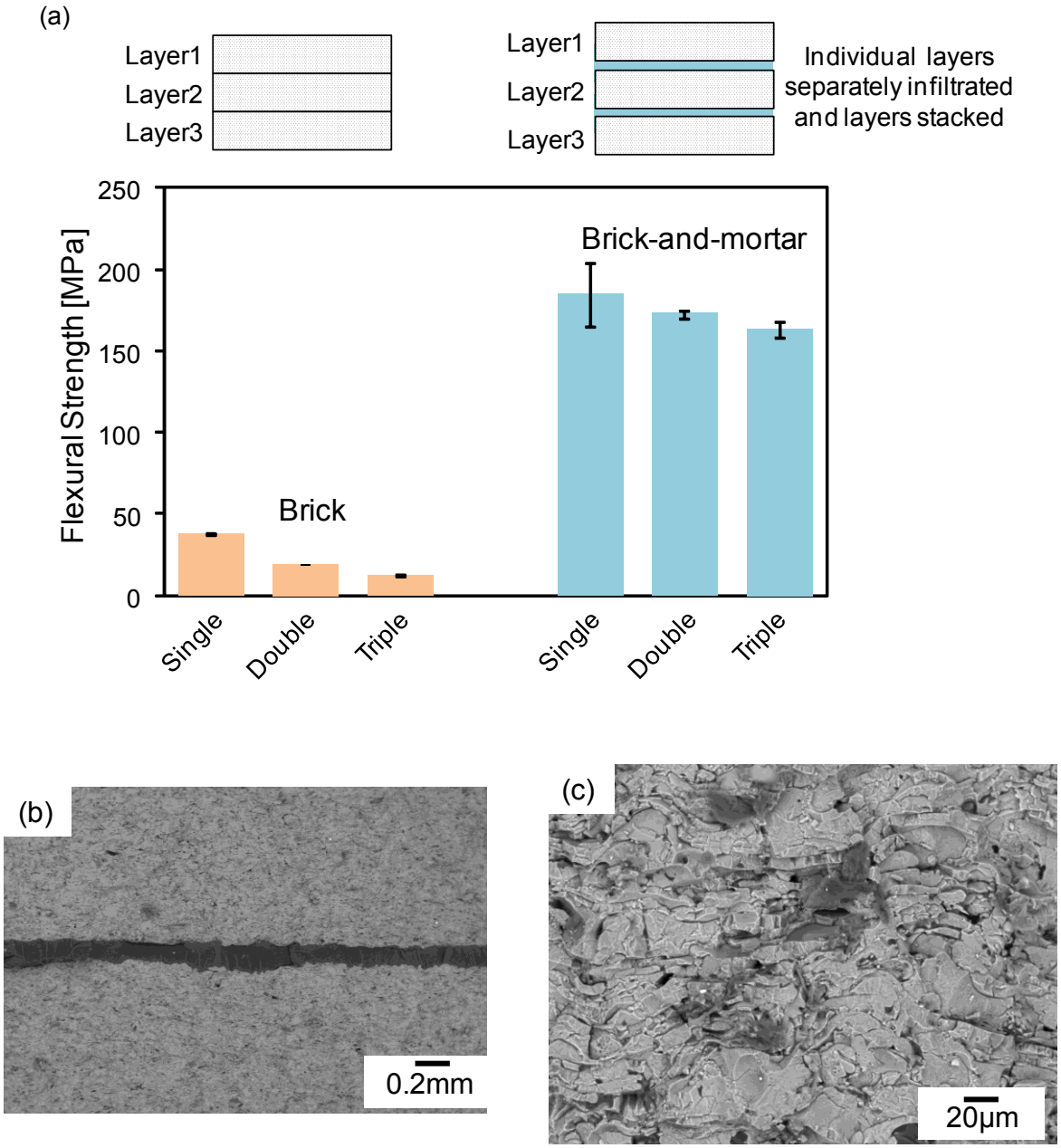

Figure 7.1. a) Flexural strength of stacked specimens. b) Fracture surface of a stacked specimen formed from three individual freestanding coatings. Each individual freestanding coating was infiltrated with epoxy and then left to cure in a stacked arrangement over night. c) As observed from a high magnification image of an individual coating from a stacked specimen, epoxy is also in the ceramic scaffold. In addition, there is a layer of approximately 50-70µm of epoxy separating each layer.

Coatings separately infiltrated and stacked together followed by a heat treatment step, show with each additional layer the flexural strength decreases. This was the same trend observed with the as sprayed coatings when an additional layer was added. The differences in the flexural strengths of the stacked sample directly related to the ease of crack propagation through the samples through thickness. For instance, when as sprayed samples are stacked and tested under three point bend loading conditions, flexural strength decreases with each additional layer. This decrease in flexural strength could be due to the fact that there is no cushioning between the layers and there is a great deal of sliding and thus the generation of frictional forces and likely crack formation due to the deflection of various layers. Under stress caused by loading the layers, their relative sliding on one another can lead to the formation of cracks. This can be surmised because if cracks were not forming, the flexural strengths observed for the stacked layers should be equal to those for the individual layers. However, this is not the case and due to the detrimental effects of stacking the as sprayed samples, the flexural strength decreases with each additional stacked layer. The same is observed for samples that have been infiltrated and heat treated with epoxy in a 5:2 ratio of resin to hardener with additional epoxy brushed on the surfaces to provide adhesion for the stacked layers.

7.2. The Effect of Sample Dimensions on Mechanical Property Measurements

Highly Porous Coatings with a Globular Porosity Arrangement

Porous flame spray coatings sprayed to yield a high porosity, Figure 7.2, were tested at several different dimensions, 2, 6, and 12mm, with a number of secondary phase infiltrates. Porous coatings were infiltrated with epoxy, 6 and 22wt% PVA, and 8 and 22wt% PMMA. Coatings were flame sprayed to have a high level of porosity, approximately 23% according to analysis conducted using ImageJ software. If this open porosity could be impregnated with a tougher phase, there exists a great deal of potential for coating property enhancements due to the high level of intrinsic porosity.

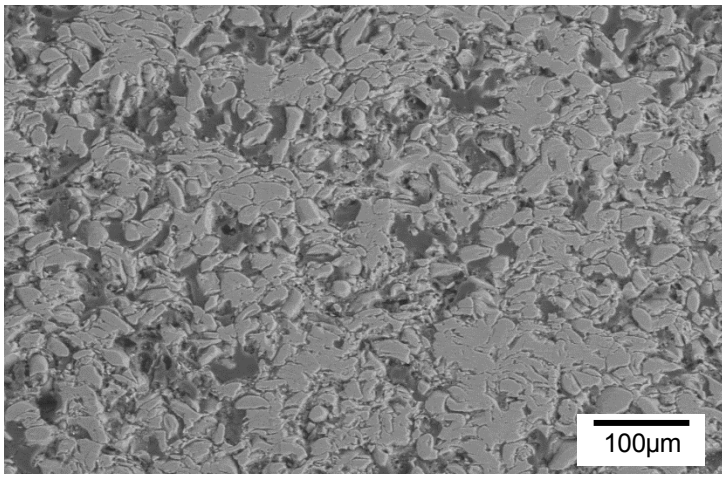

Figure 7.2. Polished cross section of highly porous flame spray alumina coatings tested at 2, 6, and 12mm sample widths with a number of polymeric secondary phases.

Interfacial modifications using a softer polymer infiltrate resulted in coatings with increased flexural strengths when compared to the as sprayed. Examination of as sprayed samples tested at 2, 6, and 12mm widths, indicate flexural strength is independent of dimension. As observed in Figure 7.3, infiltration of the flame spray alumina templates using a higher PMMA concentration results in improvements for all sample dimensions when compared with the corresponding as sprayed templates. There is also the trend for both PMMA concentrations that as the sample width decreases, the flexural strength increases. In addition, when using a higher PMMA concentration for impregnation, strain tolerance of infiltrated coating is also enhanced, Figure 7.4. This figure depicts load vs. displacement curves for the 12mm widths. Using PVA, there is an increase in the flexural strength for all sample widths when compared to their corresponding as sprayed sample widths. However, unlike with PMMA where there was the same trend observed for both concentrations, PVA did not show behavior like this that could relate sample dimension with flexural strength for the two concentrations. Another noteworthy observation is that a higher concentration did not lead to an increase in flexural strength for the flame spray alumina template with a 6mm width, but did for the 2 and 12mm cases. Just as observed in the case with a higher concentration of PMMA, a higher wt% of PVA results in an improvement in strain tolerance

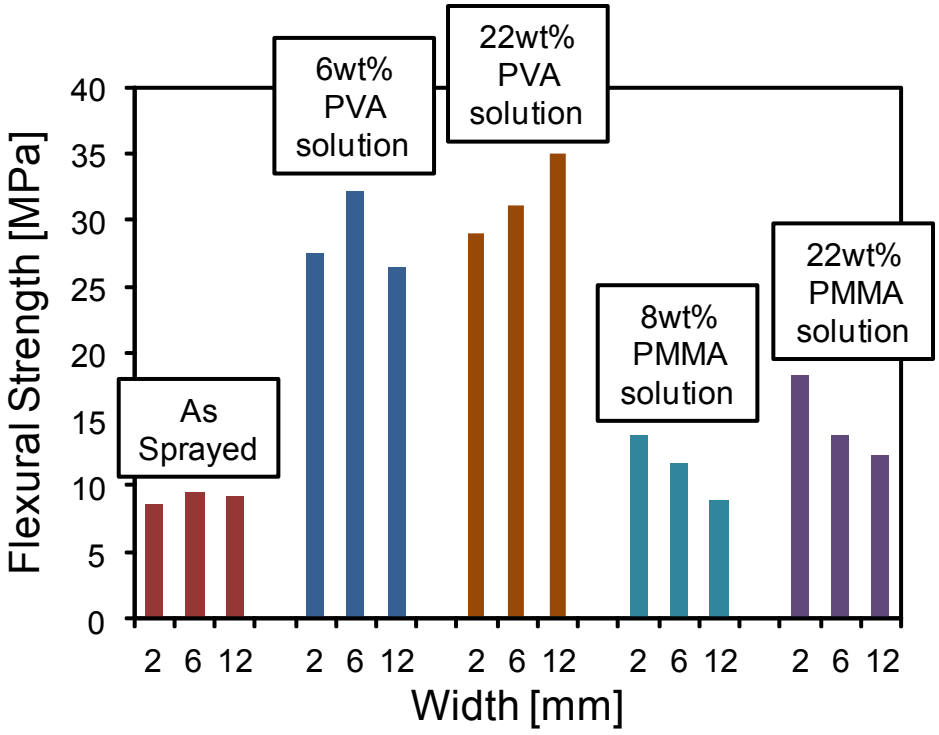

Figure 7.3. Flexural strengths for specimens tested under three-point bend loading conditions at three different widths. Flexural strength appears to be independent of sample width which is indicated by the as sprayed samples. However, when adding a secondary phase such as PVA and PMMA due to the highly defective coatings the defects present in a specific coating likely play a large role in the determination of the flexural strength. With PMMA there seems to be another factor that comes into play. Due to the high viscosity of the PMMA solution, the 2mm specimens have a higher flexural strength which is most likely due to the ease of infiltration of the smaller samples.

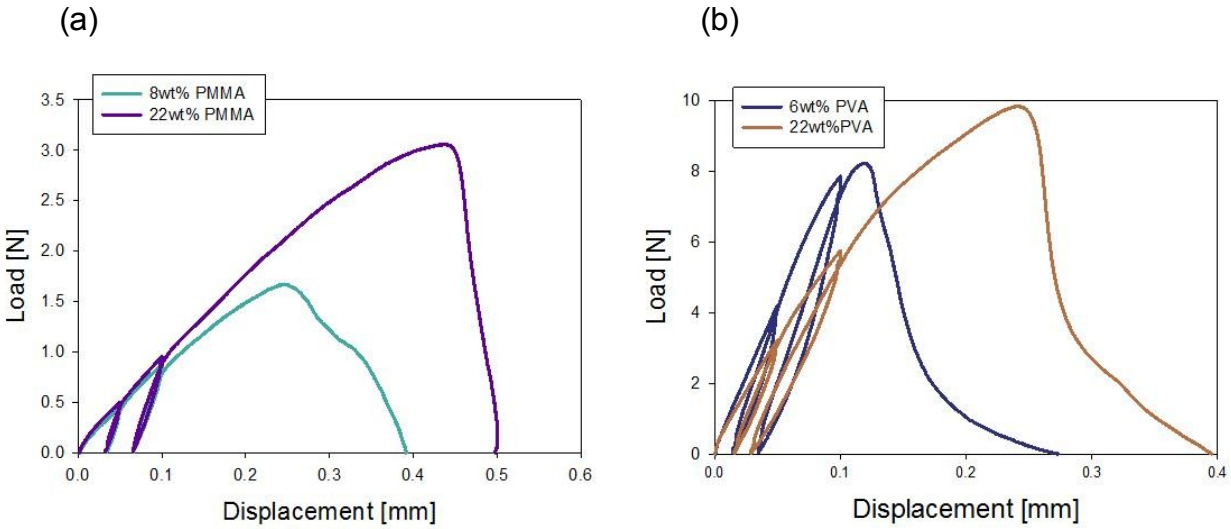

Figure 7.4. The load vs. displacement curves for the porous flame spray alumina samples with a width of 12mm that have been infiltrated with 8 and 22wt% PMMA and 6 and 22wt% PVA. As the concentration (wt%) for each polymer increases, the strain tolerance increases which is indicated by the fracture at a higher displacement.

Samples of 2, 6, and 12mm were also infiltrated with 5:2 epoxy. These coatings showed a remarkable increase in flexural strength, Figure 7.5. Just as in the case with PVA and PMMA, all of the epoxy infiltrated specimens experienced an enhancement due to the interfacial modifications caused by the epoxy presence.

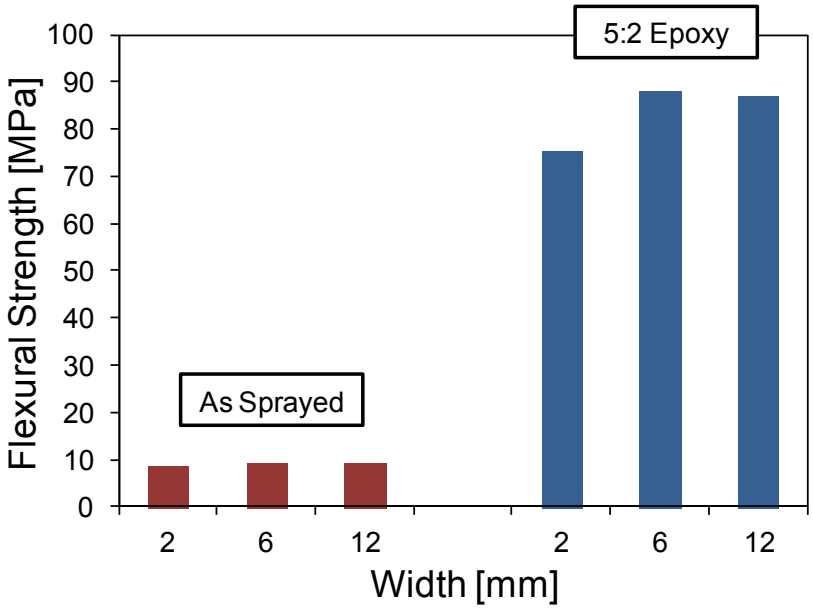

Figure 7.5. Epoxy which is the least viscous of all polymers tested so far shows the same trend as the as sprayed samples in that there is no dependence on sample flexural strength and dimension.

According to the findings, it appears flexural strength improvements are not controlled by sample dimension. This is significant because coatings can be tested in various widths and their level of enhancement is likely just a result of the integrity of the as sprayed template and polymer type and percentage. Therefore, the number of defects present in a particular sample are likely responsible for the variation in enhancement level of the flexural strengths. As observed in the SEM images, the microstructure of thermally sprayed coatings show a high number of defects and open porosity. Depending on the spray process this will vary but there is also variation within a single thermal spray run. Even when individual samples are sectioned from the same beam, there can be a difference in the number and severity of the defects on the overall coating properties. Thermally sprayed coatings tend to be highly irregular and chaotic in their microstructure. This is especially true of coatings deposited via the powder flame spray process. Based on flexural strengths of as sprayed specimens, there is not a large difference in the variation between the different sample widths. However, it is likely that with the presence of polymer the defect nature plays a greater role and that is why differences are observed. If the same pattern was observed between all polymers in that the 2mm sample widths had the highest flexural strengths then one may be able to conclude this is because the template can accommodate the highest polymer content due to the ease of infiltration resulting from the small sample dimensions. With smaller sample dimensions to get polymer into the entire through thickness there would be the lowest distance in open porosity for the polymer to flow through but this was determined not to be an issue.

Medium Porosity Coatings with an Organized/Staggered Arrangement

Regardless of sample width, flexural strength appeared independent of size for the highly porous and globular microstructures fabricated via powder flame spray, except for the case of the PMMA infiltrated samples. Further investigation into dimensionality of specimens was examined utilizing alumina rod flame spray coatings. Dimensionality was investigated by varying both thickness and width of specimens.

Specimen width was investigated using templates sprayed at a standoff of 5in with a porosity level of 14.6%. Mechanical properties were measured as sprayed (σ_{flex} approximately 40MPa, K_{IC} approximately 0.9MPa·√m) and then following infiltration by an epoxy and an epoxy heat treated mixture. Specimen dimensions tested were approximately 25.4mm x 1.2mm x 6.0mm and 25.4 x 1.2mm x 3.0mm. Results indicate property enhancements of an infiltrated coating are independent of sample width as long as sample length and thickness are not varied, Figure 7.6.

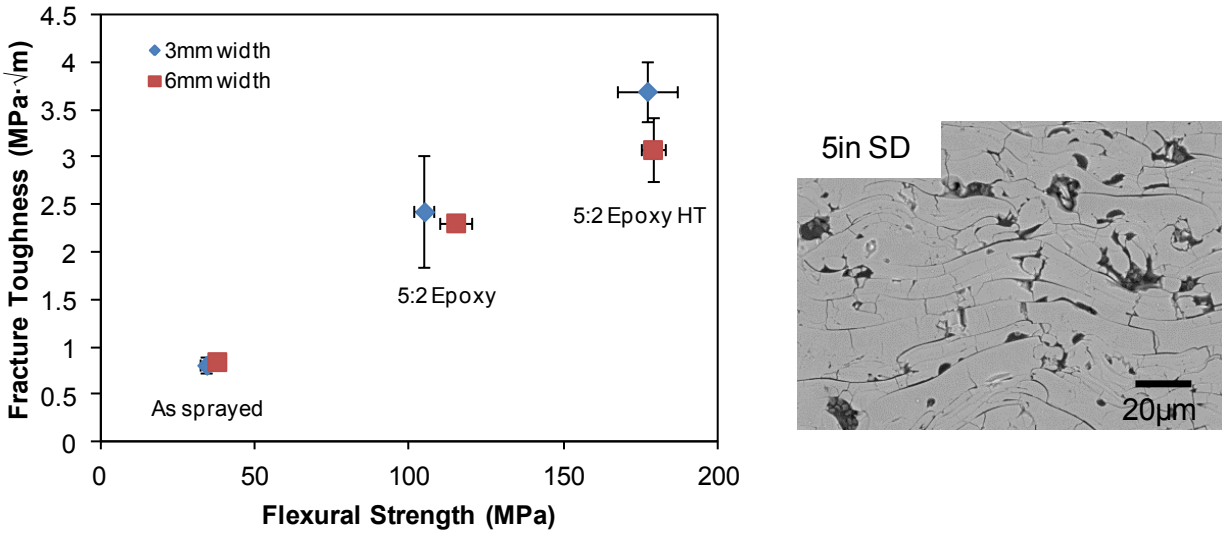

Figure 7.6. Effect of dimensionality on the fracture toughness and flexural strength of infiltrated coatings. Two different widths are plotted, 3mm and 6mm. Property enhancements are independent of width.

The effect of sample thickness was examined using a Rokide® template deposited at a 4in standoff to yield a porosity level of 12.9%. and 14.6% respectively. Starting properties were the same for the two thicknesses, 2.1mm and 1.2mm. The as sprayed flexural strength was

approximately 40MPa and the as sprayed fracture toughness was 0.9MPa·√m. Following infiltration it was determined improvements in flexural strength and fracture toughness are dependent on sample thickness. Based on the results in Figure 7.7, mechanical properties of as sprayed coatings are independent of coating thickness. However, when samples are infiltrated the coating with a 1.2mm thickness shows a higher degree of property improvements which is due to a higher polymer content per specimen. There is less through thickness for polymer to travel through to reach the center of the coating when the coating is thinner and thus there would be more complete infiltration. Epoxy infiltrated specimens deposited at a 4in standoff with a thickness of 2.1mm contain approximately 0.99wt% polymer while specimens 1.2mm thick contain about 2.63wt% polymer.

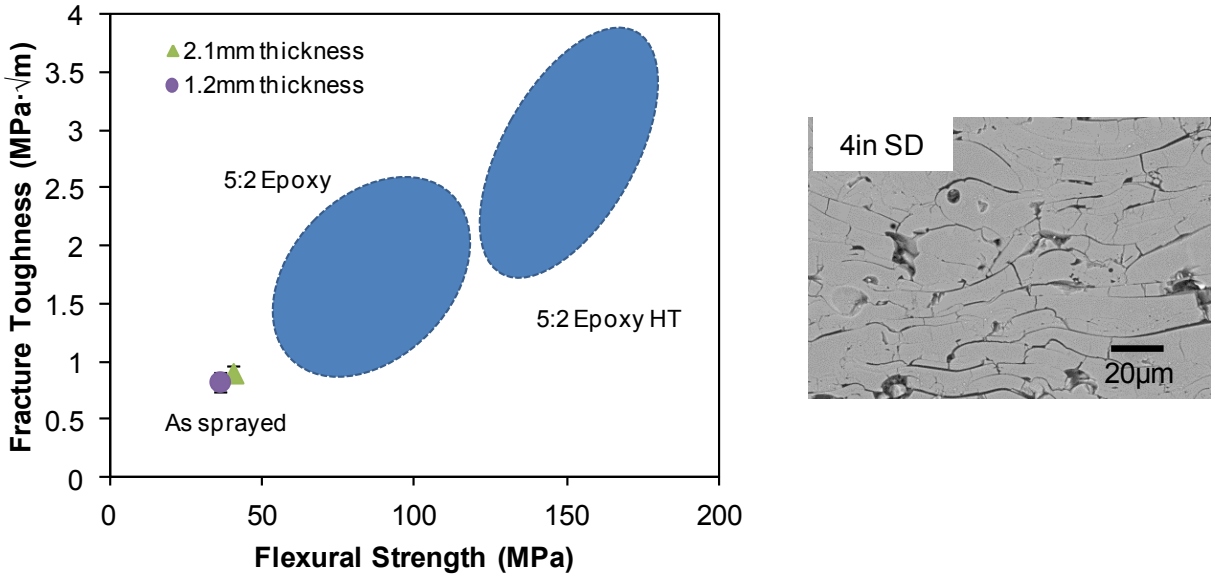

Figure 7.7. Effect of dimensionality on the fracture toughness and flexural strength of infiltrated coatings. Two different thicknesses are plotted, 1.2mm and 2.1mm. Property enhancements are dependent on thickness.

Fracture surfaces of the specimens with a 1.2mm and a 2.1mm thickness support the fact that the thinner samples are more completely filled with polymer, Figure 7.8. Fracture surfaces of the samples with a 1.2mm thickness show a greater presence of polymer. Therefore, property enhancements of coatings are dependent on specimen thickness because it is possible for thinner specimens to be more completely infiltrated and contain a greater amount of polymer.

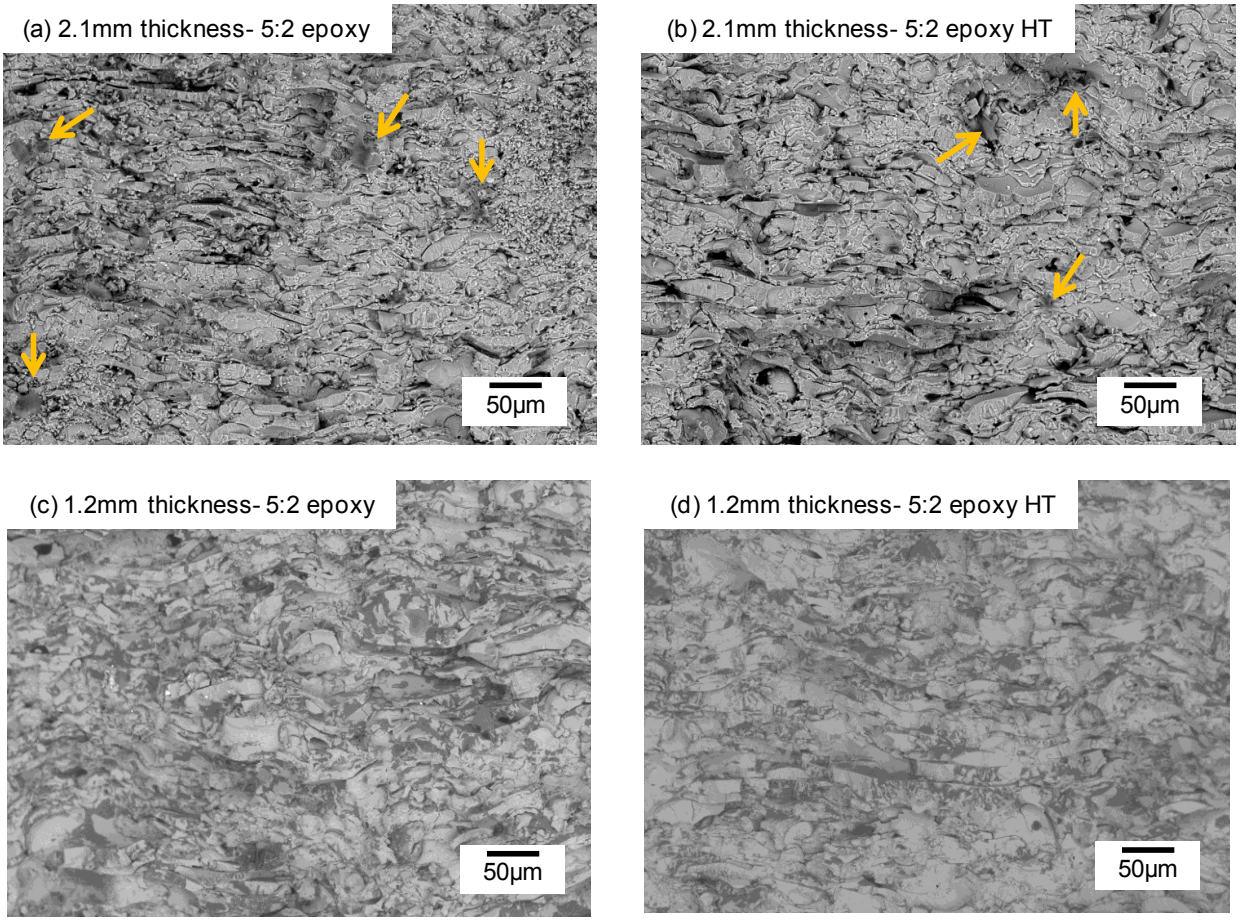

Figure 7.8. Fracture surfaces of samples sprayed at a spray distance of 4in containing 12.9% porosity. (a) and (b) are 2.1mm in thickness and contain a small polymer content compared to (c) and (d) which have a thickness of 1.2mm.

7.3. The Effect of In-situ Polymerization of PMMA into Flame Spray Coating Templates on Property Enhancements

Ceramic rod and powder flame spray coatings were deposited and prepared for three-point bend tests as discussed above. Once made freestanding through chemical means (powder flame spray) and mechanical means (ceramic rod flame spray), they were cut to the appropriate dimensions and porosity was infiltrated with polymer. Both powder and ceramic rod flame spray templates were vacuum infiltrated with 22wt% PMMA. In-situ polymerization of PMMA from MMA monomer of both coating templates was also investigated.

Previous results have shown that although vacuum impregnation of PMMA into a freestanding coating template is successful, infiltration is not optimized. Therefore, in-situ

polymerization from MMA monomers was performed on templates in order to optimize the polymer content within a coating thus possibly further enhancing mechanical properties.

The concentration as shown earlier, does have an effect on coating enhancement and therefore 22wt% PMMA was selected. For instance, as shown in Figure 7.4, there is a direct relationship between increasing flexural strength and strain tolerance with an increasing concentration of polymer in solution. With an increasing polymer content in solution, the viscosity of the solution increases which is expected because there is a higher solute content in the solvent. However, due to the high porosity content and sizes of the defects in powder flame spray coatings, this is likely not an issue. It was thought that in-situ polymerization of MMA monomer would likely have an even greater effect on the enhancements of coating properties. Almost no difference in flexural strength was observed with in-situ polymerization of the powder flame spray templates. Alumina rod flame spray templates showed a greater enhancement in flexural strength associated with polymerization, Figure 7.9.

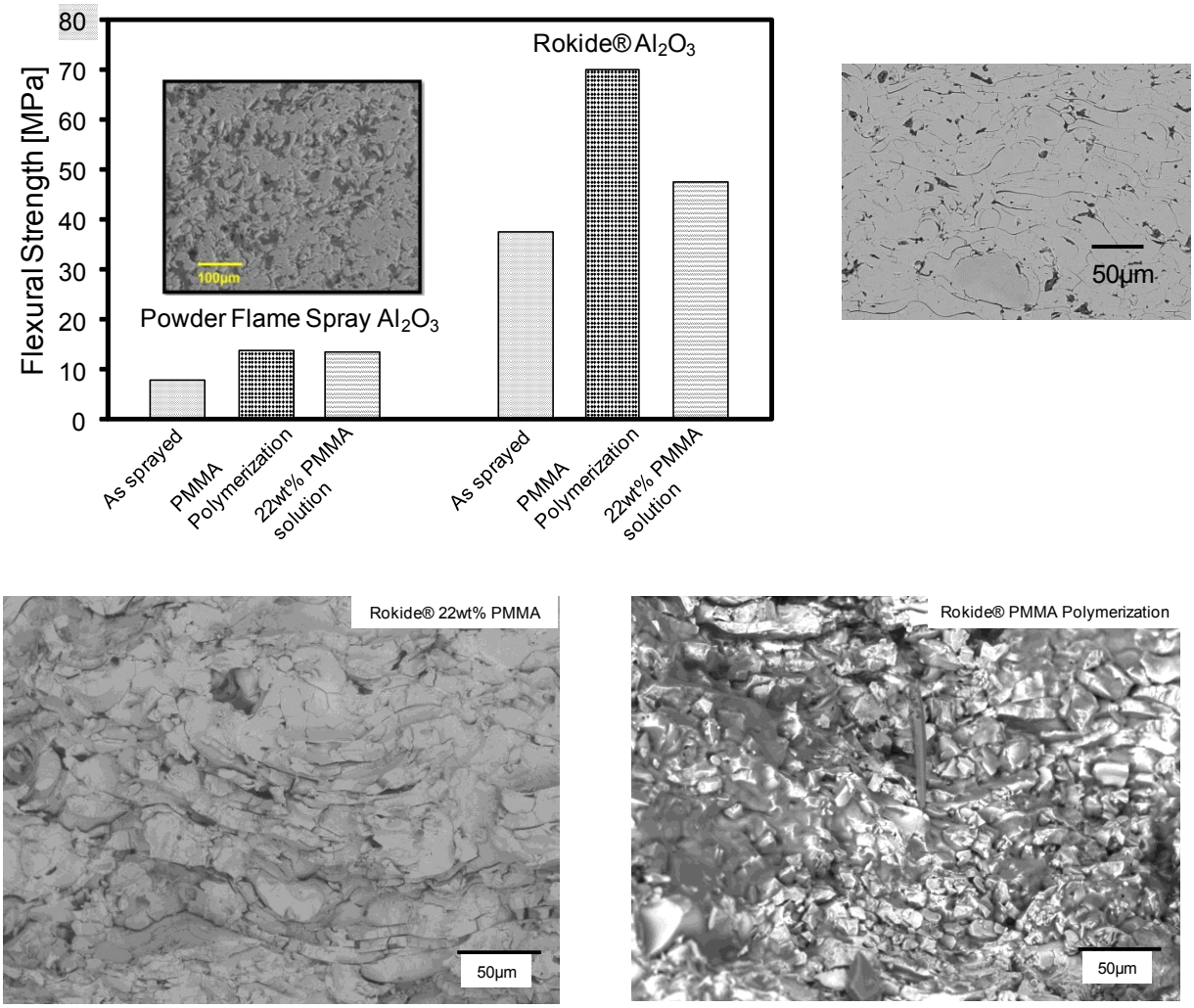

Figure 7.9. Flexural strength for an as sprayed alumina powder flame spray coating and an alumina rod flame spray coating. Each template was infiltrated with a 22wt% PMMA solution and in-situ PMMA polymerization was also completed. In both cases, PMMA polymerization results in the greatest flexural strength enhancements.

Infiltrating the porous thermal spray templates by a free radical polymerization of PMMA in bulk leads to improvements in flexural strength compared to observations when templates are infiltrated with a PMMA solution. Prior to the two polymerization reactions that are discussed in detail in the experimental section of Chapter 4, a chemical grafting procedure is performed on the samples. The purpose of the chemical grafting step is to improve adhesion between the two constituents of the bio-inspired material, ceramic and polymer. Thermal spray templates are etched in a Piranha solution for 20mins to make the surfaces reactive through the presence of hydroxyl groups. Piranha solution does not etch alumina effectively, but instead will leave hydroxyl groups on the surface. After etching, templates are rinsed in deionized water and grafted using γ-MPS: 3-(Trimethoxysilyl)propyl methacrylate diluted in acetone. Hydroxyl

groups on ceramic templates react with the grafting agent and bond to the surfaces of the ceramic template. [46, 95].

Following grafting, two polymerization reactions are carried out which are described in detail in Chapter 4. The first is run with a high initiator concentration with the purpose of maximizing the chance of radical development on the γ-MPS: 3-(Trimethoxysilyl)propyl methacrylate molecules that have become bonded to the surfaces of the ceramic template. This will lead to a chemically grafted chain of PMMA. Following the first free radical polymerization step a second one is completed but using a lower initiator concentration, to achieve complete infiltration of the thermal spray template. [46, 95].

Visual examination of the alumina rod and alumina powder flame spray cross sections clearly show a difference in terms of their porosity, Figure 7.9. Coatings deposited via powder flame spray show a higher porosity content which is verified through image analysis using ImageJ software. Templates formed via the powder flame spray process contain 22% porosity and alumina rod coating templates contain approximately 15% porosity. Examination of the porosity indicate powder flame spray coatings have large globular pores and voids while the Rokide® coatings mostly contain interfacial porosity. Differences in porosity between the two coatings can explain the very different level of enhancements in PMMA infiltration method between the two coatings. For instance, the viscous 22wt% PMMA solution can more easily infiltrate the open porosity of the powder flame spray coatings due to the large dimensions of the porosity. Therefore, in-situ polymerization of the powder flame spray leads to similar levels of flexural strength enhancements because the 22wt% PMMA solution has almost completely infiltrated the coating template.

As previously discussed in the deposition of a coating using the Rokide® spray system, all of the deposited particles are in the molten state. Particles cannot leave the torch unless in the molten state and due to their high kinetic energy and thermal mass remain fully molten until they reach the substrate. This is not the case when powder is used as a feedstock. With powder feedstock there can be a distribution of particle sizes and often the dwell time may be short which does not allow for particles to become fully molten. As a result, it is often the case powder flame spray coatings have a wider range of defects and larger defects due to the deposition of partially molten or unmolten particles and voids. Defects caused by unmelts or semimolten particles are eliminated in alumina rod flame spray which leads to significantly fewer globular pores and voids. Alumina rod flame spray coatings have narrower interfacial spacing which is the majority of their porosity and it is difficult to achieve complete infiltration with a viscous polymer solution such as 22wt% PMMA. To combat this, in-situ free radical polymerization leads to more complete infiltration of the alumina rod templates, thus leading to higher observed flexural strengths.

In addition, it is likely that due to the etching and grafting steps preceding in-situ polymerization that the strength of the PMMA and alumina bonds are increased. This leads to the slight enhancements observed in the powder flame spray template flexural strengths and contributes to the higher flexural strengths of the alumina rod templates.

7.4. The Effect of Co-Spraying Aluminum Powder and Alumina Rod Flame Spray Coatings on Property Enhancements

It was thought that it may be possible to have an even greater effect on the property enhancements by dual spraying aluminum powder and ceramic oxide rods. The aluminum was fed at a 1% feed rate so the major phase would be Rokide® alumina, Figure 7.10. Following coating deposition, the aluminum in the coating was etched by placing the entire coating in a sodium hydroxide and water solution. This etching process was repeated twice allowing for all aluminum to be etched from the templates. After the first etching step, a layer of aluminum remained in the center of the coating. The flexural strength and fracture toughness of the as sprayed coating prior to the etching steps was measured, along with the as sprayed coatings following the etching steps. At the completion of the second etching in sodium hydroxide and water, the coating was infiltrated with a 5:2 epoxy and then heat treated.

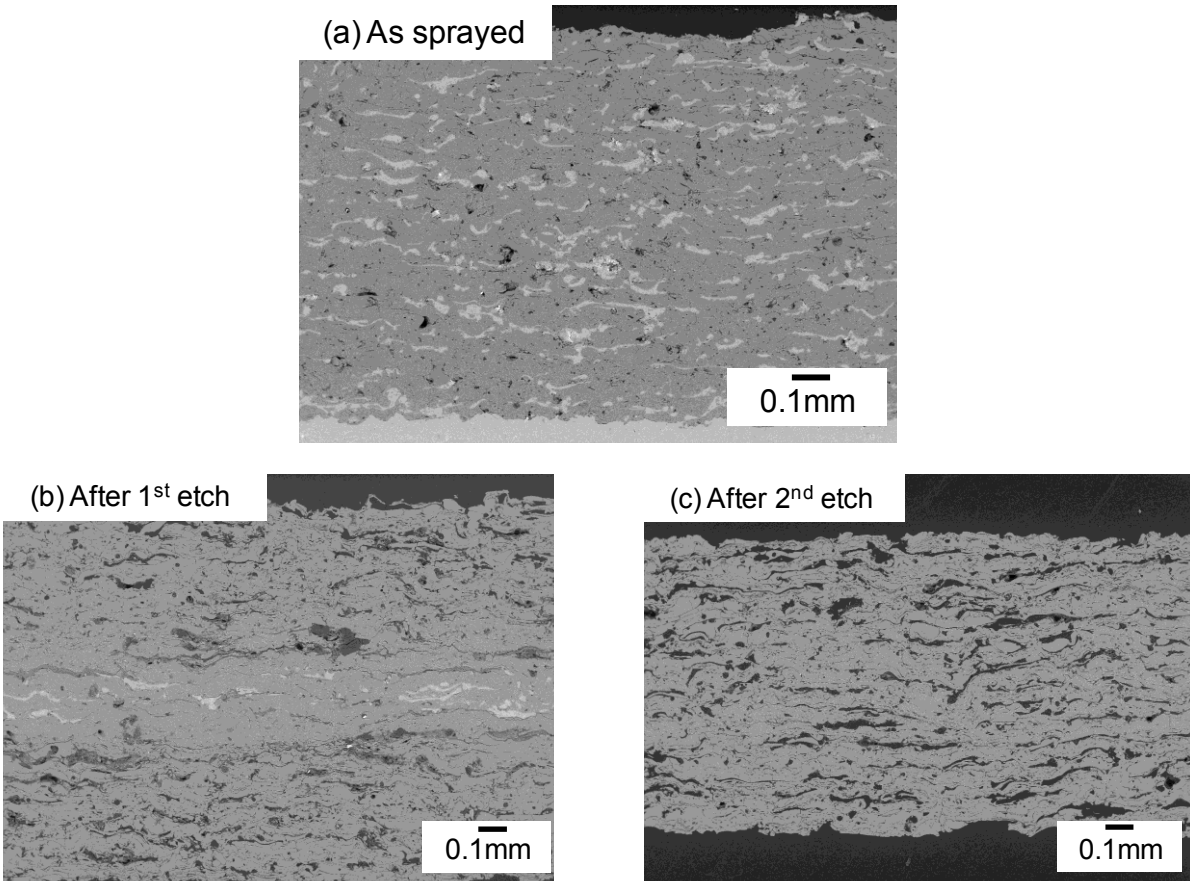

Figure 7.10. a) Cross section of a co-sprayed alumina rod and aluminum powder on an aluminum substrate. Each was sprayed using a separate torch. Following deposition the coating was removed from the substrate and immersed in a sodium hydroxide solution to etch away the aluminum within the deposited coating. b) The polished cross section after being left in a sodium hydroxide solution for one night. c) The polished cross section after being left in a sodium hydroxide solution for 36hr. After 36hr in the solution, it is clear that all of the aluminum has been etched and the alumina coating remains.

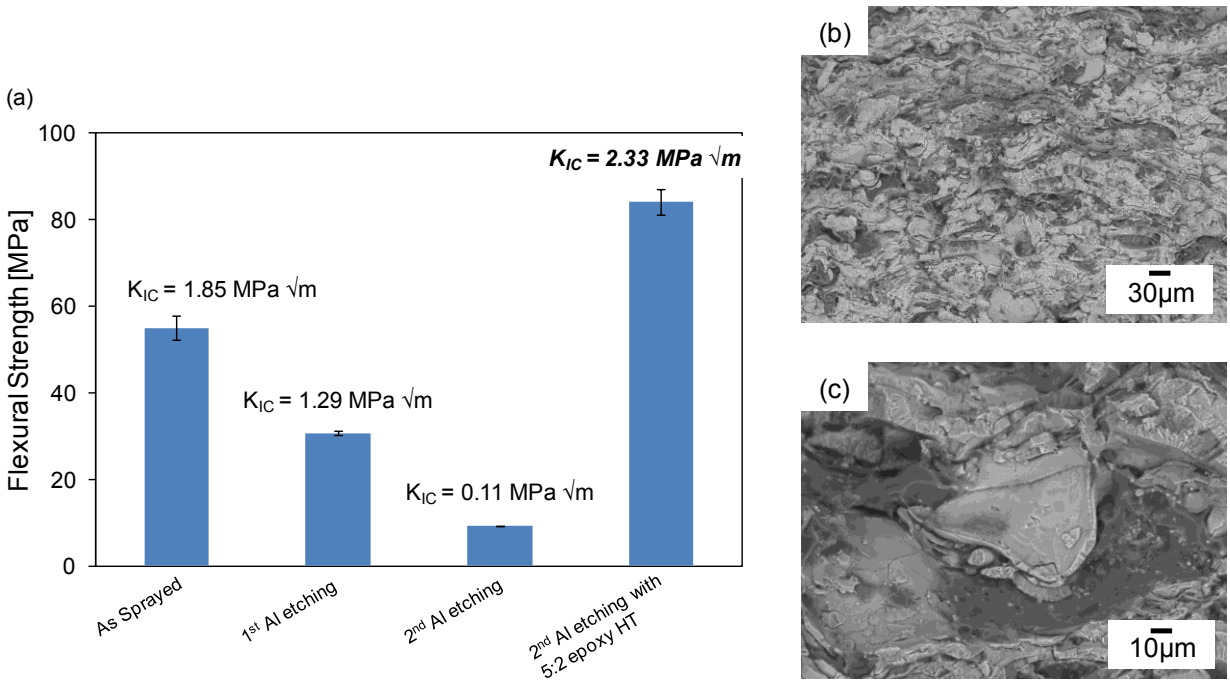

Figure 7.11. a) Rokide® alumina co-sprayed with aluminum flame spray powder tested under three-point bend loading conditions for flexural strength and fracture toughness. Coatings were tested as sprayed, after NaOH etching over night, after 36hr of NaOH etching, and after 36hr of etching infiltrated with 5:2 epoxy HT. Fracture surfaces b) and c) show a significant amount of polymer in the ceramic template.

Following aluminum removal, the heat treated infiltrated sample exhibits property improvements that are higher than the original as sprayed coating with aluminum. From the corresponding as sprayed samples that have been etched twice, the flexural strength increases by more than 800% with the presence of polymer (9.3MPa to 84.2MPa). The fracture toughness increases by over 2000% (0.11Mpa·√m to 2.33Mpa·√m) with the presence of polymer. The high polymer content, 7.71wt%, is likely the major factor that is responsible for the huge increases in fracture toughness and flexural strength. Due to the etching of the aluminum phase, the thermally sprayed templates allow for a high level of polymer because of the resultant porosity. Although there is a significant increase, the flexural strength and fracture toughness do not reach the levels of other infiltrated and heat treated Rokdie® coatings. This is probably due to the loss in organization of the overall structure of the thermally sprayed template when the aluminum was etched. This can be observed in the microstructure, Figure 7.10, showing a high level of porosity which in turn leads to low starting mechanical properties. As discussed previously, a staggered and organized structure is significant in yielding both a high strength and toughness. This concept was illustrated with the difference in microstructures of the thermally sprayed templates and is reinforced by nature in naturally laminated materials like nacre.

In addition, specimens were infiltrated with a 22wt% PVA and 22wt% PMMA solution and flexural strength and fracture toughness for each was determined through three-point bend measurements, Figure 7.12. Based on the increase for each polymer solution from the as sprayed specimen, it is obvious that the polymer presence has provided increased toughness and strength to the ceramic template. Fracture surfaces indicate that there is a high polymer content that has been incorporated into the interfacial gaps, Figure 7.12. Through co-spraying an aluminum powder to be etched away prior to testing, larger interlamellar gaps and interconnected porosity can be created allowing for a higher content of polymer. However, the ordered structure of the alumina rod flame spray templates is somewhat lost and transforms into a more globular one. In addition, the porosity level of the as sprayed coatings is so great that the template has almost no intrinsic toughness which is why properties following infiltration do not achieve the same level as the alumina rod flame spray samples presented in Chapter 5.

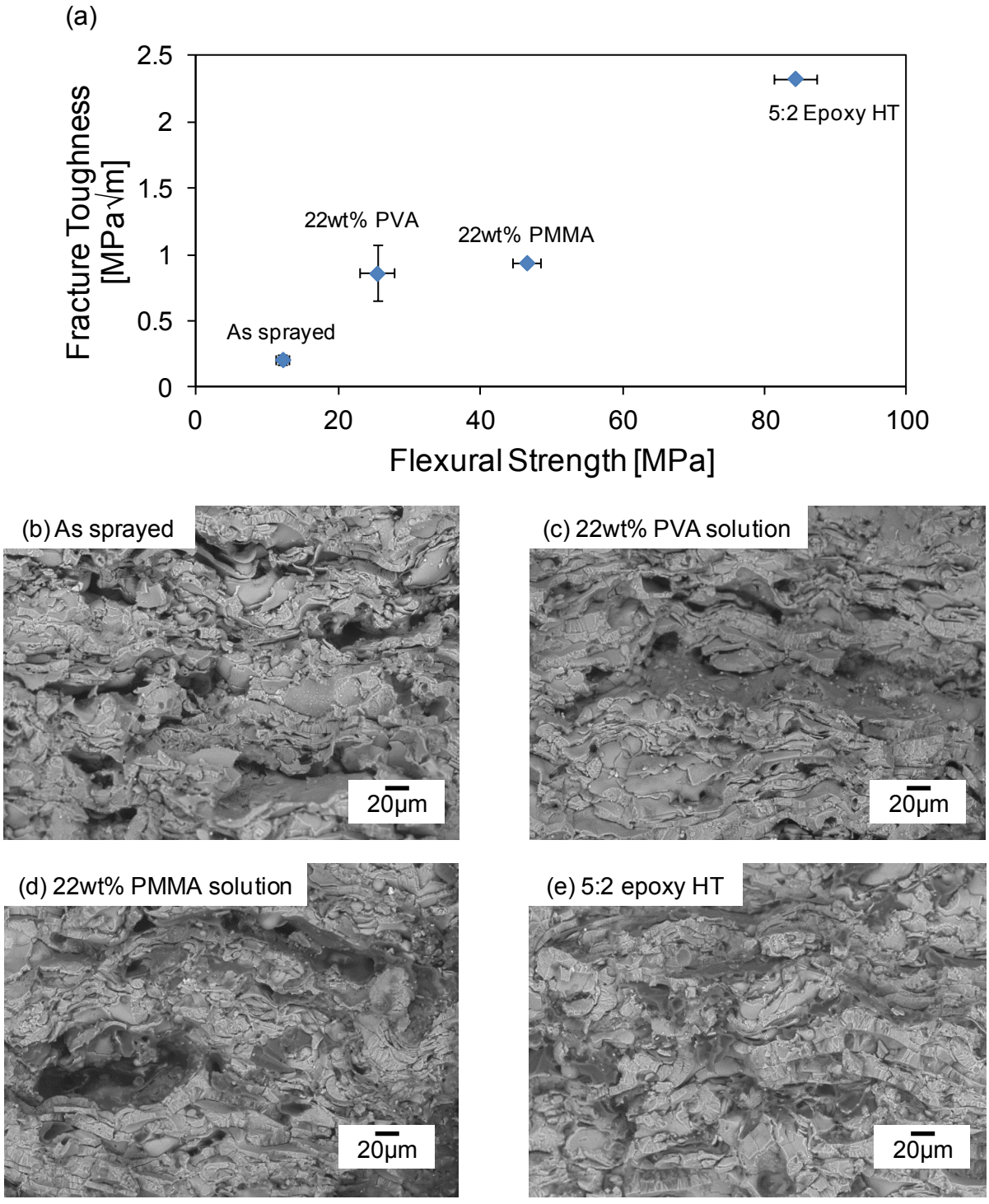

Figure 7.12. a) Fracture toughness versus flexural strength map for alumina rod flame spray with 1% feed aluminum powder flame spray. Following deposition the aluminum was completely removed and samples were infiltrated with various polymer. Fracture surfaces of tested specimens are shown, b) as sprayed (after aluminum has been etched), c) 22wt% PVA, d) 22wt% PMMA, and e) 5:2 epoxy HT. The high polymer content is clearly visible in the fracture surfaces.

7.5. Conclusions

Presented in Chapter 6 are a number of results that show the role of a ductile secondary phase and its effect on the enhancement of thermally sprayed templates. The findings support the fact that a staggered template is desired to achieve the highest flexural strength and fracture toughness. In this chapter, a number of alternate approaches are taken in order to maximize the amount of polymer in a given template to further enhance properties.

Four alternate approaches were taken and the conclusions are as follows:

- Alternate Approach I: The Effect of Stacking Thermally Sprayed Templates on Flexural Strength

Stacking of several single layer alumina rod flame spray specimens did not result in a flexural strength that was greater than an individual alumina rod flame spray specimen.

- Alternate Approach II: Effect of Sample Dimensions on Mechanical Property Measurements

Specimen width does not have an effect on mechanical properties. Sample thickness can affect the level of coating property enhancements. If a coating is too thick, polymer is not able to infiltrate the entire through thickness of the coating. This leads to a reduction in properties when compared to a similar coating that is not as thick.

- Alternate Approach III: The Effect of In-situ Polymerization of PMMA into Flame Spray Coating Templates on Property Enhancements

In-situ PMMA polymerization when compared to infiltration of a PMMA solution leads to a higher measured flexural strength.

- Alternate Approach IV: The Effect of Co-Spraying Aluminum Powder with Ceramic Rod Flame Spray Coatings on Property Enhancements

Co-spraying aluminum powder with alumina rods, followed by etching of the aluminum in a sodium hydroxide solution results in a higher degree of porosity for a given template and allows incorporation of more polymer. Although property enhancements are significant, the flexural strength and fracture toughness that is observed in alumina rod templates presented in Chapter 5 are still greater.

8. Property Enhancements of Thermally Sprayed Coatings using Industrial Sealers

Thermally sprayed coatings have a number of inherent defects that limit their use in a number of applications. Most thermally sprayed coatings have a porosity level of 2vol% to more than 15vol% [96], but this can vary based on the spray process, materials, and parameters. In addition, some of the porosity is interconnected. Most metallic coatings can be sprayed to yield a dense cross section such that the coating contains little to no porosity but ceramic coatings still contain some level of open porosity and cracks. There have been advances allowing for the deposition of coatings at higher velocities, which has led to coatings with fewer voids and open porosity [97]. However, there are still defects that allow for corrosive media to be transported throughout the through thickness of the coating where it can affect the substrate. Thus it is often necessary to treat coatings following deposition.

During their life cycle, coatings are exposed to a number of harsh conditions in which corrosive media (liquids or gases) can infiltrate their pores. This is especially problematic when there is a great deal of interconnected porosity. Eventually, corrosive fluids can cause failure of the coating brought on by corrosion of the coating or substrate material. Therefore, quite often thermally sprayed coatings are treated post deposition to improve properties such as resistance to corrosion or erosion. Treatment post deposition, using sealers is an effective method to close off surface porosity in order to protect a substrate from damage caused by its operating environment and thus helping in the prevention of premature failure of the coating. Sealing is also beneficial in preventing pullout from the surface during finishing if there is low cohesive strength.

8.1. What are Thermal Spray Sealers?

Thermal spray sealers are applied to coatings following deposition. Their main purpose is to improve the performance of the sprayed coating. The coating surface must be free from any oil, grease, moisture or other contamination so as to maximize sealant and coating adhesion. Upon drying or curing, the sealers will serve as a means of protecting the coating from hazards such as corrosive gases or liquids present in its operating environment.

Why are Sealers Necessary?

It is the nature of thermally sprayed coatings to have some degree of porosity which can reach levels greater than 20% depending on spray materials, spray process and conditions. Often, this porosity is interconnected and leads to the substrate or base material, causing premature failure. Thermally sprayed coatings are used in environments where conditions may be highly corrosive or erosive, thus porosity and interconnected porosity results in rapid degradation of coatings. Thermal spray sealers can be used to fill porosity, sealing off pathways to the base material thereby improving service life of a coating. Today it is common practice in industry to seal surface porosity of sprayed coatings post deposition.

Both ceramic and metallic coatings can be impregnated with sealers to extend their service life. Commonly sealed coatings are those that have a high degree of porosity, like ceramics, and will be used in chemical environments or metallic coatings that are more noble than their substrate. Metallic coatings that are deposited on substrates that are less noble, risk the substrate undergoing Galvanic corrosion. Metals such as aluminum, zinc, and magnesium are among some of the less noble metals while gold and platinum are two of the most noble metals.

It is important to mention that there are applications where coating porosity can be advantageous. For example, lubricants for preventing wear can be retained in porosity. However, there are a number of applications where porosity detrimental and should be sealed. Some of these cases include thin coatings or coatings whose operational use will be in a hazardous environment including:

- Sea water
- Corrosive gases
- Elevated temperatures
- Steam

In hazardous operating environments, the corrosive media becomes entrapped in open porosity, eventually damaging the coating system. If the base material or substrate becomes damaged, the bonding between the coating and substrate can fail, or the coating can fail. Application of sealers provides a means of protection to both coating and underlying substrate.

Characteristics of a Good Sealer

As previously mentioned, TS materials are porous and thus sealers are critical in some applications. There are a number of characteristics that must be present in order to make a good sealer. For a sealer to successfully improve the service life of a coating it is essential it has strong capillary action permitting impregnation of the coating. A sealer should be able to withstand its operating environment. This could include elevated temperature levels, acidic or caustic environments. Therefore, in the selection of a particular sealer, these things need to be taken into account so benefits are maximized.

In trying to fabricate materials that would exhibit the same synergistic response as nacreous assemblies, a number of thermal spray sealers were investigated. Sealers promise to provide benefits to coatings in terms of erosion and corrosion resistance. In attaining these improvements, it may be that mechanical properties like flexural strength and fracture toughness are also enhanced. The three studied sealers include:

- Diamant Dichtol
- Metcoseal AP
- Metcoseal URS

Each of these sealers has their own advantages and compatible environment for operation. For instance, Metcoseal AP has a high temperature resistance, up to 500˚C. It is an air-drying phenolic with a small percent of drying oil [98] and can penetrate quite successfully into open porosity. It can also be used as a solid lubricant because phenolics can have good friction properties. Metcoseal AP functions best in acidic environments and in applications where low friction on wear surfaces is essential. [99] It can also withstand boiling water, salt spray, oils, gasoline, greases, acids, and the majority of organic chemicals except alkalis [100]. If complete impregnation by the phenolic sealer occurs the abrasion resistance to the coating can be tremendously enhanced. Complete impregnation by Metcoseal AP can even enhance bonding of the coating to the substrate leading to an increased service life of the coating system. [99]. Metocseal URS is a urethane liquid that can be used for sealing for applications up to 205˚C. It is able to withstand a number of corrosive environments including, inorganic and organic acids, alkalis, organic solvents, aromatic hydrocarbons, and water. Metcoseal URS is resistant to impact and abrasion. It is designed for increasing the corrosion resistance to both metal and ceramic thermal spray coatings. [100].

Applications of Thermal Spray Sealers

In a wide variety of applications, the pores of a thermal spray coating can lead to detrimental effects on the coating and substrate system if corrosive elements become entrapped. For example, in high pressure industrial applications, like hydraulic rams, sealers can be applied to prevent any loss of pressure caused by fluid seeping through the pores. [100]. Sealing of aluminum and zinc coatings is commonly performed to reduce electrolytic action [98]. Other applications of sealers include:

- Pulp and paper machinery
- Farm equipment
- Bridges and trestles
- Hydraulic pistons
- Petrochemical plants
- Marine equipment and structures
- Pump seals, shafts, plungers, and housings
- Transformer cases
- Storage vessels, tanks, and waste containers [100]

Often the decision to seal sprayed coatings is an economical one in that it increases the lifetime of a coating but it also allows for a thinner coating to be deposited (less material is used) but offer the same level of protection as a thicker coating. Another benefit is that using sealers helps to improve the appearance and cleanliness of coatings. [98].

8.2. Can Coating Properties be Enhanced by Applying Sealers?

Sealants are applied to a coating surface post deposition. It is essential the coating surface is clean and dry prior to application. By impregnating the porosity of a coating, sealers provide protection by preventing erosive or corrosive media from attacking the substrate. However, previous studies in this dissertation have shown that by interfacially modifying interlamellar

spacing and filling open porosity of a freestanding coating mechanical properties are enhanced. This led to the question as to whether or not thermal spray sealers could provide any type of benefit in terms of the mechanical properties, like flexural strength and fracture toughness to a free standing coating. If the mechanical properties of a freestanding coating could be enhanced using sealers, then it is likely their application would also provide a benefit to coating and substrate systems during industrial applications.

8.2.1. Is there an Optimal Application Method for Thermal Spray Sealers

Application of thermal spray sealers to sprayed coatings is often completed at atmospheric pressure by brushing dipping, or spraying. With low-pressure impregnation methods the success is often based on the ability to remove moisture and air from defects like open porosity and cracks. With the presence of moisture and air, there are oppositional forces acting against impregnation that is being driven by capillary action of the sealer. An increased penetration depth can be achieved when excess moisture is not present. However, certain sealer formulations can help to combat this. Another factor that should be taken into consideration is that the pressure level should be such that there is not excessive evaporation of the sealer.

Freestanding coating templates were impregnated with thermal spray sealers. Sealers fill open porosity and voids of coatings penetrating open porosity by capillary action and hardening. Before conducting a number of experiments with sealants, Diamant Dichtol was chosen to investigate the best application method for sealers. Three-point bend flexural strength specimens were prepared using flame spray alumina samples. Dichtol was either brushed or impregnated into the coating via SI or VI. According to application directions, the sealer should be applied through VI or SI by leaving the coating in the sealer for 30min. It was recommended that application by brushing consist of brushing the coating several times in quick succession. Therefore, the freestanding coating was originally brushed on both sides and then one side was brushed for 15min so that the brushed surface of the coating remained wet for the entire 15min. Then the coating was flipped and the process was repeated on the other surface. Results from three-point bending indicate the presence of Dichtol at interfacial gaps and open porosity enhance the flexural strength of the templates, Figure 8.1.

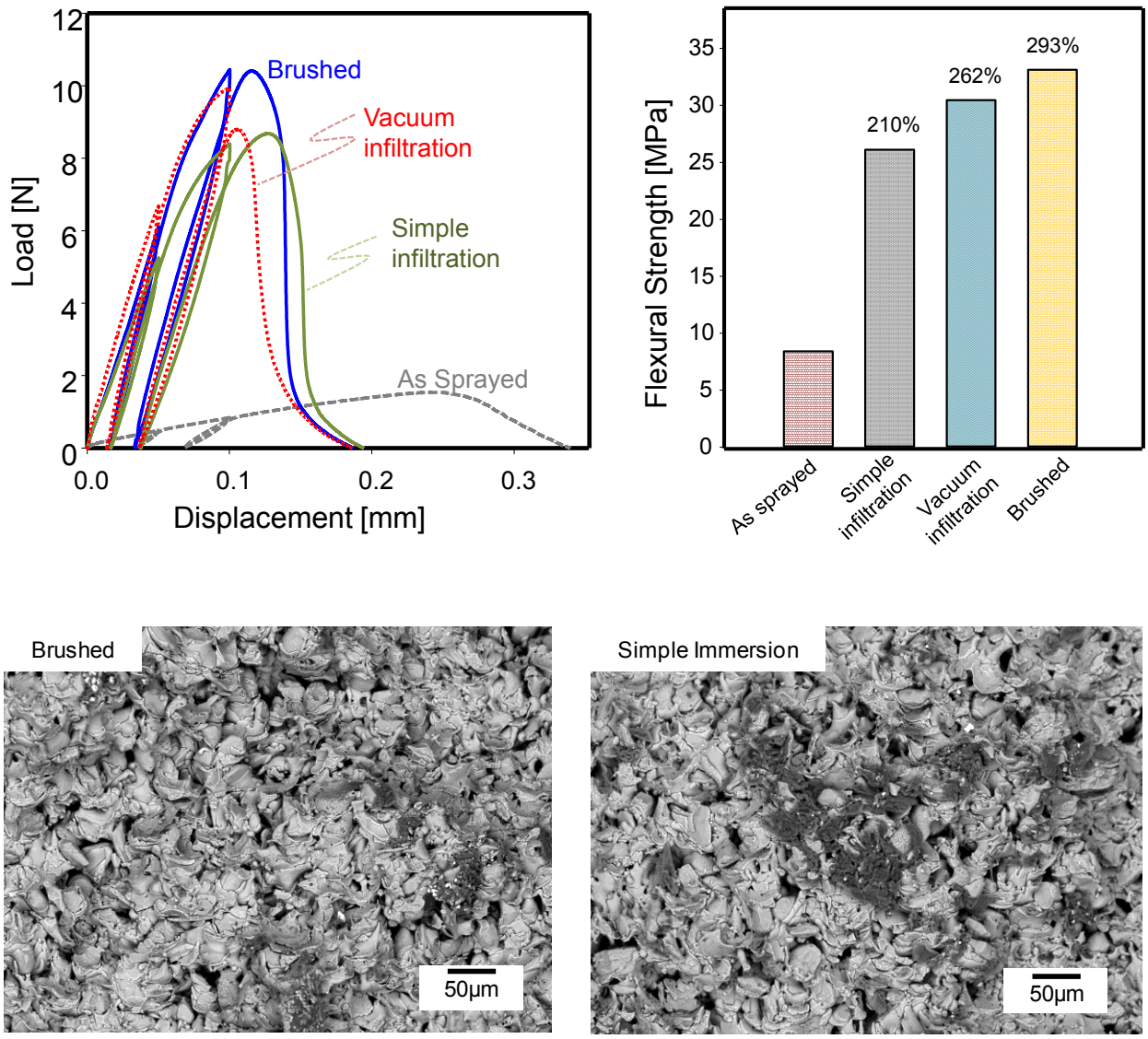

Figure 8.1. The load vs. displacement curves for Dichtol infiltrated flame spray coatings with a high porosity. The presence of Dichtol at the splat interfaces diminishes the strain tolerance but results in an increased strength. Percentages refer to the increase in flexural strength over the as sprayed coating. A fracture surface of a brushed and simple immersion specimen with Dichtol are provided.

Although each method for Dichtol impregnation results in enhanced flexural strength, applying Dichtol by brushing is the optimal method. As in section 7.1.1., VI led to a higher increase in the flexural strength than SI. The fact that sealers are designed to impregnate coatings based on capillary action and can flow easily enough without needing the force of a vacuum is significant for application for thermally sprayed coatings. Often times, parts that are sprayed with a coating are large and not easily able to be infiltrated under the pressure of a vacuum. This means that in the case of Dichtol there is not a sacrifice made in terms of flexural strength enhancements by brushing for coating impregnation. Although the presence of Dichtol in a TS

scaffold resulted in an increase in flexural strength, its presence did not have a beneficial effect on the strain tolerance, in fact, the presence of Dichtol at the interfaces of the flame sprayed coatings had a detrimental effect on the strain tolerance. However, regardless of infiltration method the strain tolerance was about the same.

Another interesting result suggest as flexural strengths of Dichtol impregnated coatings increase, Dichtol content also increases Figure 8.2. Based on these results, there is a direct relationship between sealer content and the flexural strength. Therefore, finding the ideal infiltration method to get the most polymer into the interfacial gaps will allow for the greatest enhancements observable in flexural strength and likely the highest degree of modifications of the interfaces. Based on these findings, all other sealants in this study were applied by brushing for further tests.

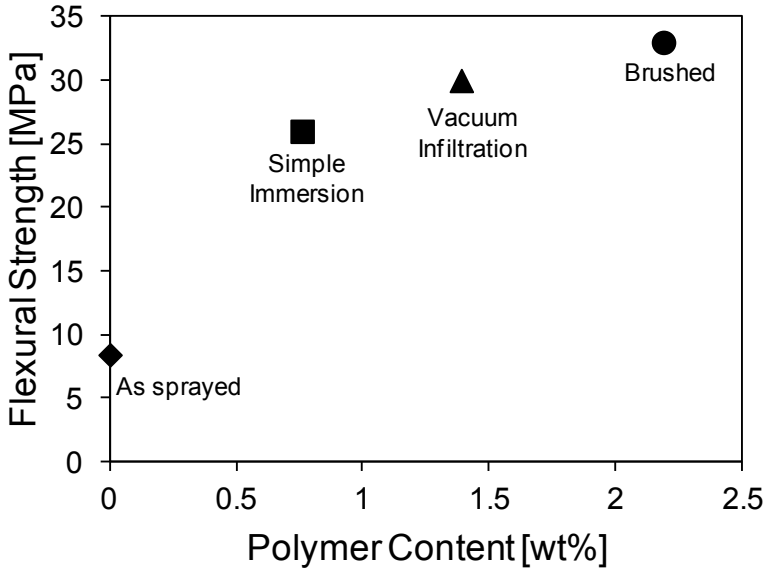

Figure 8.2. Flexural strength of flame sprayed alumina coatings and their corresponding polymer content. As polymer content increases, the flexural strength of the samples also increases.

8.3. Comparison of Coating Property Enhancements using Several Thermal Spray Sealers

Selection of a thermal spray sealer for application to a coating can be a complicated task due to not only the number of choices but based on what the coating material is and what benefits the

sealers promise to provide. For this study, three sealers were applied to a plasma sprayed YSZ coating and an Al2O3 rod flame spray coating in order to determine if sealer type does in fact contribute to mechanical properties of a coating and to what degree.

Thermal spray sealers were applied to templates previously examined in this dissertation, so it is known that the interfacial modifications of the templates by polymer improve properties. Findings for the yttria stabilized zirconia infiltrated with epoxy and several other polymers are provided in Chapter 6. Sealers were applied to Rokide® templates sprayed at a standoff distance of 4.5in and observations are presented in Chapter 5. Figure 8.3 outlines the results for the APS YSZ and Al_2O_3 FS templates brushed with Dichtol, Metcoseal AP, and Metcoseal URS.

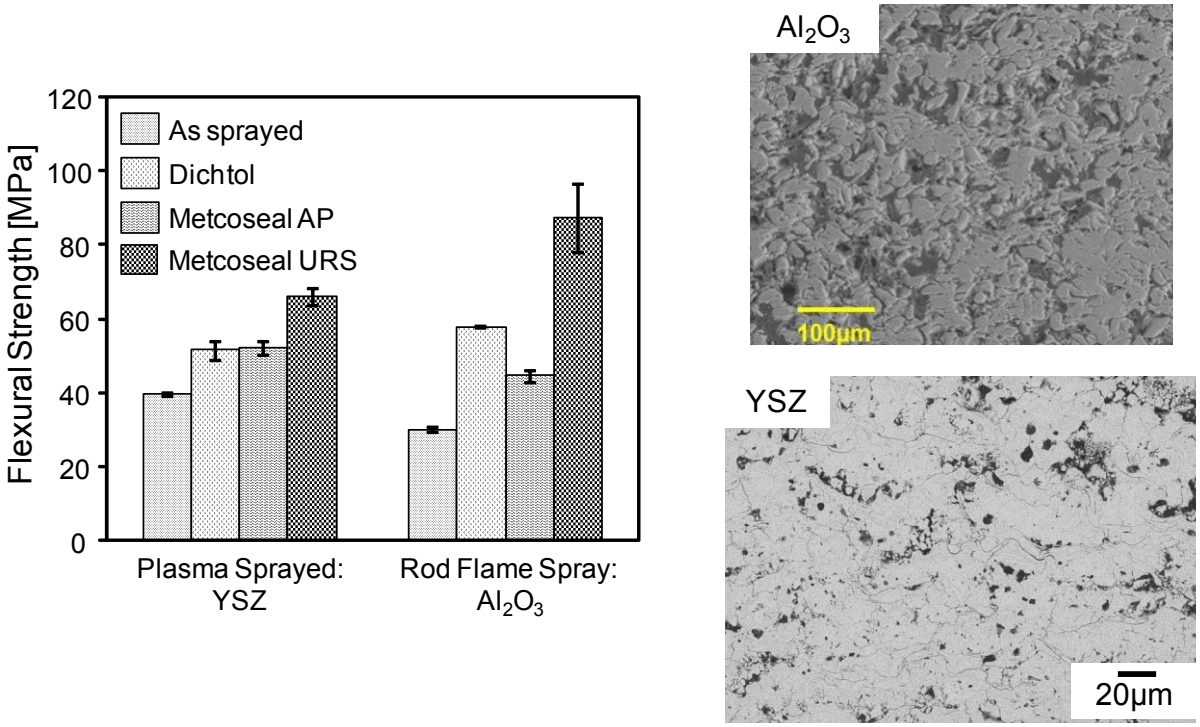

Figure 8.3. Flexural strength improvements of a plasma sprayed YSZ and Al2O3 rod flame spray templates with the application of three sealers, Dichtol, Metcoseal AP, and Metcoseal URS.

As observed in the previous chapters, when polymeric materials fill open porosity of ceramic coating scaffolds application of sealers results in improvements of mechanical properties. Examination of the coating fracture surfaces show sealers can successfully impregnate porosity, Figure 8.1. However, unlike the polymeric media which can stretch from adjacent splat surfaces, sealers appear to just fill open porosity without forming stretched ligaments. Sealers contribute to mechanical properties by filling empty space in a coating thus contributing to densification of the coating whereas polymers such as PMMA and PVA not only

contribute to densification but they can form ligaments when stress is applied. This acts as an adhesive locking splats to one another, and accommodating some degree of deformation at the macroscale prior to fracture.

Combinations of brittle ceramic YSZ templates and thermal spray sealers lead to not only improved flexural strengths of the templates but an improved modulus as well, Figure 8.4. The modulus for infiltrated YSZ coatings was measured through microindentation experiments and plotted against flexural strength. It is expected that with a secondary phase in the coating template modulus would increase. With the presence of a cured/hardened sealer in the scaffold's porosity, as the material is indented the sealer helps provide reinforcement to the coating template and prevents the scaffold from collapsing into itself. Splats are further locked into place because of greater cohesion and are less free to move as a load is applied. This allows for a higher stress level to be accommodated and thus the modulus increases.

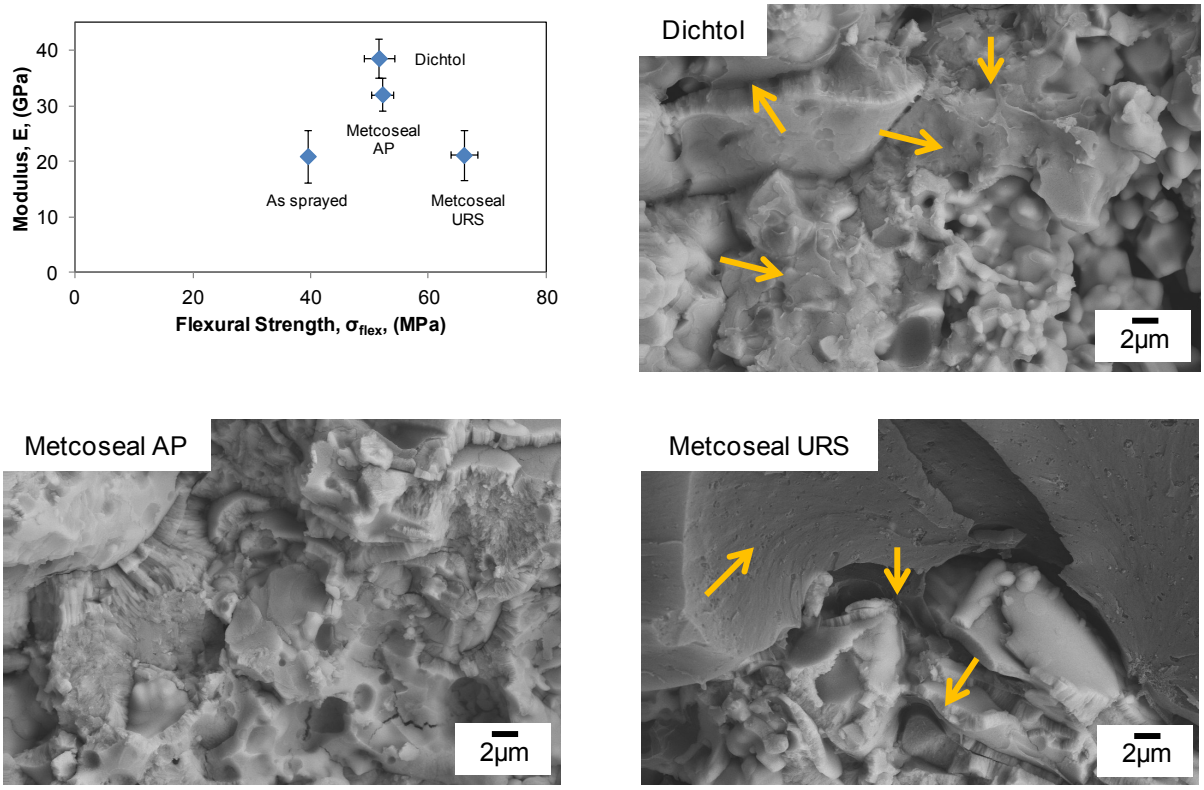

Figure 8.4. Modulus versus flexural strength of plasma sprayed YSZ coatings infiltrated with three sealers, Dichtol, Metcoseal AP, and Metcoseal URS. Corresponding fracture surfaces are provided and the presence of each sealer is indicated by arrows except in the case of Metcoseal AP in which there are no apparent interfacial modifications. However, this is not the case based on the enhanced flexural strength and fracture toughness indicated in the graph.

8.4. The Effect of Dimensionality on Improvements of Flexural Strength with the Application of Sealers

Further testing was performed on Rokide® coatings to investigate the role varying the thickness dimension has on property enhancements. As shown to be the case in Chapter 7, observed properties are dependent on coating thickness when Rokide® templates are brushed with thermal spray sealers for impregnation, Figure 8.5. With a thicker coating, there is more porosity and thus more residual air inside the pores acting against the sealer. This residual air generates an opposing force that acts against the sealer and limits its penetration depth. The affect that Metcoseal URS had on coating properties for a coating with a 2.1mm thickness was minimal. The thinner coating, 1.2mm thickness indicated that Metcoseal URS led to more significant property enhancements.

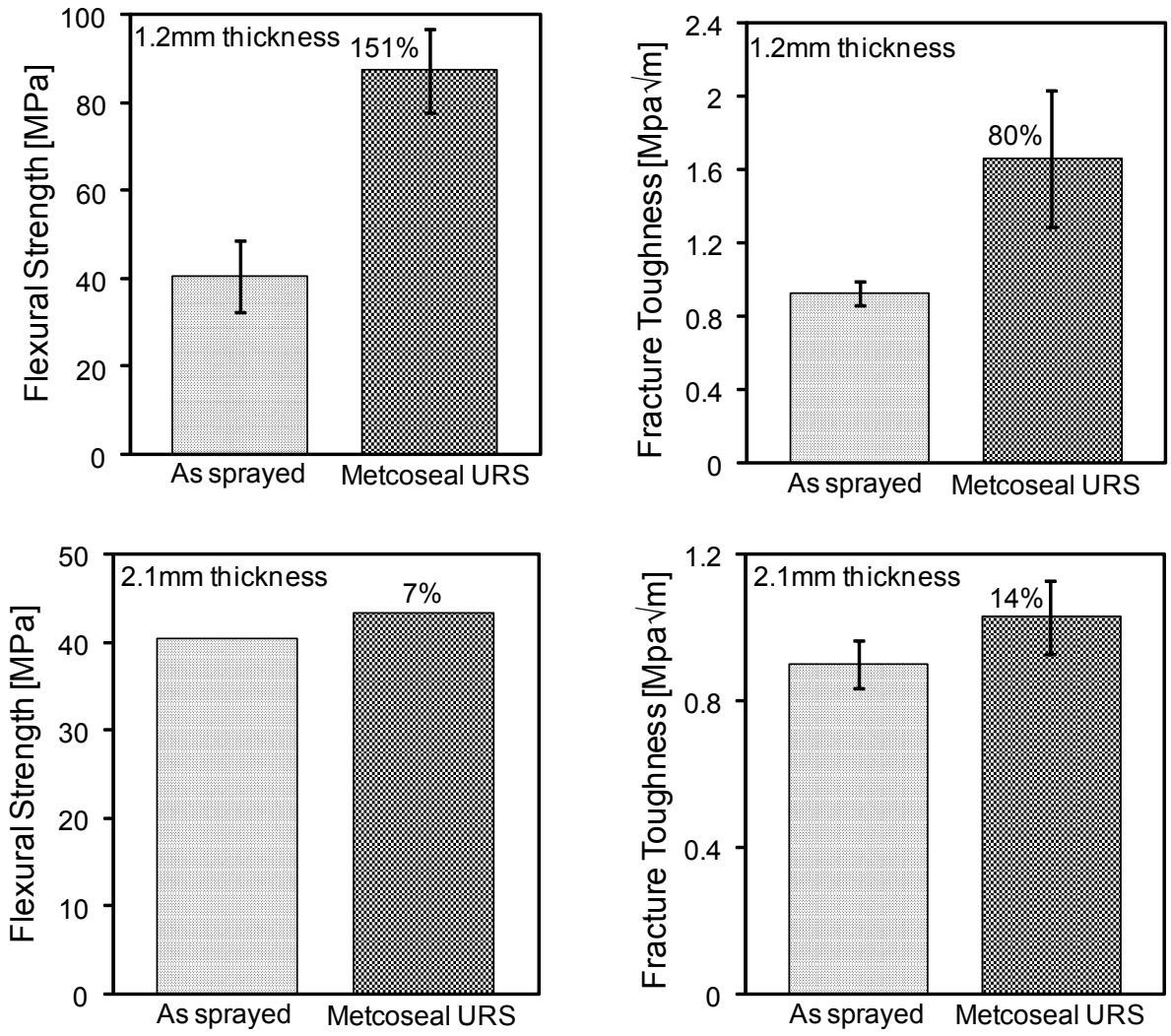

Figure 8.5. Rokide® coatings sprayed to yield two different thicknesses, 1.2mm and 2.1mm, and infiltrated with Metcoseal URS. Percentage increase for improvement over the as sprayed condition is provided.

In addition, to rather minimal flexural strength changes with sealers in the 2.1mm thick alumina rod flame spray coatings, the fracture toughness enhancements show the same trend, Figure 8.5. Although it may be advantageous for the introduction of media into a template to be able to form bridges from neighboring splats, the fact that there is some type of secondary media present in the coating's through thickness serves as a means of slowing a propagating crack. Now, the crack must take a longer path due to the presence of sealers in voids. It is hypothesized that cracks will not go through the tougher sealers but will instead be deflected to interlamellar gaps where sealers are not present resulting in increased fracture toughness. Based on the flexural strength and fracture toughness values calculated from three-point bend loading the samples with a 2.1mm thickness are too thick for a sealer to penetrate effectively due to the

oppositional force created by the residual air in the coating's porosity. Examination of the coating fracture surface does not show any Metcoseal URS sealer present in the fracture surface of the thicker coating, while there is sufficient sealer visible in the coating with a 1.2mm thickness, Figure 8.6.

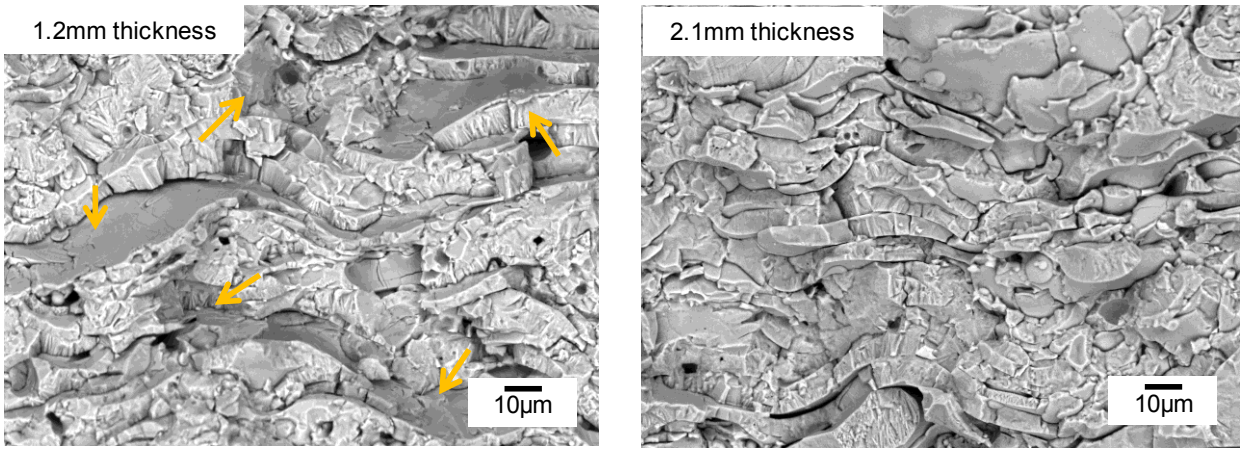

Figure 8.6. Fracture surfaces of alumina rod flame spray samples impregnated with Metcoseal URS. Specimens have thicknesses of 1.2mm and 2.1mm. There is no presence of sealer in the sample with a thickness of 2.1mm, while sealer is clearly visible in the 1.2mm thick specimen and is indicated by arrows.

8.5. Metallic Bio-Inspired Coatings

Thus far, only ceramic TS templates have been interfacially modified with polymer or thermal spray sealers. To see if these synergistic effects hold true for other scaffold materials, metallic coatings were infiltrated and tested under three-point bend loading conditions for flexural strength measurements.

Two metallic coatings were deposited, CrC-NiCr via HVOF and NiAl via APS. Coatings were made freestanding by grinding the substrate to a thickness of approximately 0.5-1mm and then bending the substrate back from the coating. After the coatings were made freestanding, Dichtol was applied by brushing. Interestingly, the sealer had a positive impact on both bio-inspired templates as observed from a typical stress/strain curve under three-point bend loading conditions for each template, Figure 8.7.

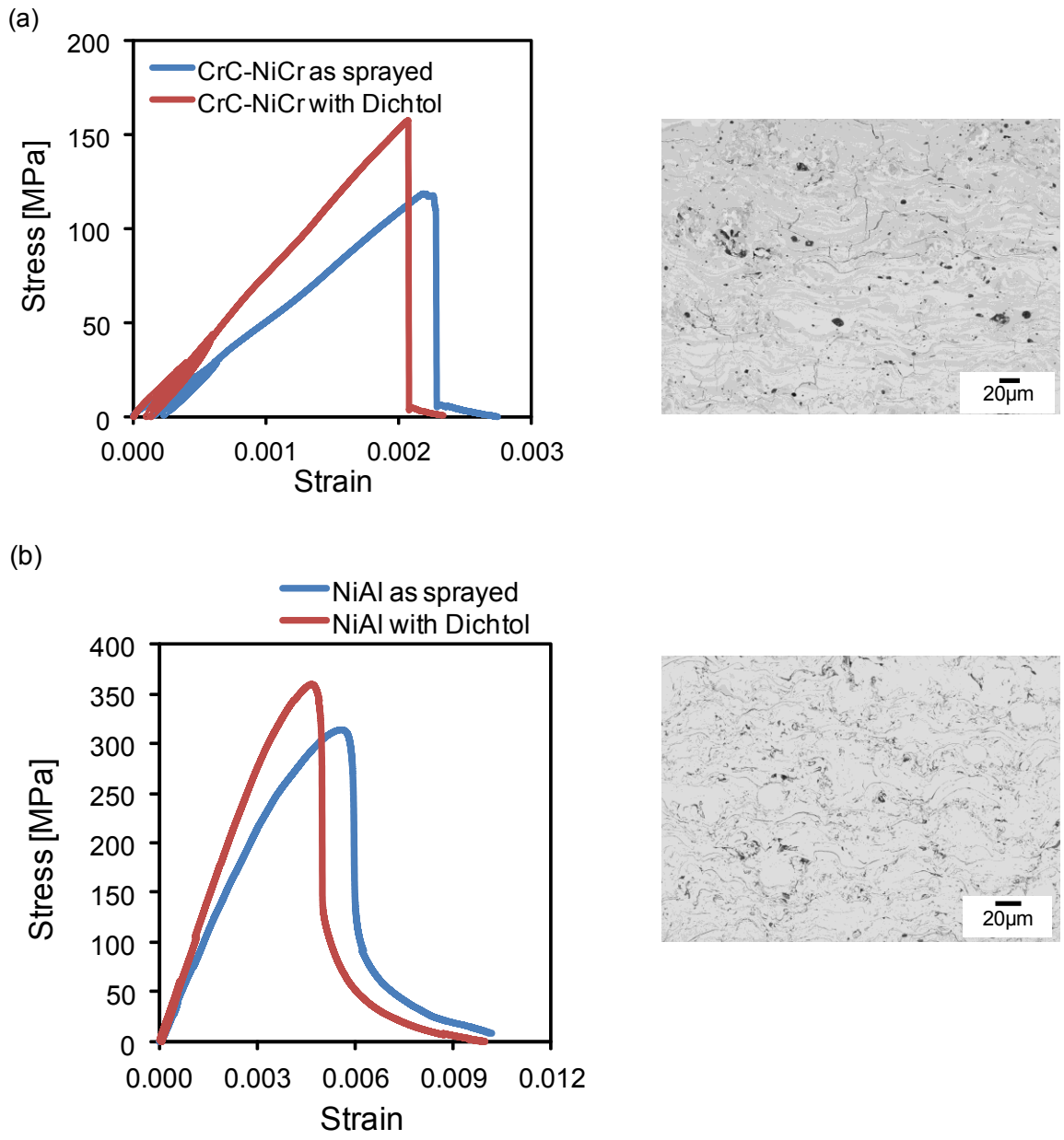

Figure 8.7. (a) Typical stress/strain behavior of an as sprayed and Dichtol infiltrated CrC-NiCr specimen and an as sprayed cross section. (b) Typical stress/strain behavior of an as sprayed and Dichtol infiltrated NiAl specimen and an as sprayed cross section. With the application of Dichtol by brushing, both coatings exhibit an increase in strength but a lower strain tolerance.

Coating enhancements of the metallic coatings were not nearly as high (referring to the percentage increase) as observed in ceramic coatings with sealers, which is expected. The strength of the metallic coatings as sprayed is higher than with the ceramic coatings and there is less porosity and interconnected porosity in the metallic coatings which provides a lesser opportunity for sealer impregnation. Metallic coatings are more ductile than thermally sprayed

ceramics and can undergo plastic deformation prior to fracture, allowing for greater stress accommodation. Due to their ability to plastically deform, sealers do not have as great of an effect. However, it is also important to know the presence of sealers will not negatively impact metallic coatings mechanical properties such as flexural strength.

8.6. Conclusions

Application of thermal spray sealers to ceramic and metallic templates lead to property enhancements including improved flexural strength, fracture toughness, and modulus. Often thermal spray sealers are applied as a means of enhancing a coatings resistance to corrosive environments or providing increased wear resistance. The findings in this chapter support that sealers such as Dichtol, Metcoseal AP, and Metcoseal URS can also provide other enhancements like flexural strength and fracture toughness.

It was determined that application of Dichtol through a simple brushing technique was the best method. Through brushing the highest flexural strength level was measured for a powder flame spray template as well as the highest percentage of Dichtol within the give template. Based on these results Metcoseal and Metcoseal URS were also applied via brushing. Another important finding is that due to air entrapped within a coating, penetration depth of a sealer can be limited and thus property enhancements can be maximized by selecting an appropriate coating thickness.

9. On the Tribological Response of Bio-Inspired Composites

Interfacial modifications of thermally sprayed templates with the introduction of polymer or sealants result in synergistic effects on properties. This is obvious based on the increased fracture toughness and flexural strength of the composite materials. Additional experiments were conducted to investigate the role of polymer infiltration on tribological properties of thermally sprayed coatings.

Tribology studies the interaction of surfaces in relative motion, friction, wear, and lubrication. The term tribology first originated in 1966 in the Jost Report, and was defined as "the science and technology of interacting surfaces in relative motion and of the practices related thereto" [101]. Although the term tribology originated relatively recently, the study of tribology has been around significantly longer. The field of tribology is multidisciplinary, including materials science (wear resistance), mechanical engineering (machine elements like bearings and gears), surface technology (surface topography and coating studies), and chemistry (dealing with the composition of lubricants and other additives) [102].

9.1. Introduction to Wear

Wear can be defined as the loss of material from a surface during a mechanical action like sliding. Friction is caused when sliding one body over another and some resistance is encountered. Wear and friction are related and by changing either, the other is changed as well. Wear is related to a number of parameters including:

- Geometry
- Sliding speed of applied force
- Material combinations

- Environment
    - Temperature
    - Humidity

It should be noted that when two surfaces are contacting each other, it may appear that the contact area is quite large because both surfaces appear flat but this is not truly the case. In fact, each surface has some degree of roughness in raised areas, or asperities, which make the actual contact area small compared to what appears to be the overall contact area. This is why it is important to finely polish the surface of the coatings.

Understanding wear is a complex issue and there is still not a general agreement regarding the classification of the mechanisms and modes. Kenneth Holmberg outlines a common classification system for wear that is helpful in understanding the issue [103]. Within his system he identifies wear mode and wear mechanism.

Wear Mode

A wear mode is a classification of the type of contact. It is characterized by the type of movement, geometry, or environment. Examples of a wear mode include sliding and rolling wear.

Wear Mechanism

A wear mechanism classifies the process by which material is removed from the contact surface. There are four basic wear mechanisms. They include:

Adhesive wear	Asperities from one surface make contact with asperities from another surface, adhering to one another. This may result in the formation of asperity junctions
Abrasive wear	This occurs when hard particles are forced into contact with a surface or one of the faces is much harder than the other.

Fatigue wear	A result of a material being cyclically loaded at a level that is unsustainable by the material numerous times. The material may be able to accommodate the load once but not when repeated.
Chemical wear	Occurs with the presence of detrimental chemical reactions in the contact. These are initiated by the environment but also include mechanical contact mechanisms.

Wear Failure Mode or Type of Wear

Some examples of wear failure modes include:

Fretting	Spalling
Pitting	Scoring
Scuffing	Galling
Gouging	Cavitation
Electrical wear	Diffusive wear
Solution wear	Mild wear
Melt wear	Severe wear
Impact wear	

Usually wear mode describes the combination of wear mechanisms and process of material removal relating to specific contact conditions acting on a surface. The subject of wear is not so clearly defined. There are a number of individuals that have described the process. However, data is not always comparable because of the variety that exists in testing equipment and test conditions. Based on the wear failure mode, one gains an idea as to the surface appearance following contact.

9.2. Coated Surfaces and Tribological Mechanisms

When it comes to tribological mechanisms governing coated systems, there are four considerations to keep in mind. These include:

- Relationship between the coating and substrate hardness
- Coating thickness
- Surface roughnesses
- Size and hardness of the debris

9.3. Effect of Polymer Infiltration on the Wear of Nacre-like Ceramic Structures using Pin-on-Disk Testing

Specimens were prepared for pin-on-disk testing according to procedures in Chapter 4. The idea was to examine the effect on friction and wear that polymer infiltration had on thermally sprayed templates when testing the wear of materials during sliding conditions using a pin-on-disk setup. The pin-on-disk setup tests adhesive wear which occurs when material is displaced due to asperities from two distinct surfaces making contact with each other. The material is removed from the surface of one material and displaced onto the surface of another. Adhesive wear often results in the presence of pitting on the surface the material is being removed from. The following parameters for the pin-on-disk test for the two thermally sprayed templates are provided in Table 6.

Table 6. Parameters for pin-on-disk tests for as sprayed and infiltrates bio-inspired templates.

	YSZ	Al_2O_3
Test duration (min)	30	30
Normal load (N)	20	20
Speed (rev/min)	120	120
Al_2O_3 ball radius (mm)	3.15	3.15

The mass of the coating and substrate system and alumina ball were measured prior to and at the conclusion of each test to determine the material loss of each. Four different coatings were examined, powder and ceramic flame sprayed alumina coatings and two different plasma sprayed zirconia coatings, Figure 9.1. The wear behavior of all as sprayed ceramic coatings is presented in Figure 9.2. Alumina coatings which are specifically used for their wear resistance, display an increased wear resistance when compared to YSZ coatings even though it is a shorter sliding distance until reaching a stable friction. The coefficient of friction for both alumina coatings remains fairly stable around 0.75 to 0.80 and they both achieve this stable level of friction at a sliding distance of around 5m. The medium porosity YSZ coating also achieves a stable coefficient of friction at 5m. The coefficient of friction for both the high and medium porosity zirconia coatings ranges from approximately 0.95 to 1. However, the friction associated with high porosity YSZ does not stabilize until a sliding distance of about 10m.

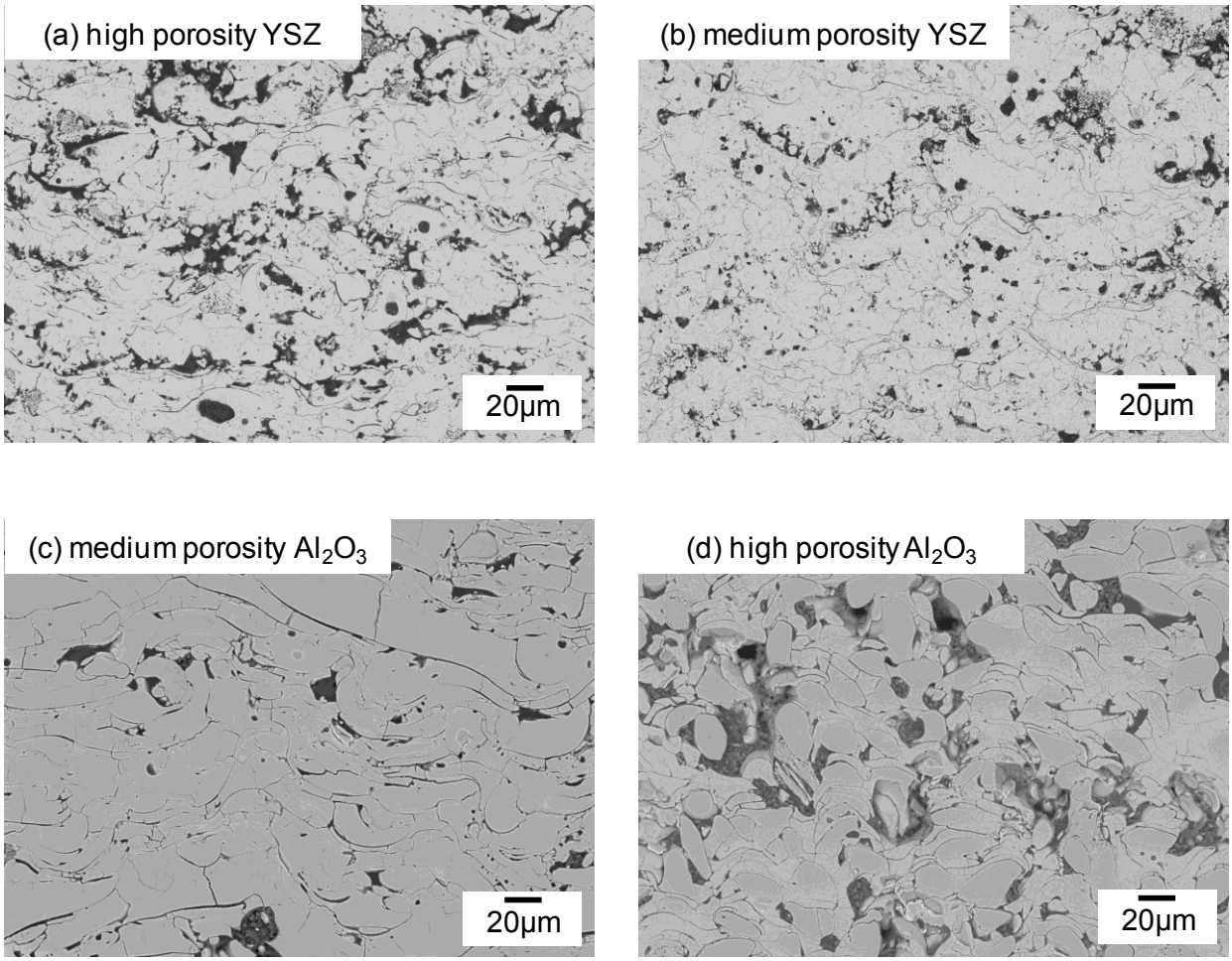

Figure 9.1. Several templates infiltrated with a 5:2 epoxy and 5:2 epoxy HT and their wear behavior was studied using a pin-on-disk apparatus. Plasma sprayed YSZ coatings were deposited a) using hollow sphere (HOSP) powder for feedstock resulting in a high porosity coating and b) using powder deposited on a rotating carousel resulting in a medium porosity coating. Tested alumina templates were deposited via c) alumina rod flame spray to yield a medium porosity staggered architecture and d) powder flame spray to yield a high porosity coating.

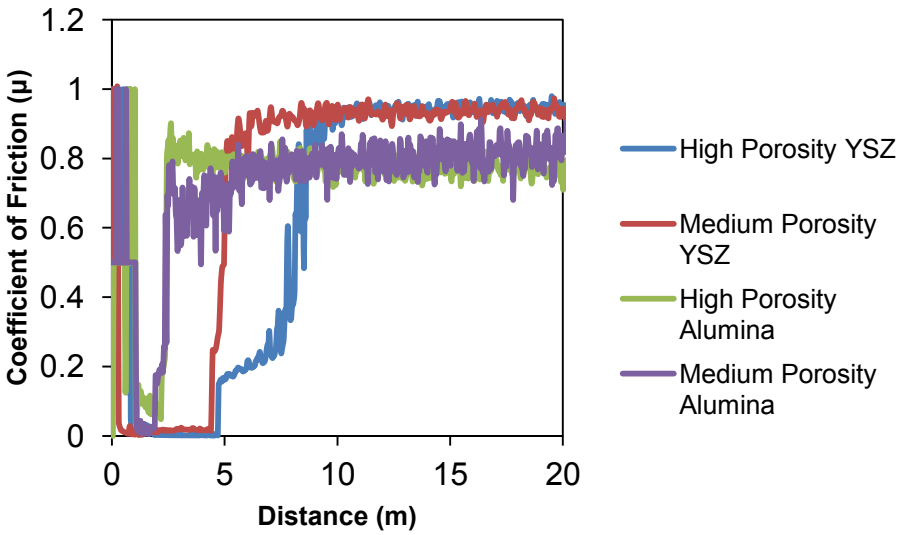

Figure 9.2. Coefficient of friction measured as a function of sliding distance.

Tested ceramic coatings were infiltrated with a 5:2 epoxy mixture and cured at room temperature. Half of the infiltrated specimens were placed in a furnace for 2h at 200˚C for a post cure treatment. Infiltrated coatings were compared to the as sprayed coatings and results are summarized in the following sections.

9.3.1. Wear Behavior of Interfacially Modified Yttria Stabilized Zirconia Coatings

The presence of a tougher and more ductile secondary phase in interconnected porosity of zirconia coatings significantly enhanced the wear resistance of the ceramic. This is evidenced by the reduced mass loss and wear track widths of the interfacially modified YSZ coatings when compared to the as sprayed, Figure 9.3. The introduction of an epoxy mixture into the coating template, seals off porosity and improves the wear response of the coating.

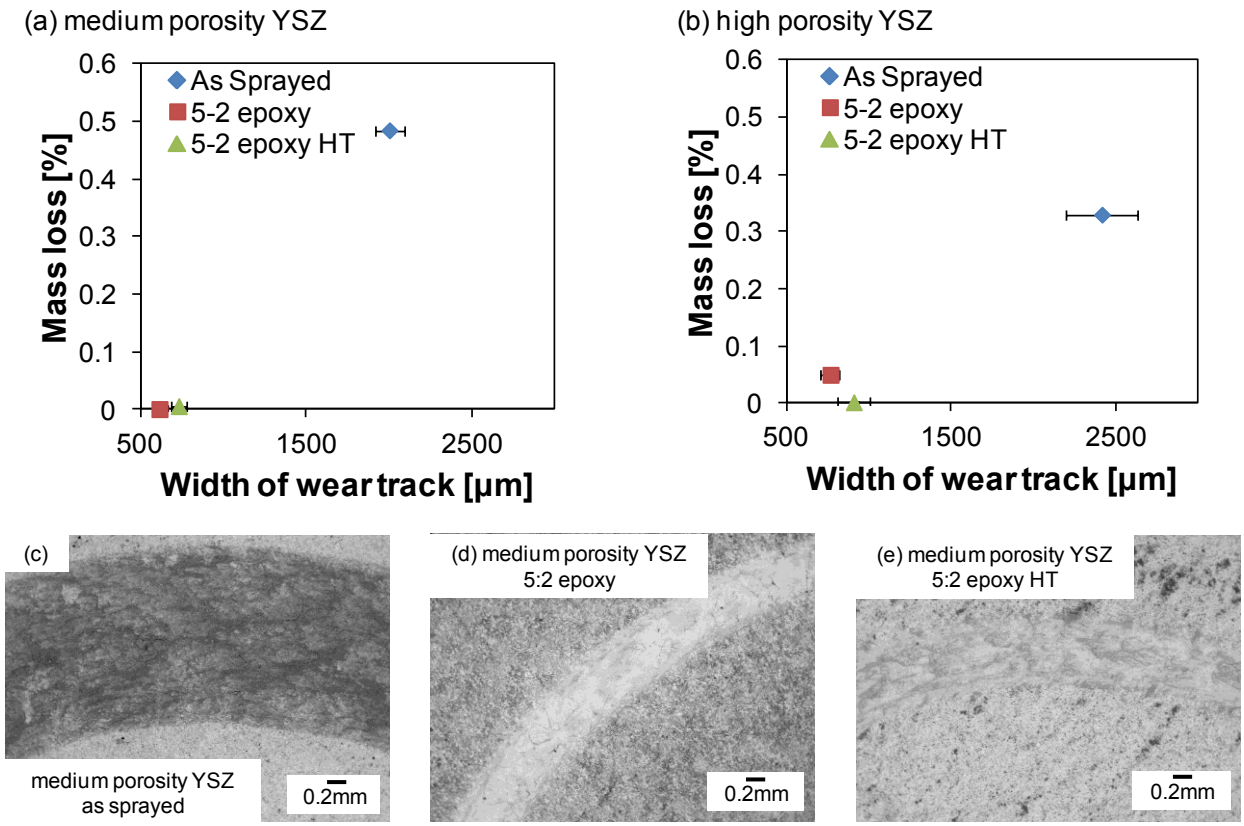

Figure 9.3. Percent mass loss plotted against the wear track width of coatings a) deposited with HOSP powder and b) on a rotating fixture. SEM top surfaces of the coatings deposited on a rotating carousel (medium porosity) following wear testing for the c) as sprayed, d) 5:2 epoxy, and e) 5:2 epoxy HT conditions. Interfacial modifications of YSZ coatings lead to enhanced wear properties indicated by less mass loss and a wear track that is reduced in size.

Filling the interconnected porosity of the coating increases the density, and a denser coating has the ability to be more robust when exposed to wear mechanisms. For instance, sealed porosity will reduce the deformation behavior with the application of a load. In the as sprayed coating, the pores are open and when load is applied the ceramic template just collapses layer by layer and the deformation begins to spread outward which is why an as sprayed specimen has a wear track width of more than double the epoxy infiltrated coatings. In addition, there is splat pull out which results in more mass loss. The wear track of the as sprayed coating appears rougher than the heat treated sample, while the epoxy infiltrated wear track is the smoothest visually. Due to the coating material being more easily removed in the as sprayed coating, following the pin-on-disk testing there was a larger presence of debris pile up on the edge of the wear track leading to coefficient of friction of almost 1.

In addition, the sliding distance for the high porosity yttria stabilized zirconia coatings impregnated with epoxy to reach a steady coefficient of friction increases from about 10m to 50m, Figure 9.4. The nacre-like coatings also stabilize at a much lower friction than the as

sprayed coating and never reach the level of the as sprayed coating. In some applications, a maximized friction level is desired because it can help to minimize wear. However, in the case of the zirconia coatings, a higher coefficient of friction was partnered with a higher level of wear. A lower coefficient of friction in nacre-like materials is likely due to the softer material acting as a lubricant, helping to alleviate detrimental effects of wear.

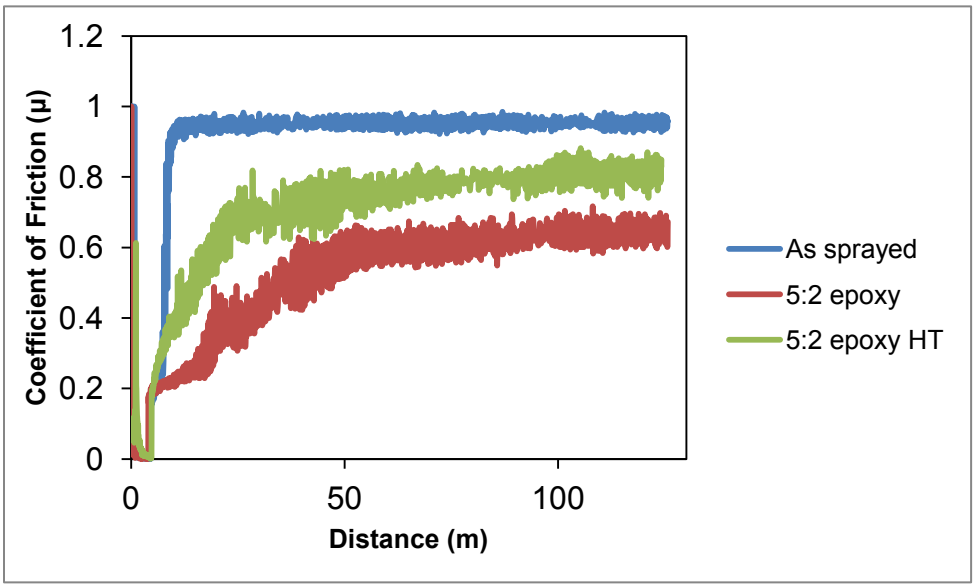

Figure 9.4. Coefficient of friction measured as a function of sliding distance for the highly porous YSZ coatings.

9.3.2. Wear Behavior of Interfacially Modified Alumina Coatings

Pin-on-disk wear testing was performed on two types of alumina coatings; high porosity powder flame spray coatings and ceramic rod flame spray coatings. As previously shown, the deposition of thermal spray alumina coatings yields a ceramic template with a high degree of resemblance to the highly organized and staggered calcium carbonate platelet arrangement of nacreous assemblies. This is especially the case for ceramic rod flame spray coatings. It has already been shown that mechanical properties like strength and toughness can be enhanced tremendously with alumina coatings that are interfacially modified. Thermally sprayed alumina coatings are often used for their ability to provide increased wear resistance to the underlying substrate. Therefore, examining whether coatings infiltrated with epoxy to more closely resemble nacre show a better wear resistance in addition to mechanical properties was investigated.

According to Figure 9.5, powder flame spray alumina coatings were positively affected through epoxy interfacial modifications. Just as in the case of YSZ coatings, epoxy infiltrated powder flame spray coatings show an improvement in wear resistance when compared with the unmodified coatings. Epoxy incorporated into a powder flame spray alumina coating enhances the wear behavior of the coating. This is significant because it shows that a coating already employed for its positive wear properties can be further enhanced through the presence of a tougher and more ductile material.

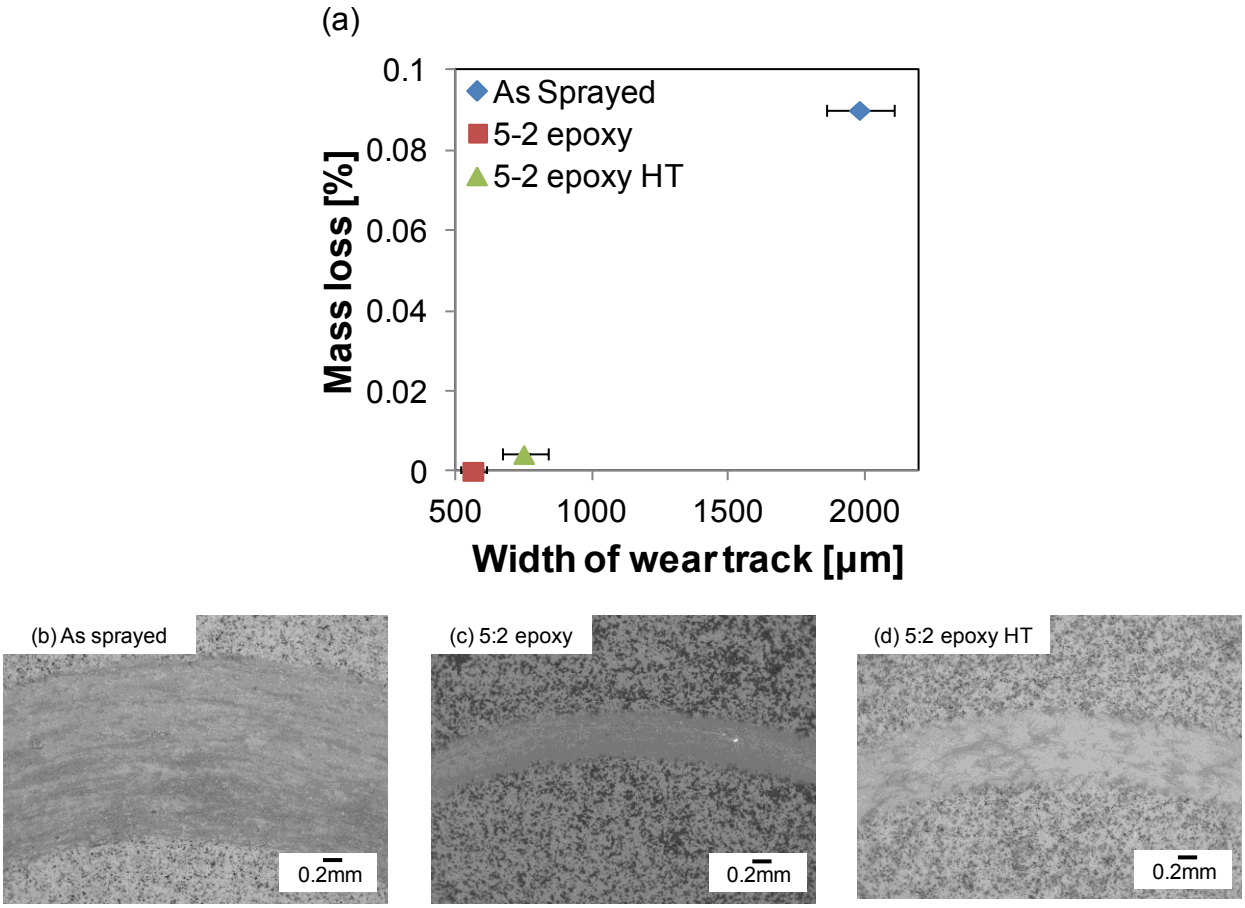

Figure 9.5. a) Percent mass loss plotted against the wear track width of the highly porous alumina flame spray coating. SEM top surfaces of the b) as sprayed, d) 5:2 epoxy, and e) 5:2 epoxy HT conditions. Interfacial modifications of the highly porous coatings lead to enhanced wear properties indicated by less mass loss and a wear track that is reduced in size.

Alumina coatings deposited via ceramic rod flame spray to yield a medium porosity microstructure showed the same response when infiltrated with epoxy and wear tested with a pin-on-disk apparatus. The response is provided in Figure 9.6. Epoxy provides the same benefit

to the Rokide® coatings, although in this case, there is no benefit associated with not heat treating the epoxy as is observed in both the powder flame spray and zirconia coatings.

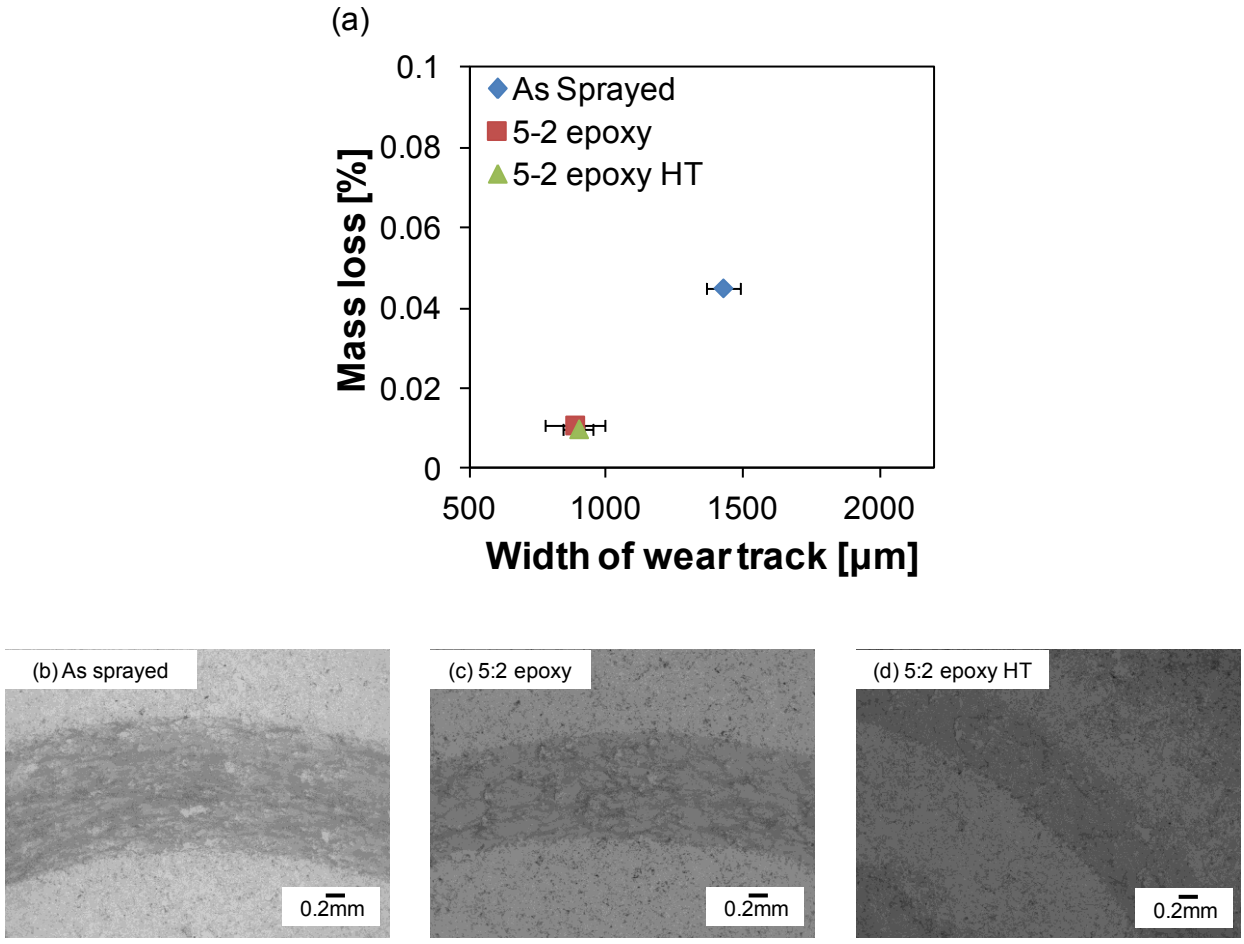

Figure 9.6. a) Percent mass loss plotted against the wear track width of the medium porosity alumina rod flame spray coating. SEM top surfaces of the b) as sprayed, d) 5:2 epoxy, and e) 5:2 epoxy HT conditions. Interfacial modifications of the coatings lead to enhanced wear properties indicated by less mass loss and a wear track that is reduced in size.

9.4. Improved Wear Resistance of Bio-Inspired Coatings Treated with Thermal Spray Sealers

Following deposition, it is quite common for thermally sprayed coatings to be treated with thermal spray sealers. Thermal spray sealers are intended to provide benefits in terms of service

life to coatings by protecting coatings from wear and corrosion that may occur during their lifetime. In Chapter 8, it was proven that another benefit, although unintended of coatings treated with sealers is a significant enhancement of mechanical properties such as strength and toughness. Here tribological properties of sealer impregnated coatings will be examined.

9.4.1. Wear Behavior of Ceramic Coatings Interfacially Modified with Thermal Spray Sealers

There are tremendous advantages associated with nacre-like coatings including their ability to display enhanced wear properties. According to Figure 9.7, the application of the thermal spray sealers by brushing affords the medium porosity Rokide® alumina coatings the same benefit of increased wear performance. There is an even lower mass loss associated with the application of Metcoseal AP and Dichtol than with epoxy impregnation.

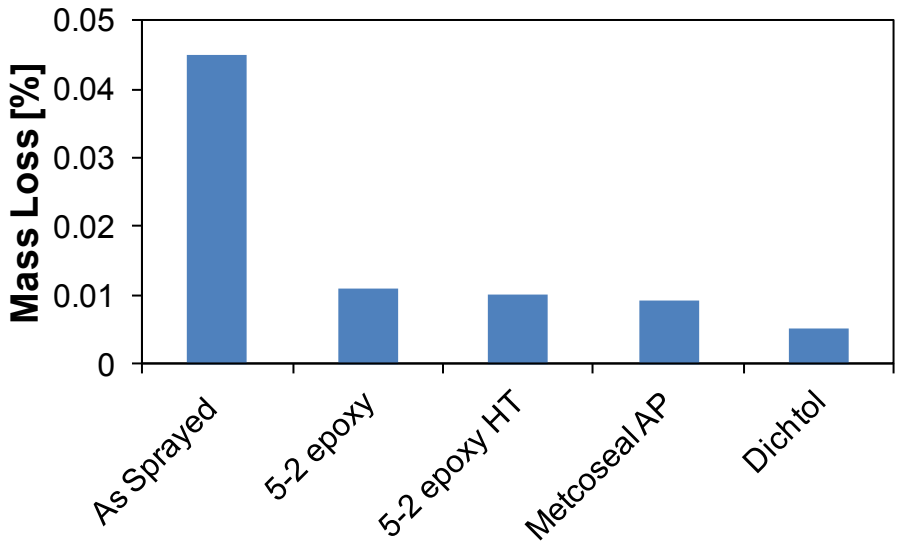

Figure 9.7. Enhanced wear properties alumina rod flame spray when infiltrated with epoxy and thermal spray sealers. The addition of a secondary phase results in a lower mass loss than with the as sprayed coating.

It is particularly interesting that although there is a lower mass loss associated with the application of Dichtol than with any other treatment, yet the width of the Dichtol wear track is greater than all of the other treatments, Figure 9.8. One explanation for this could be the depth of the Dichtol impregnated wear track is shallower than the other infiltrated coatings.

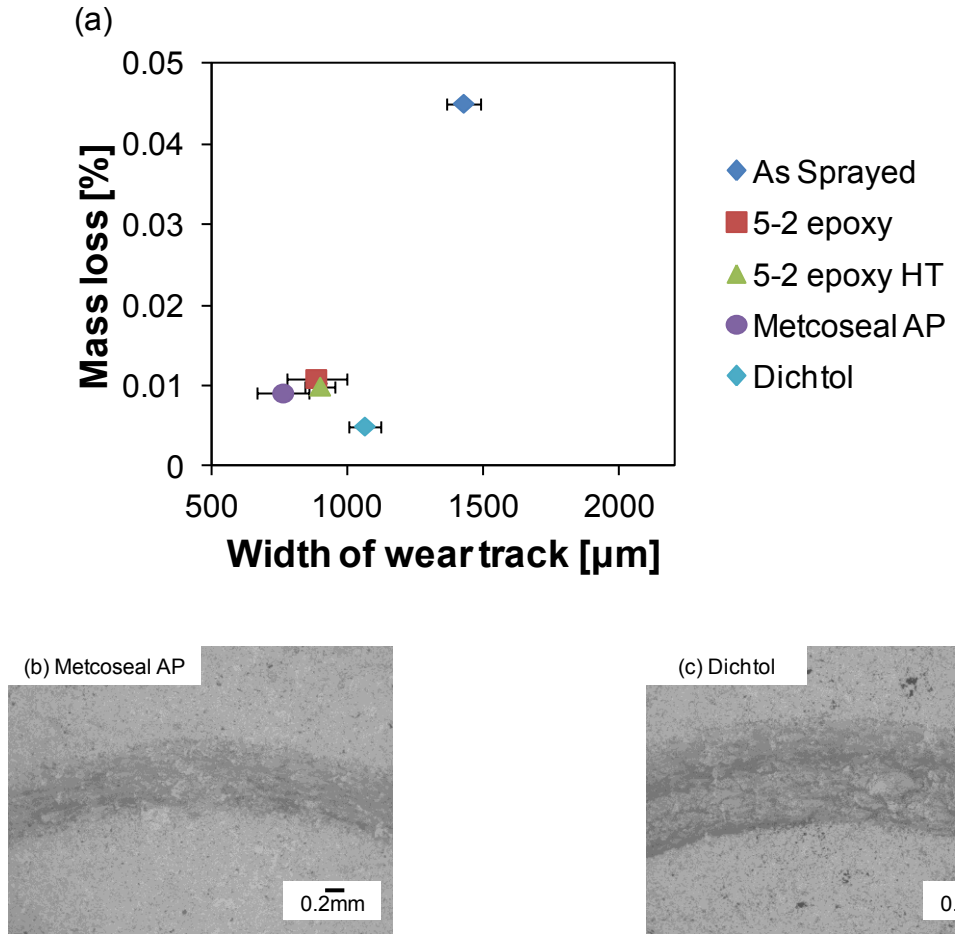

Figure 9.8. a) Percent mass loss plotted against the wear track width of the medium porosity alumina rod flame spray coating. SEM top surfaces of the coatings treated with b) Metcoseal AP and c) Dichtol. Interfacial modifications of the coatings lead to enhanced wear properties indicated by less mass loss and a wear track that is reduced in size.

9.4.2. Wear Behavior of Metallic Coatings Interfacially Modified with Thermal Spray Sealers

Two different Molybdenum-molybdenum carbide (Mo-Mo_2C) coatings were plasma sprayed on aluminum substrates. However, plasma sprayed molybdenum coatings are rather soft and do not provide adequate wear resistance [104]. Therefore, molybdenum powders with varying carbide content were plasma sprayed, Table 7. In order to deposit coatings with improved hardness and wear resistance, they are strengthened with carbides. Following deposition specimens were prepared according to the procedures outlined in the experimental section.

Table 7. Carbon percentage and particle size of the two compositions of Mo-Mo_2C powders.

Composition	Carbon (%)	Particle size (μm)
Mo-35Mo_2C	2.2	-75 +30
Mo-55Mo_2C	3.17	-75 +30

Pin-on-disk tribological testing indicates enhanced wear durability of sealer impregnated coatings when compared to as sprayed coatings, Figure 9.9. The Mo-Mo_2C with 3.17% carbon content had a higher as sprayed wear resistance than the Mo-Mo_2C with 2.2% carbon content. When thermal spray sealers were applied to the coatings, there were no major differences observed between the two coatings in the width of their wear tracks or mass loss percent. These findings are important because they show that metallic templates deposited via thermal spray and infiltrated with thermal spray sealers show improved wear resistance over as sprayed templates. This is another benefit associated with nacre-like composites formed through deposition of thermally sprayed templates infiltrated with a more ductile secondary phase.

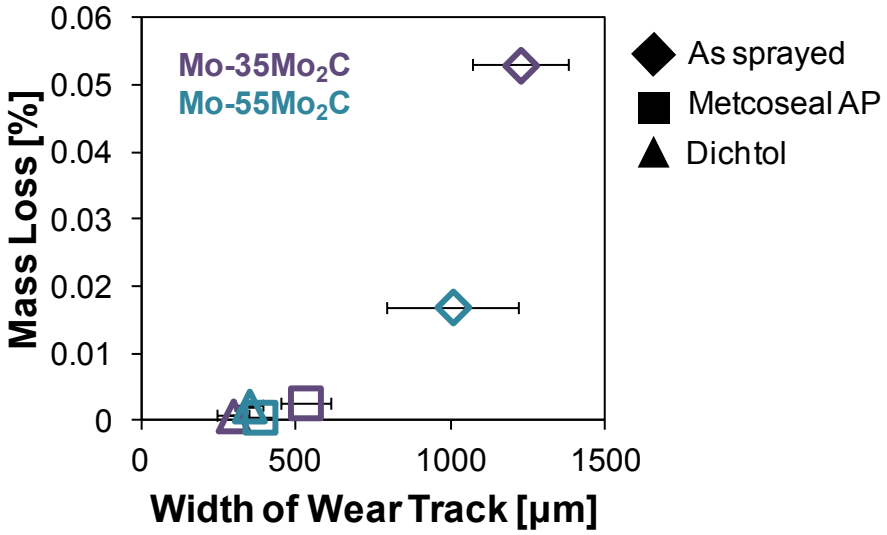

Figure 9.9. Percent mass loss plotted against the wear track width of the two Mo-Mo_2C compositions for the as sprayed and Dichtol and Metcoseal AP impregnated coatings.

Wear behavior of a nickel aluminum coating with the application of sealers led to a wear track with reduced dimensions, width and depth, Figure 9.10. This suggests that infiltration of the porous metallic template with a secondary phase can provide some benefit in terms of resisting wear. Not only is the open surface porosity sealed, but modifying interfaces that would otherwise contain air improves the ability of the coating to withstand deformation caused by the

application of a load. It could be expected that the mass loss of the sealer impregnated coatings increases following wear experimentation because the presence of a sealer adds mass to the substrate/coating system.

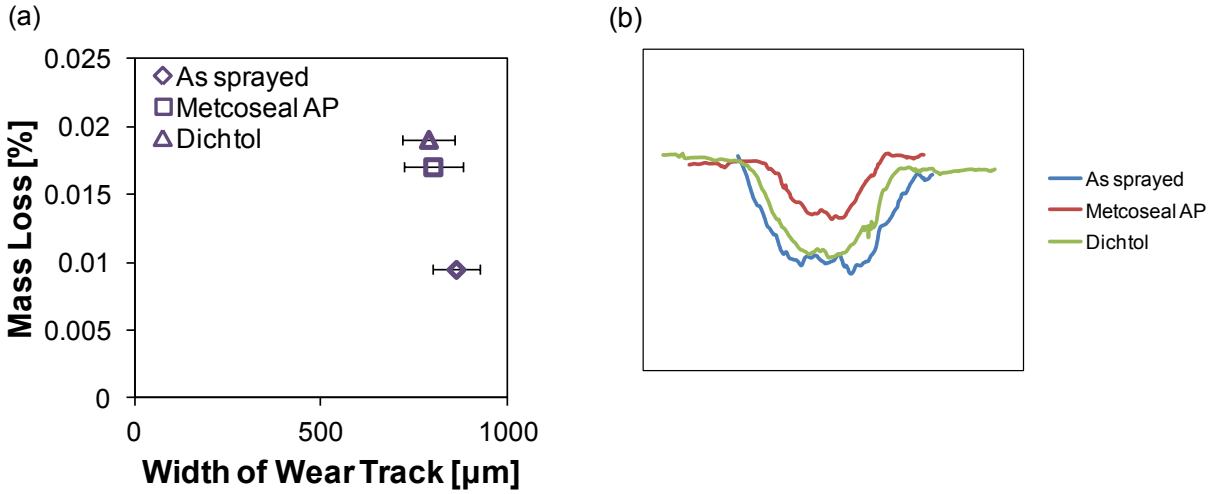

Figure 9.10. a) Percent mass loss plotted against the wear track width of the plasma sprayed NiAl coating for the as sprayed, Dichtol and Metcoseal AP impregnated coatings. b) Relative wear track depths are provided for each condition.

9.5. Summary and Conclusions

This chapter examined the response of bio-inspired materials to adhesive wear from pin-on-disk testing. The application of sealers provides enhanced wear resistance to both metallic and ceramic coatings in terms of a reduced mass loss and wear track width. Epoxy and sealer impregnation of both yttria stabilized zirconia and alumina coatings display tremendous enhancement in wear properties. Sealer impregnation also enhanced the wear properties of metallic coatings, including Mo-Mo_2C and NiAl. Unfortunately, due to limitations in sample quantities, each condition was only tested once. In the future, it is essential to perform a more in depth study including a number of other metallic coatings and varying process conditions to determine how sealers can enhance the performance of thermal spray scaffolds. It is also essential that several specimens of the same condition are investigated.

The improved wear properties of interfacially modified thermally sprayed templates have important implications. A number of costs are associated with the tribological wear of materials. For instance, wear of a part in industry can lead to failure and tremendous economic losses.

Economic losses resulting from wear could be due to replacement costs or maintenance costs, including both scheduled and unscheduled. Therefore, any way wear can be prevented or hindered is of great value especially if it is by a method as simple as the application of thermal spray sealers to a coating. Improving the wear life of materials could result in more durable products and tremendous monetary savings.

10. Improved Corrosion Resistance of Bio-Inspired Materials

The previous chapters examined the effect that thermally sprayed sealers have on properties of both ceramic and metallic coatings, including flexural strength and wear resistance. Often metallic coatings are treated following deposition to enhance their corrosion resistance. This chapter will provide some confirmatory results on metallic coatings that have been exposed to a 3.5wt% NaCl solution in deionized water to show that another benefit associated with nacre-like materials is corrosion resistance.

10.1. Introduction to Corrosion

Corrosion can be defined as a chemical or electrochemical reaction that occurs between a material, often a metal, and its surrounding environment. It is a process that occurs naturally because materials strive to reach their lowest possible energy state. Usually corrosion leads to a decline in the properties of a material and so it is an important issue. The corrosive behavior of a material is dependent on its surrounding environment which is identified by physical and chemical state, and the temperature.

The classification of corrosion is based on three factors:

- The nature of the corrosive agent; it can be wet (aqueous) or dry. The former requires some sort of liquid or moisture while the latter is mostly due to reactions with gases at elevated temperatures.

- The corrosion mechanism which can be from either direct chemical reactions or electrochemical reactions.

- The visual appearance of the corroded material. Corrosion can either occur uniformly over the entirety of a material's surface or it can be localized in areas.

Aqueous corrosion can further be divided into eight forms based on the appearance of the corroded material. However, in reality not all cases can be easily divided into one category and are usually a mixture of two or more. These eight forms include:

- Uniform corrosion
- Pitting corrosion
- Crevice corrosion
- Galvanic corrosion
- Erosion corrosion
- Intergranular corrosion
- Dealloying
- Environmentally assisted cracking

Localized corrosion can further be divided into macroscopic and microscopic corrosion. Localized corrosion at the macroscopic level includes corrosion that is either visible to the naked eye or with the use of a low-power magnifying device. Microscopic local corrosion can sometimes be more detrimental than macroscopic localized attack because often microscopic local corrosion is not observed until a high level of damage occurs.

Corrosion mitigation is a major issue due to the effects of corrosion which are both direct and indirect. For instance, a direct effect would be the loss of service life of a product while an indirect effect is how producers pass on corrosion costs to consumers when they purchase goods. There are several ways detrimental effects of corrosion can be prevented including, the application of TS coatings with a thermal spray sealer to a surface. The rest of the chapter will focus on the ability of bio-inspired nacre-like materials to provide enhanced corrosion resistance.

10.2. Potentiodynamic Polarization for Electrochemical Evaluation

There are two rather different methods that can be employed when evaluating the corrosion resistance of materials. They include a direct current (dc) electrochemical technique and alternating current (ac) electrochemical impedance spectroscopy. Of the direct current

electrochemical techniques, the most common is potentiodynamic polarization which is the method that was used for the evaluation of the benefits associated with nacre-like materials in impeding detrimental effects on properties caused by corrosion.

As previously mentioned in Chapter 4, the system supports three electrodes; the working electrode, counter electrode and reference electrode. The working electrode, or the sample serves as the anode. Platinum mesh is used as the counter electrode and serves as the cathode for the experiment. The reference electrode is used to ensure a fixed potential so the potential difference can be measured during the test. In this case, a saturated calomel electrode (SCE) is utilized for the reference electrode. The SCE reference electrode is based on the reaction between mercury and mercury (I) chloride with a saturated solution of potassium chloride in contact with the mercury and mercury (I) chloride. A stable reference electrode ensures any changes in potential can be related to any surface changes in the metal being studied providing insight into corrosion mechanisms affecting the surface.

A potentiodynamic polarization test consists of exposing a sample to a liquid electrolyte and leaving the system for some time to allow equilibration to occur. With respect to the reference electrode, the equilibrium corroding potential, E_{corr} is measured. The voltage is then swept from negative to positive values while current is measured, providing insight into corrosion behavior of the material while exposed to the electrolytic environment, which as mentioned in Chapter 4 is a 3.5wt% NaCl solution in deionized water.

During a potentiodynamic polarization experiment, a typical curve is obtained, Figure 10.1. The curve has two distinct regions, cathodic and anodic. As the voltage is swept from negative to positive the response of the system, as current, is monitored and plotted to show the two reactions occurring. The theoretical cathodic and anodic currents are observed as straight lines. The curved line shows the total current and is the sum of the anodic and cathodic currents. As the potential is swept during an experiment, the total current is the current being measured. It is important to note that a logarithmic scale is utilized due to the wide range of current values measured during potentiodynamic polarization. In fact, it is possible for measured current to vary by six orders of magnitude in one test. [89].

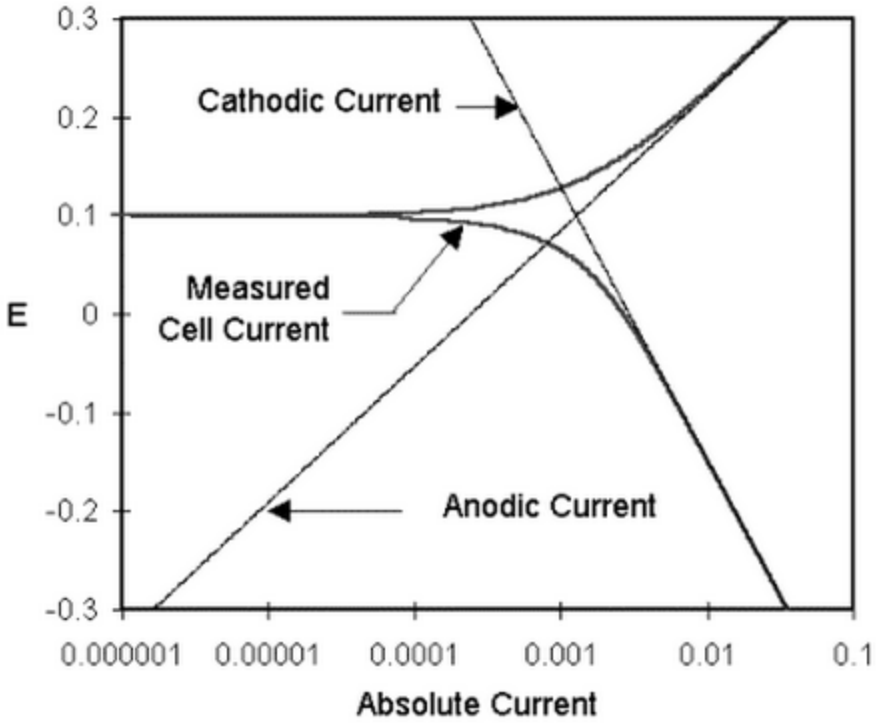

Figure 10.1. Typical curve obtained during a potentiodynamic experiment showing the anodic and cathodic components [89].

10.3. Electrochemical Corrosion Behavior of Nacre-like Nickel Aluminum Coatings

For this set of experiments, a porous nickel aluminum coating was deposited, Figure 10.2. The goal was to then apply TS sealers as a means of interfacially modifying these coatings so they would resemble nacre-like materials and thus their response to a corrosive environment could be improved. It has already been shown that the presence of a secondary phase enhances mechanical properties like fracture toughness and flexural strength, therefore corrosion resistance could be an additional benefit associated with biomimetic composites based on thermally sprayed scaffolds.

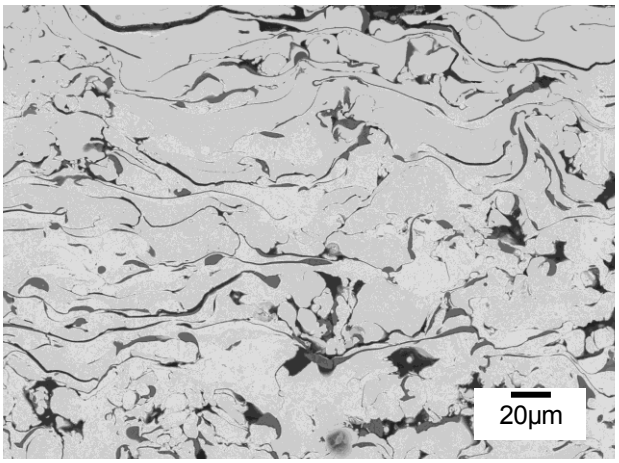

Figure 10.2. Porous APS NiAl coating deposited to investigate the corrosion response of bio-inspired thermally sprayed materials.

Potentiodynamic polarization experiments were performed in a 3.5wt% sodium chloride solution as described in the experimental section on as deposited nickel aluminum and nickel aluminum with thermal spray sealers applied following the deposition process. During a polarization experiment, the relationship between the electrochemical potential and corrosion current are continuously monitored providing insight into the metal's behavior in a corrosive environment.

The response of the nickel aluminum coating both as sprayed and with Metcoseal AP and Dichtol is depicted in Figure 10.3. It was expected the presence of sealers in the open porosity of a coating would lead to an enhanced ability of the coating to provide protection to the underlying base material. This is because the majority of the open porosity and interconnected porosity becomes sealed due to the presence of sealants limiting attack by corrosive media. This is exactly what occurred as seen in the figure. Due to the application of thermal spray sealers, the E_{oc} (open circuit potential) or E_{corr} (corrosion potential) is higher than for the as sprayed coating. In addition, the I_{corr} for the as sprayed coating is higher. The corrosion potential or open circuit potential is indicative of a materials susceptibility to corrosion, with a higher open circuit potential pointing to a higher corrosion resistance. As the potential is increased beyond the open circuit potential the current starts to increase. This region of the curve is the active region, which corresponds to the dissolution or oxidation of the metal. At a certain potential, current begins to remain constant, which corresponds to the passivation region. This region of the graph signifies the passive layer formation which provides protection against further corrosion. Application of sealers to nickel aluminum coatings provided corrosion protection to the surface as exhibited by the increased slope and passivation.

Examination of cross-sectioned coatings following electrochemical testing provided further support to the benefits associated with sealer application. Decreasing the porosity and thus increasing the density, provides coatings that are more suited to withstand corrosive environments because the corrosive media encounters more difficulty in reaching the substrate. The electrolyte solution faces more resistance in penetrating the through thickness of the coatings and reaching the substrate in sealed coatings. This can explain why the as sprayed coating in Figure 10.3 has a greater surface area of corroded substrate than the coating with Metcoseal AP or Dichtol. In addition, the coatings to which Metcoseal AP and Dichtol were applied show less oxidation at their surface. Furthermore, as evidenced in the images, part of the as sprayed coating is completely corroded away as indicated by the rough top surface of the coating and overall reduced coating thickness when compared to the infiltrated coatings. The thickness of the deposited nickel aluminum coating was approximately 500μm and following infiltration there was approximately 277μm, 300μm, and 386μm that had not been corroded for the as sprayed, Dichtol infiltrated, and Metcoseal AP infiltrated specimens respectively.

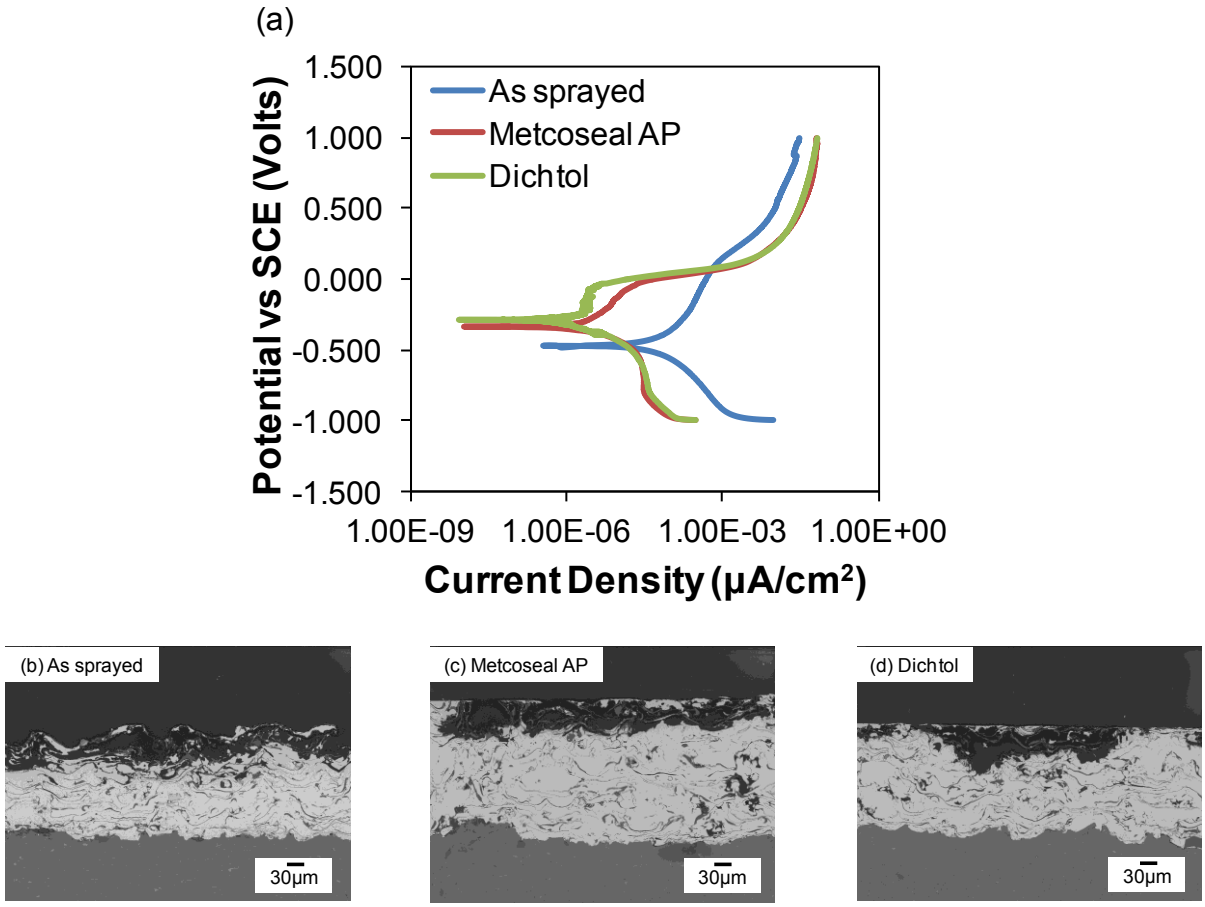

Figure 10.3. a) Potentiodynamic polarization curves for an as sprayed nickel aluminum coating and nickel aluminum coatings that have been infiltrated with the thermal spray sealers, Metcoseal AP and Dichtol. Improved corrosion resistance of the sealant infiltrated coatings is observed. Cross sections of the b) as sprayed nickel aluminum, c) Metcoseal impregnated and d) Dichtol impregnated coatings after testing.

Three major corrosion mechanisms come into play with potentiodynamic polarization of thermally sprayed materials. These are galvanic corrosion, pitting corrosion, and crevice corrosion. Galvanic corrosion occurs because the coating/substrate system is composed of two metals so the electrolyte solution will penetrate the surface of the coating and attack the coating/substrate interface. Crevice corrosion occurs when there is a localized ion concentration difference in dissolved oxygen in the crevice and the area outside the crevice. Crevices initiate oxygen starved regions leading to corrosion and possible delamination of the coating. Pitting corrosion occurs as a result of the rough surface of a thermally sprayed coating. The top surface has a number of asperities. In addition to the asperities, there are also grooves in which the corrosive media can build up. If corrosive media builds up in areas of coating roughness, then

localized attack toward the substrate is promoted. Interconnected porosity leads to pitting and crevice corrosion and allows for easy passage of corrosive media to the substrate.

Coatings infiltrated with sealers are better able to withstand the simulated salt water environment as evidenced by a greater nickel aluminum coating thickness remaining. Based on the microstructural images, the coating thickness remaining of nickel aluminum infiltrated with Metcoseal AP is the greatest, indicating the highest corrosion resistance. It is also important to note that electrochemical corrosion testing on multiple repetitions of each condition should be completed. A more intensive study would provide further insight. However, there is still an indication based on the corrosion response of the NiAl coating with and without sealers, a benefit is associated with the application of sealers.

10.4. Corrosion Behavior of Molybdenum-Molybdenum Carbide Coatings

Electrochemical testing provided some interesting findings about the corrosion behavior of Mo-Mo_2C coatings with sealers. Two Mo-Mo_2C coatings were plasma sprayed using the same parameters but the powders contained varying carbide content, Mo-35Mo_2C and Mo-55Mo_2C. Further details are provided about both powders in Table 7. The results support that coatings with a higher carbide content have better corrosion resistance which is further enhanced by the presence of thermal spray sealers, Figure 10.4 and Figure 10.5, which is the same finding for improved wear resistance in Chapter 9.

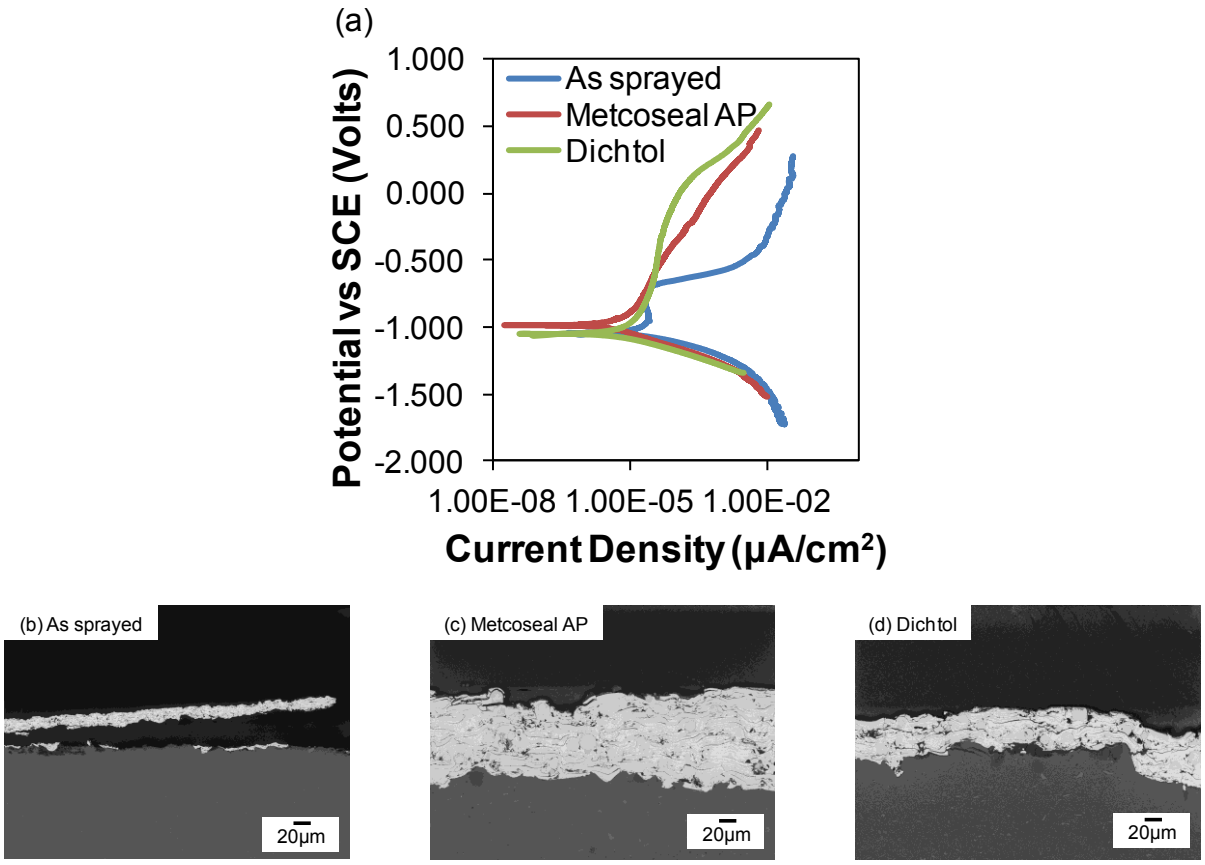

Figure 10.4. a) Potentiodynamic polarization curves for an as sprayed Mo-35Mo_2C coating and Mo-35Mo_2C coatings that have been infiltrated with the thermal spray sealers, Metcoseal AP and Dichtol. Improved corrosion resistance of the sealant infiltrated coatings is observed. Cross sections of the b) as sprayed Mo-35Mo_2C, c) Metcoseal impregnated and d) Dichtol impregnated coatings after testing.

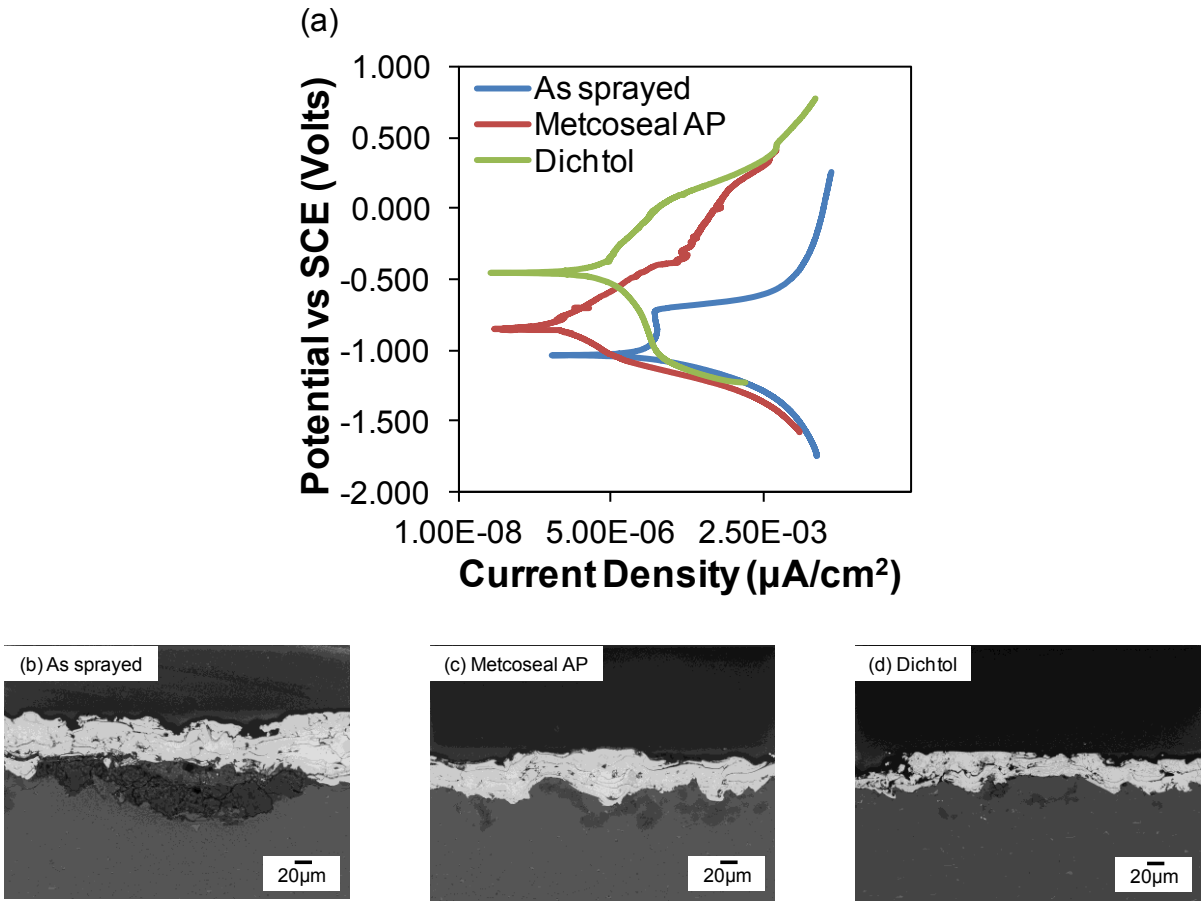

Figure 10.5. a) Potentiodynamic polarization curves for an as sprayed Mo-55Mo_2C coating and Mo-55Mo_2C coatings that have been infiltrated with the thermal spray sealers, Metcoseal AP and Dichtol. Improved corrosion resistance of the sealant infiltrated coatings is observed. Cross sections of the b) as sprayed Mo-55Mo_2C, c) Metcoseal impregnated and d) Dichtol impregnated coatings after testing.

10.5. Summary and Conclusions

Corrosion is defined as the unintended and destructive attack of a material usually beginning at the surface. Of corrosion mechanisms, the electrochemical attack of metals is one of the most important. Electrochemical corrosion is defined as corrosion that is characterized by two half reactions, an oxidation reaction and a reduction reaction. Electrochemical corrosion is an extremely costly problem with approximately 5% of an industrialized nations income spent on the prevention or maintenance of previously corroded products. Not only is corrosion an

expensive issue but it can result in failures of equipment plants, steel bridges, buildings and ships with potentially deadly consequences.

In this chapter, another advantage of interfacially modified TS coatings was presented. This time the presence of thermal spray sealers provided benefits of impeding corrosion. By filling voids and interconnected porosity, corrosive media is prevented from reaching the substrate and thus corrosion is hindered. Sealing off porosity and defects introduced as a result of the spray process leads to a denser more corrosion resistant coating. Although the results presented in this chapter, show that nacre-like materials based on TS scaffolds lead to more corrosion resistant coatings, it is essential that a greater number of specimens be studied including multiple repeats of the same condition which due to sample and time limitations was not able to be completed.

11. Structure and Mechanical Property Relations of Bio-Inspired Thermal Spray Composites

One of the most significant findings of this investigation is the structure and property relationship that leads to property enhancements when brittle TS ceramic templates are combined with polymer to fabricate bio-inspired hybrid composites. Presence of a softer organic phase is not solely responsible for governing property enhancements. The arrangement of the brittle ceramic templates is just as important. This can be surmised as nature has evolved over millions of years a natural material, nacre, which displays both a tremendous strength and toughness and is composed of highly ordered aragonite templates following a design hierarchy. In designing manmade materials, much can be gained through studying natural systems.

Nacre, a natural material provided inspiration for this investigation because of its tremendous properties exhibited despite being composed mainly of brittle calcium carbonate. Calcium carbonate platelets comprise approximately 95vol% of the natural material, while biopolymer organic interlayers make up the remaining 5vol%. Together, the combination of brittle calcium carbonate and biopolymer result in properties such as strength and toughness that far surpass those expected by the rule of mixtures.

This dissertation has sought to apply design features of nacre to ceramic and metallic scaffolds produced via thermal spray processes to achieve synergistic property enhancements in the fabricated TS composites. The goal of this dissertation was to fabricate synthetic nacre-like materials through combination of a ceramic scaffold and polymer leading to significant property enhancements. Both ceramics and polymers display poor macroscale properties but when combined achieve levels that far surpass those that would be expected based on the rule of mixtures. For instance, polymers are extremely flaw tolerant but prone to deformation at low stress levels and ceramic materials have a high strength but are brittle, making them prone to brittle fracture. However, when brittle TS ceramic templates are combined with a softer polymer, a composite with a high degree of both strength and toughness is achieved.

Fabrication of a biomimetic composite and achieving synergistic enhancements in terms of mechanical properties such as fracture toughness and flexural strength includes the design of an optimized template and successfully introducing polymer into a given template. The major aspects of this study included the template fabrication, polymer introduction, and finally observation of property enhancements. Each will be discussed.

11.1. Fabrication of Templates

One of the benefits associated with thermal spray is the relative ease associated with the deposition of a coating. Within minutes, a coating ranging from micrometers to a millimeter can be deposited through optimization of process parameters. Through appropriate tuning of the spray process and/or parameters, the coating microstructure can be significantly altered thus affecting mechanical performance of the coating, Figure 2.11. This is a major advantage of the thermal spray process for scaffold preparation which exhibits the potential for industrial scale synthesis of nacre-like synthetic structures.

The following are a list of template characteristics that were optimized during this dissertation by altering the spray process and spray parameters:

- Organization
- Porosity content
- Template material

Further processing of fabricated scaffolds can also be employed to design synthetic structures with enhanced mechanical properties. This dissertation has discussed some of these design related strategies in sections 7.1 and 7.2, namely

- Dimensionality
- Stacked layers

Perhaps the most significant parameter for template design is the organization of the coating template. Spray processes that can be utilized for scaffold fabrication were powder flame spray, ceramic rod flame spray, and plasma spray. Powder flame spray results in the deposition of a coating with a high degree of globular porosity and disorganization. The Rokide® spray system a ceramic rod flame spray process, has exhibited a highly organized coating deposit with layers of splats clearly defined. Details of these processes are provided in section 4.1. The ceramic rod flame spray process is significant because the process eliminates a number of globular pores and voids which are defects caused by the deposition of semimolten or unmolten particles. A more hybrid structure is achieved through the plasma spray process which displays both a moderate degree of globular porosity and a somewhat layered microstructure.

Image analysis confirmed the porosity levels and architecture of the three critical microstructures, Figure 6.1. It can be surmised that a layered structure combined with a tougher polymer would lead to property enhancements because this is observed in natural nacre. Ceramic rod flame spray coatings provide the most organized coating architecture and mostly

interlamellar porosity between splats lead to a starting template that is most similar to nacre, Figure 5.1. Many natural materials have highly organized composite structures that are arranged over several length scales. Obviously, these structures have evolved because they meet the design requirements of the organism. Nature applies materials to structures in such a way as to achieve the maximum benefits. If this were not the case, organisms may not be able to survive in their environment. The combination of such materials as brittle calcium carbonate and biopolymer to form nacreous assemblies in nacre also applies when it comes to synthetic materials. It was determined that alumina rod flame spray provided the greatest opportunity to synthesize an ordered microstructure, which can be seen in Figure 11.1.

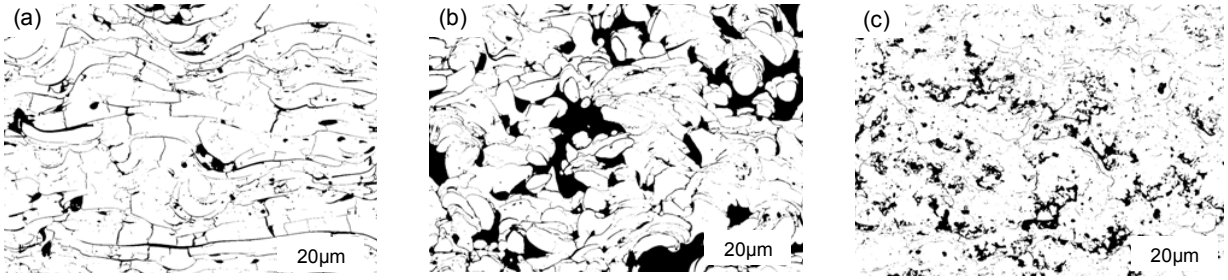

Figure 11.1. Binary images of the template architectures representing the associated features present in the coating. (a) The ceramic rod flame spray templates have porosity mostly consisting of interlamellar gaps with little globular porosity while the powder flame spray templates (b) contain mostly globular pores and voids. The plasma spray process leads to the deposition of a coating template with a hybrid structure (c).

Dimensionality has an effect on the property enhancements of biomimetic hybrid composites. Specimen width does not play a role in the level of property enhancements, Figure 7.3 and Figure 7.6, but specimen thickness was found to have a tremendous impact on the ability of properties such as flexural strength and fracture toughness to be enhanced, Figure 7.7. Specimen thickness is believed to be an important parameter in terms of the dimensionality of the specimens because polymer is not able to successfully penetrate the entire through thickness of the coating, Figure 7.8.

11.2. Optimized infiltration of templates

Infiltration methods and coating templates were investigated concurrently to determine which method would allow for the highest polymer content to be incorporated into a scaffold and whether this method was dependent on coating template and polymer type.

Initial experiments were conducted with epoxy in order to determine whether vacuum impregnation or simple immersion would lead to the highest polymer content and thus property enhancements. Results showed the introduction of polymer into plasma spray and flame spray templates was most successful by vacuum infiltration. Simple immersion and vacuum infiltration consisted of placing a coating in polymer solution. However, during the vacuum infiltration procedure the coating and polymer solution were placed in a vacuum of 0.1mm Hg. Vacuum infiltration was further explored such that the coating was initially placed in the vacuum chamber and polymer solution was then introduced to the sample. This was completed by two methods. The first allowed polymer to enter the vacuum chamber through a tube by opening a valve once the appropriate vacuum level was reached. The second method included use of a second vacuum to suspend the coating allowing it to drop into a polymer solution. The first method was ruled out because allowing polymer to enter after vacuum pressure was reached damaged the specimens. The second method was ruled out because there was no benefit observed. The vacuum infiltration process was further tailored by exploring various infiltration times and it was determined that 4 minutes was sufficient time.

PVA, PMMA, and PDMS coating impregnation was somewhat more challenging than epoxy infiltration, while coating impregnation with thermal spray sealers was not as complicated as in the case of the viscous polymers. These sealers are designed particularly for TS coatings and show easier infiltration through the defect channels. Thermal spray sealers are designed to be self wicking by capillary action. Application of thermal spray sealers by brushing was determined to lead to the highest polymer content and property enhancements. Based on these observations, the brushing procedure is the recommended infiltration procedure for sealers.

Infiltration of PDMS and 6wt% and 22wt% PVA into the three template architectures considered in this study has indicated significant challenges in infiltration primarily due to the high viscosity of the polymers, Table 2. Using a SEM to examine coating fracture surfaces, very little polymer was observed throughout the coating cross sections even with vacuum infiltration of these polymers. Further advancements in the infiltration methodologies, such as higher vacuum levels can be exercised to achieve a greater level of infiltration and hence, higher enhancements in mechanical properties. Another approach toward better infiltration can be made by altering the ratios of both components required for the cross-linking of PDMS to lower the viscosity. However, a tradeoff does exist because in general polymers with a higher viscosity tend to have higher mechanical properties such as strength. When scaffolds are infiltrated with an increasing weight percent of polymer in solution, such as 6wt% and 22wt% PVA, there is an

improved strain tolerance and comparable strength. Therefore, it may be desirable to have a polymer with high viscosity. Additionally, it may be possible to expose ceramic scaffolds to binders or coupling agents, which serve as a means of improving bonding between an organic and inorganic material, in this case, the polymer and the ceramic scaffolds.

An interesting finding occurred with the infiltration of PMMA, as introduction method is dependent on coating template. When the majority of the coating porosity is interlamellar porosity and there is little globular porosity as in the case of Rokide® coatings, specimens are more completely infiltrated by performing in-situ polymerization as opposed to vacuum infiltration with a more viscous 8wt% and 22wt% PMMA solution. As in the case of PVA and PDMS, the PMMA polymer solution is rather viscous, Table 2, that even with vacuum infiltration, little polymer was observed in coating fracture surfaces. In performing in-situ polymerization of PMMA into the ceramic scaffolds, an etching and grafting step precede the polymerization reactions. The purpose of the etching and grafting steps are to leave hydroxyl groups on the ceramic scaffold surface to increase bonding between the scaffold and organic polymer. In the case of the ceramic rod templates, the strength of composites was higher for coatings with PMMA polymerized in-situ when compared to PMMA in solution that had been infiltrated into scaffold porosity.

11.3. Synergistic Enhancements

Of particular importance, is that the benefits afforded by the polymer/ceramic combination are not equivalent for each starting microstructure suggesting there is a strong correlation between structure and properties. Powder flame spray Al_2O_3 contains higher porosity than ceramic rod flame spray Al_2O_3 due to the nature of the spray processes. Plasma sprayed YSZ has a porosity level that is in between the ceramic rod and powder flame spray processes. It is not necessary that polymer content after infiltration into these distinct templates is higher with more porosity. The powder flame spray composite had approximately 3.8wt% epoxy with approximately 22% porosity. The ceramic rod flame spray coating had approximately 2.3wt% epoxy with a porosity content of approximately 15% and there was about 4.5wt% epoxy in the YSZ plasma sprayed composite while there was approximately 12% porosity.

Flexural strength and fracture toughness enhancements vary depending on starting microstructure and polymer content with the results being more complex than simply a high polymer content (Figure 5.6, Figure 5.7, and Figure 6.7). This suggests the starting microstructure plays a critical role in observed properties following infiltration. Those ceramic templates that are more organized are able to be enhanced to the furthest degree. Part of the reason is the as deposited properties of the organized structures are higher than for the powder

flame spray templates. However, the as deposited values are rather close to those for the YSZ plasma spray. This reason is likely attributed to the fact that the hierarchical structure is ordered, which is often observed in natural materials such as nacre. Bio-inspired coatings based on laminated TS templates appear to be more able to withstand high loads and resist fracture. This could be attributed to the fact that Rokide® splats have some waviness to them. When splats experience tensile stress, they may be able to slide and the waviness of layered splats can interfere with further sliding due to locking of splats together. In addition, there is some roughness on the surface of splats due to grain growth termination sites. Surface roughness of splats can hinder splat sliding which is also more prevalent in organized structures. In addition, splat cohesion further anchors splats to one another which make a laminated coating more robust. When a second polymer phase is introduced into the TS scaffold, there is further anchoring due to polymer acting as an adhesive which further limits sliding. With a more organized and laminated structure there is more regularity to the TS composite and thus these mechanisms can occur.

Only after a suitable coating template and successful polymer introduction methods were explored could synergistic effects of brittle ceramic and tough polymer be investigated. Although interfacial modifications with a secondary phase resulted in enhanced properties of each template, only with Rokide® templates did the property enhancements reach or surpass the range of natural nacre. Ceramic rod flame spray coatings provided an organized structure while limiting defects such as globular porosity and voids which serve as a means of disrupting the organization displayed by a coating microstructure.

The synergistic effects observed when a softer and more ductile second phase is combined with a brittle ceramic phase thus depend on the interactions of the starting template structure and behavior of the polymer. This can be surmised due to the staggered alumina rod flame spray templates displaying the highest property enhancements yet containing the lowest polymer content. Further exploration of processing conditions, such as changes in standoff distance, to change the coating porosity level suggests template architecture needs to have a certain degree of porosity in order to display optimal enhancements and it is not solely a high level to allow a high polymer content, Figure 5.6, Figure 5.7, and Figure 6.7. Eventually a porosity level is reached which is too great, that mechanical property enhancements begin to stabilize. This is illustrated by altering the ceramic rod flame spray microstructures through changing the standoff distance. As the standoff distance is increased, the temperature and velocity of the particles is lowered, and thus interfacial interactions are reduced leading to a higher porosity content. Based on the results shown in section 5.4, a porosity level of 14.6% (5” standoff) was found to result in the greatest increase in flexural strength and fracture toughness compared to coatings deposited at other standoff distances. Lower porosity levels which correspond to lower standoff distances, may not have been sufficient to allow for polymer infiltration and cohesion of splats may have been too great to allow splat sliding. As porosity content in increased to 17.6% (6” standoff), the splats may be too loosely bonded to maximize the effect that sliding has on property

enhancements. In addition, the globular porosity increases, Figure 5.7. This negatively impacts the organization displayed by the alumina rod coating and also would lead to a lesser degree of sliding and splat pull out.

Starting with an optimized template, for example Rokide, the evolution of properties using epoxy are systematically presented in Figure 11.2, with the four steps in the process labeled in the figure.

- As sprayed Rokide® template is optimized.
- Template is infiltrated with epoxy that is mixed 5 parts resin to 2 parts hardener.
- Thermal spray/epoxy composite is heat treated for 2hr at 200˚C to allow the epoxy to achieve its maximum mechanical properties.
- The epoxy solution is modified by adding a toughener to the mixture which will increase the toughness of the epoxy.

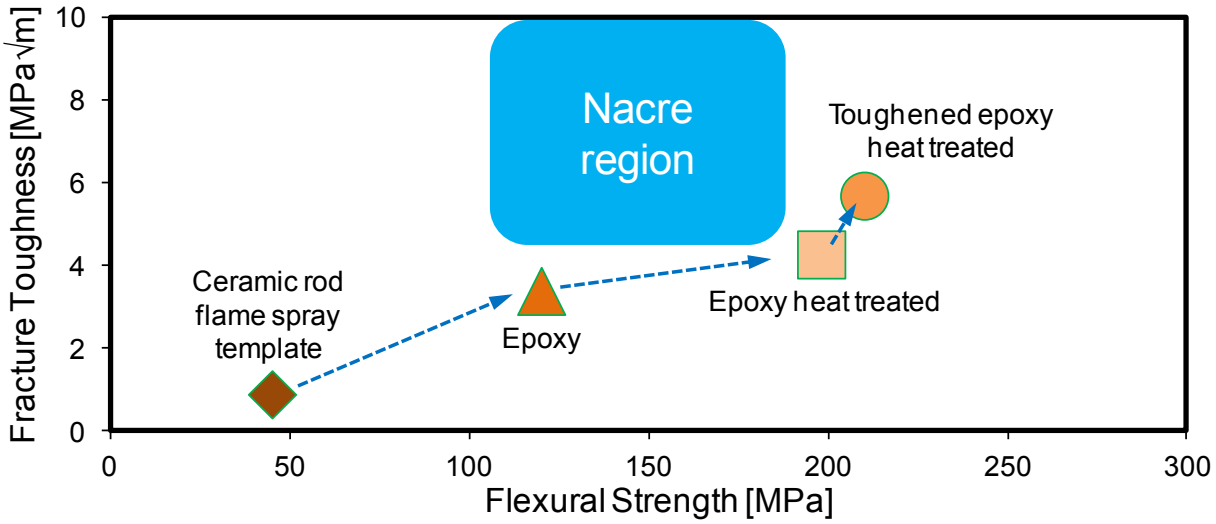

Figure 11.2. The evolution of a Rokide® thermal spray template to a biomimetic nacre-like composite with exceptional fracture toughness and strength. Properties of natural nacre are indicated. The four steps in the design include optimization of the ceramic rod template, infiltration with epoxy. The composite is heat treated so that epoxy can achieve its maximum properties and finally the epoxy is modified to increase the toughness.

The synergistic enhancements were only possible following the optimization of the thermal spray scaffold and the infiltration process. Based on the findings of this dissertation, there is a strong correlation between structure and mechanical properties of bio-inspired TS composites. In order for an infiltrated TS coating to display the highest property enhancements, it is necessary for the

scaffold to possess a moderate porosity content and a level of organization which is achieved via the ceramic rod flame spray process.

In summary, this dissertation presents a strategy or methodology for the synthesis of nacre-like composite materials which can exhibit simultaneous improvements in strength, modulus and toughness. This is not normally observed in synthetic materials which typically have either a high strength and modulus or a high toughness, meaning as one property improves, the other shows a decline. It is said synthetic materials follow a reverse banana curve which is indicated in Figure 11.3. This relationship differs for natural materials like nacre and synthetic thermal spray composites which when brittle ceramics are combined with a softer polymer display synergistic improvements in properties such as modulus and fracture toughness. Lastly, this work shows that thermal spray composites can serve as robust coatings.

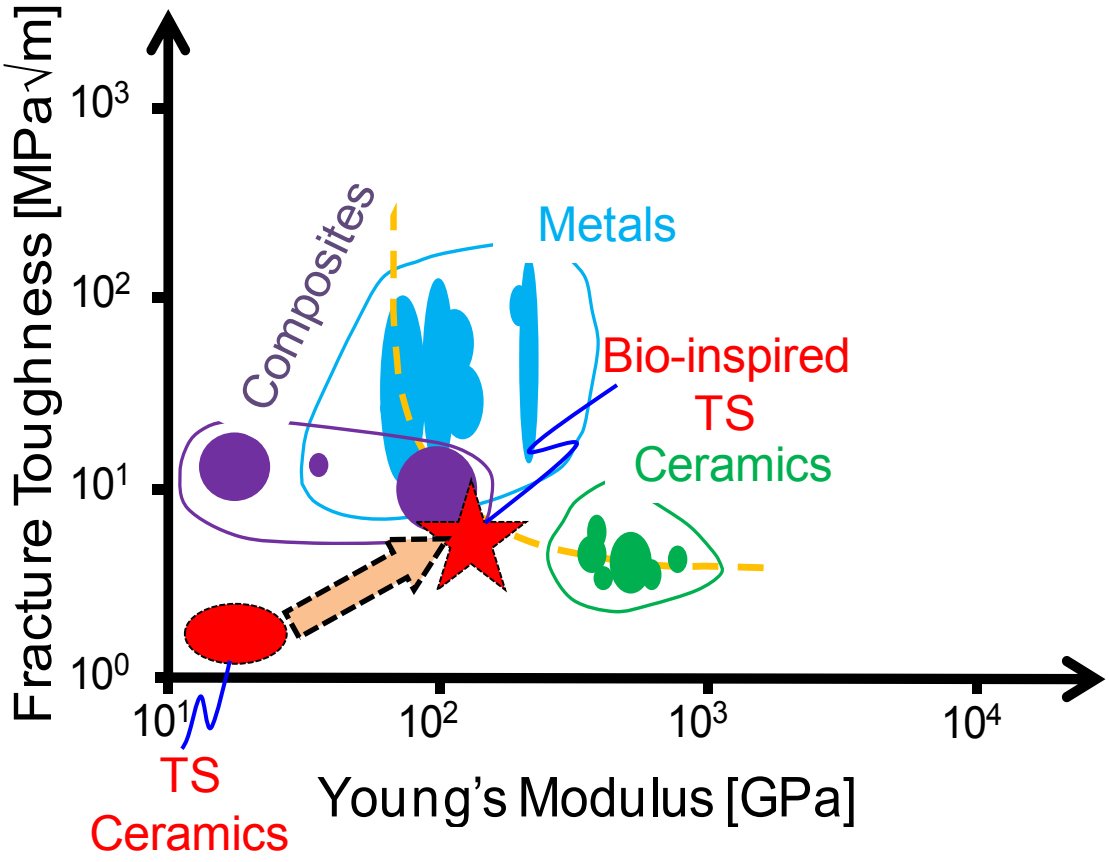

Figure 11.3. A modified figure from Qin et al. showing fracture toughness and modulus for synthetic materials. Synthetic materials display either a high fracture toughness or modulus [105]. This is not the case with bio-inspired TS composites which show both a high fracture toughness and high strength when compared with the as sprayed templates.

12. Summary and Conclusions

The research presented in this dissertation attempts to provide an analysis of the fabrication of bio-inspired materials through polymer infiltration of TS templates. Previous work by Liu *et al.* discussed anelasticity in depth and was followed by Dwivedi *et al.* Their work touched on the similarities in mechanical behavior in terms of nonlinearity and hysteresis between thermally sprayed coatings and natural laminated materials like nacre. It was noticed that both coatings and natural materials like rock, bone and nacre display anelasticity. In order for a material to be characterized as anelastic, it must display both nonlinearity and hysteresis. Nonlinearity allows for the redistribution of high levels of stress, making the material more able to withstand deformation. Hysteresis is an energy dissipative mechanism. In thermal spray materials nonlinearity is due to the opening and closing of pores with the application of loads. While the interfacial sliding of rough splat surfaces on one another leads to the presence of hysteresis. Naturally layered materials also have defects and microstructural attributes that cause these phenomena.

Not only do thermally sprayed coatings and nacre have similarities in terms of their mechanical behavior but also in terms of their microstructure. Coatings are deposited by the successive impingement of splats on a surface. This leads to the buildup of a lamellar coating that can be analogous to a brick wall. However, nacre, also a layered material can be described as having a brick and mortar microstructure. Calcium carbonate platelets are arranged in a highly organized fashion with nanometer thick interlayers of organic material surrounding the calcium carbonate inclusions.

Exploiting the similarities in thermally sprayed materials already there in terms of microstructure and mechanical behavior, biomimetic nacre-like materials can be fabricated based on templates deposited through thermal spray processes. Due to alterations in processing parameters, template architecture can be tailored to have varying degrees of porosity and type of porosity. In addition, template material can be changed and interfacial modifications can be made using a wide range of different polymers or thermal spray sealers.

Based on the investigations in this dissertation, there is a more ideal structure and type of porosity when it comes to achieving a biomimetic structure that displays synergistic effects analogous to nacre. Of all template architectures examined, ceramic rod flame spray deposited by the Rokide® spray system led to templates that show the greatest coating enhancements of flexural strength and fracture toughness when impregnated with a softer more ductile organic material. What is interesting about these templates is the lamellar microstructure is most clearly

defined. The Rokide® coatings have a staggered structure exhibiting the greatest degree of organization. Millions of years ago, nacre evolved as a highly organized laminated material. When a stiff and brittle material is combined with a second softer more ductile material, having a staggered structure is rather important in obtaining synergistic effects in fracture toughness and strength. Further evidence supports the fact that it is not solely the interfacial modifications that are necessary for coating property enhancements but the staggered arrangement and laminated structure plays a major part too. This was confirmed using thermogravimetric analysis. Even though ceramic rod flame spray coatings did not allow for the highest polymer content to be incorporated into their structure, the enhancements were the highest. Powder flame spray scaffolds accommodate the highest weight percentage of polymer which is due to their high level of globular porosity. Powder flame spray coatings have a microstructure with a high void and globular pore content which allows for a large amount of polymer. However, the structure is not highly organized. In fact it is quite lumpy and chaotic, which is not an ideal template for a biomimetic material.

Just as in nacre, where the biopolymer in combination with the aragonite templates leads to enhancements in properties such as toughness, this is also observed with thermally sprayed templates with the addition an organic phase like epoxy that serve as a biomimetic nacre like material. The nacre-like composites are formed from hard and stiff microscopic ceramic splats with a high aspect ratio. These splats are then infiltrated with a softer, more ductile material. The tablet sliding and strain hardening that occur with the application of a load are thought to be the key mechanisms for the high toughness. It is highly probable these same mechanisms lead to the enhanced fracture toughness of the infiltrated thermally sprayed materials compared to the as sprayed materials. Critical for this to occur is TS splats need to be stiff and hard with a high aspect ratio. They should also be somewhat staggered in their arrangement so that there is some overlap and organized into a dense material. Although the platelets which make up the majority of the composite should be hard and stiff, the organic phase should be more ductile and soft. The interface between the platelets and polymer should be relatively weak when compared to the splats. By incorporating weak interfaces into the structure, it is possible failure occurs there before the tablets fracture, allowing the material to maintain some integrity. This allows for the deflection of cracks from the alumina platelets so that toughening mechanisms are engaged. Eventually when the specimens do fracture, and thus fail under three-point bend loading conditions it is likely caused by splat pullout.

Both the enhanced flexural strength and fracture toughness measured at the macroscale in the manmade composites are the result of synergistic effects that occur over several length scales. For instance, there are mechanisms at work over several length scales from the millimeter, all the way down to the nanoscale grain boundaries that are found in splats. Together these mechanisms are responsible for transferring applied loads and stresses, energy dissipation, and damage tolerance including crack resistance. It is also important to note, that even with the addition of a weak polymeric second phase, there is a tremendous increase in fracture toughness

and flexural strength. This is because of the arrangement of this weak material at the interface in relation to the hard and stiff thermally sprayed splats. For example, the secondary ductile phase surrounds the splats, and even anchors them together, allowing for some degree of deformability at the macroscale making it possible for enhanced mechanical properties.

In addition to the staggered nature of the template, the porosity level of the coating should be sufficient to allow the successful infiltration by a secondary phase but not too great. For instance, interlamellar spacing of a Rokide® coating template was maximized at a standoff distance of 5in. At this spray distance, the interlamellar gaps were large enough to allow for polymer infiltration but not too large and still provided some resistance to splat sliding which is due to nanoscale surface roughness on the splats.

Dimensionality was found to be essential when designing scaffolds for polymer infiltration to synthesize biomimetic nacre-like materials. Specimen length was not varied due to restrictions in the load span of the three-point bend instrument. Various sample widths were tested and found to be independent of property enhancements. Observed property enhancements were found to be dependent on sample thickness. As a scaffold thickness is increased, the distance polymer or thermal sealer must travel to reach the center of the coating increases leading to an increased difficulty in achieving complete infiltration. It is possible that with a vacuum capable of reaching lower pressures that sample thickness would not be dependent on property enhancements.

Although the staggered structure is extremely important for a bio-inspired material to possess, it is not the whole story. Another important aspect to consider is the polymeric or secondary phase through which interfacial modifications of the template architecture will be made. The goal is to achieve synergistic effects in property enhancements when a brittle template component is combined with a ductile polymer. Ideally the fracture behavior exhibited by the combination of the two constituents would be a graceful or ductile failure mirroring that of hydrated nacre. This would indicate the material is somewhat robust and will fail gradually even after system failure rather than failing in a catastrophic manner. However, in polymer selection there is a tradeoff in terms of achieving high flexural strength and fracture toughness and achieving a somewhat ductile failure. Polymeric media that exhibit tremendous mechanical property enhancements, such as a 5:2 epoxy mixture, lead to a rather brittle fracture which can be gleaned through examination of the rather flat fracture surface as well as through analysis of the stress/strain behavior. Those polymers that display a more graceful fracture, such as PVA, do not show property improvements that reach those of an epoxy mixture.

Striving to achieve both high strength and high fracture toughness has lead to the exploration of liquid rubber phases for incorporation into an epoxy mixture. Addition of a second phase can further augment the toughness of an epoxy mixture. As a polymeric phase for interfacial modification, epoxy is beneficial because it is a thermosetting polymer and thermosets tend to be the strongest of all polymers but also the most brittle therefore, exploration of a liquid

rubber phase to enhance the toughness of epoxy could lead to tremendous improvements in the fracture behavior of modified templates. Epoxy modifications should continue to be further explored because they have the potential to offer a number of benefits.

Post deposition, thermally sprayed coatings can be treated with thermal spray sealers to seal off the coatings interconnected porosity, thus serving as a means of protection to the underlying substrate by attack from corrosive media. For this dissertation, thermal spray sealers were shown to provide corrosion resistance to the underlying base metal when applied to coatings. Interestingly enough, sealers can also provide wear resistance and enhancements to mechanical properties such as fracture toughness and flexural strength. This has important implications in that thermal spray sealers can have other advantageous effects that may be somewhat unintended.

Through selection of an appropriate TS scaffold and polymer, bio-inspired composite materials can be synthesized. These composites are somewhat independent of material selection. For instance, enhancements have been observed in ceramic and metallic templates impregnated with a number of polymer phases. Flexibility in selecting materials allows for further tailoring of these manmade systems. This is significant because there is a great potential for bio-inspired materials based on thermal spray coatings.

13. Future Work

One method that could be ideal for depositing thermally sprayed materials with a polymer phase in a brick and mortar nacre-like arrangement is to deposit both simultaneously. By spraying both phases simultaneously, the bonding between the template and polymer could be maximized. However, it is necessary for the materials to be compatible with the deposition process. Another way to accomplish property enhancements may be to deposit a number of passes and apply a layer of polymer followed by additional passes and another layer of polymer until a sufficient thickness is built up. In addition, modifications of liquid rubbers to an epoxy mixture appear promising and should be further explored. This chapter will focus on future work related to the synthesis of nacre-like biomimetic materials based on TS scaffolds.

13.1. Spraying Template Material while Alternately Introducing a Secondary Phase

Depositing alternate ceramic and polymer layers to form a composite is another option for fabricating a nacre-like coating. Deposited coatings could be formed through the buildup of a number of different template materials as well as secondary materials. A few preliminary experiments have been investigated with this technique, but more work should be completed.

One study examined the role of 6wt% PVA sprayed between deposited powder flame spray alumina passes. Samples were prepared for three-point bend to determine flexural strength. Results were repeatable for both the alumina (referred to as the as sprayed coating) and alumina/PVA coatings, Figure 13.1. Unlike with samples that had been infiltrated post deposition, those that are deposited with 6wt% PVA alternately between spray passes have mechanical properties lower than the as sprayed coatings. In this case, the PVA addition is detrimental to the overall performance of the coating. The flexural strength is similar, but strain tolerance for the alumina/PVA coatings is much lower. These observations are likely due to the increased porosity of the coatings with PVA, Figure 13.1and Figure 13.2. Due to the fact that the density of the PVA/alumina coating was measured to be 2.67g/cc and the density of the as sprayed coating was 2.74g/cc, the PVA/alumina coating has more porosity. The microstructure is more loosely bonded, thus lower cohesion, and the strength of the coating is less. Using a stream of PVA solution in between alumina spray passes, likely cools the substrate and coating buildup

thus far hindering the bond between the particles that have already been deposited and those being directed at the substrate resulting in a looser and more porous structure. This would result in the alumina/PVA system having a lower density, strength, and modulus which were all proven to be the case.

In addition, it is likely that the benefit that has been previously observed for post deposition infiltration of an organic material would be lost because the melting point of PVA is approximately 230˚C [106] and during the spray process, the temperature of the substrate and coating system likely reaches approximately 400˚C. This means that spraying PVA in between passes is actually detrimental to the overall mechanical properties of the coating because the benefits of the polymer are lost during the spray process, and the liquid solution serves as a means of cooling the deposited coating affecting the bonding of the subsequent particles being directed at the surface. Based on these findings, it may be a good idea, to experiment with other polymers with higher melting temperatures so the benefit of polymer addition is not lost.

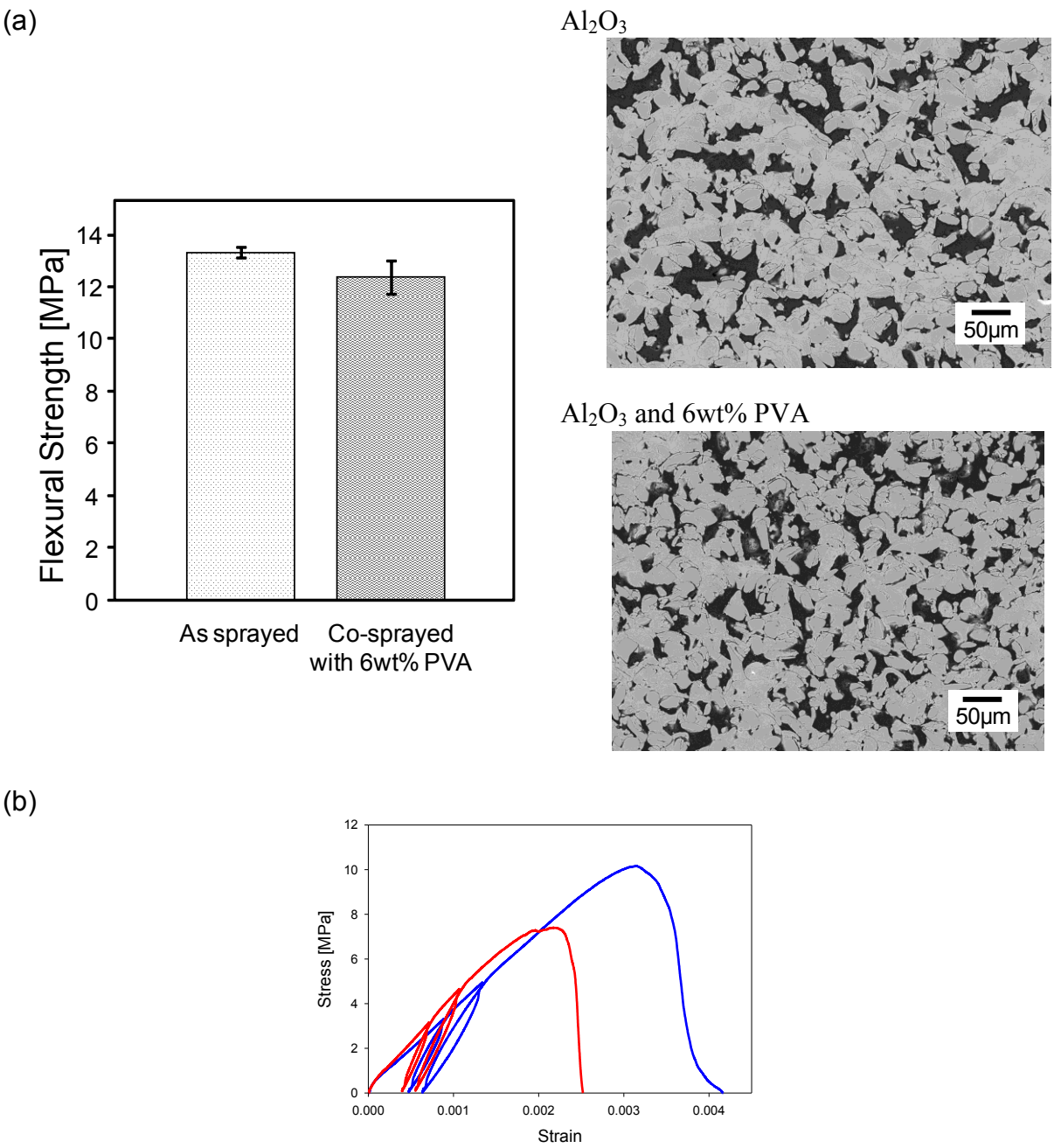

Figure 13.1. a) Flexural strengths measured through three-point bending of an alumina flame spray coating and an alumina flame spray coating that was sprayed with a 6wt% PVA solution in between alumina passes. Their corresponding microstructures are provided. b) Stress/strain behavior of the as sprayed and co-sprayed with 6wt% PVA coatings.

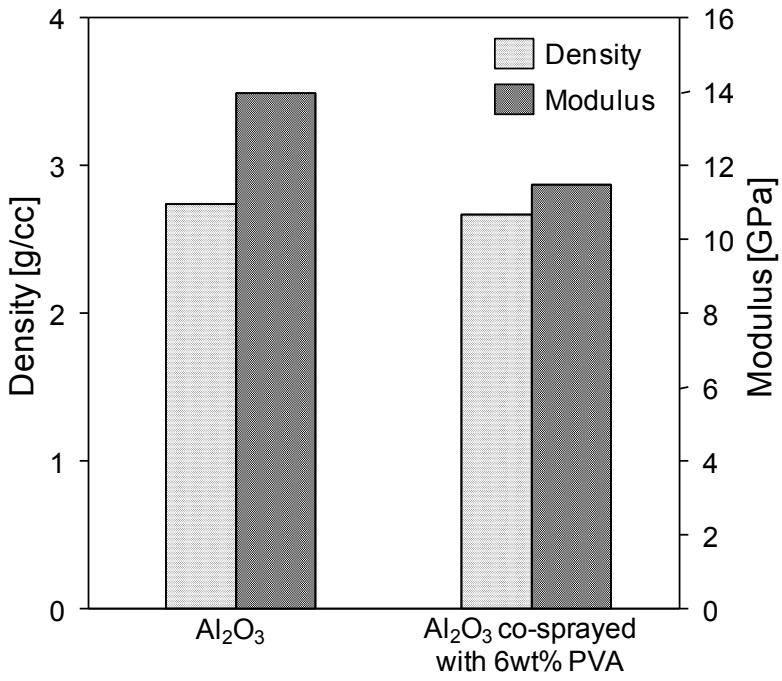

Figure 13.2. Modulus versus density for the alumina flame spray coating and alumina flame spray coating that was co-sprayed with a 6wt% PVA solution.

Alumina was plasma sprayed and Diamant Dichtol was brushed in between passes. A coating layer of 200μm was deposited and then Dichtol was brushed four times in a quick succession and left for 30min and an additional alumina layer was sprayed on top. This was done to yield a coating buildup of 800μm. A total of 4 layers of Dichtol were brushed on the sample. Samples were tested under three-point bend loading conditions to determine flexural strengths. Three samples were prepared. Substrate and coating separation was difficult. The alumina coatings were strongly adhered to the substrate and because of the Dichtol layers that were applied in between alumina deposition the system could not be placed in an aqua regia solution. Therefore, the coating had to be removed by mechanical means but this was not as simple as in the flame spray alumina case when the entire coating could be removed from the substrate in one piece. The plasma spray alumina and Dichtol coating fractured into a number of pieces during the removal process. However, three samples were able to be made from the fractured.

Results from bending experiments were rather interesting. Two of the samples had flexural strengths that were rather similar, 65.8 MPa and 63.5 MPa. The other sample (Sample 1 in Figure 13.3) had a flexural strength that was only 28.7MPa. Based upon observations from the three-point bend test, it appeared that this sample broke from the top surface, where the load was applied. This is the surface that is in compression. Usually the three-point bend samples fracture from the bottom surface in tension where the splats are being pulled apart. Another notable difference in this graph is in the way the PS alumina and Dichtol coating fractured. There is a

saw-tooth pattern to the curve which may even indicate that splats are fracturing and pulling apart. This behavior is similar to what was observed for abalone nacre. For instance, both show hysteresis and although not for the same type of test, the biopolymer interlayer shows a saw-tooth pattern in force-extension curves, Figure [44]. Smith *et al.* observed this behavior for the organic interlayers and attributed it to the organic molecules of the interlayer of nacre unfolding one at a time. The behavior observed in the alumina plasma sprayed coating with Dichtol is similar to what is caused by the unfolding of the macromolecules. Actually determining what is happening during the fracture is an important next step and whether or not this behavior is observed with other materials should be studied. In the future, this should be followed up.

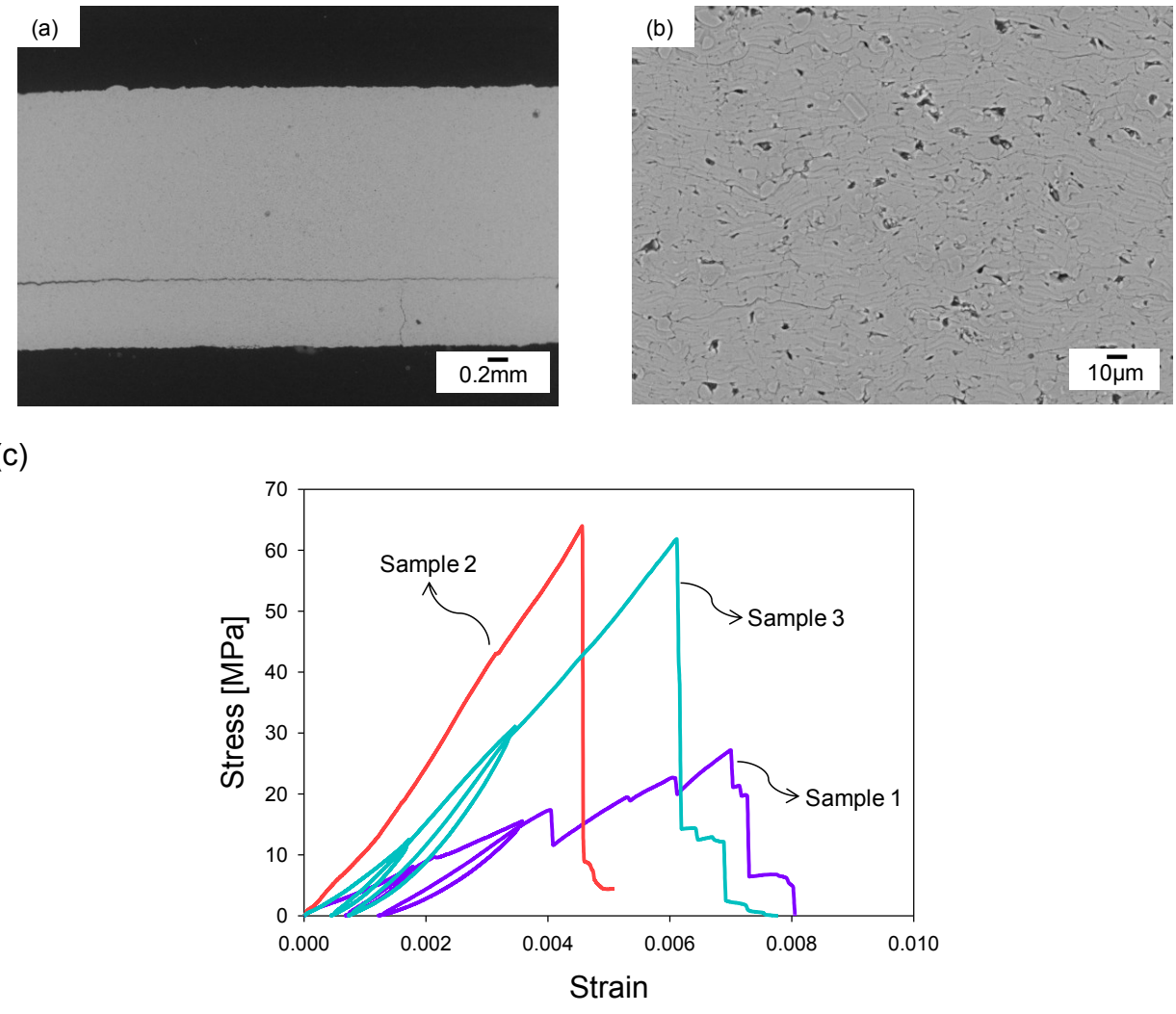

Figure 13.3. Cross sections of a plasma sprayed alumina coating deposited in layers of 200µm and then Dichtol was brushed on the freshly sprayed surface. This was repeated 4 times. b) Stress/strain behavior for the plasma sprayed alumina and Dichtol coating.

13.2. Exploration of Liquid Synthetic Rubber Modifiers to Provide Enhanced Toughening Behavior to Epoxies for Interfacial Modifications to Bio-Inspired Materials

Nacre is the most widely studied of the natural materials due its composition of mostly brittle mineral calcium carbonate platelets combined with approximately 5vol% biopolymer resulting in both a high strength and toughness. The work presented in this dissertation supports the conclusion that TS templates display similar mechanical properties to biological materials in their anelastic behavior when undergoing thermal or mechanical loading and unloading. This behavior is only enhanced when templates undergo interfacial modifications post deposition by a softer and more ductile phase closing off the interconnected porosity and defects that are inherently present in coatings due to the nature of spray processes. In fact, using Buehler a division of Illinois Tool Works Inc. EpoThin resin and EpoThin hardener in a 5:2 ratio respectively, it is possible for mechanical properties like flexural strength and fracture toughness to be tremendously enhanced. Following a staged cure, alumina ceramic rod coatings show enhancements on the same level as properties exhibited by nacreous assemblies.

Although these coatings, with the addition of epoxy, are observed to have higher strengths and toughnesses, it may be possible to further improve the fracture toughness. Thermosets are highly cross-linked polymers that are used at temperatures below their glass transition temperature. One disadvantage with epoxy infiltrated coatings, is that because epoxy is a thermoset it is thus prone to brittle failure when failure occurs. Thermosetting polymers are among the most brittle of polymer types [91]. Currently some developments have been made in improving their toughness. One such solution to this may be the addition of second-phase particles into the epoxy mixture such as rubber particles. Incorporation of a second phase of dispersed rubbery particles into an epoxy mixture need to be effectively bonded to the epoxy matrix. If this occurs then rubbery particles can prevent premature crack initiation, absorb energy behind the crack front, or via increased deformation.

Four different epoxy modifiers from Emerald Performance Materials (Moorestown, NJ) were individually mixed with the Buehler EpoThin resin and EpoThin hardener. Epoxy was made in the same 5g resin to 2g hardener with modifiers added to the mixture. The toughenners and the amounts added are as follows:

- HyPox RA840 (25 phr to the resin side of the system)
- Hypro 1300X68 (10 phr to the epoxy side of the system)
- Hypro 1300X16 (10 phr to the curative side of the system)

- Hypro 1300X21 (10 phr to the curative side of the system)

Initial findings with these toughenners are presented in Chapter 5, however, it would be beneficial to do a more in depth study. Altering the parts per hundred of the toughenners could provide further property enhancements or benefits. It is also possible altering the concentration of the secondary phase added to the epoxy that degradation of properties of the thermally sprayed hybrid composites would be observed. Therefore, it is important that a more systematic study on these four products be performed to gain a better understanding of how epoxy mixtures can be modified.

References

1. Giraud-Guille, M.M., E. Belamie, and G. Mosser, *Organic and mineral networks in carapaces, bones and biomimetic materials.* Comptes Rendus Palevol, 2004. **3**(6-7): p. 503-513.

2. Barthelat, F., *Biomimetics for next generation materials.* Philosophical Transactions of the Royal Society a-Mathematical Physical and Engineering Sciences, 2007. **365**(1861): p. 2907-2919.

3. Meyers, M., et al., *Structural biological composites: An overview.* JOM, 2006. **58**(7): p. 35-41.

4. Weiner, S. and H.D. Wagner, *THE MATERIAL BONE: Structure-Mechanical Function Relations.* Annual Review of Materials Science, 1998. **28**(1): p. 271-298.

5. Wegst, U.G.K. and M.F. Ashby, *The mechanical efficiency of natural materials.* Philosophical Magazine, 2004. **84**(21): p. 2167-2186.

6. Dastjerdi, A.K., R. Rabiei, and F. Barthelat, *The weak interfaces within tough natural composites: Experiments on three types of nacre.* Journal of the Mechanical Behavior of Biomedical Materials, 2013. **19**: p. 50-60.

7. Sanchez, C., H. Arribart, and M.M. Guille, *Biomimetism and bioinspiration as tools for the design of innovative materials and systems.* Nat Mater, 2005. **4**(4): p. 277-88.

8. Fratzl, P., et al., *Structure and mechanical quality of the collagen-mineral nano-composite in bone.* Journal of Materials Chemistry, 2004. **14**(14): p. 2115-2123.

9. Rho, J.Y., L. Kuhn-Spearing, and P. Zioupos, *Mechanical properties and the hierarchical structure of bone.* Medical Engineering & Physics, 1998. **20**(2): p. 92-102.

10. Gupta, H.S., et al., *Cooperative deformation of mineral and collagen in bone at the nanoscale.* Proceedings of the National Academy of Sciences, 2006. **103**(47): p. 17741-17746.

11. Tai, K., F.-J. Ulm, and C. Ortiz, *Nanogranular Origins of the Strength of Bone.* Nano Letters, 2006. **6**(11): p. 2520-2525.

12. Peterlik, H., et al., *From brittle to ductile fracture of bone.* Nature Materials, 2006. **5**(1): p. 52-55.

13. Nalla, R.K., et al., *Mechanistic aspects of fracture and R-curve behavior in human cortical bone.* Biomaterials, 2005. **26**(2): p. 217-231.

14. Barthelat, F., J.E. Rim, and H.D. Espinosa, *A Review on the Structure and Mechanical Properties of Mollusk Shells – Perspectives on Synthetic Biomimetic Materials*, in *Applied Scanning Probe Methods XIII*, B. Bhushan and H. Fuchs, Editors. 2009, Springer Berlin Heidelberg. p. 17-44.

15. Rabiei, R., S. Bekah, and F. Barthelat, *Failure mode transition in nacre and bone-like materials.* Acta Biomaterialia, 2010. **6**(10): p. 4081-4089.

16. Espinosa, H.D., et al., *Merger of structure and material in nacre and bone - Perspectives on de novo biomimetic materials.* Progress in Materials Science, 2009. **54**(8): p. 1059-1100.

17. Olson, I.C., et al., *Mollusk Shell Nacre Ultrastructure Correlates with Environmental Temperature and Pressure.* Journal of the American Chemical Society, 2012. **134**(17): p. 7351-7358.

18. Weiner, L.A.a.S., *Biomineralization: A pavement of pearl.* Nature, 1997. **389**(6654): p. 4.

19. Metzler, R.A., et al., *Architecture of Columnar Nacre, and Implications for Its Formation Mechanism.* Physical Review Letters, 2007. **98**(26): p. 268102.

20. Checa, A.G., J.H.E. Cartwright, and M.-G. Willinger, *The key role of the surface membrane in why gastropod nacre grows in towers.* Proceedings of the National Academy of Sciences, 2009. **106**(1): p. 38-43.

21. Rousseau, M., et al., *Multiscale structure of sheet nacre.* Biomaterials, 2005. **26**(31): p. 6254-6262.

22. Cartwright, J.H.E., et al., *Spiral and target patterns in bivalve nacre manifest a natural excitable medium from layer growth of a biological liquid crystal.* Proceedings of The National Academy of Sciences, 2009. **106**(26): p. 10499-10504.

23. Currey, J.D., *MECHANICAL-PROPERTIES OF MOTHER OF PEARL IN TENSION.* Proceedings of the Royal Society of London Series B-Biological Sciences, 1977. **196**(1125): p. 443-&.

24. Jackson, A.P., J.F.V. Vincent, and R.M. Turner, *THE MECHANICAL DESIGN OF NACRE.* Proceedings of the Royal Society of London Series B-Biological Sciences, 1988. **234**(1277): p. 415-&.

25. Luz, G.M. and J.F. Mano, *Biomimetic design of materials and biomaterials inspired by the structure of nacre.* Philosophical Transactions of the Royal Society a-Mathematical Physical and Engineering Sciences, 2009. **367**(1893): p. 1587-1605.

26. Li, X.D., et al., *Nanoscale structural and mechanical characterization of a natural nanocomposite material: The shell of red abalone.* Nano Letters, 2004. **4**(4): p. 613-617.

27. Currey, J.D., *MECHANICAL-PROPERTIES OF MOTHER OF PEARL IN TENSION.* Proceedings of the Royal Society Series B-Biological Sciences, 1977. **196**(1125): p. 443-+.

28. Bonderer, L.J., A.R. Studart, and L.J. Gauckler, *Bioinspired design and assembly of platelet reinforced polymer films.* Science, 2008. **319**(5866): p. 1069-1073.

29. Okumura, K. and P.G. de Gennes, *Why is nacre strong? Elastic theory and fracture mechanics for biocomposites with stratified structures.* European Physical Journal E, 2001. **4**(1): p. 121-127.

30. Clegg, W.J., et al., *A SIMPLE WAY TO MAKE TOUGH CERAMICS.* Nature, 1990. **347**(6292): p. 455-457.

31. Currey, J.D., et al., *Mechanical properties of nacre and highly mineralized bone.* Proceedings of the Royal Society of London Series B-Biological Sciences, 2001. **268**(1462): p. 107-111.

32. Walsh, J.B., *The effect of cracks on the uniaxial elastic compression of rocks.* Journal of Geophysical Research, 1965. **70**(2): p. 399-411.

33. Brace, W.F. and M.I.o.T.I.L. Program, *Brittle Fracture of Rocks*. 1963: Massachusetts Institute of Technology, Industrial Liaison Program.

34. Karl, J.J., T.D. Dwight, and A. Ozan, *Observations of Damage in Bone*, in *Bone Mechanics Handbook, Second Edition*. 2001, CRC Press. p. 17-1-17-18.

35. Lemaître, J., *A course on damage mechanics*. 1996: Springer.

36. Fondrk, M., et al., *Some viscoplastic characteristics of bovine and human cortical bone.* Journal of Biomechanics, 1988. **21**(8): p. 623-630.

37. Carter, D.R., et al., *Fatigue Behavior of Adult Cortical Bone: The Influence of Mean Strain and Strain Range.* Acta Orthopaedica, 1981. **52**(5): p. 481-490.

38. Carter, D.R. and W.C. Hayes, *Compact bone fatigue damage—I. Residual strength and stiffness.* Journal of Biomechanics, 1977. **10**(5–6): p. 325-337.

39. Pattin, C.A., W.E. Caler, and D.R. Carter, *Cyclic mechanical property degradation during fatigue loading of cortical bone.* Journal of Biomechanics, 1996. **29**(1): p. 69-79.

40. Zioupos, P., X.T. Wang, and J.D. Currey, *Experimental and theoretical quantification of the development of damage in fatigue tests of bone and antler.* Journal of Biomechanics, 1996. **29**(8): p. 989-1002.

41. Zioupos, P. and A. Casinos, *Cumulative damage and the response of human bone in two-step loading fatigue.* Journal of Biomechanics, 1998. **31**(9): p. 825-833.

42. Herkowitz, H.N. and I.S.S.L. Spine, *The Lumbar Spine*. 2004: Lippincott Williams & Wilkins.

43. Ashby, M.F., *Hybrids to fill holes in material property space.* Philosophical Magazine, 2005. **85**(26-27): p. 3235-3257.

44. Smith, B.L., et al., *Molecular mechanistic origin of the toughness of natural adhesives, fibres and composites.* Nature, 1999. **399**(6738): p. 761-763.

45. Munch, E., et al., *Tough, Bio-Inspired Hybrid Materials.* Science, 2008. **322**(5907): p. 1516-1520.

46. E. Munch, M.E.L., D. H. Alsem, E. Saiz, A. P. Tomsia, R. O. Ritchie, *Supporting Online Material for Tough, Bio-Inspired Hybrid Materials.* Science, 2008. **322**: p. 1516.

47. Finnemore, A., et al., *Biomimetic layer-by-layer assembly of artificial nacre.* Nat Commun, 2012. **3**: p. 966.

48. Tang, Z.Y., et al., *Nanostructured artificial nacre.* Nature Materials, 2003. **2**(6): p. 413-U8.

49. Sellinger, A., et al., *Continuous self-assembly of organic-inorganic nanocomposite coatings that mimic nacre.* Nature, 1998. **394**(6690): p. 256-260.

50. Walther, A., et al., *Large-Area, Lightweight and Thick Biomimetic Composites with Superior Material Properties via Fast, Economic, and Green Pathways.* Nano Letters, 2010. **10**(8): p. 2742-2748.

51. Deville, S., et al., *Freezing as a path to build complex composites.* Science, 2006. **311**(5760): p. 515-518.

52. Barthelat, F., *Nacre from mollusk shells: a model for high-performance structural materials.* Bioinspiration & Biomimetics, 2010. **5**(3).

53. Herman, H., S. Sampath, and R. McCune, *Thermal spray: Current status and future trends.* Mrs Bulletin, 2000. **25**(7): p. 17-25.

54. Davis, J.R. and A.I.T.S.S.T. Committee, *Handbook of Thermal Spray Technology*. 2004: ASM International.

55. Wang, Z., et al., *Effects of pores and interfaces on effective properties of plasma sprayed zirconia coatings.* Acta Materialia, 2003. **51**(18): p. 5319-5334.

56. Kulkarni, A., et al., *Processing effects on porosity-property correlations in plasma sprayed yttria-stabilized zirconia coatings.* Materials Science and Engineering: A, 2003. **359**(1–2): p. 100-111.

57. Dwivedi, G., *On the Anelasticity of Plasma Sprayed Ceramic Coatings: Observations, Characterizations and Applications*, in *Materials Science and Engineering*. 2011, Stony Brook University: Stony Brook.

58. Liu, Y., *Anelastic Behavior of Thermal Spray Coatings and Associated Relationships with Processing Conditions*, in *Mechanical Engineering*. 2007, Stony Brook University.

59. Kulkarni, A., et al., *Comprehensive microstructural characterization and predictive property modeling of plasma-sprayed zirconia coatings.* Acta Materialia, 2003. **51**(9): p. 2457-2475.

60. Kuroda, S., T. Dendo, and S. Kitahara, *QUENCHING STRESS IN PLASMA-SPRAYED COATINGS AND ITS CORRELATION WITH THE DEPOSIT MICROSTRUCTURE.* Journal of Thermal Spray Technology, 1995. **4**(1): p. 75-84.

61. Matejicek, J. and S. Sampath, *Intrinsic residual stresses in single splats produced by thermal spray processes.* Acta Materialia, 2001. **49**(11): p. 1993-1999.

62. Liu, Y., et al., *Anelastic Behavior of Plasma-Sprayed Zirconia Coatings.* Journal of the American Ceramic Society, 2008. **91**(12): p. 4036-4043.

63. Lawn, B.R. and D.B. Marshall, *Nonlinear stress-strain curves for solids containing closed cracks with friction.* Journal of the Mechanics and Physics of Solids, 1998. **46**(1): p. 85-113.

64. Yagmur, L., S. Fank, and B. Aydemir, *Effect of microstructure on modulus loss at flexural mode and stress in sensor materials.* Sensors and Actuators A: Physical, 2007. **136**(1): p. 261-266.

65. Nakamura, T. and Y. Liu, *Determination of nonlinear properties of thermal sprayed ceramic coatings via inverse analysis.* International Journal of Solids and Structures, 2007. **44**(6): p. 1990-2009.

66. Kroupa, F. and J. Plesek, *Nonlinear elastic behavior in compression of thermally sprayed materials.* Materials Science and Engineering: A, 2002. **328**(1–2): p. 1-7.

67. Kachanov, M., I. Tsukrov, and B. Shafiro, *Effective Moduli of Solids With Cavities of Various Shapes.* Applied Mechanics Reviews, 1994. **47**(1S): p. S151-S174.

68. Dwivedi, G., T. Nakamura, and S. Sampath, *Controlled Introduction of Anelasticity in Plasma-Sprayed Ceramics.* Journal of the American Ceramic Society, 2011. **94**: p. S104-S111.

69. Lawn, B., *Fracture of Brittle Solids*. 1993: Cambridge University Press.

70. Currey, J.D., *Mechanical Properties of Mother of Pearl in Tension.* Proceedings of the Royal Society of London. Series B, Biological Sciences, 1977. **196**(1125): p. 443-463.

71. Gao, H., et al., *Materials become insensitive to flaws at nanoscale: Lessons from nature.* Proceedings of the National Academy of Sciences, 2003. **100**(10): p. 5597-5600.

72. Ji, B. and H. Gao, *Mechanical properties of nanostructure of biological materials.* Journal of the Mechanics and Physics of Solids, 2004. **52**(9): p. 1963-1990.

73. Barthelat, F., et al., *On the mechanics of mother-of-pearl: A key feature in the material hierarchical structure.* Journal of the Mechanics and Physics of Solids, 2007. **55**(2): p. 306-337.

74. Jackson, A.P., J.F.V. Vincent, and R.M. Turner, *THE MECHANICAL DESIGN OF NACRE.* Proceedings of the Royal Society Series B-Biological Sciences, 1988. **234**(1277): p. 415-+.

75. Barthelat, F. and H.D. Espinosa, *An experimental investigation of deformation and fracture of nacre-mother of pearl.* Experimental Mechanics, 2007. **47**(3): p. 311-324.

76. Wang, R.Z., et al., *Deformation mechanisms in nacre.* Journal of Materials Research, 2001. **16**(9): p. 2485-2493.

77. *Technical Bulletin; Rokide® A (Aluminum Oxide) Ceramic Rod for Thermal Spraying*, in *Saint-Gobain Coating Solutions*, S.-G.C. Solutions, Editor., Saint-Gobain Coating Solutions.

78. (ITSA), I.T.S.A., *What is Thermal Spray?*, I.T.S.A. (ITSA), Editor., International Thermal Spray Association (ITSA): Fairport HArbor, OH.

79. Osswald, T.A. and G. Menges, *Materials Science of Polymers for Engineers*. 2003: Hanser Publishers.

80. Clegg, D.W., A.A. Collyer, and I.o. Materials, *The Structure and Properties of Polymeric Materials*. 1993: Institute of Materials.

81. López, O.B.L., G.L. Sierra, and G.A.I. Mejía, *Biodegradability of poly(vinyl alcohol).* Polymer Engineering & Science, 1999. **39**(8): p. 1346-1352.

82. *Safety Data Sheet 1907/2006/EC- REACH (GB)*, Buehler, Editor. 2006. p. 10.

83. Fouassier, J.P. and J. Lalevée, *Photoinitiators for Polymer Synthesis: Scope, Reactivity, and Efficiency*. 2013: Wiley.

84. *Sigma-Aldrich Co. LLC poly(vinyl alcohol)*. Sigma-Aldrich poly(methyl methacrylate), PMMA 2014 [cited 2014 July 21, 2014].

85. *Sigma-Aldrich Co. LLC poly(methyl methacrylate), PMMA*. Sigma-Aldrich Co. LLC poly(methyl methacrylate), PMMA [cited 2014 July 21,2014].

86. Callister, W.D., *(WCS)Materials Science and Engineering: An Introduction, 7th Edition Binder Ready Version*. 2007: John Wiley & Sons Canada, Limited.

87. Fischer-Cripps, A.C., *Introduction to Contact Mechanics*. 2nd ed, ed. F.F. Ling. 2007, United States of America: Springer Science+Business Media, LLC.

88. *Simultaneous Thermal Analysis; Method, Technique, Applications*, N. Group, Editor., NETZSCH-Geratebau GmbH: Germany. p. 1-16.

89. *Basics of Electrochemical Corrosion Measurements*. Gamry Instruments. p. 8.

90. Launey, M.E., et al., *Designing highly toughened hybrid composites through nature-inspired hierarchical complexity.* Acta Materialia, 2009. **57**(10): p. 2919-2932.

91. Young, A.J.K.a.R.J., *Fracture Behavior of Polymers*. 1983, Northern Ireland: Applied Science Publishers Ltd. 496.

92. Zuo, S. and Y. Wei, *Microstructure observation and mechanical behavior modeling for limnetic nacre.* Acta Mechanica Sinica, 2008. **24**(1): p. 83-89.

93. Corni, I., et al., *A review of experimental techniques to produce a nacre-like structure.* Bioinspiration & Biomimetics, 2012. **7**(3): p. 031001.

94. Humburg, H., et al., *Bio-inspired tapered fibers for composites with superior toughness.* Composites Science and Technology, 2012. **72**(9): p. 1012-1019.

95. *Procedure of in-situ polymerization into plasma-sprayed alumina scaffolds*. 2012, VTT Technical Research Centre of Finland: Finland.

96. Tucker, R.C., *ASM Handbook, Volume 5A: Thermal Spray Technology*. Vol. 5A. 2013: ASM International and Thermal Spray Society.

97. Knuuttila, J., P. Sorsa, and T. Mantyla, *Sealing of thermal spray coatings by impregnation.* Journal of Thermal Spray Technology, 1999. **8**(2): p. 249-257.

98. Ingham, H.S., *Metco Flame Spray Handbook: Wire process*. 1959: Metco.

99. Ingham, H.S., *Metco Flame Spray Handbook: Volume 3: Plasma Flame Process*. 1965: Metco.

100. *Material Product Data Sheet; Sealers for Thermal Spray Coatings*, S. Metco, Editor. 2012, Sulzer Metco. p. 1-6.

101. Education, G.B.D.o. and Science, *Lubrication (tribology), education and research: a report on the present position and industry's needs*. 1966: H. M. Stationery Off.

102. Mang, T., K. Bobzin, and T. Bartels, *Industrial Tribology: Tribosystems, Friction, Wear and Surface Engineering, Lubrication*. 2011: Wiley.

103. Holmberg, K. and A. Matthews, *Coatings Tribology: Properties, Mechanisms, Techniques and Applications in Surface Engineering*. 2009: Elsevier Science.

104. Sampath, S. and S.F. Wayne, *Microstructure and properties of pLASMA-sPRAYED Mo-Mo2C composites.* Journal of Thermal Spray Technology, 1994. **3**(3): p. 282-288.

105. QIN, Z., et al., *ROBUSTNESS-STRENGTH PERFORMANCE OF HIERARCHICAL ALPHA-HELICAL PROTEIN FILAMENTS.* International Journal of Applied Mechanics, 2009. **01**(01): p. 85-112.

106. Nadras Othman, N.A.A., Hanafi Ismail, *Thermal Properties of Polyvinyl Alcohol (PVOH)/Corn Starch Blend Film.* Malaysian Polymer Journal, 2011. **6**.